# CHARACTERIZING AND RESCUING ABERRANT PROTEOSTASIS IN MODELS OF *GABRG2(Q390X)*-ASSOCIATED DRAVET SYNDROME

By

Sarah Elizabeth Marie Poliquin

Dissertation

Submitted to the Faculty of the

Graduate School of Vanderbilt University

in partial fulfillment of the requirements

for the degree of

DOCTOR OF PHILOSOPHY

in

Neuroscience

May 12, 2023

Nashville, Tennessee

Approved:

Christine Konradi, Ph.D.

Martin Gallagher, M.D., Ph.D.

Andre LaGrange, M.D., Ph.D.

Brad Grueter, Ph.D.

Jing-Qiong Kang, M.D., Ph.D.

# Acknowledgements

I thank my PI, Katty Kang, for accepting me into the lab and appreciate her boundless enthusiasm for science. I thank my committee – Christine Konradi, Andre LaGrange, Brad Grueter, and Marty Gallagher – for all of their varied scientific expertise.

I would like to thank Jake Bauer and Cipo Bazan for their unwavering support through this entire journey. Perhaps most importantly, they were just as supportive whenever I was tempted – yet again – to drop out of science forever. They've ensured I've had a fulfilling and exciting life outside the lab, whether that be climbing the mountains of Colorado or getting lost (literally!) in the Tennessee wilderness, sweating at the gym, and laughing. Cipo has provided patient wisdom, going all the back to the beginning with the stress of grad school applications, and interminable groan-worthy puns. Jake especially deserves a shout-out for keeping me company through so many late nights in the lab, and patiently tolerating the weekends interrupted by experiments, as well as eager assistance in consuming the products of many culinary experiments performed to cope with failed laboratory experiments.

Emily Schroeder has been a wonderful best friend. She's provided endless encouragement and fresh perspectives, as well as silly pictures of her cats.

My Dungeons and Dragons group and friends at my dance studios helped reset me. I especially want to thank dance, for providing the opportunity to temporarily shut off the worries of classes and experiments and grants and manuscripts and presentations and conferences, and instead exist in the moment.

I thank all the past and present members of the Kang lab. Wangzhen Shen has been a font of technical expertise, helping to troubleshoot so many experiments. Gerald Nwosu performed dozens of surgeries to implant EEG head mounts on mice. Felicia Mermer brought wonderful energy that made the lab a fun place to be. Kirill Zavalin has provided advice on the PhD journey and given feedback on manuscripts.

I'd also like to thank Olivia Cox and Manuel Giannoni for their friendship and scientific support.

My colleagues at COMBINEDBrain have been so supportive and given me a sense of belonging and purpose. The opportunity to work with such wonderful people, doing such important and impactful projects, gave me hope for the future when I wasn't sure why I was drudging through the PhD. I'm glad I stuck with it and finished the journey, and can't wait to see what amazing things we do together for patients with rare diseases.

.

# Table of Contents

# List of Tables

# List of Figures

# 1 Introduction

This chapter is adapted from “Disruption of the ubiquitin-proteasome system and elevated endoplasmic reticulum stress in epilepsy” published in *Biomedicines* and has been reproduced with the permission of the publisher and my co-author, Jing-Qiong Kang.
Citation: Poliquin S, Kang JQ. Disruption of the ubiquitin-proteasome system and elevated endoplasmic reticulum stress in epilepsy. *Biomedicines*. 2022;10(3):647. doi: 10.3390/biomedicines10030647

## 1.1 Abstract

The epilepsies are a broad group of conditions characterized by repeated seizures, and together are one of the most common neurological disorders. Additionally, epilepsy is comorbid with many neurological disorders, including lysosomal storage diseases, syndromic intellectual disability, and autism spectrum disorder. Despite the prevalence, treatments are still unsatisfactory: Approximately 30% of epileptic patients do not adequately respond to existing therapeutics, which primarily target ion channels. Therefore, new therapeutic approaches are needed. Disturbed proteostasis is an emerging mechanism in epilepsy with profound effects on neuronal health and function. Proteostasis – the dynamic balance of protein synthesis and degradation – can be directly disrupted by epilepsy-associated mutations in various components of the ubiquitin-proteasome system (UPS), or the impairments can be secondary to seizure activity or misfolded proteins. Endoplasmic reticulum (ER) stress can arise from failed proteostasis and result in neuronal death. In light of this, several treatment modalities that modify components of proteostasis show promise in the management of neurological disorders. This includes chemical chaperones to assist proper folding of

proteins, inhibitors of overly active protein degradation, and enhancers of endogenous proteolytic pathways such as the UPS. This review summarizes recent work on the pathomechanisms of abnormal protein folding and degradation in epilepsy, and treatment development targeting this area.

## 1.2 Introduction

Proteins are crucial to nearly every function in a cell, including both general functions found in nearly every cell such as energy production and DNA replication, as well as neuron-specific processes like maintenance of the membrane potential and synaptic vesicle release. Proteins must be folded properly in order to fulfill their functions, but protein folding is incredibly complex, and thus misfolding is common.[1] Up to one-third of newly synthesized proteins are degraded due to problems with synthesis or folding.[1] This inefficiency can pose problems, as not only is the native protein function lost by the misfolding, toxic protein aggregates may form.[1] Therefore, there are many quality control mechanisms in the cell to minimize these problems, ranging from methods to assist folding to machinery to degrade misfolded or aggregated proteins, or, in the case of severe proteostasis problems, programmed cell death.

A large proportion of newly synthesized proteins are folded in the endoplasmic reticulum (ER). The ER is equipped to facilitate proper folding, as its oxidizing environment promotes disulfide bond formation, and it contains many proteins that act as chaperones to further assist folding and act as quality control.[1] Complex oligosaccharides are added posttranslationally to proteins, often further stabilizing them and enhancing interactions with chaperones.[1,2]

Proteostasis is the careful balance between protein synthesis and degradation, and disruptions of proteostasis are implicated in numerous diseases, including neurological conditions such as epilepsy. Neuronal function depends on a vast array of membrane proteins, such as voltage-gated sodium channels and neurotransmitter receptors, and membrane proteins in particular are prone to rapid degradation, as their complex structure results in inefficient folding and assembly.[2] The $GABA_A$ receptor (GABR) subunits are one example related to epilepsy, but this trend applies to other membrane proteins as well, such as cystic fibrosis transmembrane conductance regulator and peripheral myelin protein.[2]

As mentioned above, GABR subunits are inefficiently trafficked to the cell surface, due to their complex structures, as well as the necessity of assembling with other subunits to form a complete pentameric receptor.[2–4] It is estimated that only approximately 20-30% of newly synthesized GABR protein successfully reaches the cell surface.[2] Proper insertion of a full receptor into the membrane is further compromised by many epilepsy-linked mutations, such as α1(A322D) or γ2(Q390X), that result in ER retention of the misfolded protein or impaired heteropentamer assembly.[4–8]

When a protein cannot be folded properly, it is degraded. Protein degradation is a crucial function in the cells, to properly balance protein synthesis and to eliminate misfolded or mutated proteins.[9,10] There are two primary pathways in eukaryotic cells: macroautophagy and the ubiquitin-proteasome system (UPS). Macroautophagy, henceforth referred to simply as autophagy, involves the enveloping of the cargo in a double-membrane compartment known as the autophagosome, and therefore can target large cellular components such as organelles, complex protein complexes, and

protein aggregates.[9,11] In contrast, the UPS – which degrades the majority of intracellular proteins – primarily degrades individual proteins, as the target must be able to enter the narrow entrance.[11,12] These two pathways are interconnected, as they rely on shared components like ubiquitin, and disruptions to one pathway can alter the other.[9,11]

### 1.3 Ubiquitin-proteasome system

The UPS is critical in maintaining appropriate levels of regulatory proteins, such as those involved in the cell cycle, metabolism, and apoptosis, as well as degrading misfolded proteins.[9,12,13] Dysfunction of the UPS is therefore associated with many diseases, ranging from cancer to neurological diseases.[9,12,14,15]

#### 1.3.1 Unfolded protein response

In the case of misfolded proteins, the degradation process can begin in the ER with activation of the unfolded protein response (UPR). The UPR is activated in response to ER stress caused by factors such as accumulation of misfolded proteins or oxidative stress.[16–18] The function of the UPR is to restore proteostasis, which can be aided by several mechanisms: boosting the folding capacity of the ER by enlarging the ER and upregulating chaperones; decreasing the number of proteins to fold via increased ER-to-Golgi trafficking and halted protein translation; and/or enhancing protein degradation.[1,16,19] If these attempts fail, the UPR induces apoptosis.[16–18,20] There are three arms to the UPR – PERK, IRE1, and ATF6 – but there is overlap in function as all three can be both pro-apoptotic and protective.[4,16,18] The UPR plays a role in some of

the neuronal damage observed in epilepsy: Seizures can cause excessive ER stress and result in neuronal apoptosis.[16]

### 1.3.2 Endoplasmic reticulum-associated degradation

One of the results of the UPR is enhancing protein degradation, through autophagy or through ER-associated degradation (ERAD).[1,18] ERAD is a major removal pathway for misfolded proteins, both wildtype and mutant, and is induced when an ER chaperone such as BiP recognizes a misfolded protein.[1,5,21,22] The misfolded protein is targeted for degradation via ubiquitination, which will be described in more detail below. After ubiquitination, the protein is retrotranslocated from the ER to the cytosol, where the proteasome is located.[1,23] The ATPase valosin-containing protein (VCP) provides the energy to move the protein through a retrotranslocation channel in the ER membrane.[1,23] Membrane proteins like ion channels can be especially challenging to extract from the ER, as the hydrophobic membrane-spanning regions must be exposed to the cytosol during extraction.[1] ERAD plays an intrinsic role in epilepsies: For example, overactive ERAD contributes to seizure pathology in some genetic epilepsies.[2,22]

### 1.3.3 Proteasome

When proteins are targeted by ERAD, they are passed to the 26S proteasome. There are multiple types of proteasomes, but the 26S proteasome is found in all cell types and degrades damaged proteins.[24] The 26S proteasome is a large, complex cellular machine consisting of at least 33 subunits and weighing 2.5 MDa.[1,9,12,24] It is composed of a 20S core particle and a 19S regulatory particle, and the core particle can be singly capped at one end by the regulatory 19S particle or doubly capped at both

ends.[1,9,10,24,25] The heptameric 20S core is made of two outer rings of alpha subunits and two inner rings of beta subunits.[9,10,24] The beta subunit rings are the site of proteolytic activity, which takes three forms: caspase-like (β1), trypsin-like (β2), and chymotrypsin-like (β5).[1,9,10,24] This results in polypeptides of 2-30 amino acids that are then further broken down by other processes.[1] The 19S regulatory particle is involved in substrate recognition, followed by unfolding of the substrate polypeptide and translocation into the catalytic 20S core.[9,24] The 19S particle is made up of a base of 10 proteins and a lid of 9 more.[9,10] The expression of all these subunits is tightly regulated, and alterations to subunit expression have been observed in genetic epilepsy.[9,26] Excess excitatory transmission, such as occurs during a seizure or stroke, can also modulate the activity of the 26S proteasome.[10]

### 1.3.4 Ubiquitin

The first step in proteasome-mediated protein degradation is ubiquitination (Figure 1). The process of ubiquitination can be broken up into multiple stages: ubiquitin must first be activated by ATP with E1 enzymes, then transferred to ubiquitin-conjugating enzyme E2, and then moved to the target protein by E3 ubiquitin ligases.[1,10,11,13] The E3 ligases are substrate-specific and over 600 have been identified in mammalian cells.[1,11,27] Some of these E3 ligases are directly implicated in epilepsy, and will be discussed in more detail below. Further ubiquitin proteins are added to lysine residues of the initial ubiquitin, resulting in a polyubiquitin chain.[1,11,13,24]

Once ubiquitinated, the substrate is recognized by the proteasome, either through direct binding of the polyubiquitin chain to 19S subunits or though adaptor proteins that are associated with the proteasome.[1,24] In order to initiate degradation, there must also

be an unstructured site on the ubiquitinated protein.[24] If there is no unstructured site, the stochastic unfolding and refolding can temporarily create an initiation site, but these proteins are more likely to escape the 19S subunits or 19S adaptors and thus not be degraded.[24] Unstructured proteins can directly enter uncapped 20S proteasomes for proteolysis that is ubiquitin- and ATP-independent.[9,24] For ubiquitin-dependent degradation, the ubiquitin protein is removed from the substrate prior to degradation by deubiquitinases (DUBs) so that it can be reused.[1,10,24] DUBs can also remove the ubiquitin prior to association with the proteasome, allowing the substrate to avoid degradation.[1,24]

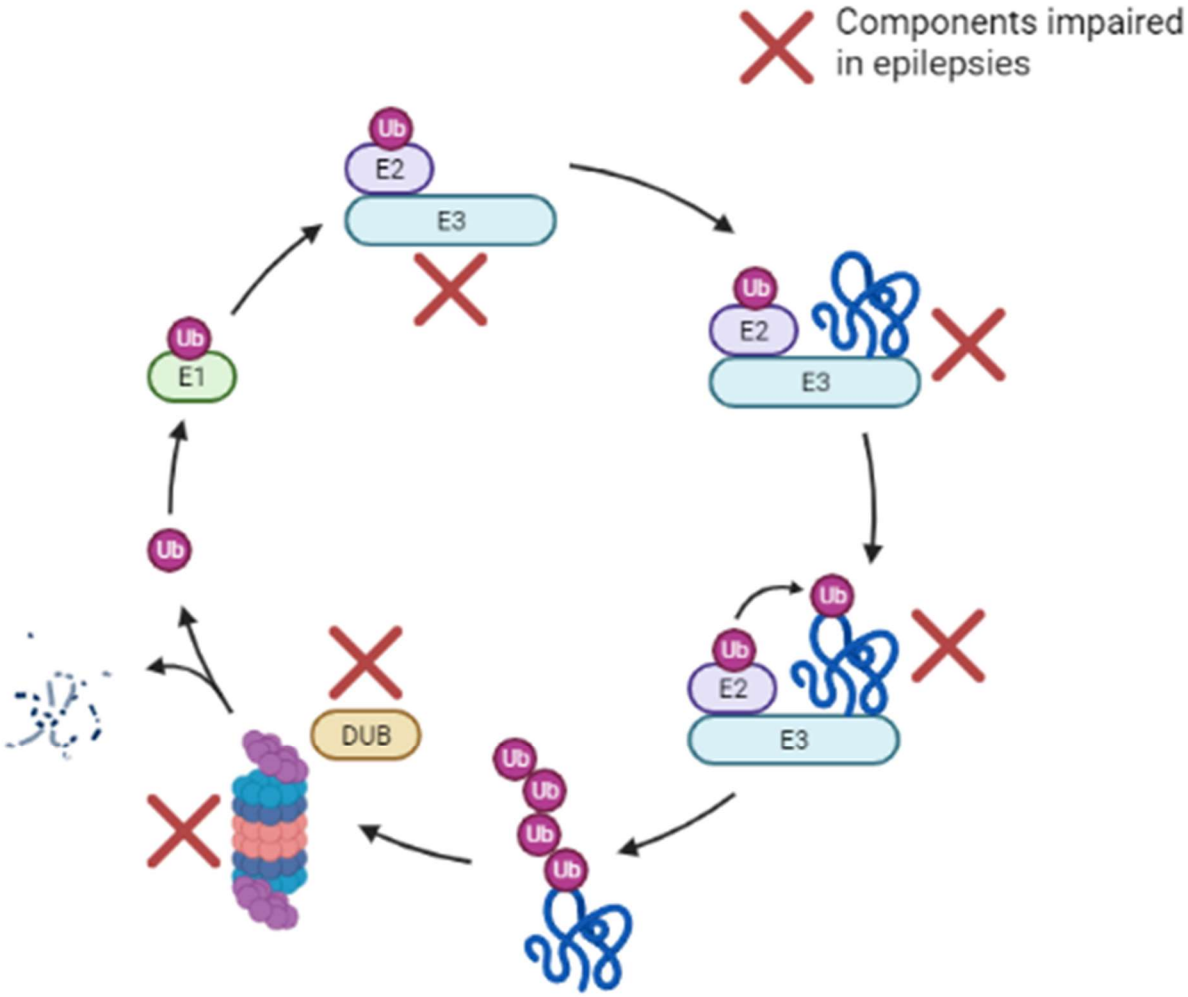


***Figure 1.1. Ubiquitination and proteasomal degradation of proteins.***
A ubiquitin-activating E1 enzyme hydrolyzes ATP to bind to ubiquitin (Ub), and then transfers the ubiquitin to a ubiquitin-conjugating E2 enzyme. The substrate-specific E3 ubiquitin ligase recognizes a protein and transfers the ubiquitin from the E2 enzyme to the substrate protein. A polyubiquitin chain can then be formed by adding to the initial ubiquitin. The 26S proteasome recognizes the ubiquitinated substrate and hydrolyzes it into small peptides. A deubiquitinase (DUB) removes the ubiquitin molecules before they can be degraded, so that they can be reused. Several steps of this process can be compromised in epilepsies, including downregulation or mutation of E3 ligases, impaired substrate recognition or ubiquitination, inappropriate DUB activity, and dysregulation of the proteasome itself.

## 1.4 The role of the UPS in the proteostasis of synaptic signaling

Efficient degradation of proteins is especially important for neurons, which, due to their post-mitotic state, have a more difficult time clearing toxic proteins.[28] When proteins are not degraded efficiently, prolonged ER stress and impaired UPS function can occur, and these factors are considered likely causes of neurodegeneration.[10,16,29] Proper UPS activity is crucial for correct neurotransmission: Not only are both pre- and postsynaptic proteins regulated by the UPS, the growth of dendrites and spines and the formation of new synapses are also controlled by the UPS.[13,14,25,27,30] When excitatory and inhibitory neurotransmission is imbalanced, seizures can occur.[31] Thus, insight from the interconnection of synaptic signaling and the UPS may further understanding of epilepsy.

### 1.4.1 The UPS is affected by synaptic signaling

In order to ensure proper neurotransmission, there is complex feedback between the UPS and synaptic signaling: the UPS both regulates and is regulated by neuronal activity. Induced synaptic activity in cultured neurons results in increased ubiquitination in postsynaptic densities (PSDs), and elevated UPS activity was observed within minutes in dendrites.[13,25] Conversely, activity blockade via TTX results in decreased ubiquitination and UPS activity.[13,25] The decreased dendritic UPS activity after synaptic blockade is mediated by $Ca^{2+}$ influx through NMDA receptors activating CaMKII, which phosphorylates the 19S subunit Rpt6.[25]

NMDA receptors in particular have been shown to have effects on the UPS. Bingol and Shuman (2006) showed that, in cultured hippocampal neurons, acute NMDA receptor activation resulted in a greater number of proteasomes in dendritic spines,

primarily due to a 6-fold decrease in the rate at which proteasomes exited the spines, but also aided by a subtler increase in the rate at which proteasomes were trafficked into the spines.[32] This change in localization is caused by active sequestering of proteasomes in the spines, mediated by an NMDA-dependent promotion of the association between proteasome subunits and the actin cytoskeleton.[32] In line with the findings above, the increase in proteasomes after excitatory stimulation was paired with augmented proteasomal activity, but there was a concomitant decrease in the amount of ubiquitinated proteins in dendritic spines.[32]

Interestingly, a decrease in ubiquitinated proteins that was accompanied by depressed 26S proteasome activity was found in a study by Tai et al (2010), after inducing long-term synaptic plasticity in cultured hippocampal neurons via NMDA exposure.[12] The decrease in both UPS activity and in the amount of ubiquitinated proteins indicates that protein ubiquitination is reduced, and this is supported by the downregulation of E3 ligases such as UBE3A and HUWE1.[12] Another study found that excitotoxic levels of glutamate stimulation of cultured hippocampal neurons temporarily dampened 26S proteasomal activity due to disassembly into 20S and 19S particles.[10] However, at this high concentration of NMDA, in contrast to the previous study, NMDA resulted in more polyubiquitinated proteins, possibly due to an observed reduction of DUB activity.[10]

### 1.4.2 Regulation of synaptic signaling by the UPS

While the UPS is influenced by neuronal activity, the UPS can also exert control over synaptic signaling, which has clear applicability to diseases of dysregulated synaptic transmission such as epilepsy. The turnover of several crucial synaptic proteins have

been demonstrated to be regulated by the UPS, including PSD-95, Shank, GKAP, AKAP, SPAR, and GRIP1.[13,25] Activity-dependent alterations in UPS activity result in widespread changes to the protein expression profile in postsynaptic densities, and inhibition of the UPS replicates the shifts in protein expression seen in inactive synapses.[13] In addition, pharmacological inhibition of the proteasome in cultured hippocampal neurons resulted in a larger pool of recycling synaptic vesicles (vesicles that both exocytosed and endocytosed in response to K+ stimulation).[33] This effect is activity dependent, as coapplication of TTX and antagonists of AMPA and NMDA receptors with the proteasome inhibitor abolished the change to vesicle pool size, although the blockers without proteasome inhibition had no effect.[33] This has important ramifications for synaptic function, as long-term UPS impairment could result in sustained changes to the pool of synaptic vesicles.[33]

Various parts of the UPS besides the proteasome itself can influence signaling. FBXO2 is a substrate-recognizing component of an E3 ligase complex known to regulate NMDARs, and *Fbxo2*$^{-/-}$ mice were shown to have altered NMDAR expression, with elevated GluN1 and GluN2A.[34] These mice were also observed to have a large increase in the number of axo-dendritic synapses, which are normally rare, and it is likely that these shaft synapses are the location of the excess GluN1 and GluN2A.[34] This dramatic promotion of unusual excitatory synapses could lead to epileptogenic activity.[34] The GluN2D NMDAR subunit, meanwhile, interacts with the E3 ligase Nedd4, and overexpression of Nedd4 abates GluN1/GluN2D receptor-mediated currents.[35] Nedd4 also regulates endocytosis and degradation of another excitatory receptor, mGlu7.[36] Additionally, the kainite receptor subunit GluK2 is regulated by parkin, an E3

ligase implicated in Parkinson's disease, such that mutant parkin leads to excess GluK2 and enhanced excitotoxicity in brain slices.[37] In combination with the effect of NMDA receptor stimulation on UPS activity discussed in the previous section, glutamate receptors thus have an intricate relationship with the UPS.

Proper proteasome balance is also necessary for other ion channels. The calcium-activated potassium channels in the $K_{Ca}2$ family are responsible for the medium afterhyperpolarizing potentials (mAHP) that play a role in the regulation of neuronal excitability.[38] In chronically epileptic rats, $K_{Ca}2.2$ was transcriptionally down-regulated; likewise, in hippocampal slices incubated with the GABA receptor blocker gabazine, $K_{Ca}2.2$ is reduced.[38] $K_{Ca}2.2$ is a substrate of the E3 ligase UBE3A so the decreased protein level is hypothesized to be due to UPS proteolysis.[38] Indeed, the reduction was blocked by MG132, and MG132 also lessened the epileptiform discharges in slices.[38]

Another E3 ligase that regulates components of neurotransmission is SCRAPPER (encoded by *FBXL20*).[39–41] SCRAPPER is enriched in the presynaptic membrane throughout the brain and controls levels of Rab3-interacting molecule 1 (RIM1).[39,41] RIM1 assists in priming synaptic vesicles for release and is necessary for synaptic plasticity.[39,41] Unsurprisingly, then, as a result of upregulated RIM1 in *Scrapper*$^{-/-}$ mice, there is a greater density of synaptic vesicles in the active zone.[39] Brain slices from *Scrapper*$^{-/-}$ mice have reduced paired-pulse facilitation (PPF) and increased mEPSC frequency.[39] Additionally, *Scrapper*$^{-/-}$ mice have elevated glutamate and GABA concentrations throughout the brain.[40] Conversely, lentiviral overexpression of SCRAPPER in rats results in decreased RIM1 and is protective against seizures after

pilocarpine administration.[41] SCRAPPER therefore plays an important role in regulating presynaptic neurotransmission.

## 1.5 ER stress and epilepsy

The epilepsies are a broad group of neurological disorders characterized by repeated unprovoked seizures, and together are one of the most common neurological disorders.[16,42] Approximately 30% of epilepsy patients do not respond to existing anti-epilepsy drugs (AEDs), which primarily target various ion channels.[16,20] Therefore, approaches that leverage other pathways have great potential for currently-intractable seizures. As noted above, excessive excitatory input can alter the UPS, which in turn shifts protein expression.[10] Beyond immediate changes to synapse composition, impaired proteostasis can result in ER stress.[16] ER stress is an adaptive response to oxidative stress, ion balance disruptions, or misfolded proteins.[1,16,18] Genetic epilepsies, too, can directly cause ER stress by the continued presence of misfolded protein.[43,44] Excessive ER stress can result in apoptosis, and indeed neuronal death is observed after seizures.[16,18,45] Managing ER stress, then, may alleviate some pathology associated with epilepsy.

### 1.5.1 Acquired epilepsy

ER stress is seen in multiple animal models of epilepsy as well as human brain tissue. In rats treated with kainic acid (KA) to induce seizures, multiple signs of ER stress were observed.[45] After KA administration, the ER chaperone BiP/Grp78 had enhanced expression, as did the ER stress-mediated proapoptotic factor CHOP.[45] A target of CHOP, TRIB3, became elevated at 24 hr and remained high for days, as did

other downstream apoptotic factors Bax and cleaved caspase 3.[45] Similarly, in mice treated with PTZ to induce seizures, BiP and CHOP were elevated.[20] And, in hippocampal tissue resected from patients undergoing surgery for temporal lobe epilepsy, elevated levels of markers of ER stress were found.[42] Immunoreactivity for the KDEL motif shared by the chaperones BiP and Grp94 was stronger and more prevalent than in control brains, as was immunoreactivity for another ER chaperone, calnexin.[42]

This induction of ER stress is detrimental, as suggested by the electron micrographs of rat hippocampal tissue after KA administration, revealing swollen mitochondria and swollen rough ER, which is indicative of neuronal injury.[45] This was supported by greater TUNEL staining compared to control animals.[45] In the human tissue, various proapoptotic caspases, such as cleaved caspases 6, 7, and 9 were nearly absent in control brains but clearly expressed in epileptic brains.[42]

### 1.5.2 Genetic epilepsy

Genetic epilepsy can be directly linked to ER stress, independent of seizures. A Dravet syndrome-associated mutation, *GABRG2(Q390X)*, results in intracellular accumulation of misfolded protein.[43,44] This triggers ER stress, as shown by heightened expression of the ER-stress-induced pro-apoptotic factor GADD153/CHOP.[43,44] In transfected cells, the induction of GADD153 is correlated with increasing amounts of cDNA, suggesting that the accumulation of this overly-stable misfolded protein has negative consequences.[44] Indeed, neuronal death is seen in *Gabrg2*$^{+/Q390X}$ mice.[43] Elevated cleaved caspase 3, a marker of cell death, is detected in mice as early as 5-6 months, and more prominently at 12 months.[43] Additionally, the cleaved caspase 3 is colocalized with γ2 aggregates.[43] Increased TUNEL staining at 12 months also supports

the idea of neurodegeneration, and, in 14-18 month old *Gabrg2*$^{+/Q390X}$ mice, a decrease in the number of cells positive for NeuN (a neuronal marker) is observed in the somatosensory cortex.[43] Finally, the neurotoxicity is at least partially intrinsic to the direct effects of the misfolded protein, and not only a result of a lifetime of severe seizures, as cultured neurons from P0 pups also display higher amounts of cleaved caspase 3.[43] Furthermore, other *GABRG2* truncation mutations – W429X and W461X – have been shown to mimic the effect of Q390X on ER stress, as expression of these mutant γ2 results in more GADD153 relative to wildtype γ2, and the induction of GADD153 corresponded to the amount of cDNA transfected into the cells.[43,44]

Additional evidence for a connection between genetic epilepsy and ER stress comes from mutations in RNF13.[17] RNF13 is a key activator of the JNK-mediated pathway of ER stress, via activation of the ER stress sensor IRE1α.[17] Three individuals with epilepsy and profound ID were found to harbor missense mutations in RNF13, and a study of patient-derived cells revealed increased ER stress signaling and ER stress-induced apoptosis.[17] Thus, these epilepsy-linked mutations produce a toxic gain-of-function in regard to ER stress.[17]

### 1.6 Acquired epilepsy and the UPS

The UPS is known to be impaired by the protein aggregates of neurodegenerative disorders, as well as by brain ischemia and traumatic brain injury.[1,10,14] Seizure disorders, too, are being shown to have a complex relationship with the UPS, which is not surprising, given how interrelated even normal neurotransmission and the UPS are, as discussed above (Figure 1).

In two mouse models of induced status epilepticus (SE) (kainic acid and pilocarpine administration models), there was an accumulation of polyubiquitinated proteins in the hippocampus.[14] This was accompanied by diminished UPS activity that was intriguingly most prominent in regions most resistant to seizure-induced cell death (DG and CA1).[14] Investigation into individual cell types showed that impaired UPS activity was first seen almost exclusively in neurons, but after 24 hr astrocytes became the affected population, with some contributions from microglia.[14] When mice had reached the chronic epilepsy stage after convulsant administration, there was still an elevation in polyubiquitinated proteins, but proteasome activity was actually increased, and more 20S subunits were present.[14] At this later timepoint, neurons were again the cell type with dampened UPS activity, while astrocytes were not impaired.[14] Another study using a pilocarpine-treated rodent model also found time-dependent changes in the UPS.[15] In this model, ubiquitin was found to be downregulated in the acute (2 hr post pilocarpine administration) and latent (3 weeks post-administration) stages of epileptogenesis, but upregulated in the chronic (8 weeks post-administration) stage.[15]

The E3 ligase Nedd4-2, which regulates ion channels, was also downregulated in both the acute and chronic stages but not in the latent period.[15] Pilocarpine also depresses another E3 ligase, SCRAPPER encoded by *FBXL20*, in mice.[41] Similarly, in hippocampal resection samples from patients with intractable epilepsy, there was decreased expression of SCRAPPER, but interestingly the synaptic protein it regulates, RIM1, was also reduced compared to control patients, underscoring a complex relationship between *FBXL20* and epilepsy.[41] E3 ligase downregulation has also been observed in vitro, after shifts in synaptic activity[12].

In line with the correlation of dampened UPS activity in areas with the least cell death, that study found proteasomal inhibition to be neuroprotective.[14] When cultured hippocampal neurons were exposed to an excitotoxic concentration of KA, proteasomal inhibition with small amounts of epoxomicin or MG132 was neuroprotective, and acute epoxomicin treatment was also shown to prevent neuronal death in two mouse models of epilepsy.[14] However, the other study found the opposite: when rats were pre-treated with MG132 before pilocarpine, they displayed heightened irritability and seizure frequency, and further loss of Nedd4-2.[15] Additionally, neuronal cell loss in the hippocampus was aggravated by MG132 at all stages after SE.[15] The reorganization of mossy fibers of granule cells in the hippocampus appeared earlier and to greater extents in the MG132 pretreated animals, compared to animals that only received pilocarpine.[15]

A complementary study found that inhibition of a DUB exasperated neuronal injury after KA-evoked SE in mice.[46] Downregulation of the neuronally-expressed DUB ubiquitin carboxyl-terminal hydrolase isozyme L1 (UCHL1) was seen 24 hours after SE, in line with findings that NMDA-mediated excitotoxicity downregulates DUBs in vitro.[10,46] Similar to the findings of regional differences above, UCHL1 was most depressed in the vulnerable CA3 region of the hippocampus.[46] Inhibition of UCHL1 with LDN-57444 downregulates monomeric ubiquitin and decreases UPS activity.[46] LDN-57444 treatment of mice prior to KA administration resulted in more neuronal death in the CA3 region of the hippocampus than in animals that did not receive LDN-57444, suggesting a neuroprotective role of UCHL1.[46] The UPS, therefore, seems to have a complex relationship with seizures and neuron death.

## 1.7 Genetic epilepsy and the UPS

Genetic epilepsy has an especially complex relationship with the UPS and proteostasis. In addition to the mechanisms discussed in the prior three sections – whereby elevated synaptic transmission can impact the UPS and therefore profoundly change the expression profile of synaptic proteins, and seizure activity can cause proapoptotic ER stress – the mutated proteins can exert their own effect on the UPS. Many mutations directly dysregulate components of the UPS, such as E3 ligases, while other epilepsy-causing mutations alter the proteostatic network with their rate of degradation (Figure 2).

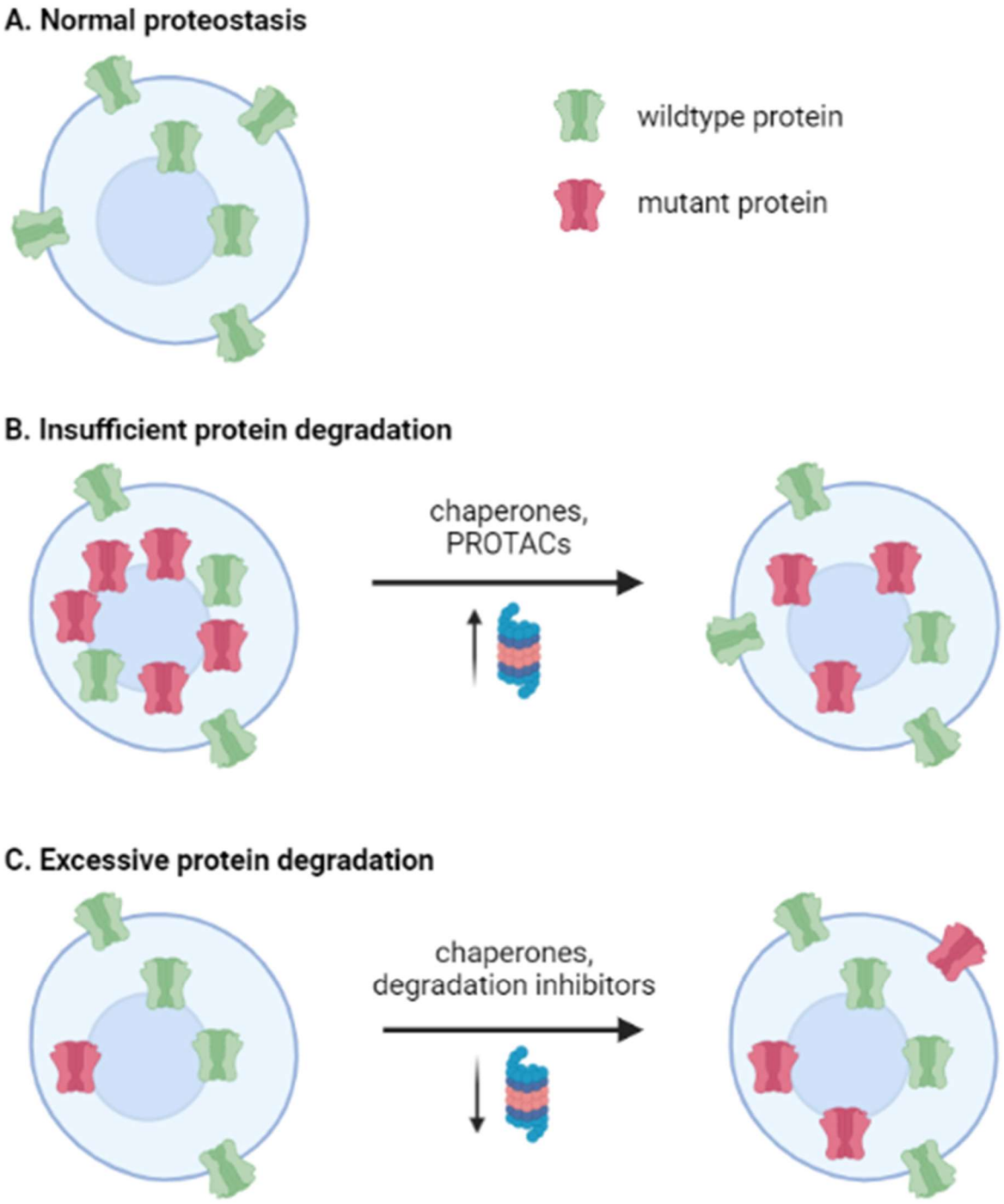


***Figure 1.2. Rescue of dysregulated proteostasis in epilepsy.***
**A.** Under healthy conditions, there is appropriate expression and trafficking of proteins. Here, a membrane channel is shown as an example. **B.** Insufficient protein degradation can occur in epilepsies, due to factors such as aggregation-prone mutants, decreased E3 ubiquitin ligase activity, or loss of deubiquitinase function. Potential rescue mechanisms include chaperones to prevent aggregation of mutant proteins and

PROTACs to enhance degradation of specific substrates. **C.** Excessive protein degradation is also seen in epilepsies, when a mutant protein with only partial loss of function is not permitted to reach its final location in order to exert function. Chaperones may help the protein fold properly, allowing proper trafficking, as would inhibition of the select components involved in the degradation of that protein.

### 1.7.1 Overactive ERAD

Unnecessary degradation of mutant – yet still functional – protein is associated with several diseases, notably cystic fibrosis[1,4] but also several epilepsies connected to genes in the GABAergic pathway, such as *GABRA1*, *GABRG2*, and *SLC6A1* (Table 1). This overactive degradation results in lower levels of functional protein, potentially causing haploinsufficiency phenotypes, and also places a burden on the protein quality control mechanisms.[1]

***Table 1.1. Proteostatic impairments in genetic epilepsies and neurological disorders with comorbid seizures.***

| disease | gene involved | proteostatic impairment | accumulation of misfolded proteins? | reference |
|---|---|---|---|---|
| autosomal dominant juvenile mycolic epilepsy | *GABRA1* | overactive ERAD | no | 2,5,21,47–49,96 |
| febrile seizures | *GABRG2* | overactive ERAD | no | 22 |
| generalized epilepsy with febrile seizures plus (GEFS+) | *GABRG2* | overactive ERAD | no | 50 |
| *SLC6A1*-associated disorders | *SLC6A1* | ER retention | possibly | 51–54 |
| Lafora disease | *EPM2A, EPM2B* | loss of E3 ligase activity | yes | 27,55–59 |
| Angelman syndrome | *UBE3A* | loss of E3 ligase activity | no | 27,60 |
| duplication 15q syndrome (Dup15q) | *UBE3A* | excess E3 ligase | no | 27,60 |
| fragile X syndrome | *FMR1* | decreased ubiquitination | no | 27,69 |
| 15q13.3 microdeletion syndrome | *OTUD7A* | decreased 20S expression | yes | 26,70 |
| *STXBP1* encephalopathy | *STXBP1* | protein aggregation | yes | 72,73 |
| Dravet syndrome | *GABRG2* | protein aggregation | yes | 8,43,44,74,75 |
| familial encephalopathy with neuroserpin inclusion bodies (FENIB) | *SERPINI1* | protein aggregation | yes | 23,76–79 |
| progressive myoclonus epilepsy type 1 (EPM1) | *StB* | protein aggregation | yes | 80 |

#### 1.7.1.1 GABRA1

The A322D mutation of the GABR subunit *GABRA1* causes autosomal dominant juvenile myoclonic epilepsy, and produces a mutant protein with partial loss of function.[47] When expressed in HEK293T cells with the partnering subunits β2 and γ2, peak GABA-evoked currents from α1(A322D)β2γ2 receptors were depressed to 10% of control cells containing wildtype α1.[48] But, expression of α1(A322D) is also dramatically

reduced, by 94% in HEK293T cells and 39% in transfected neurons.[48,49] What little protein remains is almost entirely retained within the ER.[48] Importantly, the misfolded α1(A322D) is still capable of interacting with β2 and γ2 subunits, and therefore traps the partnering subunits in the ER, resulting in a dominant-negative pathology.[49] This mutant subunit is subject to enhanced ERAD, as supported by a 3-fold increase in association with the chaperone calnexin, compared to wildtype α1, and the decreased half-life.[5,21] Knockdown of various factors in the pathway of ERAD of α1 augmented levels of α1(A322D) and increased GABA-evoked current.[2] Thus, the observed diminishment in ion current flow is only partially due to direct effects of the mutation on GABR function; some of the seizure pathology is due to trafficking problems and overactive ERAD.[2]

#### 1.7.1.2 GABRG2

Overactive ERAD has also been documented for another GABR subunit, *GABRG2*. The R177G mutation linked with febrile seizures has impaired trafficking, having reduced surface trafficking and a lower proportion of mature glycosylation.[22] Additionally, intracellular γ2(R177G) was subject to higher rates of ERAD than wildtype.[22] However, the R177G mutant is capable of assembling with α1 and β2 into pentameric receptors that insert into the plasma membrane, and these mutant receptors still have appreciable function (whole cell current density approximately 41% that of wildtype).[22] Therefore, the accelerated ERAD is decreasing the pool of functional receptors and likely contributing to seizures.[22]

Two mutations connected to generalized epilepsy with febrile seizures plus (GEFS+), γ2(R82Q) and γ2(P83S), are also retained with the ER.[50] When mutant subunits successfully traffic beyond the ER, however, they are capable of forming surface receptors, albeit with poor efficiency.[50] This study did not investigate the

degradation rate of these mutants, but the authors speculate the mutant subunits are subject to enhanced ERAD like α1(A322D) and γ2(R177G).[50]

#### 1.7.1.3 GAT1

Another gene in the GABAergic signaling pathway, *SLC6A1*, encoding GABA transporter 1 (GAT1), is associated with ER retention of epilepsy-causing mutations. Several studies from the Kang lab have found that GAT1 mutations manifesting with clinically diverse symptoms have similar cellular phenotypes. Three mutations – G234S linked with Lennox-Gastaut syndrome, P361T associated with epilepsy and autism, and V125M identified in two siblings with epilepsy and ADHD – were found to have decreased total and surface protein expression, as well as diminished GABA uptake.[51–53] All three mutant proteins are partially retained in the ER, and the observed reduction in total protein expression is suggestive of enhanced ERAD.[51–53] Investigation of an additional 20 varied mutations also revealed trafficking problems, as all 20 mutations had lower surface expression, while total protein expression was not always reduced.[54] Further investigation into one mutation, S295L associated with epilepsy and developmental delay, revealed prominent ER retention, which may result in ER stress.[54]

### 1.7.2 E3 ubiquitin ligases

A number of epilepsies and neurological disorders with comorbid seizures are due to genetic abnormalities that affect E3 ligases (Table 1). Because E3 ligases are involved in almost cellular process, E3 ligase dysfunction can result in a range of pathological changes, such as the accumulation of metabolic intermediates, decreased expression of proteasome subunits, and generally disrupted proteostasis of many key neuronal proteins (Figure 2).

#### 1.7.2.1 Lafora disease

Lafora disease (LD) is a fatal, neurodegenerative disease belonging to the group of progressive myoclonic epilepsies.[55–59] It is generally caused by autosomal recessive mutations in *EPM2A* or *EPM2B*, although recently mutations in the related gene *PRMD8* have been implicated in LD.[27,55–57] *EPM2A* encodes the phosphatase laforin, and *EPM2B* (also called *NHLRC1*) encodes malin, an E3 ubiquitin ligase. Lafora disease is characterized by the presence of Lafora bodies – intracellular accumulations of insoluble glycogen-like carbohydrates – in the brain and other tissues.[27,55,57,58] Loss of function of malin or laforin diminishes the ability of the laforin-malin complex to regulate enzymes responsible for glycogen synthesis, resulting in Lafora bodies.[27,55,58]

The exact mechanisms by which laforin or malin mutations result in epilepsy and neurodegeneration are unknown, but hypotheses include altered energy homeostasis and impairments of the UPS.[27,56–58] Due to the dysregulation of the glycogen synthesis machinery, improperly-branched glycogen-like polyglucosans accumulate and these are resistant to hydrolysis by α-amylase into glucose.[27,58] Glycogenolysis is the most important energy source for the brain, so reduced glycogenolysis can interfere with basic processes of neuronal metabolism and result in hyperexcitable neurons.[27,58]

Involvement of proteostasis pathways in LD is supported by the finding that Lafora bodies contain 6-28% protein, in addition to polyglucosans.[57,59] The components of this protein in Lafora bodies include malin, ubiquitin, 20S proteasome subunits, and the Hsc70/Hsp70 chaperones.[57] Mutant malin expression can result in aggregates that recruit Hsp70 and are associated with cell death.[57] The sequestering of Hsp70 may be deleterious, as overexpression of Hsp70 abated malin aggregation and cell death.[57] Mutant malin also caused depressed UPS activity and a concomitant increase in

ubiquitinated proteins.[57] Interestingly, in *Epmb*$^{-/-}$ mice with no malin, elevations in ubiquitinated proteins is also seen, suggesting this phenotype is due to the loss of E3 ligase function and not due to the presence of mutant protein.[59]

#### 1.7.2.2 UBE3A mutations

Deletion or loss-of-function mutations in maternally-imprinted Ubiquitin Protein Ligase E3A (*UBE3A*) result in the neurodevelopment disorder Angelman syndrome, while duplication of the maternal allele of the chromosomal region that spans the UBE3A gene, 15q11.2-q13.1, results in another neurodevelopmental disorder, Duplication 15q syndrome (Dup15q).[27,60] Both Angelman syndrome and Dup15q often have comorbid seizures.[27] UBE3A is an especially interesting E3 ligase as some evidence suggests it ubiquitinates the proteasome itself to regulate proteolytic activity.[60] At the cellular level, UBE3A disruptions are associated with many neuronal abnormalities, such as altered synapse formation and maintenance, dysregulation of ion channels, and disruption of the mTOR pathway.[27,60] The mechanism underlying epilepsy in Dup15q patients is not entirely clear but some evidence points to a target of UBE3A, the Na+/K+ pump ATPα responsible for ion homeostasis.[27] For Angelman syndrome, seizure activity may be due to the loss of UBE3A in GABAergic neurons.[27,60]

#### 1.7.2.3 CUL3-associated mutations

Cullin 3 (CUL3) is a scaffold for the E3 ligase class Cullin-RING ligases (CRL).[61,62] Two patients with intellectual disability and infantile spasms were found to have missense mutations (V285A and R46Lfs*32) in CUL3, and analysis of the V285A mutant revealed a decreased ability to bind to KEAP1 – another component of the CRL complex – suggesting diminished stability of the E3 complex.[61]

Mutations in another CUL3-associated protein, rho-related BTB domain-containing protein 2 (RHOBTB2), have been found in several patients with epileptic encephalopathy.[62,63] RHOBTB2 is both a substrate of CUL3 and an adaptor protein that assists CUL3 in targeting substrates for degradation.[62] The patient mutations showed higher expression of RHOBTB2 in heterologous cells, and overexpressing HA-CUL3 did not lower expression of the mutants like it did the wildtype protein, indicating a CUL3-mediated deficit in degradation.[62,63] Although the details of the relationship between excessive RHOBTB2 and seizures are not known, there may be dendritic abnormalities.[63]

Additionally, a CUL3 substrate, potassium channel tetramerization domain-containing protein 7 (KCTD7), has been implicated in epilepsy.[64] Two siblings with PME and neuronal ceroid lipofuscinosis (NCL) have a homozygous R184C mutation.[64] This mutant protein has impaired trafficking, as decreased membrane staining and pronounced cytoplasmic aggregates were observed in heterologous cells, and has greatly decreased association with CUL3, which likely results in excess KCTD7, although the functional consequences of this are unknown.[64]

#### 1.7.2.4 HECW2 mutations

Multiple reports have identified mutations in the HECT, C2, and WW domain-containing E3 ubiquitin protein ligase 2 gene (*HECW2*) in patients with severe epilepsy, intellectual disability, and hypotonia..[65–68] HECW2, also called NEDD4-like ubiquitin protein ligase-2 (NEDL2), stabilizes p73, a tumor suppressor protein involved in neurodevelopment.[65,66] Although *Hecw2* knockout mice do not display CNS abnormalities, zebrafish with knockdown of the *HECW2* ortholog *hecw2a* had severe morphological abnormalities of the brain and spinal cord, as well as cell death.[66]

Therefore, although detailed mechanisms are unknown, HECW2 is another E3 ligase implicated in epilepsy pathogenesis.

#### 1.7.2.5 Fragile X syndrome

Fragile X syndrome (FXS) is the most common inherited form of intellectual disability and is caused by loss of function of the *FMR1* gene that codes for the fragile X mental retardation protein (FMRP).[69] In addition to autism and ID, some patients have epilepsy, and the *Fmr1* knockout mouse has neuronal hyperexcitability.[27,69] This hyperexcitability seems to be due to multiple factors. A study reported that, following PTX treatment of cultured neurons, *Fmr1*$^{-/-}$ neurons failed to show ubiquitination of the AMPA receptor subunits GluA1 and GluA2 that was seen in wildtype neurons.[69] This lack of homeostatic ubiquitination was mediated by impaired association of the E3 ligase Nedd4-2 with GluA1, as Nedd4-2 was inappropriately dephosphorylated after PTX treatment in the *Fmr1*$^{-/-}$ neurons.[69] Nedd4-2 disruptions were also observed in pilocarpine-treated mice, supporting the role of Nedd4-2 in epilepsy.[15] Other studies in the *Fmr1*$^{-/-}$ mouse have shown an absence of E3 ligase Mdm2-mediated ubiquitination of PSD95, leading to an excess of excitatory synapses.[27]

### 1.7.3 Deubiquitinases

Alterations to the ubiquitination process beyond the substrate recognition and ubiquitination steps mediated by E3 ligases can also result in seizures (Table 1). Deubiquitinases (DUBs) cleave ubiquitin moieties from proteasome substrates so that the ubiquitin can be reused; shifts to DUB activity can therefore alter ubiquitin homeostasis (Figure 2), which has implications for seizures, as seen in the kainic acid mouse model of epilepsy discussed previously.[1,10,24,46]

#### 1.7.3.1 OTUD7A mutations

15q13.3 microdeletion syndrome is characterized by a wide range of neuropsychiatric phenotypes, including epilepsy, developmental delay, and/or autism spectrum disorder.[26,70] The microdeletion spans two genes, *CHRNA7* (encoding the neuronal nicotinic acetylcholine receptor subunit alpha-7) and *OTUD7A* (ovarian tumor deubiquitinase 7A).[26,70] Knockout of *Otud7a*, a DUB, in mice replicates much of the human phenotype and thus is believed to be the causative gene of 15q13.3 microdeletion syndrome.[26]

Further support for the involvement of *OTUD7A* in epilepsy came when a patient with epileptic encephalopathy and severe developmental delay was found to have a homozygous missense mutation in *OTUD7A*, L233F.[26] Fibroblasts from this patient were cultured and the proteasome activity in them was analyzed.[26] The patient-derived fibroblasts had greatly decreased 20S proteasome activity, which was found to be due to lower expression of the proteasome activator protein PA28-α and many 20S subunits.[26] The 19S regulatory subunits, however, were unaffected.[26] Additionally, the patient-derived fibroblasts showed an increase in polyubiquitinated proteins, indicating impairment in UPS function.[26]

In 2021, another patient with epilepsy and developmental delay, as well as severe hypotonia, was reported to have an *OTUD7A* mutation, a homozygous de novo frameshift E375Dfs*11, in addition to a 15q13.3 microdeletion spanning part of *OTUD7A*.[70] To investigate the role of the frameshift mutation, a *Caenorhabditis elegans* model was created with a frameshift corresponding to the human mutation, in the *OTUD7A* homolog *otub-2*.[70] The homozygous *otub-2(ta112)* worms showed impaired

locomotion, supporting the link between the patient's hypotonia and the E375Dfs*11 *OTUD7A* mutation.[70]

#### 1.7.3.2 USP9X mutations

Another deubiquitinase, Ubiquitin Specific Peptidase 9 X-Linked (USP9X), has been connected to genetic epilepsy. A patient with epileptic encephalopathy was found to have a de novo missense mutation (S1012P) at a conserved residue and another patient with infantile spasms was found to have the missense mutation G1890E.[71] Interestingly, however, in *Drosophila*, loss-of-function mutations in the ortholog of *USP9X*, *faf*, were shown to confer resistance to seizures when crossed with the *prickle* model of epilepsy, $pk^{sple}$/+.[71] In the same vein, treatment of homozygous $pk^{sple}$ flies with the USP9X inhibitor Degrasyn/WP1130 was also seizure-protective.[71] The authors postulate that the discrepancy may be due to the *Drosophila* mutant alleles generating no protein product, while the human mutations do produce mutant protein, implicating a possible dominant-negative effect.[71]

## 1.8 Protein misfolding and genetic epilepsies

In addition to the seizure-related disorders with direct connections to the UPS discussed above, a number of other epilepsies have misfolded proteins that are prone to aggregation (Table 1). While alterations to proteasomal function may not yet have been found for all these diseases, given the strong link between neurodegenerative diseases, protein aggregates, and impaired UPS, it is likely that there are some similarities with the following disorders. A failure of proteostasis is, however, clear from the presence of aggregates.

### 1.8.1 STXBP1 encephalopathy

Syntaxin binding protein 1 (STXBP1), or Munc18-1, is part of the machinery involved in the release of synaptic vesicles.[72,73] Mutations in this gene are linked with multiple neurological disorders, primarily developmental and epileptic encephalopathies.[72,73] Interestingly, some patients with STXBP1 encephalopathy later develop juvenile-onset parkinsonism, and changes to STXBP1 levels are seen in Alzheimer's disease, together suggesting a connection between STXBP1 and neurodegenerative diseases with protein aggregates.[72,73] Disease-causing missense mutations were predicted to be less stable than wildtype STXBP1 by in silico structural modeling, and this was corroborated by cycloheximide experiments in vitro.[72,73] Despite the decreased stability and shorter half-life of the mutant STXBP1, the mutants are prone to aggregation, as determined by Triton X-100 solubility and tryptic digestion assays.[73]

Although the aggregates do not appear to be cytotoxic, they do represent a dominant-negative feature of mutant STXBP1: wildtype STXBP1 forms dimers, and the mutant proteins retain the ability to assemble with the wildtype protein.[72,73] Consequently, the aggregate-prone misfolded proteins also trap wildtype STXBP1 in aggregates, leading to lower expression of functional STXBP1 protein in transfected mouse neurons than expected for simple haploinsufficiency.[72] Because the mutant proteins are less stable, the association with wildtype protein also reduces the half-life of the wildtype STXBP1, further lowering the pool of functional protein.[72] Thus, improper folding leads to excessive protein degradation, as part of the pathomechanism for this severe epilepsy.

### 1.8.2 *GABRG2* mutations

Several mutations in *GABRG2* cause epilepsy, including *GABRG2(Q390X)* found in Dravet syndrome. The truncation of the γ2 protein results in a hydrophilic domain in place of the hydrophobic TM4, and this hydrophilic domain fails to stably insert into the membrane.[43] As a result, the mutation turns γ2(Q390X) from a membrane protein into a globular cytosolic protein.[43] Wildtype γ2 is already the GABR subunit most prone to self-dimerization due to proportionally high hydrophobicity, and the remaining exposed hydrophobic domains of γ2(Q390X) make this mutant especially prone to aggregation, due to interactions between the hydrophobic domains.[43,74] γ2(Q390X) is retained in the ER as stable dimers and larger oligomers, and has a dominant-negative effect on wildtype γ2, α1, and β2, trapping these other subunits in the ER as well and reducing their surface expression.[8,44,75] The misfolded mutant is extensively ubiquitinated, more so than wildtype, although total levels of all polyubiquitinated proteins are identical.[44] As previously discussed in the section on ER stress above, the γ2(Q390X) oligomers cause extensive ER stress and eventual neurodegeneration.[43,44]

Although the clinical phenotype of Dravet syndrome connected to *GABRG2(Q390X)* is amongst the most severe epilepsies, other disease-associated mutations in GABR subunits share some of the molecular pathomechanisms. Several other truncation mutations in γ2 have been studied, and many form dimers and multimers, although not to the extent of γ2(Q390X). For instance, while γ2(R136X) is not prone to aggregation, W429X, which is linked to febrile seizures and generalized tonic-clonic seizures, does display moderate dimerization tendencies.[44,74] Yet even without protein aggregation, R136X, W429X, and W461X have trafficking aberrations and are retained within the

ER.[6,44] Non-truncating mutations such as R82Q also show this deficit.[7] All of these mutations share with γ2(Q390X) the toxic ability to trap partnering α1 and β2 subunits within the ER, lowering surface expression and decreasing the relative amounts of mature, fully-glycosylated protein.[6,44]

### 1.8.3 Familial encephalopathy with neuroserpin inclusion bodies (FENIB)

Familial encephalopathy with neuroserpin inclusion bodies (FENIB) is a neurodegenerative disorder with a range of symptom severity.[23,76–78] At its most severe, patients develop severe epilepsy as a child.[76] FENIB is caused by mutations in neuroserpin, a primarily CNS-expressed serine protease inhibitor that is involved in synaptic plasticity.[23,76–79] The mutated proteins misfold and form neuroserpin inclusion bodies in the ER, and the most severe clinical phenotypes are associated with the mutants that polymerize most rapidly.[23,76,78] In part due to the correlation between clinical severity and presence of inclusion bodies, these inclusion bodies are believed to be part of the disease pathomechanism.[23] The mutant neuroserpin is targeted by ERAD for UPS-mediated degradation, but as the UPS becomes less efficient with age, the mutant protein can accumulate.[23,76,79] The E3 ligases implicated in mutant neuroserpin degradation are HRD1 – which also interacts with other epilepsy-causing proteins[3] – and gp78.[23,76] When a transgenic FENIB mouse model was crossed with a model genetic impairment of the UPS, twice as many neuroserpin inclusions were observed as in the control FENIB mouse, demonstrating the connection between the UPS and this protein-folding disease with seizures.[79]

### 1.8.4 Progressive myoclonus epilepsy type 1

Progressive myoclonus epilepsy type 1 (EPM1), also known as Unverricht-Lundborg disease, is a neurodegenerative disease caused by mutations in Stefin B (StB).[80,81] StB, or cystatin B (CSTB), is a cysteine protease inhibitor.[80,81] While the majority of EPM1 cases have a repeat expansion in the promoter region of StB that results in decreased transcription and consequentially lower protein levels, loss-of-function point mutations have also been found.[80,81] Two of these mutations, G4R and R68X, were investigated and found to form perinuclear aggregates that were associated with reduced cell viability in transfected cells.[80] The mutant aggregates costained both with autophagy proteins and 20S and 26S proteasomes, indicating failure of the UPS to maintain proteostasis.[80] Interestingly, loss of function of StB (in a knockout mouse without mutant protein) results in the formation of aggregates of other proteins, and these aggregates contained almost no proteasome subunits and very few chaperones.[81] Therefore, lack of StB is associated with an impairment of the UPS.[81]

### 1.8.5 *KCNQ2* epileptic encephalopathy

*KCNQ2* encodes the $K_V7.2$ subunit of the neuronal $K_V7$ potassium channel, which is responsible for the M-current that suppresses neuronal excitability.[31] Mutations in the $K_V7$ channel cause epilepsies of varying severity.[31] The $K_V7.2$(M518V) mutation, identified in a patient with early-onset epileptic encephalopathy, was found to have poorer trafficking to the axon initial segment (AIS) and greater ubiquitination compared to wildtype $K_V7.2$ protein.[31] Treatment with MG132 blocked the enhanced degradation of $K_V7.2$(M518V) and resulted in aggregation of the mutant protein, demonstrating the involvement of the UPS in this disease.[31] Interestingly, coexpression with the partnering

subunit $K_V7.3$ also stabilized the mutant $K_V7.2$ and enhanced aggregation.[31] The intracellular accumulation of $K_V7.2$(M518V) caused cell shrinkage and nuclei condensation – features of apoptosis – in HEK293T cells.[31] In transfected neurons, $K_V7.2$(M518V) also increased cell death.[31] These in vitro findings perhaps explain the MRI findings in a patient with the mutation, where there were small frontal lobes, a thin corpus callosum, and large ventricles, indicative of neuronal loss.[31] A lack of sufficient proteasome-mediated degradation of this mutant protein, then, may result in neurodegeneration as well as severe epilepsy.

### 1.8.6 Other misfolded proteins associated with epilepsy

*GRIN1*-related neurodevelopmental disorder is characterized predominantly by ID, epilepsy, and other neurological symptoms like hypotonia.[82,83] Missense mutations may have dominant-negative effects on NMDAR receptor assembly, as heterozygous null mutations such as deletions or truncations of *GRIN1* do not generally cause clinical phenotypes.[82,83] Instead, heterozygous missense mutations might suppress the pool of functional receptors by assembling with wildtype subunits in the ER and trapping them there.[83]

*SPTAN1* encodes non-erythrocyte αII spectrin, and several patients with epileptic encephalopathies have been reported with *SPTAN1* mutations.[84] Spectrins form the cytoskeletal structure of the plasma membrane and are thus normally distributed evenly across a cell.[84] Imaging of fibroblasts from the patients showed instead aggregates of varying intensities, although aggregates were not observed in all patients.[84] Interestingly, however, despite the obvious presence of protein aggregates, the patient-

derived fibroblasts did not seem to be more vulnerable to apoptosis, but neurons may have increased susceptibility.[84]

## 1.9 Therapeutic implications

### 1.9.1 Anti-epilepsy drugs that impact UPS

A few existing, common AEDs have been found to have secondary effects on proteostasis and the UPS, in addition to their manipulation of neurotransmission (Table 2). Zonisamide is an AED that is used in low doses as an add-on therapy for Parkinson's disease.[85,86] Zonisamide helps to treat PD by upregulating SEL1L, which in turn stabilizes the E3 ligase HRD1, boosting the levels of HRD1.[18,85,86] This enhancement of HRD1 is protective against cell death from ER stress-inducing compounds tunicamycin or 6-OHDA.[86] Additionally, in type 2 diabetic mice, many ER stress-related proteins are elevated, and zonisamide treatment returned expression of most of the investigated proteins to control levels.[18] The cognitive impairment of the mice was rescued, potentially due to lessened ER stress-induced neurotoxicity.[18] HRD1 is expressed in neurons in many regions of the brain and is involved in the degradation of the mutant neuroserpin responsible for FENIB and with *GABRA1*.[2,3,23,76]

The AED valproic acid (VPA) is one of the most commonly used AEDs, and has a complex mechanism of action.[20] In regards to proteostasis, VPA upregulates the transcription of the ER stress proteins BiP, Grp94, and calreticulin 26, and this yields greater protein expression.[87] VPA also prevented increases in BiP and CHOP in mice after injection with the convulsant PTZ, as well as preventing apoptosis as measured by TUNEL staining and cleaved caspase 3 expression.[20] VPA is also useful for abating ER

stress in Wolfram syndrome, a multisystemic disease with several neurological components, caused by mutations of an ER membrane protein.[88]

Carbamazepine (CBZ) is an AED and mood stabilizer that also has been shown to affect protein degradation. CBZ has been shown in vitro to reduce both mutant huntingtin and mutant α-synuclein, via autophagy enhancement.[89] The liver disease α1-antitrypsin deficiency (ATD) is a serinopathy like the neurodegenerative disease FENIB discussed in the previous section and is likewise characterized by a deleterious accumulation of proteins in the ER – in this case, mutant α1-antitrypsin Z (ATZ).[77,90] CBZ effectively enhances autophagy to reduce ATZ aggregates and hepatic fibrosis.[90] In addition to autophagy, CBZ modulates proteasomal protein degradation: A study on the breast cancer protein Her-2 found that CBZ increases acetylation of Hsp90, which then lessens the ability of Hsp90 to interact with Her-2.[91] This resulted in a decrease in Her-2 protein that was blocked by MG132 treatment, showing that CBZ can promote protein degradation through multiple mechanisms.[91]

### 1.9.2 Chaperones and chaperone upregulators

To relieve the burden on the UPS and restore proteostasis, chaperones that aid in protein folding may be of use in seizure-associated diseases like those discussed above (Table 2, Figure 2). Molecular chaperones are endogenous proteins such as the various heat shock proteins that aid in protein folding, and can be induced by some small molecules, such as BIX (discussed below).[1] Chemical or osmolyte chaperones provide a more favorable environment for protein folding by altering the chemical environment of the ER, thereby stabilizing folded states and/or reducing aggregation tendencies.[1,73] Pharmacological chaperones like PBA, meanwhile, directly interact with the misfolding-

prone protein instead of altering the general folding environment.[1,73,92] This may lower the free energy state of the protein to help it fold, or it may cover exposed hydrophobic regions of a misfolded protein to prevent aggregation.[1,73]

***Table 1.2. Drugs with effects on proteostasis with potential use for epilepsies.***

| drug | mechanism | reference |
|---|---|---|
| *antiepileptic drugs* | | |
| zonisamide | upregulates E3 ligase HRD1 | 85,86 |
| valproic acid | upregulates ER chaperones | 20,87,88 |
| carbamezepine | enhances proteasomal and lysosomal degradation | 89–91 |
| | | |
| *chaperones* | | |
| 4-phenylbutyrate (PBA) | hydrophobic chaperone, HDAC inhibitor | 19,59,73,85,88,94 |
| Ambroxol | pharmacological chaperone | 92 |
| suberanilohydroxamic acid (SAHA) | upregulates BiP | 95–97 |
| BiP inducer X (BIX) | upregulates BiP | 4,98 |
| Dinoprost (DNP) | suppression of HRD1 and SEL1L, facilitated substrate association with BiP and calnexin | 3 |
| Dihydroergocristine (DHEC) | suppression of HRD1 and SEL1L, facilitated substrate association with BiP and calnexin | 3 |
| | | |
| *degradation inhibitors* | | |
| Eer1 | VCP inhibitor | 97 |
| 17AAG | Hsp90 inhibitor | 100 |
| HSP990 | Hsp90 inhibitor | 101 |
| | | |
| *degradation enhancers* | | |
| PROTACs | promote interactions between E3 ligases and substrates | 24,30,102 |

#### 1.9.2.1 4-phenylbutyrate (PBA)

4-phenylbutyrate (PBA) is sold as the FDA-approved drug Buphenyl for the treatment of urea cycle disorders, but has shown promise for a variety of neurological disorders with misfolded proteins.[19] PBA has several mechanisms of action. It is a hydrophobic pharmacological chaperone, preventing aggregation of misfolded proteins by interacting with exposed hydrophobic regions.[73] PBA is also an inhibitor of histone deacetylases (HDAC), and perhaps via this effect, PBA upregulates the molecular chaperones BiP, Hsp70, and Hsp90.[1,59]

For aggregation-prone STXBP1 mutants, PBA not only increased the total levels of STXBP1 – including wildtype – but it also decreased the fraction of detergent-insoluble protein, indicating that less of it was in aggregates and thus even more was functional.[73] Importantly, no negative effect was observed from overexpression of wildtype STXBP1, indicating that concerns from boosting the mutant protein, in non-aggregated forms, should be minimal.[73] Aggregates were also decreased in worms expressing the various mutants, and localization of the protein within the ventral nerve cord was restored.[73] Furthermore, PBA rescued locomotion deficits in mutant worms.[73]

PBA improved motor and neurobehavioral phenotypes in the Lafora disease model *Epm2b*$^{-/-}$ mice.[59] This was due to a reduction of polyglucosan inclusions and polyubiquitinated protein aggregates in the brain, which prevented neuronal loss and dampened reactive gliosis.[59] For ATP1A3 mutants associated with a range of neurological impairments from hypotonia to severe infantile epilepsy, PBA promoted expression of the mutant protein in vitro by stabilizing them and promoting proper trafficking through the Golgi apparatus.[19] PBA also ameliorated trafficking defects for an ER-retained LGI1 mutant associated with autosomal dominant lateral temporal lobe epilepsy, LGI1(E383A).[93] When the protein was able to be secreted, it was able to correctly bind to its receptor, and thus PBA ameliorated the epilepsy phenotype in mouse models.[93] Creatine transporter deficiency syndrome has several neurological symptoms including epilepsy and developmental delay, and is caused by mutations in the creatine transporter 1 (hCRT-1).[94] These mutations result in a misfolded protein that is retained in the ER, and PBA treatment restored trafficking to the plasma membrane and creatine uptake functionality of several mutants.[94] In a non-epileptic neurological

disorder, PBA also decreases ER stress resulting from dominant-negative mutations of Wolfram syndrome-causing WSF1.[88] Additionally, PBA improves behavioral phenotypes in Parkinson's disease and Alzheimer's disease mouse models, and aids folding of the protein Pael-R implicated in autosomal recessive juvenile parkinsonism.[85]

#### 1.9.2.2 Ambroxol

Ambroxol is a common mucolytic agent that crosses the blood-brain barrier and also acts as a pharmacological chaperone for acid β-glucosidase (GCase), the causative enzyme in Gaucher disease.[92] Gaucher is a lysosomal storage disorder that can have neurological presentations including intractable epilepsy.[92] Ambroxol can bind to mutant GCase at neutral pH, such as what is found in the ER, to promote proper folding, but it dissociates at low pH.[92] Because GCase localizes to the acidic lysosome, that means ambroxol does not interfere with function.[92] Ambroxol treatment has improved the symptoms of patients both with neuropathic and non-neuropathic GD.[92] Of note, efficacy of ambroxol for a given individual can potentially be screened using cultured fibroblasts from that patient.[92] For a patient whose fibroblasts showed no benefit from ambroxol, ambroxol treatment was initiated regardless, due to the severity of his symptoms, but his symptoms did not improve.[92] Intriguingly, another patient who shared the same mutation (L444P) as the previous, ambroxol-resistant patient, did show improvement in fibroblasts.[92] This suggests that there are other factors at play, and underscores the usefulness of in vitro screening before initiating therapy in patients.[92]

#### 1.9.2.3 Suberanilohydroxamic acid (SAHA)

Suberanilohydroxamic acid (SAHA), also called Vorinostat, is an FDA-approved drug used for the treatment of cutaneous T-cell lymphoma.[95] Additionally, it has been extensively studied *in vitro* for GABR mutations linked to epilepsy, as it acts through BiP

to stabilize misfolded proteins via upregulation of BiP transcription.[95–97] In HEK293T cells expressing α1(A322D)β2γ2 $GABA_A$ receptors, SAHA application substantially upregulated α1, increasing protein levels 5-fold, and the half-life of a1(A322D) was tripled from 40 min to 125 min.[96] Partnering β2 and γ2 subunits were also upregulated.[96] Additionally, SAHA enhanced the trafficking efficiency of the α1(A322D) subunit, preventing degradation and thereby augmenting the amount of fully mature α1(A322D).[96] Further, the GABA-evoked currents were increased, showing that SAHA treatment resulted in functional α1(A322D)β2γ2 $GABA_A$ receptors on the cell surface.[96]

SAHA also rescues γ2 mutations that have reduced surface expression due to ER retention, such as N79S, R82Q, P83S, and R177G.[95] GABAergic currents for these mutations were partially or completely restored to wildtype currents, in regards to both amplitude and kinetics.[95] Interestingly, γ2(K328M), which does not have trafficking defects and only accelerates deactivation of the receptor, was not affected by SAHA treatment, further supporting the idea that SAHA functions as a chaperone for ER-retention-prone mutants.[95] SAHA therefore can directly ameliorate haploinsufficiency mechanisms by boosting functional receptors, and prevent overburdening of the UPS by directing salvageable proteins away from ERAD. It is a promising option, due to being already FDA approved, non-cytotoxic, and able to cross the blood-brain barrier.[95,96]

#### 1.9.2.4 Molecular chaperone Bip inducer X (BIX)

BiP inducer X (BIX), or 1-(3,4-dihydroxy-phenyl)-2-thiocyanate-ethanone, induces expression of the molecular chaperone BiP and prevents neuronal death from ER stress.[4] Cells exposed to the ER stress inducer thapsigargin did not show an increase in cleaved caspase 3 when also treated with BIX, and BIX halved the activity of caspases 3 and 7.[98] BIX is also neuroprotective in vivo, increasing BiP and protecting mice from

neuronal apoptosis after cerebral ischemia.[98] Additionally, the epilepsy-causing α1(A322D) GABR subunit displayed elevated surface expression after BIX treatment.[4] This was via enhanced trafficking efficiency of the mutant subunit, as indicated by an increase in the mature, endo H-resistant glycoform.[4] GABA-induced current was also increased, showing that BIX stabilization of the α1(A322D) subunit results in a greater number of functional receptors.[4]

#### 1.9.2.5 DNP and DNEC

Dinoprost (DNP) is a synthetic analogue of prostaglandin $F_{2\alpha}$ that crosses the blood-brain barrier.[3] Dihydroergocristine (DHEC) is used to treat high blood pressure and dementia.[3] Both compounds were identified in a screening of a library of FDA-approved drugs as promoting total α1 subunit in HEK293T cells, and were subsequently tested on two epilepsy-associated mutations, α1(A322D) and α1(D219N).[3] DNP and DHEC elevated surface expression of both mutants by 2-3 fold, compared to untreated cells, and this corresponded to greater peak GABA-induced currents.[3] The higher expression was due to decreased ERAD of the misfolded subunits, via suppressed transcription and expression of HRD1 and SEL1L.[3] Additionally, the drugs enhanced the interaction of α1(A322D) with BiP and calnexin, resulting in a greater proportion of folded α1, which is then able to assemble with β2.[3] Two epilepsy-associated γ2 mutants were also tested, R82Q and R177G, and DNP and DHEC likewise enhanced the incorporation of those subunits into functional $GABA_A$ receptors.[3] Of note, DNP and DHEC worked additively with SAHA, implying different but complementary mechanisms.[3] Finally, the drugs were demonstrated to be useful for neuronopathic Gaucher disease as well.[3] The most common mutation identified in Gaucher disease, GCase(L444P), is subject to

excessive ERAD, and both DNP and DHEC increased the amount of functional GCase protein in patient-derived fibroblasts.[3]

#### 1.9.2.6 Other chaperones

Multiple other chemical chaperones have shown promise for neurological disorders with epilepsy. A class of oxysterol derivatives were demonstrated to act as pharmacological chaperones for NPC1, the protein causing Niemann-Pick type C1, a lysosomal storage disorder with many neurological manifestations including seizures.[99] The oxysterol derivatives enhance folding and function of mutant NPC1, attenuating the accumulation of cholesterol in fibroblasts derived from a patient.[99] Another group of drugs – the azole anti-fungals itraconazole, posaconazole, and ketoconazole – have also been shown to chaperone NPC1.[99] These compounds boost the expression of NPC1 by decreasing the rate of degradation.[99] Other osmolytic chaperones include sorbitol, used in STXBP1 models,[73] and trehalose under investigation for both Lafora disease and STXBP1.[59,73]

### 1.9.3 Protein degradation inhibitors

#### 1.9.3.1 Eer1

Valosin-containing protein (VCP) is part of the retrotranslocation machinery that transports polyubiquitinated proteins from the ER to the cytosol for degradation via the UPS.[3,97] Eer1 is an inhibitor of VCP, and application of Eer1 prevented the excessive ERAD linked to the GABR mutation α1(A322D) without impacting partnering subunits β2 or γ2.[97] Eer1 did so by facilitating proper trafficking of α1(A322D), which led to an increase in the mature, post-ER glycoform, heightened surface expression, and increased GABA-induced peak current.[97] In line with suppression of the over-aggressive

ERAD, less ubiquitination of α1(A322D) was seen after Eer1 treatment and the mutant had a longer half-life.[97] However, because the protein degradation pathways are interconnected, suppression of ERAD may boost autophagy.[1] Interestingly, the chaperone SAHA worked additively, further stabilizing and elevating functional α1(A322D) levels.[97]

#### 1.9.3.2 Hsp90 inhibitors

The heat shock chaperone Hsp90β recruits the glutamate transporter GLT-1 (also referred to as EAAT2) to the 20S proteasome.[100] In tissue from humans with temporal lobe epilepsy, Hsp90β is upregulated in astrocytes, a change also seen in rodent models of epilepsy.[100] This increase may be pathological, as Hsp90β inhibition by 17AAG elevated GLT-1 levels and glutamate uptake in astrocytes, and pretreatment of mice with 17AAG reduced the number of seizures following injection of the convulsant kainic acid.[100] Importantly, in mice that had already developed chronic seizures, 17AAG also lessened the number of seizures and increased the percentage of seizure-free days.[100] Additionally, in the *Tsc1*$^{GFAP}$CKO model of tuberous sclerosis complex, 17AAG decreased seizure frequency, although drug administration began weeks before normal seizure onset.[100] HSP990 is another potent inhibitor of Hsp90 proteins, with greater blood-brain barrier permeability and less toxicity than 17AAG.[101] Similarly to 17AAG, HSP990 also upregulates GLT-1 in astrocytes, and greater latency to seizures when given to mice prior to the convulsant PTZ.[101] Spontaneous seizures were also reduced by HSP990 in the kainic acid models of temporal lobe epilepsy in both mice and cynomolgus monkeys.[101]

### 1.9.4 Other manipulations of UPS

#### 1.9.4.1 PROTACs

A technology recently receiving a lot of attention is proteolysis targeting chimerics (PROTACs). PROTACs enhance the endogenous interactions between E3 ligases and their substrates by utilizing a heterobifunctional molecule that consists of an E3 ligase ligand and a ligand to bind the substrate.[24,30,102] The ubiquitination of substrates by E3 ligases is the rate-limiting step of ubiquitination.[27] By facilitating this interaction, the E3 ligase can then more efficiently ubiquitinate the target protein, so it can then be degraded by the UPS.[30,102] PROTACs are exciting because they can hopefully be used to target so-called undruggable proteins – proteins that do not have a clear function to modulate with small molecules – by boosting degradation of the protein. PROTACs are already being utilized in clinical trials, for cancer and autoimmune disorders, and ones for neurological disorders are being developed.[102]

Several PROTACs targeting tau have been discovered, including TH006, which reduced tau levels in vitro, and in a mouse model of Alzheimer's disease, lessened the neurotoxicity of Aβ.[30] The first few discovered used a small peptide sequence as the ligands, but small-molecule PROTACs were discovered in 2019 that degraded tau in human neurons.[30] For Huntington's disease, there are also small-molecule PROTACs that reduced the amount of huntingtin in patient-derived fibroblasts.[30] These drugs were also effective for degrading other polyglutamine-expansion proteins, such as ataxin 3 and 7, responsible for spinocerebellar ataxia types 3 and 7.[30] Parkinson's disease-associated A53T α-synuclein is degraded in vitro by multiple small molecule PROTACs.[30] These promising studies are likely only the beginning – so far only around 10 E3 ligases have been used, out of the 600 in the human body, [102] so it is hopeful that

many more PROTACs will likely emerge as more E3 ligases are investigated, such as the many E3 ligases addressed in this review.

## 1.10 Conclusion

The interrelationship between neuronal transmission, epilepsy, protein quality control, and the ubiquitin proteasome system is complex and multidirectional. For example, excitatory synaptic activity – such as after NMDA receptor activation – can result in complex changes to proteasome localization and activity and to ubiquitination patterns, thereby modifying the entire profile of proteins found in postsynaptic densities.[10,12,13,25,32] Loss of function of several E3 ubiquitin ligases, meanwhile, impacts multiple glutamate receptors, which results in enhancements to epileptic activity and excitotoxicity.[34–37] Elimination of an E3 ligase also causes changes to the pool of synaptic vesicles, as does inhibition of the UPS.[33,39] Neuronal excitability can also be regulated by the UPS via degradation of ion channels such as $K_{Ca}2.2$.[38]

Unsurprisingly, given the effects even normal neuronal activity has on the UPS, status epilepticus can cause dramatic changes to the UPS, including downregulation of UPS activity and deubiquitinase expression that vary in magnitude across brain regions and cell types.[14,46] The UPS plays a complex role in the neuronal death that is often observed after SE, as decreased UPS activity is found in the most resilient neurons yet pharmacological UPS inhibition results in increased neuronal loss after SE.[14,15]

Like the UPS, ER stress is also interlinked with neuronal loss and epilepsy. Epilepsy can cause impairments to the protein folding machinery in the ER, resulting in ER stress that can progress to apoptosis. Multiple animal models have demonstrated that seizures

can cause elevations in ER stress-related factors such as BiP and CHOP, and human epileptic brain tissue also shows increases in both ER chaperones and proapoptotic caspases.[20,42,45] ER stress can also arrive independently from seizure activity and instead be the result of misfolded and mistrafficked proteins, as seen in genetic epilepsies such as Dravet syndrome.[43,44] ER stress can even be causative of epilepsy, as mutations in a component of the ER stress pathway result in epilepsy.[17] Regardless of the cause of ER stress, however, it is still associated with neuronal death.[17,43]

Epileptic disorders can be due to misfolded proteins that are degraded too quickly, or to misfolded proteins that accumulate in aggregates. Accelerated degradation of misfolded proteins that still maintain at least partial function is seen in *GABRA1*, *GABRG2*, and *SLC6A1* mutations.[5,22,47–54]. Dampening this overactive ERAD allows the protein to traffic beyond the ER, where it had been retained, and become a functional membrane receptor.[2,3,97] It is likely that the elevated ERAD demonstrated for some of these mutations may be accompanied by ER stress.

Dysregulated degradation can also arise from mutations that alter the function of E3 ligases or their partnering proteins, or even via alterations to a substrate protein that impairs the ability of its associated E3 ligase to degrade it, as is the case for the CUL3 substrates, RHOBTB2 and KCTD7.[62–64] Both too little and too much E3 ligase activity can result in seizures, as seen in the UBE3A-implicated genetic disorders Dup15q and Angelman syndrome.[27,60] Conversely, shifts in synaptic signaling can modulate levels of E3 ligases, underscoring the interconnectedness of neurotransmission and proteostasis.[12] Mutations to DUBs, too, can disrupt the UPS and result in epilepsy.[26,70,71]

Further connections between epilepsies and compromised proteostasis can be found in the variety of genetic epilepsies that have intracellular protein aggregates. Proteins like STXBP1 and Stefin B are prone to aggregation even in wildtype forms, and epilepsy-associated mutations exacerbate aggregation.[72,73,80] Unsurprisingly, given the well-studied relationship of protein aggregates with neurodegenerative disorders such as Alzheimer's disease and Parkinson's disease, some of these aggregate-forming epilepsy mutants also result in neuronal death, such as γ2(Q390X) and $K_V$7.2(M518V).[31,43,44]

In terms of treatment, then, multiple modulations of proteostasis show promise for these many epilepsies. For proteins with partial function that are subject to accelerated ERAD, selectively inhibiting their associated components of the degradation pathway may be beneficial, such as VCP inhibition via Eer1 for α1(A322D).[97] Conversely, when there is insufficient degradation, as is the case for fragile X syndrome or FENIB, the interaction between substrate proteins and the appropriate E3 ligase can be boosted by PROTACs.[23,30,69,76,79,102] Existing antiepileptic drugs with effects on the UPS, like valproic acid, can potentially be leveraged for conditions with elevated ER stress. Various chemical chaperones like PBA and inducers of molecular chaperones like BIX show great promise for almost any genetic epilepsy. Chaperones aid protein folding, and thus can potentially both prevent mutated proteins like STXBP1 from aggregating and stabilize functional mutants like GAT-1 that are prone to rapid degradation. In addition, because many membrane proteins – including neurotransmitter receptors – are inefficiently folded, chaperones may be able to elevate the wildtype protein in cases

of haploinsufficiency. Additionally, chaperones can reduce ER stress, such as what has been documented after SE, and thereby help prevent neuronal death.

### 1.10.1 Further applications

Impaired proteostasis is a common feature in many other diseases, both neurological and not. Neurodegenerative disorders including amyotrophic lateral sclerosis, Huntington's disease, Alzheimer's disease, Parkinson's disease, and spinocerebellar ataxias are known to involve accumulation of misfolded proteins and impairments of the UPS.[30,72] Decreased proteasome activity is also seen in Down syndrome, as well as overactivation of the unfolded protein response.[103] The neurohypophyseal form of diabetes insipidus is caused by mutations in vasopressin that result in ER retention and coaggregation with wildtype protein, and eventual cell death.[104] A similar pathology is seen in the liver disease α1-antitrypsin deficiency.[90] Other disorders involving altered proteostasis include cystic fibrosis, type 2 long QT syndrome, and retinitis pigmentosa.[4] Thus, study of aberrant protein trafficking, ER stress, and proteasomal activity has great promise to bring treatments to a number of seizure disorders and many other pathologies.

## 1.11 Acknowledgements

I thank JQK, JB, CB, and ES for assistance editing the manuscript.
Figures were created with BioRender.com.

## 1.12 Summary of previous findings on the *GABRG2(Q390X)* mutation

### 1.12.1 The *GABRG2(Q390X)* mutation results in a truncated, hydrophobic protein

A truncation mutation of *GABRG2* was identified in a patient with Dravet syndrome in 2002.[105] This truncation, Q390X, is the result of a c.1168C>T mutation that creates a premature stop codon (PTC), removing 78 amino acids from the C-terminus of the γ2 protein.[8,43,105] Q390 is located between transmembrane domains 3 and 4, in the cytoplasmic loop, so the PTC removes the fourth transmembrane α-helix.[43,105] In place of the hydrophobic TM4, structural modeling suggests a new α-helix is formed in the γ2(Q390X) subunit, with many charged amino acids, and this hydrophilic domain fails to stably insert into the membrane.[43] Thus, the mutation turns the γ2(Q390X) subunit from a membrane protein into a globular cytosolic protein.[43] The wildtype γ2 subunit is already the GABR subunit most prone to self-dimerization due to proportionally high hydrophobicity, and the remaining exposed hydrophobic domains of γ2(Q390X) protein make this mutant especially prone to aggregation, due to interactions between the hydrophobic domains.[43,74]

Despite the PTC, *GABRG2(Q390X)* is not subject to nonsense-mediated mRNA decay (NMD). NMD only recognizes PTCs ~50-55 nucleotides upstream of an exon-exon junction, so because *GABRG2(Q390X)* is in the last exon, the mRNA is translated.[8,44] This was demonstrated *in vitro* through the use of a minigene that contained the first eight exons of *GABRG2*, intron 8, and exon 9. When HEK293T cells were transfected with the mutant Q390X version of this minigene, mRNA of the same nucleotide length as properly-spliced wildtype mRNA was detected, and at similar

levels.[8] Additionally, abundant protein is detected by an anti-γ2 antibody at the predicted band size of ~40 kDa.[43]

### 1.12.2 ER retention of the γ2(Q390X) subunit

In fact, the γ2(Q390X) subunit shows increased protein expression compared to the wildtype γ2 subunit. Additionally, high molecular weight bands are detected, indicating dimers and larger oligomers. However, this mutant protein does not reach the cell surface – surface biotinylation of transfected HEK293T cells showed that, compared to wildtype α1β2γ2 (1:1:1) GABR, mixed α1β2γ2/γ2(Q390X) GABR had only 43% as much surface γ2 protein, and mutant α1β2γ2(Q390X) had virtually no detectable protein.[8] This is in contrast to the hemizygous condition (1:1:0.5 α1β2γ2 GABR) that had 68% of the wildtype γ2 surface expression, which indicates that the γ2(Q390X) protein has a dominant-negative effect.[8]

Confocal microscopy in transfected COS-7 cells revealed that, compared to the widely-distributed wildtype γ2 subunit, mixed α1β2γ2/γ2(Q390X) and mutant α1β2γ2(Q390X) conditions result in ER retention of γ2 protein.[8,75] Further experiments with pHluorin – which fluoresces only at the cell surface – supported the indication of impaired protein trafficking. Using a pHfluorin-tagged γ2L subunit coexpressed with α1 and β2 subunits in cultured neurons, plentiful fluorescent signal was seen with wildtype $\gamma2L^{pHfluorin}$ while almost none was detected for $\gamma2L(Q390X)^{pHfluorin}$.[8] In contrast to the γ2S subunit splicing isoform, which has some ability to traffic to the surface without a full α1β2γ2 receptor, the γ2L subunit isoform can only insert into the cell membrane when assembled with other subunits; thus, the fluorescent puncta seen in the wildtype

condition reflect functional receptors, and the lack of puncta in the mutant condition suggests the γ2(Q390X) subunit could not traffic properly.[8]

Furthermore, differential digestion with glycosidases showed that the γ2(Q390X) protein does not traffic beyond the ER. The glycosidase Endo H removes only immature glycans post-translationally added to proteins in the ER, while PNGase F cleaves all glycans, including mature glycans processed in the Golgi apparatus.[8] The wildtype γ2 subunit presents as a wide, smeared band on immunoblots, and digestion with Endo-H results in two bands – a lower band for the immature unglycosylated protein and an Endo-H resistant band representing mature protein that has reached the Golgi.[8] PNGase F digestion results in only the lower band.[8] The relative intensity of the Endo-H resistant band, compared to the total intensity, reveals the proportion of fully mature protein. When γ2(Q390X) protein is digested, the Endo-H and PNGase F conditions appear identical, with no Endo-H resistant upper band present, indicating that the γ2(Q390X) subunit does not reach the Golgi for glycan processing.[8] In mixed conditions with both wildtype and mutant protein, the relative proportion of the Endo-H insensitive band for wildtype γ2 protein is decreased compared to the α1β2γ2 condition, suggesting that the presence of the γ2(Q390X) subunit is causing ER retention of the γ2 subunit.[8] This is consistent with the findings from surface biotinylation.

In addition to ER retention of the wildtype γ2 subunit, γ2(Q390X) protein also associates with α1 and β2 subunits and traps those subunits in the ER as well.[8,44] This is revealed through biotinylation showing decreased surface expression and through glycosidase digestion showing decreased mature protein.[8,44]

### 1.12.3 The γ2(Q390X) subunit forms stable aggregates

This ER-retained mutant forms stable dimers and larger oligomers. Although the rate of synthesis is the same for wildtype and mutant γ2 subunits, the half-life of the γ2(Q390X) subunit is more than twice as long as the γ2 subunit (4 hours vs ~100 minutes).[75] While both wildtype and mutant γ2 subunits form dimers cotranslationally in the ER, the γ2(Q390X) subunit forms them to a much greater extent, as intense bands at seen at 80 and 160 kDa on immunoblots.[75] Additionally, the self-oligomerization tendency of wildtype γ2 protein is greatly attenuated by the presence of binding partners α1 and β2 subunits in adequate levels.[75] The aggregation of the γ2(Q390X) subunit seems to be at least partially driven by a disulfide bond between C151 and C165, as mutation of both or either cysteine to alanine resulted in dramatically fewer oligomers, as well as monomeric protein.[75]

The greater stability of the γ2(Q390X) subunit seen *in vitro* is recapitulated *in vivo*, in the *Gabrg2*$^{+/Q390X}$ mouse. Immunohistochemistry reveals accumulation of γ2 protein in the cortex of young adult mice (2-4 months) and old mice (16 months), as well as neonatal P0 mice.[43] At 6 months, the *Gabrg2*$^{+/Q390X}$ mice have increased γ2 protein staining in the somata region of neurons compared to wildtype littermates, but less in synaptosomes or at the cell surface, further supporting the previous findings of impaired trafficking.[43]

### 1.12.4 The γ2(Q390X) subunit results in decreased GABAergic current

The dominant-negative effect of the γ2(Q390X) subunit on the trafficking of wildtype γ2 subunits is also reflected in the function of GABR. In α1β2γ2/γ2(Q390X) transfected HEK293T cells, GABA-evoked peak currents are only 35% of the wildtype α1β2γ2

condition, in contrast to 61% for the hemizygous 1:1:0.5 α1β2γ2 condition, so the presence of the γ2(Q390X) protein reduced the current by another 43% compared to what a haploinsufficient loss-of-function mutation may do.[8] The mutant condition with α1β2γ2(Q390X) resulted in very small currents.[8] Similar results were found in transfected neurons in which the endogenous γ2 was knocked out with siRNA.[8] In addition, the amplitude and frequency of mIPSCs were reduced in these neurons in the mixed mutant condition.[8] This finding was replicated in cortical layer VI neurons of *Gabrg2*$^{+/Q390X}$ mice, while *Gabrg2*$^{+/-}$ knockout mice had no difference compared to wildtype littermates.[43]

### 1.12.5 Proteasomal and lysosomal degradation of the γ2(Q390X) subunit

Like other GABR subunits,[2,8,97] the γ2 subunit is degraded by the UPS. γ2(Q390X) degradation is also mediated via the UPS, as treatment with the proteasome inhibitor lactacystin slows its degradation.[75] Interestingly, however, in contrast to the wildtype γ2 subunit, the rate of degradation of which is unaffected by lysosomal inhibition with chloroquine, the γ2(Q390X) subunit is a substrate of lysosomal degradation as chloroquine treatment resulted in slower degradation.[75] The misfolded mutant is extensively ubiquitinated, more so than wildtype, although total levels of polyubiquitination are identical.[44] Elevated ubiquitination could have dramatic effects on cellular fitness, as ubiquitin has many vital roles beyond protein degradation, including DNA repair and transcription, cell differentiation, and synaptic plasticity.[44] Therefore, if the γ2(Q390X) subunit is monopolizing the cell's ubiquitin pool, these other crucial processes may not be as efficient. Moreover, the γ2(Q390X) subunit associates with the ER chaperones BiP/GRP78 and calnexin approximately 4-fold as much as the γ2

subunit does, further supporting the hypothesis that the γ2(Q390X) mutant protein sequesters the cell's proteostatic resources.[106]

The tendency of the γ2(Q390X) subunit to oligomerize with other subunits results in alterations to their degradation patterns as well – when coexpressed with γ2(Q390X) subunits, the α1 subunit is more sensitive to lactacystin than when coexpressed with γ2 subunits, as the rate of degradation is depressed more.[8] This explains how the γ2(Q390X) protein reduces the expression of α1 and β2 subunits, by enhancing the proteasomal degradation of these subunits.[8]

### 1.12.6 Neurobehavioral characterization of *Gabrg2*$^{+/Q390X}$ mice

A mouse line was generated bearing the γ2(Q390X) mutation, *Gabrg2*$^{+/Q390X}$, and it mimics the phenotype of Dravet syndrome. These mice have spontaneous generalized tonic-clonic seizures (GTCSs) and EEG recordings reveal 4-7 Hz spike-wave discharges (SWDs), myoclonic jerks, and intense activity corresponding to GTCSs.[43,107] Additionally, the mice are more susceptible to seizure induction via the GABR antagonist pentylenetetrazol (PTZ) or elevated temperature, and have more severe seizures in response to these stimuli.[107] Interestingly, *Gabrg2*$^{+/Q390X}$ mice in the DBA/2J background had less severe susceptibility than heterozygous mice in the C57BL/6J background, speaking to the polygenetic nature of epilepsy, even in those with strongly epilepsy-causative mutations such as *GABRG2(Q390X)*.[107] Adult *Gabrg2*$^{+/Q390X}$ mice were found to have poorer temperature regulation compared to wildtype littermates, as during the seizure induction protocol, their core body temperature rose faster than that of the control mice.[107] Adolescent mice, however, had no genotype differences.[107] Another age-dependent phenotype that emerged is that, in response to heat exposure,

adult mice displayed increased jumping behavior, which is thought to be a correlate of anxiety, but adolescent mice did not.[107] Anxiety is also demonstrated during the elevated zero maze and open field test.[43] The severe seizure phenotype is a reflection of the dominant-negative function of the γ2(Q390X) subunit as heterozygous knockout *Gabrg2*$^{+/-}$ mice have been reported to have no seizures or only mild absence seizures, but anxiety is likely the result of haploinsufficiency as both *Gabrg2*$^{+/Q390X}$ and *Gabrg2*$^{+/-}$ display anxiety-related behaviors.[43] Another observation in line with Dravet syndrome is that *Gabrg2*$^{+/Q390X}$ mice have a higher mortality rate than their wildtype littermates at all times across their lifespan, which may reflect SUDEP.[43] In addition, in a mixed background strain, heterozygous and homozygous mutants are born at reduced Mendelian ratios, and any homozygous mice that are born die on the day of birth.[43]

### 1.12.7 Neurodegeneration, ER stress, and inflammation

Another vital component of the pathophysiology of the *GABRG2(Q390X)* mutation – and one of great interest – is the association of the mutant γ2(Q390X) subunit with neurodegeneration. The mutant protein triggers ER stress, as shown by increased expression of the ER-stress-induced pro-apoptotic factor GADD153/CHOP.[43,44,106] In transfected cells, the induction of GADD153 is correlated with increasing amounts of cDNA, suggesting that the accumulation of this stable misfolded protein has negative consequences.[44] Indeed, neuronal death is seen in *Gabrg2*$^{+/Q390X}$ mice.[43] Elevated cleaved caspase 3, a marker of cell death, is detected in mice as early as 5-6 months, and more prominently at 12 months.[43] Additionally, the cleaved caspase 3 is colocalized with γ2 aggregates.[43] Increased TUNEL staining at 12 months also supports the idea of neurodegeneration, and, in 14-18 month old *Gabrg2*$^{+/Q390X}$ mice, a decrease in the

number of cells positive for NeuN (a neuronal marker) is observed in the somatosensory cortex.[43] Finally, the neurotoxicity is at least partially intrinsic to the direct effects of the misfolded protein, and not only a result of a lifetime of severe seizures, as cultured neurons from P0 pups also display increased amounts of cleaved caspase 3.[43]

In addition to ER stress, the γ2(Q390X) protein causes neuroinflammation. In *Gabrg2*$^{+/Q390X}$ mice, the cytokines tumor necrosis factor (TNF), interleukin-1 β (IL-1β), and interleukin-6 (IL-6) are elevated in all brain regions examined, as early as two weeks of age and prior to seizure onset.[106] Fascinatingly, pro-inflammatory conditions did not result in further expression of cytokines in these animals, while wildtype animals had a robust increase in cytokine expression.[106] In contrast, *Gabrg2*$^{+/-}$ mice – which have a much milder seizure phenotype and no mutant protein – had normal cytokine levels at baseline and showed a similar response to inflammatory conditions as wildtype mice.[106] Furthermore, neurons cultured from *Gabrg2*$^{+/Q390X}$ mice fail to increase TNF in response to the ER stress inducer tunicamycin, while neurons from wildtype and *Gabrg2*$^{+/-}$ mice both upregulated TNF.[106] These findings suggest that the γ2(Q390X) protein dampens the ability of cells to respond to stressors and results in a ceiling effect on these physiological processes.

### 1.12.8 Rescue via overexpression of the γ2 subunit

Much of the molecular, circuitry, and seizure phenotypes were greatly restored in *Gabrg2*$^{+/Q390X}$ mice by overexpressing wildtype γ2 protein. This was accomplished by crossing them with a transgenic line that expresses human HA-tagged *GABRG2* under control of the endogenous *hGABRG2* promoter, Tg(*hGABRG2*$^{HA}$).[108] In adult mice 2-4 months old, expression of functional γ2 subunits (combination of endogenous wildtype

mouse γ2 and introduced human $\gamma2^{HA}$) was restored to control levels of wildtype littermates.[108] In addition to γ2, α1 and β2 subunits were partially rescued.[108] The result of increased GABR subunits was that mIPSC amplitude was restored in cortical layer VI pyramidal neurons, although mIPSC frequency was not.[108] Furthermore, the oscillations of the thalamocortical network returned to normal.[108] The overexpression of *hGABRG2* also resulted in a reduction of PTZ-induced seizure threshold to that of control animals and the mortality rate from the induced seizures was also identical to control.[108] These findings are promising, as they suggest that γ2 and γ2(Q390X) subunits may compete with each other for dimerization and for assembling with α1 and β2 subunits, so increasing the amount of wildtype γ2 subunit results in the mutant being outcompeted and thus an attenuation of the dominant-negative effect.[108]

## 1.13 Dissertation goals

I have described in detail how proteostasis can be impaired, in both genetic and acquired epilepsies. I then summarized prior findings on the *GABRG2(Q390X)* mutation, including how the γ2(Q390X) subunit results in impaired trafficking and excessive degradation of wildtype GABR subunits; forms stable intracellular aggregates; and causes neuronal death. However, the ways in which the *GABRG2(Q390X)* mutation alters proteostasis have not yet been elucidated. Furthermore, therapeutics to treat *GABRG2(Q390X)* Dravet syndrome are currently lacking. This brings me to the primary goals of my dissertation projects:

1. **Characterize the proteostasis network in models of *GABRG2(Q390X)* Dravet syndrome, including the UPS and macroautophagy**
2. **Rescue total and surface expression of wildtype GABR subunits**
3. **Facilitate degradation of γ2(Q390X)**

The roles of the UPS and autophagy in genetic epilepsies have so far been poorly studied, and my work aims to further the understanding of proteostasis in *GABRG2(Q390X)* Dravet syndrome and other epileptic encephalopathies. A better understanding of the pathophysiology of genetic epilepsies will hopefully inspire treatments that not only suppress seizures but are truly disease-modifying.

The second and third aims are interconnected, as I hypothesize that decreasing expression of the γ2(Q390X) subunit should also result in partial rescue of wildtype subunit trafficking, as this should alleviate the dominant-negative retention of those

subunits within the ER. However, chemical and molecular chaperones may rescue wildtype subunit surface trafficking independently of any effects on the γ2(Q390X) subunit. Additionally, chaperones may facilitate degradation of the γ2(Q390X) subunit by making the protein more accessible to the degradation machinery and inhibiting the formation of aggregates. Regardless of whether chemical chaperones affect the γ2(Q390X) subunit, stabilizing the wildtype subunits should still promote surface trafficking. Increasing the wildtype subunits should result in these subunits out-competing the γ2(Q390X) and thus partially attenuating the dominant-negative suppression. This effect has been shown to occur in a γ2(Q390X) model, via overexpression of a transgene *in vivo*,[108] and is also supported by analogous findings in other genetic diseases with dominant-negative mutations.[109–112] My goal is to achieve this rescue by a more clinically applicable method.

Finally, I aim to mitigate the deleterious effects of the γ2(Q390X) protein by decreasing its expression. To that end, I leverage the endogenous ERAD machinery, first by overexpressing ERAD components *in vitro*, and then by administering a proteostasis-regulating small molecule *in vivo*.

## 1.14 References


1. Guerriero CJ, Brodsky JL. The Delicate Balance Between Secreted Protein Folding and Endoplasmic Reticulum-Associated Degradation in Human Physiology. *Physiol Rev*. 2012;92(2):537-576. doi:10.1152/physrev.00027.2011

2. Di XJ, Wang YJ, Han DY, et al. Grp94 Protein Delivers γ-Aminobutyric Acid Type A (GABAA) Receptors to Hrd1 Protein-mediated Endoplasmic Reticulum-associated Degradation. *J Biol Chem*. 2016;291(18):9526-9539. doi:10.1074/jbc.M115.705004

3. Di XJ, Wang YJ, Cotter E, et al. Proteostasis Regulators Restore Function of Epilepsy-Associated GABAA Receptors. *Cell Chem Biol*. 2021;28(1):46-59.e7. doi:10.1016/j.chembiol.2020.08.012

4. Fu YL, Han DY, Wang YJ, Di XJ, Yu HB, Mu TW. Remodeling the endoplasmic reticulum proteostasis network restores proteostasis of pathogenic GABAA receptors. *PloS One*. 2018;13(11):e0207948. doi:10.1371/journal.pone.0207948

5. Gallagher MJ, Ding L, Maheshwari A, Macdonald RL. The GABAA receptor α1 subunit epilepsy mutation A322D inhibits transmembrane helix formation and causes proteasomal degradation. *Proc Natl Acad Sci*. 2007;104(32):12999-13004. doi:10.1073/pnas.0700163104

6. Johnston AJ, Kang JQ, Shen W, et al. A Novel GABRG2 Mutation, p.R136*, in a family with GEFS+ and extended phenotypes. *Neurobiol Dis*. 2014;64:131-141. doi:10.1016/j.nbd.2013.12.013

7. Kang JQ, Kang J, Macdonald RL. The GABAA receptor gamma2 subunit R43Q mutation linked to childhood absence epilepsy and febrile seizures causes retention of alpha1beta2gamma2S receptors in the endoplasmic reticulum. *J Neurosci Off J Soc Neurosci*. 2004;24(40):8672-8677. doi:10.1523/JNEUROSCI.2717-04.2004

8. Kang JQ, Shen W, Macdonald RL. The GABRG2 mutation, Q351X, associated with generalized epilepsy with febrile seizures plus, has both loss of function and dominant-negative suppression. *J Neurosci Off J Soc Neurosci*. 2009;29(9):2845-2856. doi:10.1523/JNEUROSCI.4772-08.2009

9. Rousseau A, Bertolotti A. Regulation of proteasome assembly and activity in health and disease. *Nat Rev Mol Cell Biol*. 2018;19(11):697-712. doi:10.1038/s41580-018-0040-z

10. Caldeira MV, Curcio M, Leal G, et al. Excitotoxic stimulation downregulates the ubiquitin-proteasome system through activation of NMDA receptors in cultured hippocampal neurons. *Biochim Biophys Acta*. 2013;1832(1):263-274. doi:10.1016/j.bbadis.2012.10.009

11. Pohl C, Dikic I. Cellular quality control by the ubiquitin-proteasome system and autophagy. doi:10.1126/science.aax3769

12. Tai HC, Besche H, Goldberg AL, Schuman EM. Characterization of the Brain 26S Proteasome and its Interacting Proteins. *Front Mol Neurosci*. 2010;3:12. doi:10.3389/fnmol.2010.00012

13. Ehlers MD. Activity level controls postsynaptic composition and signaling via the ubiquitin-proteasome system. *Nat Neurosci*. 2003;6(3):231-242. doi:10.1038/nn1013

14. Engel T, Martinez-Villarreal J, Henke C, et al. Spatiotemporal progression of ubiquitin-proteasome system inhibition after status epilepticus suggests protective adaptation against hippocampal injury. *Mol Neurodegener*. 2017;12(1):21. doi:10.1186/s13024-017-0163-2

15. Wu L, Peng J, Kong H, et al. The role of ubiquitin/Nedd4-2 in the pathogenesis of mesial temporal lobe epilepsy. *Physiol Behav*. 2015;143:104-112. doi:10.1016/j.physbeh.2015.02.026

16. Fu J, Tao T, Li Z, Chen Y, Li J, Peng L. The roles of ER stress in epilepsy: Molecular mechanisms and therapeutic implications. *Biomed Pharmacother Biomedecine Pharmacother*. 2020;131:110658. doi:10.1016/j.biopha.2020.110658

17. Edvardson S, Nicolae CM, Noh GJ, et al. Heterozygous RNF13 Gain-of-Function Variants Are Associated with Congenital Microcephaly, Epileptic Encephalopathy, Blindness, and Failure to Thrive. *Am J Hum Genet*. 2019;104(1):179-185. doi:10.1016/j.ajhg.2018.11.018

18. He YX, Shen QY, Tian JH, et al. Zonisamide Ameliorates Cognitive Impairment by Inhibiting ER Stress in a Mouse Model of Type 2 Diabetes Mellitus. *Front Aging Neurosci*. 2020;12:192. doi:10.3389/fnagi.2020.00192

19. Arystarkhova E, Ozelius LJ, Brashear A, Sweadner KJ. Misfolding, altered membrane distributions, and the unfolded protein response contribute to pathogenicity differences in Na,K-ATPase ATP1A3 mutations. *J Biol Chem*. 2021;296:100019. doi:10.1074/jbc.RA120.015271

20. Fu J, Peng L, Wang W, et al. Sodium Valproate Reduces Neuronal Apoptosis in Acute Pentylenetetrzole-Induced Seizures via Inhibiting ER Stress. *Neurochem Res*. 2019;44(11):2517-2526. doi:10.1007/s11064-019-02870-w

21. Bradley CA, Taghibiglou C, Collingridge GL, Wang YT. Mechanisms involved in the reduction of GABAA receptor alpha1-subunit expression caused by the epilepsy mutation A322D in the trafficking-competent receptor. *J Biol Chem*. 2008;283(32):22043-22050. doi:10.1074/jbc.M801708200

22. Todd E, Gurba KN, Botzolakis EJ, Stanic AK, Macdonald RL. GABAA receptor biogenesis is impaired by the γ2 subunit febrile seizure-associated mutation, GABRG2(R177G). *Neurobiol Dis*. 2014;69:215-224. doi:10.1016/j.nbd.2014.05.013

23. Ying Z, Wang H, Fan H, Wang G. The endoplasmic reticulum (ER)-associated degradation system regulates aggregation and degradation of mutant neuroserpin. *J Biol Chem*. 2011;286(23):20835-20844. doi:10.1074/jbc.M110.200808

24. Schrader EK, Harstad KG, Matouschek A. Targeting proteins for degradation. *Nat Chem Biol*. 2009;5(11):815-822. doi:10.1038/nchembio.250

25. Djakovic SN, Schwarz LA, Barylko B, DeMartino GN, Patrick GN. Regulation of the proteasome by neuronal activity and calcium/calmodulin-dependent protein kinase II. *J Biol Chem*. 2009;284(39):26655-26665. doi:10.1074/jbc.M109.021956

26. Garret P, Ebstein F, Delplancq G, et al. Report of the first patient with a homozygous OTUD7A variant responsible for epileptic encephalopathy and related proteasome dysfunction. *Clin Genet*. 2020;97(4):567-575. doi:10.1111/cge.13709

27. Zhu J, Tsai NP. Ubiquitination and E3 Ubiquitin Ligases in Rare Neurological Diseases with Comorbid Epilepsy. *Neuroscience*. 2020;428:90-99. doi:10.1016/j.neuroscience.2019.12.030

28. Fassio A, Falace A, Esposito A, Aprile D, Guerrini R, Benfenati F. Emerging Role of the Autophagy/Lysosomal Degradative Pathway in Neurodevelopmental Disorders With Epilepsy. *Front Cell Neurosci*. 2020;14:39. doi:10.3389/fncel.2020.00039

29. Nowakowska M, Gualtieri F, von Rüden EL, et al. Profiling the Expression of Endoplasmic Reticulum Stress Associated Heat Shock Proteins in Animal Epilepsy Models. *Neuroscience*. 2020;429:156-172. doi:10.1016/j.neuroscience.2019.12.015

30. Hyun S, Shin D. Chemical-Mediated Targeted Protein Degradation in Neurodegenerative Diseases. *Life Basel Switz*. 2021;11(7):607. doi:10.3390/life11070607

31. Kim EC, Zhang J, Pang W, et al. Reduced axonal surface expression and phosphoinositide sensitivity in Kv7 channels disrupts their function to inhibit neuronal excitability in Kcnq2 epileptic encephalopathy. *Neurobiol Dis*. 2018;118:76-93. doi:10.1016/j.nbd.2018.07.004

32. Bingol B, Schuman EM. Activity-dependent dynamics and sequestration of proteasomes in dendritic spines. *Nature*. 2006;441(7097):1144-1148. doi:10.1038/nature04769

33. Willeumier K, Pulst SM, Schweizer FE. Proteasome inhibition triggers activity-dependent increase in the size of the recycling vesicle pool in cultured hippocampal neurons. *J Neurosci Off J Soc Neurosci*. 2006;26(44):11333-11341. doi:10.1523/JNEUROSCI.1684-06.2006

34. Atkin G, Moore S, Lu Y, et al. Loss of F-box Only Protein 2 (Fbxo2) Disrupts Levels and Localization of Select NMDA Receptor Subunits, and Promotes Aberrant Synaptic Connectivity. *J Neurosci*. 2015;35(15):6165-6178. doi:10.1523/JNEUROSCI.3013-14.2015

35. Gautam V, Trinidad JC, Rimerman RA, Costa BM, Burlingame AL, Monaghan DT. Nedd4 is a specific E3 ubiquitin ligase for the NMDA receptor subunit GluN2D. *Neuropharmacology*. 2013;74:96-107. doi:10.1016/j.neuropharm.2013.04.035

36. Lee S, Park S, Lee H, et al. Nedd4 E3 ligase and beta-arrestins regulate ubiquitination, trafficking, and stability of the mGlu7 receptor. Goda Y, Aldrich R, Sans N, eds. *eLife*. 2019;8:e44502. doi:10.7554/eLife.44502

37. Maraschi A, Ciammola A, Folci A, et al. Parkin regulates kainate receptors by interacting with the GluK2 subunit. *Nat Commun*. 2014;5:5182. doi:10.1038/ncomms6182

38. Müller S, Guli X, Hey J, et al. Acute epileptiform activity induced by gabazine involves proteasomal rather than lysosomal degradation of KCa2.2 channels. *Neurobiol Dis*. 2018;112:79-84. doi:10.1016/j.nbd.2018.01.005

39. Yao I, Takagi H, Ageta H, et al. SCRAPPER-dependent ubiquitination of active zone protein RIM1 regulates synaptic vesicle release. *Cell*. 2007;130(5):943-957. doi:10.1016/j.cell.2007.06.052

40. Eto F, Sato S, Setou M, Yao I. Region-specific effects of Scrapper on the abundance of glutamate and gamma-aminobutyric acid in the mouse brain. *Sci Rep*. 2020;10(1):7435. doi:10.1038/s41598-020-64277-w

41. Fu P, Wen Y, Xiong Y, et al. Abnormal Expression of FBXL20 in Refractory Epilepsy Patients and a Pilocarpine-Induced Rat Model. *Neurochem Res*. 2016;41(11):3020-3031. doi:10.1007/s11064-016-2021-y

42. Yamamoto A, Murphy N, Schindler CK, et al. Endoplasmic reticulum stress and apoptosis signaling in human temporal lobe epilepsy. *J Neuropathol Exp Neurol*. 2006;65(3):217-225. doi:10.1097/01.jnen.0000202886.22082.2a

43. Kang JQ, Shen W, Zhou C, Xu D, Macdonald RL. The human epilepsy mutation GABRG2(Q390X) causes chronic subunit accumulation and neurodegeneration. *Nat Neurosci*. 2015;18(7):988-996. doi:10.1038/nn.4024

44. Kang JQ, Shen W, Macdonald RL. Trafficking-deficient mutant GABRG2 subunit amount may modify epilepsy phenotype. *Ann Neurol*. 2013;74(4):547-559. doi:10.1002/ana.23947

45. Zhang J, Han Y, Zhao Y, et al. Role of endoplasmic reticulum stress-associated gene TRIB3 in rats following kainic acid-induced seizures. *Int J Clin Exp Pathol*. 2019;12(2):599-605.

46. Reynolds JP, Jimenez-Mateos EM, Cao L, et al. Proteomic Analysis After Status Epilepticus Identifies UCHL1 as Protective Against Hippocampal Injury. *Neurochem Res*. 2017;42(7):2033-2054. doi:10.1007/s11064-017-2260-6

47. Gallagher MJ, Song L, Arain F, Macdonald RL. The juvenile myoclonic epilepsy GABA(A) receptor alpha1 subunit mutation A322D produces asymmetrical, subunit position-dependent reduction of heterozygous receptor currents and alpha1 subunit protein expression. *J Neurosci Off J Soc Neurosci*. 2004;24(24):5570-5578. doi:10.1523/JNEUROSCI.1301-04.2004

48. Gallagher MJ, Shen W, Song L, Macdonald RL. Endoplasmic reticulum retention and associated degradation of a GABAA receptor epilepsy mutation that inserts an aspartate in the M3 transmembrane segment of the alpha1 subunit. *J Biol Chem*. 2005;280(45):37995-38004. doi:10.1074/jbc.M508305200

49. Ding L, Feng HJ, Macdonald RL, Botzolakis EJ, Hu N, Gallagher MJ. GABAA receptor alpha1 subunit mutation A322D associated with autosomal dominant juvenile myoclonic epilepsy reduces the expression and alters the composition of wild type GABAA receptors. *J Biol Chem*. 2010;285(34):26390-26405. doi:10.1074/jbc.M110.142299

50. Huang X, Hernandez CC, Hu N, Macdonald RL. Three epilepsy-associated GABRG2 missense mutations at the γ+/β- interface disrupt GABAA receptor assembly and trafficking by similar mechanisms but to different extents. *Neurobiol Dis*. 2014;68:167-179. doi:10.1016/j.nbd.2014.04.015

51. Poliquin S, Hughes I, Shen W, et al. Genetic mosaicism, intrafamilial phenotypic heterogeneity, and molecular defects of a novel missense SLC6A1 mutation associated with epilepsy and ADHD. *Exp Neurol*. 2021;342:113723. doi:10.1016/j.expneurol.2021.113723

52. Cai K, Wang J, Eissman J, et al. A missense mutation in SLC6A1 associated with Lennox-Gastaut syndrome impairs GABA transporter 1 protein trafficking and function. *Exp Neurol*. 2019;320:112973. doi:10.1016/j.expneurol.2019.112973

53. Wang J, Poliquin S, Mermer F, et al. Endoplasmic reticulum retention and degradation of a mutation in SLC6A1 associated with epilepsy and autism. *Mol Brain*. 2020;13(1):76. doi:10.1186/s13041-020-00612-6

54. Mermer F, Poliquin S, Rigsby K, et al. Common molecular mechanisms of SLC6A1 variant-mediated neurodevelopmental disorders in astrocytes and neurons. *Brain J Neurol*. 2021;144(8):2499-2512. doi:10.1093/brain/awab207

55. Ibrahim F, Murr N. Lafora Disease. In: *StatPearls*. StatPearls Publishing; 2022. Accessed January 12, 2022. http://www.ncbi.nlm.nih.gov/books/NBK482229/

56. Garyali P, Siwach P, Singh PK, et al. The malin-laforin complex suppresses the cellular toxicity of misfolded proteins by promoting their degradation through the ubiquitin-proteasome system. *Hum Mol Genet*. 2009;18(4):688-700. doi:10.1093/hmg/ddn398

57. Rao SNR, Maity R, Sharma J, et al. Sequestration of chaperones and proteasome into Lafora bodies and proteasomal dysfunction induced by Lafora disease-associated mutations of malin. *Hum Mol Genet*. 2010;19(23):4726-4734. doi:10.1093/hmg/ddq407

58. García-Gimeno MA, Knecht E, Sanz P. Lafora Disease: A Ubiquitination-Related Pathology. *Cells*. 2018;7(8):E87. doi:10.3390/cells7080087

59. Berthier A, Payá M, García-Cabrero AM, et al. Pharmacological Interventions to Ameliorate Neuropathological Symptoms in a Mouse Model of Lafora Disease. *Mol Neurobiol*. 2016;53(2):1296-1309. doi:10.1007/s12035-015-9091-8

60. Lopez SJ, Segal DJ, LaSalle JM. UBE3A: An E3 Ubiquitin Ligase With Genome-Wide Impact in Neurodevelopmental Disease. *Front Mol Neurosci*. 2018;11:476. doi:10.3389/fnmol.2018.00476

61. Nakashima M, Kato M, Matsukura M, et al. De novo variants in CUL3 are associated with global developmental delays with or without infantile spasms. *J Hum Genet*. 2020;65(9):727-734. doi:10.1038/s10038-020-0758-2

62. Belal H, Nakashima M, Matsumoto H, et al. De novo variants in RHOBTB2, an atypical Rho GTPase gene, cause epileptic encephalopathy. *Hum Mutat*. 2018;39(8):1070-1075. doi:10.1002/humu.23550

63. Straub J, Konrad EDH, Grüner J, et al. Missense Variants in RHOBTB2 Cause a Developmental and Epileptic Encephalopathy in Humans, and Altered Levels Cause Neurological Defects in Drosophila. *Am J Hum Genet*. 2018;102(1):44-57. doi:10.1016/j.ajhg.2017.11.008

64. Staropoli JF, Karaa A, Lim ET, et al. A homozygous mutation in KCTD7 links neuronal ceroid lipofuscinosis to the ubiquitin-proteasome system. *Am J Hum Genet*. 2012;91(1):202-208. doi:10.1016/j.ajhg.2012.05.023

65. Heide EC, Puk O, Biskup S, et al. A novel likely pathogenic heterozygous HECW2 missense variant in a family with variable expressivity of neurodevelopmental delay, hypotonia, and epileptiform EEG patterns. *Am J Med Genet A*. 2021;185(12):3838-3843. doi:10.1002/ajmg.a.62427

66. Lu Q, Zhang MN, Shi XY, et al. Association of HECW2 variants with developmental and epileptic encephalopathy and knockdown of zebrafish hecw2a. *Am J Med Genet A*. 2021;185(2):377-383. doi:10.1002/ajmg.a.61958

67. Halvardson J, Zhao JJ, Zaghlool A, et al. Mutations in HECW2 are associated with intellectual disability and epilepsy. *J Med Genet*. 2016;53(10):697-704. doi:10.1136/jmedgenet-2016-103814

68. Yanagishita T, Hirade T, Shimojima Yamamoto K, et al. HECW2-related disorder in four Japanese patients. *Am J Med Genet A*. 2021;185(10):2895-2902. doi:10.1002/ajmg.a.62363

69. Lee KY, Jewett KA, Chung HJ, Tsai NP. Loss of fragile X protein FMRP impairs homeostatic synaptic downscaling through tumor suppressor p53 and ubiquitin E3 ligase Nedd4-2. *Hum Mol Genet*. 2018;27(16):2805-2816. doi:10.1093/hmg/ddy189

70. Suzuki H, Inaba M, Yamada M, et al. Biallelic loss of OTUD7A causes severe muscular hypotonia, intellectual disability, and seizures. *Am J Med Genet A*. 2021;185(4):1182-1186. doi:10.1002/ajmg.a.62054

71. Paemka L, Mahajan VB, Ehaideb SN, et al. Seizures are regulated by ubiquitin-specific peptidase 9 X-linked (USP9X), a de-ubiquitinase. *PLoS Genet*. 2015;11(3):e1005022. doi:10.1371/journal.pgen.1005022

72. Lanoue V, Chai YJ, Brouillet JZ, et al. STXBP1 encephalopathy: Connecting neurodevelopmental disorders with α-synucleinopathies? *Neurology*. 2019;93(3):114-123. doi:10.1212/WNL.0000000000007786

73. Guiberson NGL, Pineda A, Abramov D, et al. Mechanism-based rescue of Munc18-1 dysfunction in varied encephalopathies by chemical chaperones. *Nat Commun*. 2018;9(1):3986. doi:10.1038/s41467-018-06507-4

74. Wang J, Shen D, Xia G, et al. Differential protein structural disturbances and suppression of assembly partners produced by nonsense GABRG2 epilepsy mutations: implications for disease phenotypic heterogeneity. *Sci Rep*. 2016;6:srep35294. doi:10.1038/srep35294

75. Kang JQ, Shen W, Lee M, Gallagher MJ, Macdonald RL. Slow degradation and aggregation in vitro of mutant GABAA receptor gamma2(Q351X) subunits associated with epilepsy. *J Neurosci Off J Soc Neurosci*. 2010;30(41):13895-13905. doi:10.1523/JNEUROSCI.2320-10.2010

76. Roussel BD, Newton TM, Malzer E, et al. Sterol metabolism regulates neuroserpin polymer degradation in the absence of the unfolded protein response in the dementia FENIB. *Hum Mol Genet*. 2013;22(22):4616-4626. doi:10.1093/hmg/ddt310

77. Galliciotti G, Glatzel M, Kinter J, et al. Accumulation of mutant neuroserpin precedes development of clinical symptoms in familial encephalopathy with neuroserpin inclusion bodies. *Am J Pathol*. 2007;170(4):1305-1313. doi:10.2353/ajpath.2007.060910

78. López-González I, Pérez-Mediavilla A, Zamarbide M, et al. Limited Unfolded Protein Response and Inflammation in Neuroserpinopathy. *J Neuropathol Exp Neurol*. 2016;75(2):121-133. doi:10.1093/jnen/nlv011

79. Schipanski A, Oberhauser F, Neumann M, et al. Lectin OS-9 delivers mutant neuroserpin to endoplasmic reticulum associated degradation in familial encephalopathy with neuroserpin inclusion bodies. *Neurobiol Aging*. 2014;35(10):2394-2403. doi:10.1016/j.neurobiolaging.2014.04.002

80. Ceru S, Layfield R, Zavasnik-Bergant T, et al. Intracellular aggregation of human stefin B: confocal and electron microscopy study. *Biol Cell*. 2010;102(6):319-334. doi:10.1042/BC20090163

81. Polajnar M, Zavašnik-Bergant T, Škerget K, et al. Human Stefin B Role in Cell's Response to Misfolded Proteins and Autophagy. *PLOS ONE*. 2014;9(7):e102500. doi:10.1371/journal.pone.0102500

82. Lemke JR, Geider K, Helbig KL, et al. Delineating the GRIN1 phenotypic spectrum: A distinct genetic NMDA receptor encephalopathy. *Neurology*. 2016;86(23):2171-2178. doi:10.1212/WNL.0000000000002740

83. Benke TA, Park K, Krey I, et al. Clinical and therapeutic significance of genetic variation in the GRIN gene family encoding NMDARs. *Neuropharmacology*. 2021;199:108805. doi:10.1016/j.neuropharm.2021.108805

84. Syrbe S, Harms FL, Parrini E, et al. Delineating SPTAN1 associated phenotypes: from isolated epilepsy to encephalopathy with progressive brain atrophy. *Brain J Neurol*. 2017;140(9):2322-2336. doi:10.1093/brain/awx195

85. Omura T, Kaneko M, Okuma Y, Matsubara K, Nomura Y. Endoplasmic reticulum stress and Parkinson's disease: the role of HRD1 in averting apoptosis in neurodegenerative disease. *Oxid Med Cell Longev*. 2013;2013:239854. doi:10.1155/2013/239854

86. Omura T, Asari M, Yamamoto J, et al. HRD1 levels increased by zonisamide prevented cell death and caspase-3 activation caused by endoplasmic reticulum stress in SH-SY5Y cells. *J Mol Neurosci MN*. 2012;46(3):527-535. doi:10.1007/s12031-011-9638-8

87. Bown CD, Wang JF, Chen B, Young LT. Regulation of ER stress proteins by valproate: therapeutic implications. *Bipolar Disord*. 2002;4(2):145-151. doi:10.1034/j.1399-5618.2002.t01-1-40201.x

88. Batjargal K, Tajima T, Jimbo EF, Yamagata T. Effect of 4-phenylbutyrate and valproate on dominant mutations of WFS1 gene in Wolfram syndrome. *J Endocrinol Invest*. 2020;43(9):1317-1325. doi:10.1007/s40618-020-01228-2

89. Sarkar S, Floto RA, Berger Z, et al. Lithium induces autophagy by inhibiting inositol monophosphatase. *J Cell Biol*. 2005;170(7):1101-1111. doi:10.1083/jcb.200504035

90. Hidvegi T, Ewing M, Hale P, et al. An autophagy-enhancing drug promotes degradation of mutant alpha1-antitrypsin Z and reduces hepatic fibrosis. *Science*. 2010;329(5988):229-232. doi:10.1126/science.1190354

91. Meng Q, Chen X, Sun L, Zhao C, Sui G, Cai L. Carbamazepine promotes Her-2 protein degradation in breast cancer cells by modulating HDAC6 activity and acetylation of Hsp90. *Mol Cell Biochem*. 2011;348(1-2):165-171. doi:10.1007/s11010-010-0651-y

92. Ciana G, Dardis A, Pavan E, et al. In vitro and in vivo effects of Ambroxol chaperone therapy in two Italian patients affected by neuronopathic Gaucher disease and epilepsy. *Mol Genet Metab Rep*. 2020;25:100678. doi:10.1016/j.ymgmr.2020.100678

93. Yokoi N, Fukata Y, Kase D, et al. Chemical corrector treatment ameliorates increased seizure susceptibility in a mouse model of familial epilepsy. *Nat Med*. 2015;21(1):19-26. doi:10.1038/nm.3759

94. El-Kasaby A, Kasture A, Koban F, et al. Rescue by 4-phenylbutyrate of several misfolded creatine transporter-1 variants linked to the creatine transporter deficiency syndrome. *Neuropharmacology*. 2019;161:107572. doi:10.1016/j.neuropharm.2019.03.015

95. Durisic N, Keramidas A, Dixon CL, Lynch JW. SAHA (Vorinostat) Corrects Inhibitory Synaptic Deficits Caused by Missense Epilepsy Mutations to the GABAA Receptor γ2 Subunit. *Front Mol Neurosci*. 2018;11:89. doi:10.3389/fnmol.2018.00089

96. Di XJ, Han DY, Wang YJ, Chance MR, Mu TW. SAHA enhances Proteostasis of epilepsy-associated α1(A322D)β2γ2 GABA(A) receptors. *Chem Biol*. 2013;20(12):1456-1468. doi:10.1016/j.chembiol.2013.09.020

97. Han DY, Di XJ, Fu YL, Mu TW. Combining valosin-containing protein (VCP) inhibition and suberanilohydroxamic acid (SAHA) treatment additively enhances the folding, trafficking, and function of epilepsy-associated γ-aminobutyric acid, type A (GABAA) receptors. *J Biol Chem*. 2015;290(1):325-337. doi:10.1074/jbc.M114.580324

98. Kudo T, Kanemoto S, Hara H, et al. A molecular chaperone inducer protects neurons from ER stress. *Cell Death Differ*. 2008;15(2):364-375. doi:10.1038/sj.cdd.4402276

99. Shioi R, Karaki F, Yoshioka H, et al. Image-based screen capturing misfolding status of Niemann-Pick type C1 identifies potential candidates for chaperone drugs. *PloS One*. 2020;15(12):e0243746. doi:10.1371/journal.pone.0243746

100. Sha L, Wang X, Li J, et al. Pharmacologic inhibition of Hsp90 to prevent GLT-1 degradation as an effective therapy for epilepsy. *J Exp Med*. 2017;214(2):547-563. doi:10.1084/jem.20160667

101. Sha L, Chen T, Deng Y, et al. Hsp90 inhibitor HSP990 in very low dose upregulates EAAT2 and exerts potent antiepileptic activity. *Theranostics*. 2020;10(18):8415-8429. doi:10.7150/thno.44721

102. Qi SM, Dong J, Xu ZY, Cheng XD, Zhang WD, Qin JJ. PROTAC: An Effective Targeted Protein Degradation Strategy for Cancer Therapy. *Front Pharmacol*. 2021;12:692574. doi:10.3389/fphar.2021.692574

103. Lanzillotta C, Tramutola A, Meier S, et al. Early and Selective Activation and Subsequent Alterations to the Unfolded Protein Response in Down Syndrome Mouse Models. *J Alzheimers Dis JAD*. 2018;62(1):347-359. doi:10.3233/JAD-170617

104. Spiess M, Beuret N, Prescianotto Baschong C, Rutishauser J. Amyloid-like aggregation of provasopressin. *Vitam Horm*. 2020;113:55-77. doi:10.1016/bs.vh.2019.08.014

105. Harkin LA, Bowser DN, Dibbens LM, et al. Truncation of the GABAA-receptor gamma2 subunit in a family with generalized epilepsy with febrile seizures plus. *Am J Hum Genet*. 2002;70(2):530-536. doi:10.1086/338710

106. Shen W, Poliquin S, Macdonald RL, Dong M, Kang JQ. Endoplasmic reticulum stress increases inflammatory cytokines in an epilepsy mouse model Gabrg2+/Q390X knockin: A link between genetic and acquired epilepsy? *Epilepsia*. 2020;61(10):2301-2312. doi:10.1111/epi.16670

107. Warner TA, Liu Z, Macdonald RL, Kang JQ. Heat induced temperature dysregulation and seizures in Dravet Syndrome/GEFS+ Gabrg2(+/Q390X) mice. *Epilepsy Res*. 2017;134:1-8. doi:10.1016/j.eplepsyres.2017.04.020

108. Huang X, Zhou C, Tian M, et al. Overexpressing wild-type γ2 subunits rescued the seizure phenotype in Gabrg2(+/Q390X) Dravet syndrome mice. *Epilepsia*. 2017;58(8):1451-1461. doi:10.1111/epi.13810

109. Fritsch A, Spassov S, Elfert S, et al. Dominant-negative effects of COL7A1 mutations can be rescued by controlled overexpression of normal collagen VII. *J Biol Chem*. 2009;284(44):30248-30256. doi:10.1074/jbc.M109.045294

110. Pochampally RR, Horwitz EM, DiGirolamo CM, Stokes DS, Prockop DJ. Correction of a mineralization defect by overexpression of a wild-type cDNA for COL1A1 in marrow stromal cells (MSCs) from a patient with osteogenesis imperfecta: a strategy for rescuing mutations that produce dominant-negative protein defects. *Gene Ther*. 2005;12(14):1119-1125. doi:10.1038/sj.gt.3302514

111. Yang C, Tan W, Whittle C, et al. The C-terminal TDP-43 fragments have a high aggregation propensity and harm neurons by a dominant-negative mechanism. *PloS One*. 2010;5(12):e15878. doi:10.1371/journal.pone.0015878

112. Schaap D, van der Wal J, Howe LR, Marshall CJ, van Blitterswijk WJ. A dominant-negative mutant of raf blocks mitogen-activated protein kinase activation by growth factors and oncogenic p21ras. *J Biol Chem*. 1993;268(27):20232-20236.

# 2 Characterization of the Ubiquitin-Proteasome System in *GABRG2(Q390X)* Models

## 2.1 Introduction

As laid out in the main introduction, the ubiquitin proteasome system (UPS) is often disrupted in epilepsies. This dysregulation is bidirectional, as changes in UPS activity can both cause and be caused by epilepsy. Because severe seizures are part of the phenotype of Dravet syndrome, it would be expected that the UPS would be altered in the *Gabrg2*$^{+/Q390X}$ mouse model of Dravet syndrome. But, the *GABRG2(Q390X)* mutation likely has a multifactorial effect on the UPS: In addition to the seizures, this mutation also results in the intracellular accumulation of misfolded protein.[1,2]

Protein aggregates are known to interfere with the UPS. In Alzheimer's disease, amyloid-β (Aβ) aggregates inhibit UPS activity by blocking the opening of the proteasome, preventing entry of other substrates into the catalytic core.[3] Similarly, aggregated prion protein binds the outside of the 20S proteasome and allosterically favors the closed position, preventing substrate entry.[4] Aggregates of mutant huntingtin protein have also been shown to decrease UPS activity, via multiple methods including irreversible inhibition of the catalytic core.[3,5] Another polyglutamine expansion protein, ataxin-7 associated with spinocerebellar ataxia type 7, also reduces UPS activity, although the mechanism is not clear.[6] The neurodegenerative disorder Lafora disease is characterized by intracellular inclusions of protein and polyglucosans called Lafora bodies. These inclusions sequester protein quality control components including

molecular chaperones and the 20S proteasome, thereby resulting in decreased UPS activity.[7]

Therefore, I wanted to investigate what intrinsic effect the aggregate-prone γ2(Q390X) subunit might have directly on the UPS, independent of the seizures. To do this, I utilized *in vitro* models with non-excitable cells. I also compared γ2(Q390X) with GAT1(S295L), a mutant protein encoded by *SLC6A1(S295L)* that is associated with neurodevelopmental delay and is retained within the ER, like γ2(Q390X).[8] Our unpublished data suggest that GAT1(S295L) may also be dominant-negative like γ2(Q390X), by trapping the wildtype protein in the ER and lowering wildtype total and/or surface expression. However, unlike γ2(Q390X), GAT1(S295L) does not form aggregates. It therefore represents membrane protein that misfolds and taxes the protein quality control system, but in a manner perhaps slightly different from the aggregate-forming γ2(Q390X).

## 2.2 Methods

### 2.2.1 Cell culture and polyethyleneimine transfection

Human embryonic kidney 293 T (HEK293T) cells were grown in Dulbecco's Modified Eagle's Medium (DMEM) supplemented with 10% FBS and 1% penicillin/streptomycin. 24 hours after plating the cells, they were transfected with cDNA for wildtype rat GABR γ2S, γ2S(Q390X), γ2S(W461X) subunits (referred to hereafter simply as γ2, γ2(Q390X), and γ2(W461X) subunits, respectfully), human GABR α1 subunit, human GABR β2 subunit, rat GAT1, rat GAT1(S295L), and/or empty vector pcDNA. cDNA was combined with polyethyleneimine (PEI) at a ratio of 2.5 μL PEI per 1 μg cDNA. Additional cDNA

included myc-tagged HRD1 and HA-tagged SEL1L, kindly shared by Dr. Nobuko Hosokawa at the Institute for Frontier Life and Medical Sciences, Kyoto University. Lactacystin (Tocris 2667), MG132 (Tocris 1748), celastrol (Sigma-Aldrich C0869), 4-phenylbutyric acid (PBA) (Sigma-Aldrich P21005), and zonisamide (ZNS) (Tocris 2625) were dissolved in dimethyl sulfoxide (DMSO).

### 2.2.2 Immunoblot

Cells were harvested 48 hr after transfection. Cells were washed with cold phosphate buffered saline (PBS) and lysed with RIPA-PI solution containing 20 mM Tris, 20 mM EGTA, 1 mM DTT, 1 mM benzamidine, 0.01 mM PMSF, 0.005 µg/mL leupeptin, and 0.005 µg/mL pepstatin. Protein concentration was measured and samples were subjected to standard sodium dodecyl sulfate (SDS) polyacrylamide gel electrophoresis (SDS-PAGE) procedures and immunoblotted. Primary antibodies used were anti-γ2 1:1,000 (Synaptic Systems 224003), anti-GAT1 1:1,000 (Synaptic Systems 274102), anti-green fluorescent protein (GFP) 1:100 (Sigma-Aldrich G6539), anti-β-actin 1:6,000 (ABclonal AC006), anti-glyceraldehyde 3-phosphate dehydrogenase (GAPDH) 1:6,000 (Millipore Sigma CB1001), and anti-ATPase 1:1,000 (Developmental Studies Hybridoma Bank a6F). Secondary antibodies were LI-COR IRDye 680LT Goat anti-Mouse IgG Secondary Antibody (926-68020) and IRDye 800CW Goat anti-Rabbit IgG Secondary Antibody (926-32211), both 1:10,000.

Blots were imaged with an Odyssey DLx digital fluorescence scanner and LI-COR Image Studio Lite 5.2 software. Protein bands were quantified by circumscribing the band of interest and correcting for background signal. Integrated density values (IDVs) for the protein of interest were normalized to the IDV for the loading control, ATPase.

The values were then normalized to loading controls and then the normalized IDV of the control lane (generally, wildtype or untreated), which was arbitrarily taken as equal to 1.

### 2.2.3 20S proteasome activity assay for cultured cells

Cells were harvested 48 hr post transfection, washed with PBS, and lysed in cell lysis buffer containing 150 mM NaCl, 50 mM HEPES (pH 7.5), 5 mM ethylenediaminetetraacetic acid (EDTA), 1% Triton X-100, and 2 mM ATP. Protein concentrations were determined and 30 µg of protein was added to a sample tube. The volume of each sample was normalized to 90 µL using assay buffer (25 mM HEPES [pH 7.5], 0.5 mM EDTA, 0.05% NP-40, 0.001% SDS). Separately, positive controls were prepared by serial dilution of purified 20S proteasomes (Millipore Sigma APT280) in assay buffer. 10 µL of substrate solution containing 0.5 mM Suc-LLVY-AMC (Boston Biochem S-280) in assay buffer was added to sample tubes and positive control tubes. Tubes were then incubated at 37°C for 1 hr. Meanwhile, a standard curve was prepared by serial dilution of 7-amino-4-methylcoumarin (AMC) (Sigma-Aldrich A9891) in assay buffer, to create a range from 0.39 µM to 12.5 µM AMC. The contents of all tubes were then transferred to an opaque 96-well plate. The fluorescence was measured using a POLARstar Omega plate reader (BMG Labtech) with a 355 nm/460 nm (excitation/emission) filter, acquired with Omega software (version 5.11 R4). Samples were performed in duplicate and values were averaged. These values were then normalized to the control (generally, wildtype or untreated), which was arbitrarily taken as equal to 1.

### 2.2.4 Mice

The generation of the *Gabrg2*$^{+/Q390X}$ mouse is described previously[1] and the line was maintained in C57BL/6J (Jackson Labs stock #000664). Animals were housed in standard facilities with ad libitum food and water access.

### 2.2.5 Drug administration and brain tissue preparation in *Gabrg2*$^{+/Q390X}$ mice

Beginning at 1-1.5 months of age, heterozygous *Gabrg2*$^{+/Q390X}$ animals and wildtype littermates, both male and female, were treated daily with vehicle, 20 mg/kg ZNS, or 100 mg/kg PBA injected intraperitoneally for 7 days. ZNS (Tocris 2625) and PBA (Sigma-Aldrich P21005) were dissolved in 10% dimethyl sulfoxide (DMSO) and 90% 0.9% saline, for a final concentration of 5 mg/mL or 20 mg/mL, respectively. After 7 days of treatment, the mice were anesthetized with isoflurane and decapitated. The brain was removed, and the somatosensory cortex, cerebellum, thalamus, and hippocampus were dissected.

### 2.2.6 20S proteasome activity assay for mouse brain tissue

Dissected brain regions were lysed in tissue lysis buffer containing 20mM Tris-HCl (pH 7.6), 20 mM KCl, 10 mM Mg acetate, 2 mM dithiothreitol (DTT), and 10% glycerol. Samples were centrifuged at 25,000 g for 45 min at 4°C, to separate soluble proteins into the supernatant. The assay was then performed as described above for cultured cells.

### 2.2.7 Data analysis

Data were analyzed using GraphPad Prism 9.4 and is reported as mean ± standard error of the mean (SEM). For the cell culture experiments, two-way analysis of variance

(ANOVA) tests were performed and post-hoc analyses were performed as reported in the text, corrected for multiple comparisons. For the mouse immunohistochemistry experiments, one-way ANOVAs and Šídák's multiple comparisons post-hoc analysis were performed. Statistical significance was taken as $p < 0.05$ throughout.

## 2.3 Results

### 2.3.1 Neither γ2(Q390X) subunit nor GAT1(S295L) alter levels of the UPS activity reporter GFPu *in vitro*

To study proteasome activity *in vitro*, I took advantage of a HEK293T cell line stably expressing the construct GFPu. GFPu is green fluorescent protein (GFP) fused with a degron, a short chain of amino acids targeting a protein for degradation; specifically, the CL1 degron is 16 amino acids fused to carboxyl terminus of GFP.[9] GFPu is constitutively expressed and quickly destroyed via the UPS.[9] Therefore, it can be used as a proxy for UPS activity. When the UPS is inhibited, substrates like GFPu accumulate, while under conditions of increased UPS activity, GFPu is degraded more quickly and thus protein expression levels fall.

I transfected HEK293T GFPu cells with increasing amounts of wildtype γ2 or mutant γ2(Q390X) cDNA and then measured GFPu expression via Western blotting. I found no statistical difference in GFPu expression between wildtype and mutant ($p = 0.9490$), nor was there any effect for µg cDNA ($p = 0.9091$) or any interaction between genotype and cDNA amount ($p = 0.9052$). Expression of γ2 protein was, as expected, correlated with the amount of cDNA transfected into the cells (Figure 1).

***Table 2.1. p values of analysis of GFPu expression in cells transfected with different amounts of γ2 or γ2(Q390X) cDNA.***

| γ2 | Mean ± SEM | *p*, vs 0.5 |
|---|---|---|
| 0.5 | 0.951 ± 0.048 | |
| 1 | 0.914 ± 0.081 | 0.9892 |
| 2 | 0.872 ± 0.092 | 0.9123 |
| 4 | 0.905 ± 0.104 | 0.9796 |
| | | |
| γ2(Q390X) | | |
| 0.5 | 0.927 ± 0.071 | |
| 1 | 0.840 ± 0.115 | 0.8929 |
| 2 | 0.916 ± 0.135 | 0.9996 |
| 4 | 0.978 ± 0.196 | 0.9789 |

Significant values ($p < 0.05$) are bolded. Two-way ANOVA, Dunnett's multiple comparisons, $n$ = 4-5.

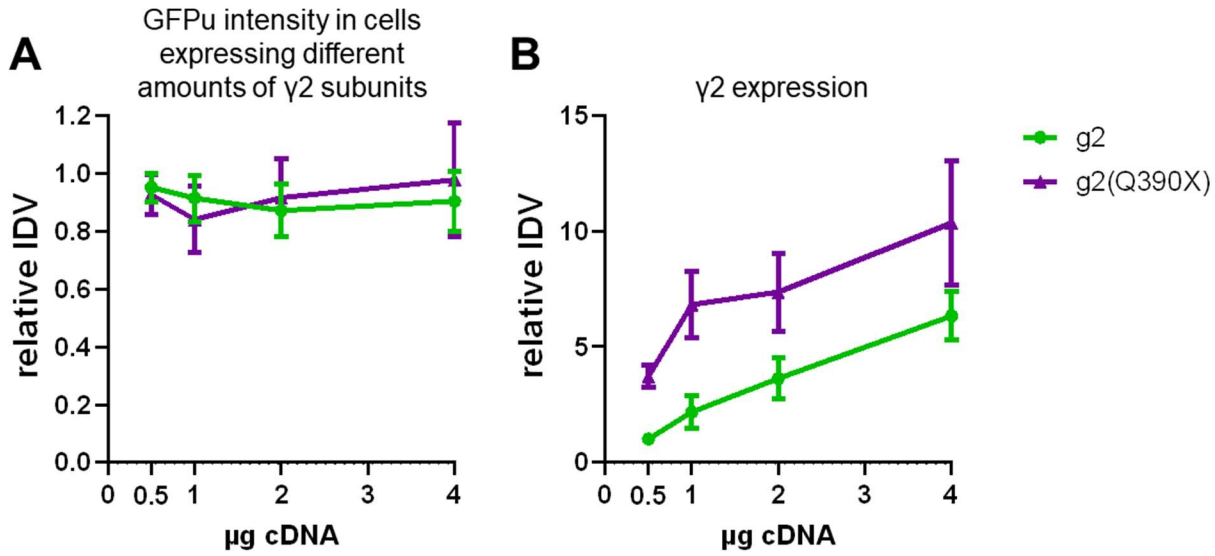


***Figure 2.1. Increased expression of neither γ2 nor γ2(Q390X) had any effect on GFPu intensity.***

A. Relative IDV of GFPu, normalized to untransfected controls. B. Relative IDV of γ2, normalized to 0.5 µg cDNA γ2.

I also performed the same experiment with GAT1 and GAT1(S295L). GAT1(S295L) is a mutation identified in a patient with neurodevelopmental delay. This mutation has almost no GABA uptake activity and has impaired protein trafficking, as it is heavily retained within the ER.[8] As with γ2, there was no effect on GFPu expression by genotype ($p$ = 0.2153), cDNA amount ($p$ = 0.8294), or any interaction between the factors ($p$ = 0.6450).

***Table 2.2. p values of analysis of GFPu expression in cells transfected with different amounts of GAT1 or GAT1(S295L) cDNA.***

| GAT1 | Mean ± SEM | *p*, vs 0.5 |
|---|---|---|
| 0.5 | 0.978 ± 0.072 | |
| 1 | 1.003 ± 0.118 | 0.9984 |
| 2 | 1.062 ± 0.186 | 0.9496 |
| 4 | 1.223 ± 0.167 | 0.4574 |
| | | |
| GAT1(S295L) | | |
| 0.5 | 0.899 ± 0.101 | |
| 1 | 0.971 ± 0.119 | 0.9674 |
| 2 | 1.021 ± 0.172 | 0.8671 |
| 4 | 0.883 ± 0.129 | 0.9996 |

Significant values ($p$ < 0.05) are bolded. Two-way ANOVA, Dunnett's multiple comparisons, $n$ = 6

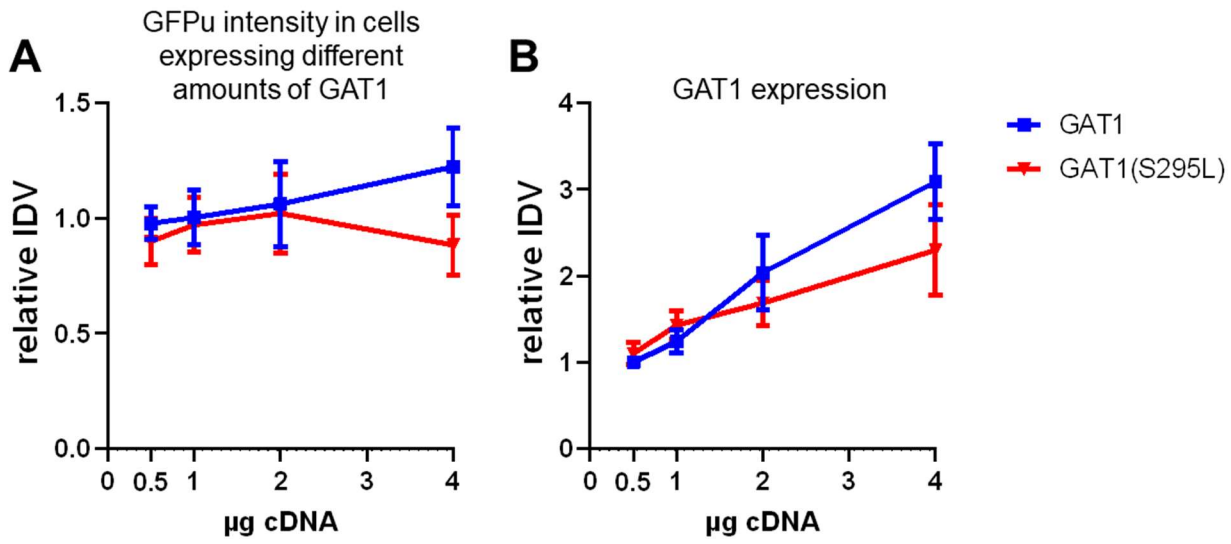


***Figure 2.2. Increased expression of neither GAT1 nor GAT1(S295L) had any effect on GFPu intensity.***
A. Relative IDV of GFPu, normalized to untransfected controls. B. Relative IDV of GAT1, normalized to 0.5 µg cDNA GAT1.

However, an interesting trend was noticed: the spread of the data seemed to increase at higher doses. This led to a hypothesis that I may have been measuring at an inflection point, where the relative activity of the proteasome begins to change, for the conditions with higher amounts of cDNA. Therefore, the same transfection conditions were replicated but cells were harvested at multiple time points, to get a clearer picture. Interestingly, differences did emerge. At 12 hours, there was a significant interaction between genotype and µg cDNA ($p$ = 0.0268). Genotype ($p$ = 0.3263) and cDNA amount ($p$ = 0.5041) were not directly associated with differences. Unexpectedly, a significant interaction was also found at 48 hours (our standard time post-transfection to harvest cells), despite no difference in the prior experiment (interaction $p$ = 0.0304, µg cDNA $p$ = 0.6213, genotype $p$ = 0.9956).

To better visualize the data, I performed simple linear regressions of the data and plotted the resulting lines. Data were grouped by genotype and hours post transfection, with µg cDNA as the independent variable. As a whole, there appears to be a slight upward trend for γ2, while all γ2(Q390X) lines slope downward, although only two of these ten equations had slopes significantly different from zero (γ2 at 48 hr: y = 0.1153*x + 0.6967; γ2(Q390X) at 12 hr: y = -0.06742*x + 0.9539).

***Table 2.3. p values of analysis of GFPu expression in cells transfected with different amounts of γ2 or γ2(Q390X) cDNA.***

| Time (hr) | Interaction | µg cDNA | Genotype |
|---|---|---|---|
| 12 | **0.0268** | 0.5041 | 0.3263 |
| 24 | 0.1464 | 0.8521 | 0.7996 |
| 36 | 0.2614 | 0.7651 | 0.5465 |
| 48 | **0.0304** | 0.6213 | 0.9956 |
| 60 | 0.6007 | 0.9645 | 0.8407 |

Significant values ($p < 0.05$) are bolded. Two-way ANOVA, n = 5-7.

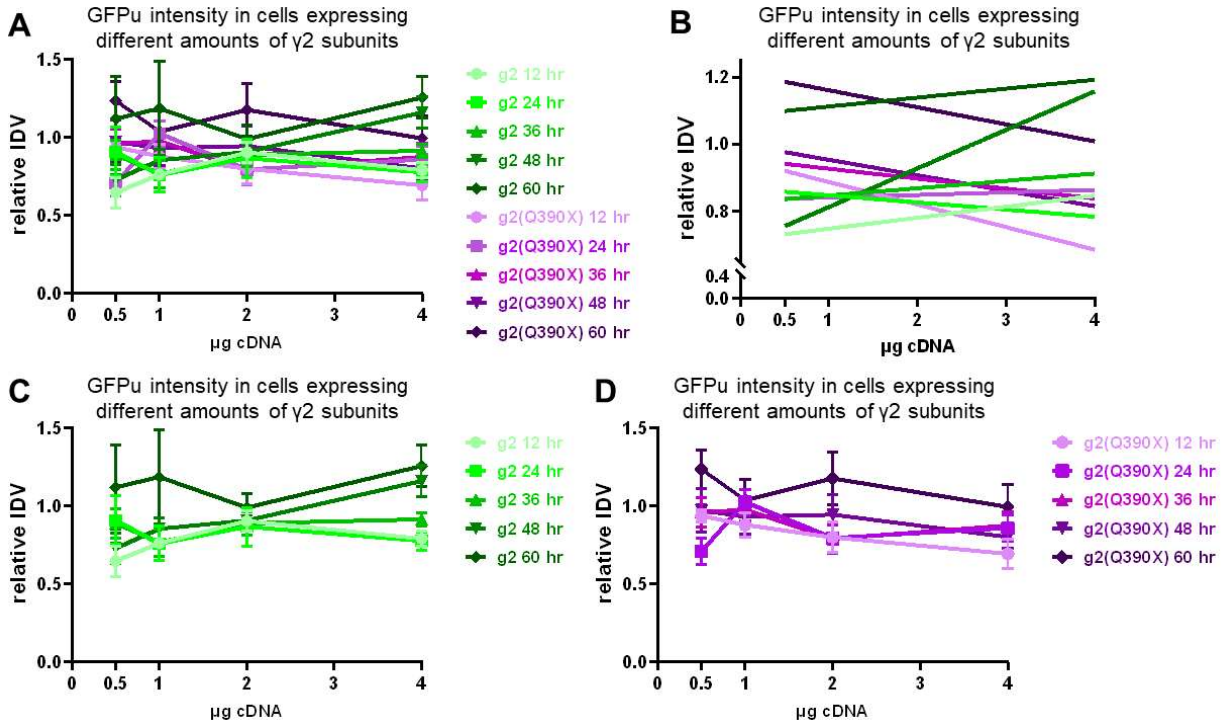


***Figure 2.3. Subtle changes in GFPu intensity, in response to increased expression of γ2 and γ2(Q390X).***
A. Relative IDV of GFPu, normalized to untransfected controls collected at the corresponding time point. B. Simple linear regressions of the data in panel A, to better show trends. C. Same as panel A, selecting only wildtype γ2. D. Same as panel A, selecting only mutant γ2(Q390X).

Unpublished preliminary data from Dr. Katty Kang, however, did show significant differences, using flow cytometry to measure GFPu abundance. In her experiments, using 0.5, 1, 2.5, 5, and 10 µg cDNA, the fluorescence intensity for all wildtype γ2 conditions is unchanged, compared to untransfected controls. For γ2(Q390X), however, the GFPu fluorescence intensity was lower than that of wildtype γ2 and untransfected controls at lower cDNA amounts (0.5 and 1 µg) and then rose above these controls at higher amounts (5 and 10 µg). This indicates that the UPS was upregulated by small

amounts of mutant γ2(Q390X) but then began to fail in the presence of high γ2(Q390X) expression.

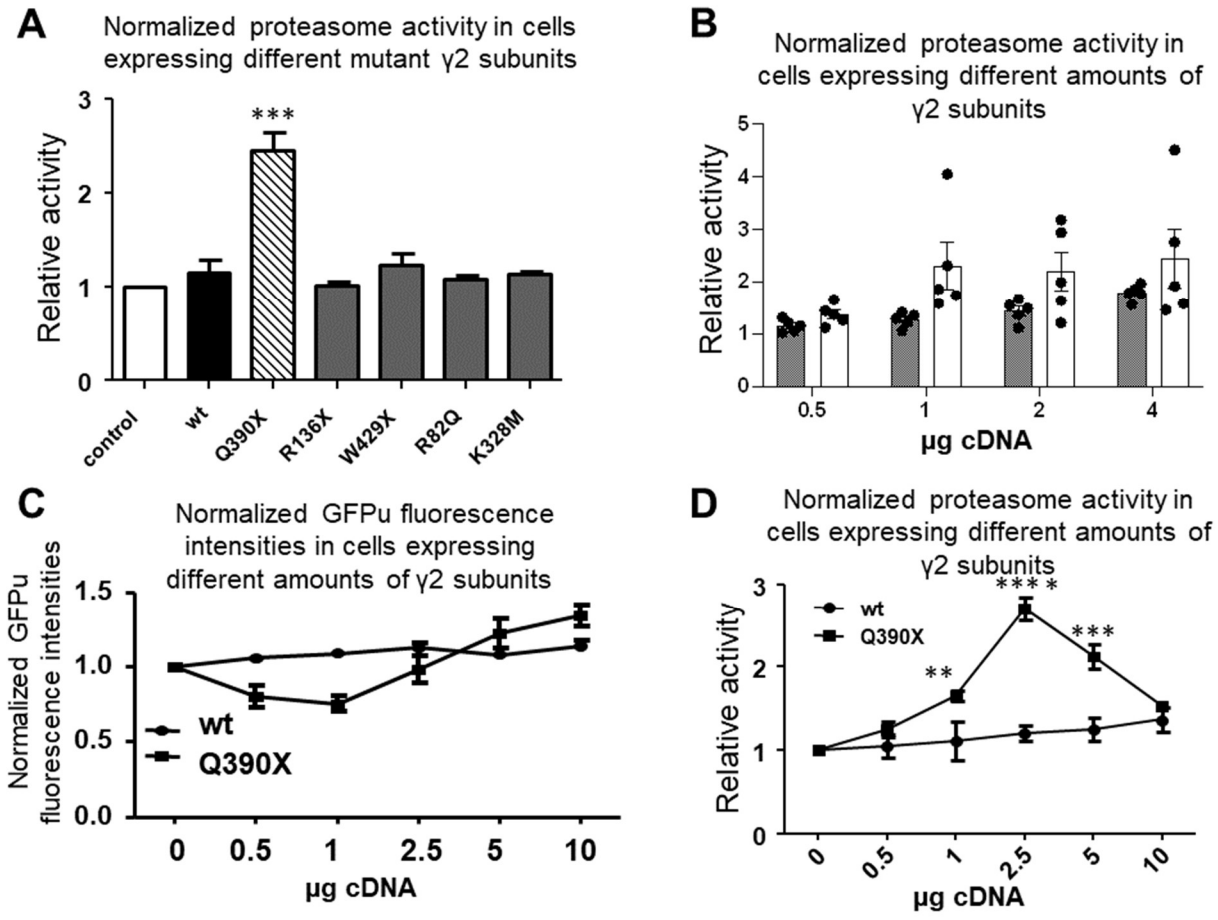


***Figure 2.4. γ2(Q390X) – but not other γ2 mutations – alter proteasome activity.*** A. Proteasome activity in cells transfected with 3 µg cDNA of wildtype or mutant γ2, normalized to untransfected controls. B, D. Proteasome activity in cells transfected with varying amounts of cDNA of wildtype or mutant γ2, normalized to untransfected controls. C. Relative GFPu fluorescence intensity in cells transfected with varying amounts of cDNA of wildtype or mutant γ2, normalized to untransfected controls. *All data collected by Katty Kang.*

In order to validate that changes can be detected by Western blot, I treated cells with a variety of conditions that could impact UPS activity. These included the conventional, known UPS inhibitors MG132 (5 μM, 6 hr) and lactacystin (10 μM, 6 hr); celastrol (1 μM, 6 hr), which is reported to inhibit the UPS in tumor cells;[10] PBA (2 mM, 24 hr), which normalizes UPS activity in some disease states;[11–13] and transfection with the ERAD components HRD1 or SEL1L, which may increase UPS activity by facilitating the identification and movement of substrates from the ER to the cytoplasmic proteasome. This was underpowered (n = 3-4), as it was only a proof-of-principle experiment, but MG132 significantly increased the amount of GFPu (3.506 ± 0.2563, $p = 0.0163$), and lactacystin showed a strong upward trend (2.583 ± 0.5612, $p = 0.1795$). Thus, large decreases in UPS activity can clearly be detected by immunoblotting against GFP, for GFPu cell lysates.

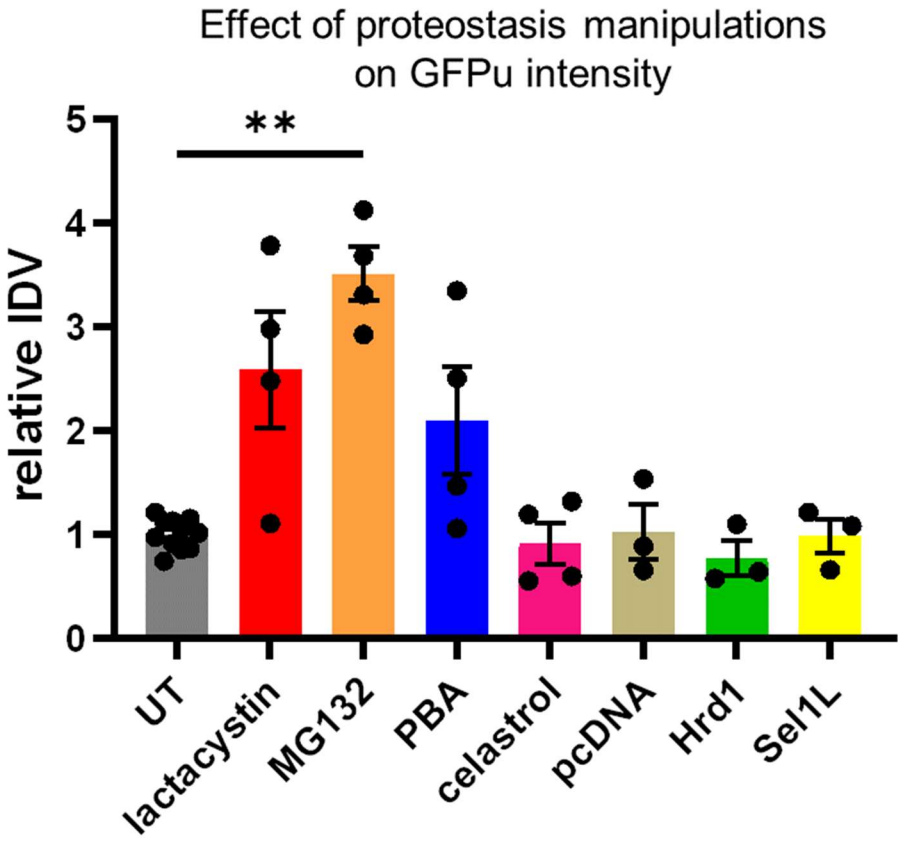


***Figure 2.5. Immunoblotting of GFP detects changes in GFPu expression, reporting alterations in UPS activity.***

### 2.3.2 γ2(Q390X) subunit does not alter proteasome chymotrypsin-like activity *in vitro*

Next, I directly measured 20S proteasome activity, via metabolism of a fluorophore. Suc-LLVY-AMC is cleaved by the chymotrypsin-like activity of the proteasome, releasing the AMC fluorophore. Prior data from the lab utilizing this technique does indicate potential differences in proteasome activity between experimental conditions. This suggests that this direct measurement of proteasome activity may be more sensitive to subtle changes than Western blotting of GFPu. However, this data – collected by Hongmei Wang and Sean Moran – has a very limited *n* so no scientific

conclusions can be drawn from it; the value at present is that it supports the use of this methodology for my experiments.

Therefore, HEK293T cells were transfected with increasing amounts of cDNA for wildtype γ2 or γ2(Q390X) as before, and proteasome activity was measured via Suc-LLVY-AMC fluorescence. Again, there was no change (two-way ANOVA: cDNA dose $p = 0.9277$, genotype $p = 0.1708$, interaction $p = 0.8532$, $n = 5$).

If the γ2(Q390X) mutant protein results in a reduced reserve capacity to respond to stressors – as hypothesized – healthy cells under physiological conditions may show no change, but differences will emerge under conditions of cellular stress. Heat stress is a particularly relevant source of cellular stress, as it not only results in ER stress, it also mimics the specific conditions of febrile seizures that are common in Dravet syndrome. Incubation at 40°C has been shown to alter proteostasis of GABRs containing febrile seizure associated γ2 mutants (R82Q, K328M, and Q390X), as heat exposure rapidly reduces surface expression of γ2 and increases intracellular expression.[14] So, I subjected HEK293T cells to 40°C for 2 hours before collection. As in the previous experiment, there was no difference from any factor (two-way ANOVA: cDNA dose $p = 0.9817$, genotype $p = 0.9750$, interaction $p = 0.9150$, $n = 5$) (normalized to UT at 37°C)

Interestingly, this is in contrast to Katty's prior data that had suggested a dramatic upregulation of proteasome activity in cells transfected with high amounts of γ2(Q390X) (Figure 4). I combed through Hongmei's data and pooled together the untreated controls from multiple experiments testing various drugs. With this higher sample size ($n = 9$-10), I could perform meaningful statistical analyses. This data shows a moderate change: 3 µg cDNA of γ2(Q390X) resulted in UPS activity slightly elevated above that of

cells transfected with 3 μg cDNA of γ2 (γ2 1 ± 0, γ2(Q390X) 1.347 ± 0.1453, $p$ = 0.0441) (Figure 6D).

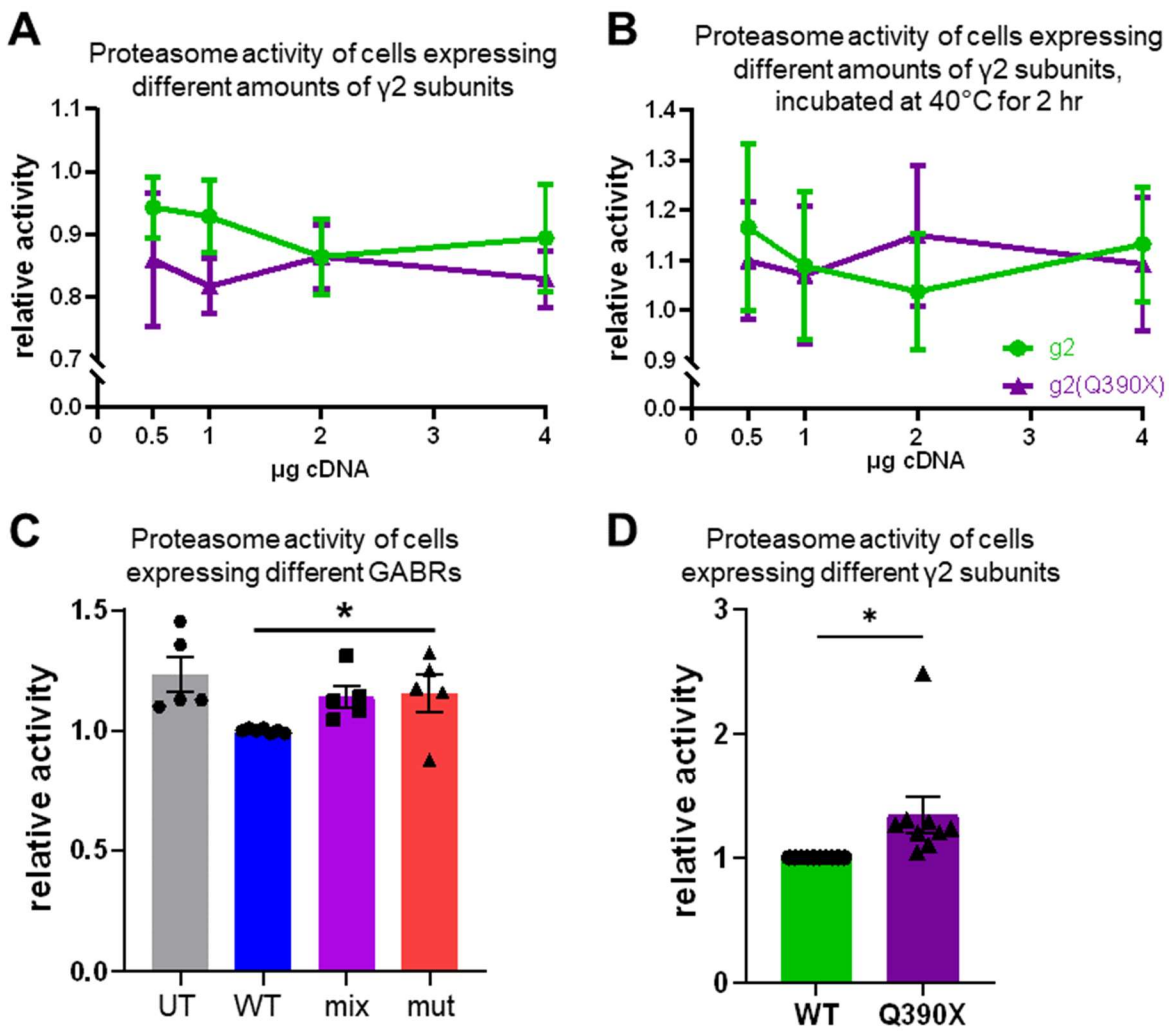


***Figure 2.6. The γ2(Q390X) subunit may alter UPS activity, compared to wildtype γ2.***

A, B. Proteasome activity in cells transfected with varying amounts of cDNA of wildtype or mutant γ2, normalized to untransfected controls. $n = 5$ for both experiments. For B, cells were incubated for 2 hr at 40°C before collecting. Values are normalized to an untransfected control left at 37°C. C. Proteasome activity in cells transfected with α1β2γ2 (1:1:1) (WT), α1β2γ2/γ2(Q390X) (1:1:0.5:0.5) (mix), or α1β2γ2(Q390X) (1:1:1) (mut), or untransfected. Values are normalized to WT condition. One-way ANOVA, Dunnett's multiple comparisons post hoc analysis. D. Proteasome activity in cells transfected with 3 µg cDNA of wildtype or mutant γ2, normalized to wildtype. Two-tailed *t*-test. * indicates $p < 0.05$. *Data in D was collected by Hongmei Wang.*

Similarly, I pooled together untreated α1β2γ2, α1β2γ2/γ2(Q390X), and α1β2γ2(Q390X) data points from my experiments utilizing various drugs (celastrol, PBA, and zonisamide, discussed below). Here, I did find a subtle increase in the mixed and mutant conditions (1 ± 0.0035 wt, 1.140 ± 0.0455 mixed, 1.156 ± 0.0756 mutant), although the mixed fails to reach statistical significance ($p$ = 0.0732 for mixed vs wt, $p$ = 0.0456 mutant vs wt) (n = 5-7).

### 2.3.3 No effect of proteostasis regulators on proteasome chymotrypsin-like activity *in vitro*

In addition to testing the individual γ2 and γ2(Q390X) subunits, I also investigated GABRs consisting of α1β2γ2, α1β2γ2/γ2(Q390X), and α1β2γ2(Q390X), and the effects of celastrol, PBA, and zonisamide (ZNS) on these different GABRs. Celastrol is reported to upregulate molecular chaperones and PBA is a chemical chaperone. Therefore, both compounds could potentially ameliorate aggregation of γ2(Q390X), which would prevent any of the negative effects of protein aggregates on proteasome activity (as discussed in the introduction). Additionally, celastrol and PBA are predicted to stabilize wildtype subunits, so that there is not the enhanced degradation that normally occurs when they are retained in the ER with γ2(Q390X). Thus, there should be less burden on the UPS.

ZNS is reported to upregulate HRD1, an E3 ligase that potentially ubiquitinates Q390X and the overexpression of which we have shown reduces expression of γ2(Q390X). ZNS would therefore likely help to protect the proteasome from negative effects of γ2(Q390X) subunit aggregation, but also places more burden on the UPS by increasing γ2(Q390X) degradation.

Because PBA and the molecular chaperones upregulated by celastrol (such as HSP70) can stabilize proteins, and γ2(Q390X) is more stable than wildtype γ2, the drug treatments may exacerbate the toxic accumulation of γ2(Q390X) protein. Therefore, I also included γ2(W461X). This is another truncation mutation associated with epilepsy, like γ2(Q390X), but the protein is less stable and is rapidly degraded, rather than forming intracellular aggregates. I hypothesized that the response to drug treatment would be similar between cells expressing γ2(W461X) and those expressing wildtype γ2.

However, data thus far does not indicate any robust effects of either celastrol or PBA on the UPS in transfected HEK293T cells. Before proceeding with this experiment, I sought to verify that the doses we standardly use in the lab (2 mM PBA for 24 hr, 1 μM celastrol for 6 hr), were appropriate for this experiment.

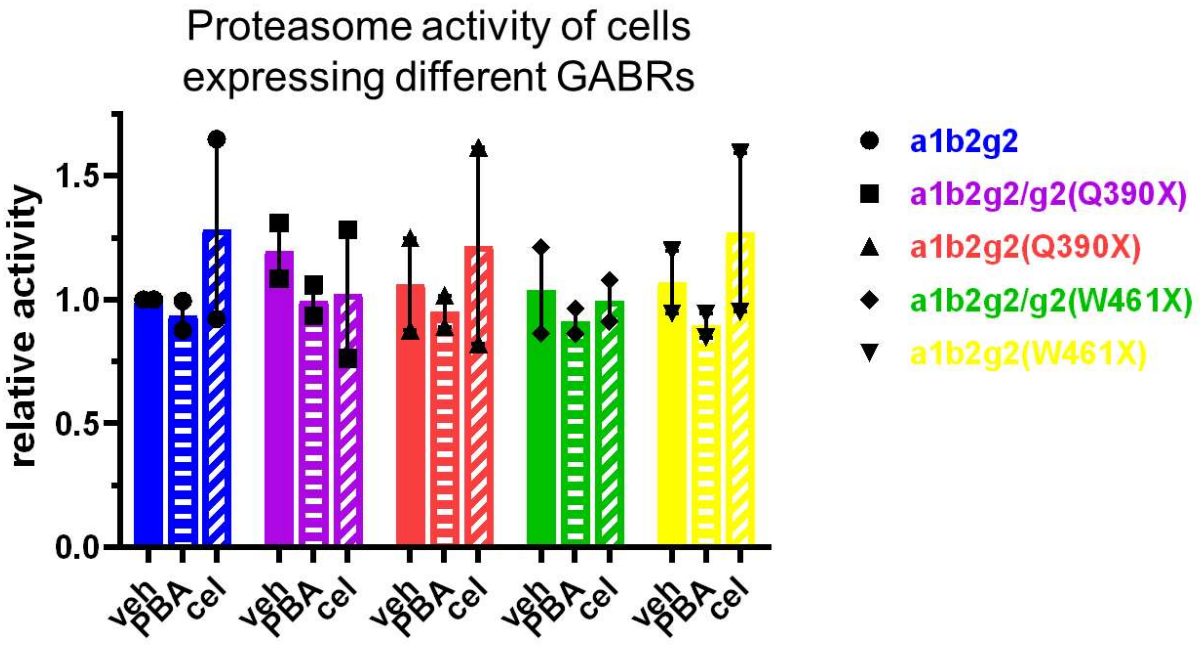


***Figure 2.7. Preliminary data comparing the effects of PBA (2 mM, 24 hr) and celastrol (1 μM, 6 hr) on cells transfected with various GABRs.***
Wildtype α1β2γ2 (1:1:1), mixed α1β2γ2/γ2(Q390X) (1:1:0.5:0.5), mutant α1β2γ2(Q390X) (1:1:1), mixed α1β2γ2/γ2(W461X) (1:1:0.5:0.5), and mutant α1β2γ2(W461X) (1:1:1). *n* = 2

Our work with GAT1 mutations had shown that the ideal dose of PBA was 2 mM for 24 hr, in regards to boosting GAT1 expression and function. GABR, however, may respond differently. Thus, I investigated 0.5, 1, 2, and 4 mM for 6, 12, and 24 hr. I used untransfected HEK293T cells to test for intrinsic effects of the compound on the UPS, and cells transfected with wildtype α1β2γ2, because the overexpression of exogenous protein may modify how the proteostasis network responds to drug treatments. Preliminary data from untransfected cells (*n* = 2) and GABR-transfected cells (*n* = 3) do not seem to suggest any direct effect on UPS activity by PBA. However, wildtype

proteins that fold properly may not be assisted as much by a chemical chaperone like PBA as misfolding-prone mutant proteins.

I also gathered preliminary data on celastrol and UPS activity. Utilizing 0.1, 0.5, and 1 μM celastrol for 3, 6, and 24 hr, I measured UPS activity in untransfected HEK293 cells and HEK293 cells transfected with wildtype GABR (α1β2γ2, 1:1:1 cDNA). This preliminary data ($n$ = 4 for both) does not indicate a direct effect.

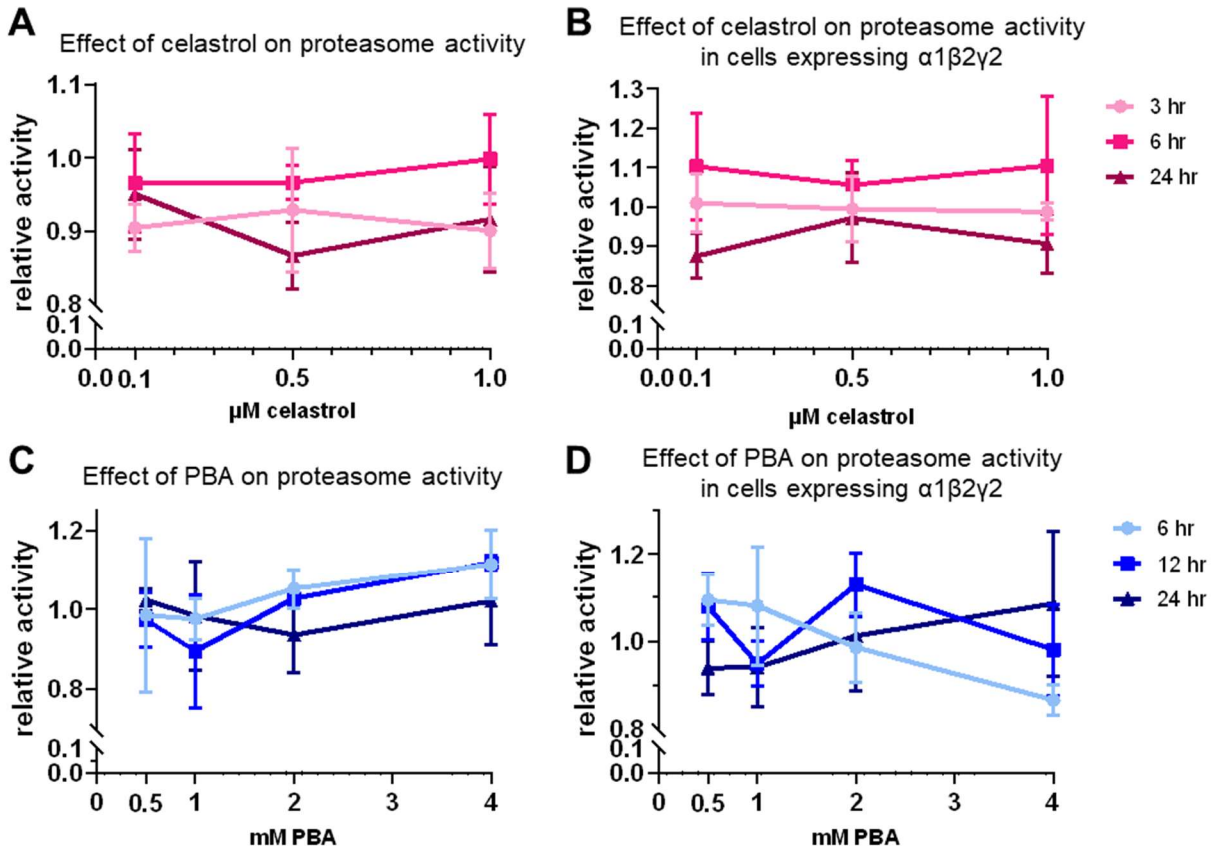


***Figure 2.8. Neither celastrol nor PBA has robust effects on UPS activity.***
A, B. Proteasome activity in cells treated with 0.1, 0.5, or 1 μM celastrol for 3, 6, or 24 hr. Values normalized to untreated controls. C, D. Proteasome activity in cells treated with 0.5, 1, 2, or 4 mM PBA for 6, 12, or 24 hr. Values normalized to untreated controls. In B and D, all cells have been transfected with wildtype GABR (α1β2γ2, 1:1:1).

ZNS also does not appear to have robust effects on UPS activity, in untransfected HEK293T cells or in cells transfected with wildtype or mutant GABRs. The data is, however, preliminary at *n* = 3.

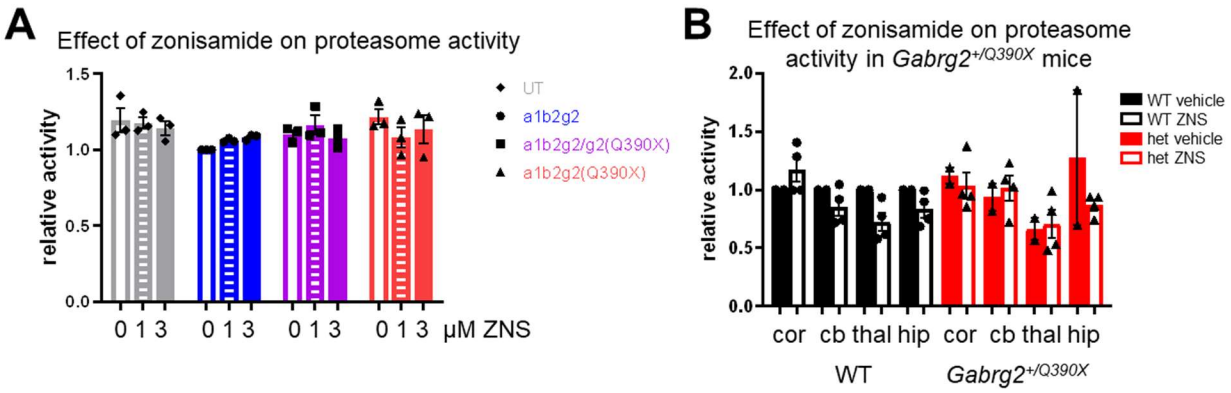


***Figure 2.9. ZNS has no effect on UPS activity.***
A. Cells were transfected with wildtype α1β2γ2 (1:1:1), mixed α1β2γ2/γ2(Q390X) (1:1:0.5:0.5), or mutant α1β2γ2(Q390X) (1:1:1) GABR, or untransfected. Each transfection condition was treated with 1 or 3 μM ZNS, or vehicle. Values are normalized to vehicle-treated wildtype controls. B. 1-1.5 month old *Gabrg2*$^{+/Q390X}$ mice and littermate controls were treated with ZNS (20 mg/kg/day for 7 days) or vehicle. Values are normalized to vehicle-treated wildtype controls, for each brain region. Values are not normalized across regions.

### 2.3.4 Investigation into the effect of proteostasis regulators on proteasome chymotrypsin-like activity in brains of *Gabrg2*$^{+/Q390X}$ mice

Transfected HEK293T cells are a useful tool that allow me to investigate the elements of γ2(Q390X) pathophysiology that do not involve electrical activity. However, GABR subunits are endogenously expressed in neurons, and the UPS in neurons is known to be influenced by neuronal activity and seizures.[15] Thus, it is necessary to

study *in vivo* proteasome activity, and so I began investigating *Gabrg2*$^{+/Q390X}$ mice and wildtype littermates.

Young mice (1-1.5 months old, shortly after seizure onset) were treated with PBA (100 mg/kg/day for 7 days) or ZNS (20 mg/kg/day for 7 days), and proteasome activity was measured using the suc-LLVY-AMC assay. The data I have so far is preliminary, with only 2-4 animals per group (wildtype vehicle, heterozygous vehicle, wildtype drug, heterozygous drug) (Figure 9 for ZNS-treated mice; PBA data not shown). I also collected preliminary data on older mice (7-8 months old) treated with ZNS, but there are 1 or 2 animals per group. More work is needed here before any discussion can be had.

Because the drug treatment experiments are underpowered, I pooled together the data from the vehicle-treated controls of each group of 1-1.5 month old mice, for an $n$ of 4 for each genotype. This data suggests a possibility of brain region specific changes, where proteasome activity in the cortex of *Gabrg2*$^{+/Q390X}$ mice is unchanged compared to wildtype littermates (1 vs 1.007 ± 0.1145, $p = 0.9553$), but the cerebellum (0.8213 ± 0.0813, $p = 0.1154$) and thalamus (0.8184 ± 0.1447, $p = 0.2982$) have decreased activity and the hippocampus (1.414 ± 0.2500, $p = 0.1961$) has increased activity, relative to controls. None of these changes are statistically significant with this initial sample size, however.

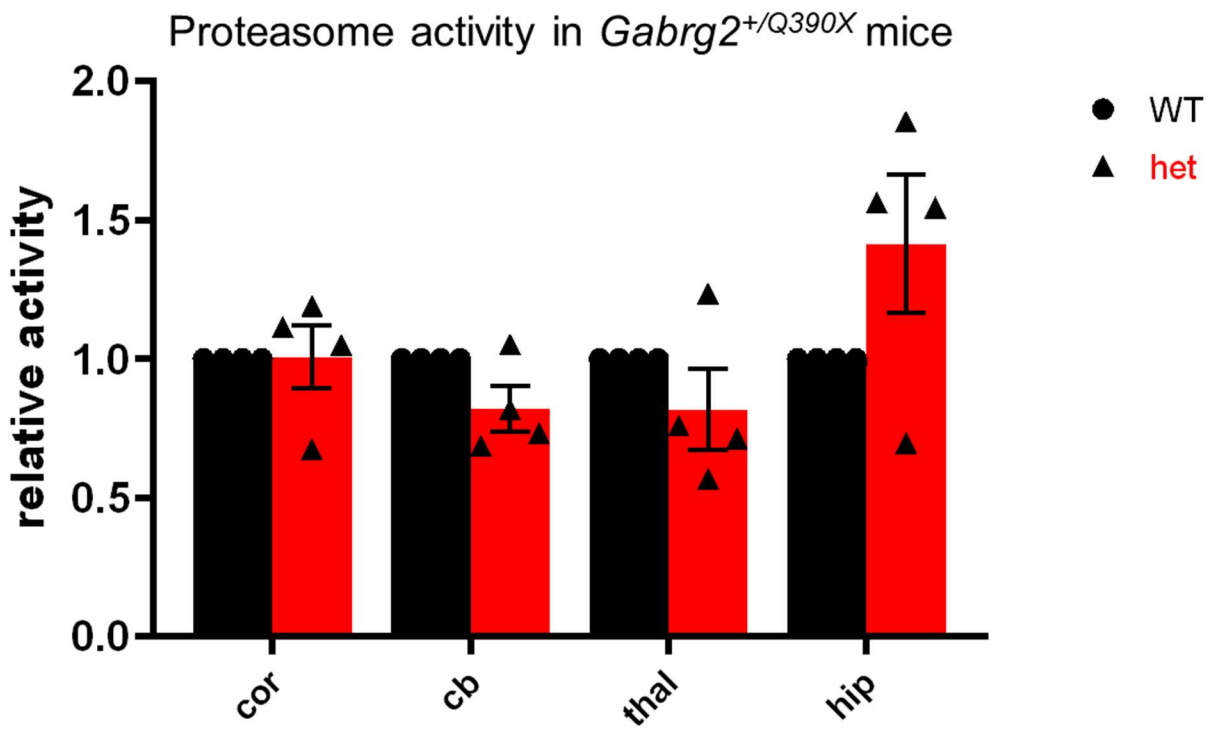


***Figure 2.10. The brains of* Gabrg$^{2+/Q390X}$ *mice may have region-specific changes in UPS activity, compared to wildtype littermates.***
Mice were 1-1.5 months of age.

## 2.4 Conclusions

### 2.4.1 Conflicting reports of the effect of the γ2(Q390X) subunit on UPS activity *in vitro*

Overall, these data present a confused picture of UPS activity in γ2(Q390X) models. Using Western blotting to measure expression of the UPS reporter GFPu, my experiments investigating the effects of increasing amounts of γ2 and γ2(Q390X) cDNA on the UPS failed to find a difference between wildtype and mutant conditions. However, using flow cytometry to measure GFPu, Katty had previously shown that γ2(Q390X) alters the UPS.

GFPu may not be sensitive to small perturbations of the UPS, especially using a semi-quantitative technique like Western blotting. It has been reported that, for pharmacological inhibitors of the chymotryptic activity of the proteasome, inhibition must exceed 70% before changes in GFPu expression are detected.[9] The use of flow cytometry may have allowed Katty to detect a difference too subtle for Western blots, and indeed the differences she reports are moderate, around 25%. Another possibility is that GFPu mRNA levels were altered between various conditions, as has been described for the similar UPS reporter $Ub^{G76V}$-GFP.[16] Additionally, constructs such as GFPu rely upon endogenous ubiquitylation machinery.[17] Given the substrate specificity of E3 ligases, it is possible that GFPu may not be affected by a dysregulation of the UPS. Furthermore, if an experimental condition modifies any component of the ubiquitylation machinery, GFPu may not be recognized and targeted for degradation in the same way in cells expressing γ2 versus γ2(Q390X). This could potentially mask other changes to the UPS, or mistakenly suggest a more global, profound dysfunction than is actually present.[18]

The discrepancies between datasets collected via suc-LLVY-AMC fluorescence are more alarming. With this technique, Katty consistently reports that γ2(Q390X) can elevate proteasome function 2-3-fold over γ2. Using the same assay, Hongmei's data shows that γ2(Q390X) only causes an increase of 35%. And, I found no difference in UPS activity via suc-LLVY-AMC fluorescence. It is only when I compared full GABRs instead of the γ2 subunit alone that I found any changes: a slight increase of 16% in cells expressing α1β2γ2(Q390X) relative to the wildtype α1β2γ2 condition.

It is possible that small differences in methodology may have a large impact. Katty's data, both with GFPu and with suc-LLVY-AMC, show a complex dose-dependent change, wherein the γ2(Q390X) mutation can result in UPS activity that is higher or lower than – or even equal to – activity in cells expressing γ2. Thus, an experimenter may inadvertently have created conditions under which all measurements are in that area of overlap. Extensive troubleshooting may be wise, including use of different transfection techniques and systematic investigation of dose-response curves with various reagents (e.g., suc-LLVY-AMC and sample protein) to ensure optimal detection of biological changes.

There are limitations to the use of fluorophores to assay chymotrypsin-like activity of the 20S core. The trypsin-like and caspase-like activity can also be measured, via fluorophores analogous to suc-LLVY-AMC. However, inclusion of these other assays is still limited to the catalytic activity of the 20S proteasome. Additional components of the complex UPS include the availability of free ubiquitin, recognition and ubiquitination of substrates by E3 ligases, recognition by the 19S regulatory particle, and unfolding of a substrate for entry to the 20S core particle.[17,19] Furthermore, spatial expression of the proteasome may change within a cell, subunit composition can change, and the activity of DUBs may become dysregulated.[15,19] Because γ2(Q390X) is highly ubiquitinated,[20] a decrease in the availability of free ubiquitin should be considered.

The extent of UPS impairments may not be apparent under physiological conditions. It is necessary to study multiple conditions to understand the impact of cell stress and how the reserve capacity of the UPS may be altered. For instance, under normal conditions, SH-SY5Y cells transfected with GFP containing a 80-glutamine repeat

(representing polyglutamine expansion disorders) do not have differences in UPS activity compared to cells transfected with control 19-glutamine GFP, but when exposed to heat shock, these cells are unable to upregulate UPS activity like control cells do.[21] Similarly, fibroblasts from patients with HD are not able to respond to overexpression of the proteasome activator PA28, which in healthy fibroblasts results in increased proteasome activity.[22] It will thus be valuable to continue investigating how the γ2(Q390X) mutant protein impacts the ability of a cell to respond to non-physiological conditions, such as the presence of low concentrations of a proteasome inhibitor or to proteasome activators.

### 2.4.2 Lack of effect of proteostasis regulators on UPS

The lack of direct effect of PBA on UPS activity in untransfected HEK293T cells is not surprising: PBA has been described as a normalizer, and so may have minimal effects on the proteasome of healthy cells. To determine what effect it may have on cells expressing α1β2γ2(Q390X) will take a higher *n* than I report here. Given that I found that the mutant condition only increases UPS activity 16%, with a standard deviation of 17%, a power analysis suggests *n* must be 99, if PBA were to alleviate the perturbation by half (so that UPS activity was only 8% higher than wildtype controls).

The effects of celastrol on the proteasome, however, have been extensively reported on. Celastrol acts as an inhibitor of the proteasome – in tumor cells, which are more sensitive to proteasomal inhibition than healthy cells.[10,23–26] Few studies have examined the effect of celastrol on the UPS in noncancerous cells, but one did find strong inhibition of UPS in human fibroblasts at 0.8 μM.[27] Therefore, my use of 0.1-1 μM for HEK293T cells is likely an appropriate range.

Celastrol is a compound for which the effects are highly dose-dependent, with a narrow therapeutic range. Much of the neuroprotective effects of celastrol are attributed to its upregulation of HSP70, but at concentrations higher than 1 μM, celastrol begins downregulating HSP70 in a dose-dependent manner.[28] Celastrol can be quite cytotoxic, at doses just barely higher than therapeutic doses – many studies report decreased cell viability with concentrations higher than 1 μM.[29–33] Cytotoxicity has even been reported at lower doses, such as 0.3 μM[34] or 0.75 μM.[28] However, I did not evaluate cell viability or cell health in my experiments; nevertheless, I used equal quantities of protein for all samples, which should minimize the impact of confounding factors.

In a lactacystin model of Parkinson's disease, administration of 1 μM celastrol not only fails to protect mouse and human neurons from lactacystin-induced cell death, it actually increased death compared to lactacystin alone.[31] Additionally, the benefits of celastrol can also be specific to particular mutations.[35] Interestingly, one study found that celastrol was most protective against oxidative damage at 0.1 μM, but did not increase HSP70 expression until 0.4 μM, suggesting that HSP70 may not be responsible for all the benefits of celastrol.[29]

These findings should all be taken under consideration, to guide understanding of how to best leverage celastrol for neurological disorders such as Dravet syndrome. It may be necessary to thoroughly characterize the kinetics of celastrol in HEK293T cells, and note that cells expressing γ2(Q390X) may respond differently from untransfected cells. Further study will also be required to determine by which mechanism celastrol is altering the physiology of cells expressing γ2(Q390X), because celastrol has diverse

functions including modulation of molecular chaperones and inflammatory factors, in addition to proteasome inhibition (see Chapter 4 for further discussion).

There have been no published studies on the effect of ZNS on proteasomal activity. Although one paper reports that ZNS prevents the parkinsonism that develops in mice treated with the proteasome inhibitor lactacystin, the paper did not address UPS function.[36]

### 2.4.3 Evaluation of UPS activity *in vivo*

The use of transfected HEK293T cells has several limitations. The most prominent limitation is also one of the benefits of using these cells: they have no electrical activity. While this allowed me to isolate the effects on proteasomal activity directly due to the accumulation of misfolded protein, this is only one component of the disease *in vivo*. The γ2(Q390X) protein is expressed in the brain, where the mutation alters the electrical activity of neurons and results in spontaneous seizures.[1] Both normal neuronal activity and seizures are known to affect the UPS, so some of the influences of γ2(Q390X) on the UPS are likely specific to neurons.[15] Another consideration is that HEK293T cells are generally collected 48 hr post transfection, meaning that they are only expressing γ2(Q390X) protein for that amount of time. Humans with the *GABRG2(Q390X)* mutation, meanwhile, express the mutant protein for years, beginning *in utero*. Finally, general protein degradation machinery is conserved across cell types, but neurons do differ from other cell types in some ways.[37,38] Transgenic mice are thus a more faithful model, as they recapitulate the epilepsy phenotype and chronically express γ2(Q390X) in neurons for weeks or months before tissue is harvested.

In mouse brains, it is not too surprising that there may not be prominent disruptions to the UPS at young ages. Impairments may only become detectable in older mice, as the γ2(Q390X) subunits accumulate and neurons become more vulnerable and begin dying. In some models of neurodegenerative diseases, deficits in proteasome activity have been reported in mice 4-6 weeks old,[39,40] but depending on the particular disease model, proteasome activity might not be altered until 3 months[18,41] or even 1 year and older.[19,40,42,43]

UPS function in genetic epilepsy is poorly studied in comparison to neurodegenerative diseases of aging, but there has been some investigation. In patient-derived cells, reduced 20S activity has been reported for DEEs resulting from mutations in the deubiquitinases OTUD7A and OTUD6B.[44,45] Additionally, fibroblasts from a patient with epilepsy and parkinsonism-pyramidal syndrome resulting from truncated FBXO7 – a component of an E3 ligase complex – show decreased 20S activity.[46] However, because these experiments did not utilize mouse brain tissue, it is difficult to extrapolate comparable ages of *Gabrg2*$^{+/Q390X}$ mice for testing.

Further experiments should test *Gabrg2*$^{+/Q390X}$ mice at multiple ages. Not only might dysfunctions not appear until later than the age used here (1.5 months), the degree or even direction of the changes may vary over time. In a mouse model of ALS, although a reduction in proteasome activity was first detected at postnatal day 45, the impairment became more severe over time.[39] Similarly, in AD Tg2576 mice, 20S activity steadily goes down between 5 and 22 months.[43] Another possibility is that an initial deficit may normalize with time, as was seen with 3xTg AD mice,[41] and activity might increase over baseline in dying neurons.[19] Prominent γ2 aggregates are not observed until

*Gabrg2*$^{+/Q390X}$ mice are 6 months old, and decreases in neuron number do not occur until 14-18 months, although signs of apoptosis such as cleaved caspase 3 and positive TUNEL staining are seen at 12 months.[1] So, in addition to mice 1.5 months old, it may be insightful to examine the 20S proteasome activity of mice at 3-4 months, 6-7 months, and 12+ months.

An additional factor to consider is the possibility of changes specific to certain types of cells, or to subcellular locations. γ2 is only expressed in neurons, so the use of whole brain lysates – which include glia and even vascular tissue – may water down proteasome changes and make them difficult to detect, if the changes are specific to neurons. Brain-region-specific changes are quite likely,[47] and may be more granular than my brain dissections: within the hippocampus, the dentate gyrus and CA1 region responded to seizures differently than other hippocampal regions.[48] Aberrations may also depend upon the health of a particular neuron, as upregulation of proteasome activity was seen specifically in degenerating neurons in a HD model.[19] Additionally, proteasomes at the synapse may react differently to disease states than proteasomes in the soma, as was found in a separate HD study.[40] Because γ2(Q390X) is retained within the ER, perhaps proteasomes near the ER will be taxed by the mutant protein more than distal proteasomes. Moreover, the overexcitation associated with epileptic activity could be preferentially impacting proteasomes near dendrites.[49–51]

My data from mice is preliminary, but it will be of interest to continue these *in vivo* experiments. It is very likely that *Gabrg2*$^{+/Q390X}$ mice have alterations in the UPS compared to wildtype mice, due to the aggregates of misfolded protein and seizures – two factors known to alter the UPS.[15] The experiments with PBA and ZNS should also

be continued, as I have shown that these proteostasis regulators reduce seizures (see Chapters 4 and 5), so these compounds likely normalize the UPS perturbations caused by epilepsy. This could have implications for the longevity of patients by preserving neuronal health into old age.

## 2.5 References


1. Kang JQ, Shen W, Zhou C, Xu D, Macdonald RL. The human epilepsy mutation GABRG2(Q390X) causes chronic subunit accumulation and neurodegeneration. *Nat Neurosci*. 2015;18(7):988-996. doi:10.1038/nn.4024

2. Harkin LA, Bowser DN, Dibbens LM, et al. Truncation of the GABAA-receptor gamma2 subunit in a family with generalized epilepsy with febrile seizures plus. *Am J Hum Genet*. 2002;70(2):530-536. doi:10.1086/338710

3. Türker F, Cook EK, Margolis SS. The proteasome and its role in the nervous system. *Cell Chem Biol*. 2021;28(7):903-917. doi:10.1016/j.chembiol.2021.04.003

4. Deriziotis P, André R, Smith DM, et al. Misfolded PrP impairs the UPS by interaction with the 20S proteasome and inhibition of substrate entry. *EMBO J*. 2011;30(15):3065-3077. doi:10.1038/emboj.2011.224

5. Holmberg CI, Staniszewski KE, Mensah KN, Matouschek A, Morimoto RI. Inefficient degradation of truncated polyglutamine proteins by the proteasome. *EMBO J*. 2004;23(21):4307-4318. doi:10.1038/sj.emboj.7600426

6. Wang HL, He CY, Chou AH, Yeh TH, Chen YL, Li AH. Polyglutamine-expanded ataxin-7 decreases nuclear translocation of NF-kappaB p65 and impairs NF-kappaB activity by inhibiting proteasome activity of cerebellar neurons. *Cell Signal*. 2007;19(3):573-581. doi:10.1016/j.cellsig.2006.08.006

7. Rao SNR, Maity R, Sharma J, et al. Sequestration of chaperones and proteasome into Lafora bodies and proteasomal dysfunction induced by Lafora disease-associated mutations of malin. *Hum Mol Genet*. 2010;19(23):4726-4734. doi:10.1093/hmg/ddq407

8. Mermer F, Poliquin S, Rigsby K, et al. Common molecular mechanisms of SLC6A1 variant-mediated neurodevelopmental disorders in astrocytes and neurons. *Brain J Neurol*. 2021;144(8):2499-2512. doi:10.1093/brain/awab207

9. Bence NF, Bennett EJ, Kopito RR. Application and analysis of the GFPu family of ubiquitin-proteasome system reporters. *Methods Enzymol*. 2005;399:481-490. doi:10.1016/S0076-6879(05)99033-2

10. Yang H, Chen D, Cui QC, Yuan X, Dou QP. Celastrol, a triterpene extracted from the Chinese “Thunder of God Vine,” is a potent proteasome inhibitor and suppresses human prostate cancer growth in nude mice. *Cancer Res*. 2006;66(9):4758-4765. doi:10.1158/0008-5472.CAN-05-4529

11. Santos-Laso A, Izquierdo-Sanchez L, Rodrigues PM, et al. Proteostasis disturbances and endoplasmic reticulum stress contribute to polycystic liver disease: New therapeutic targets. *Liver Int Off J Int Assoc Study Liver*. 2020;40(7):1670-1685. doi:10.1111/liv.14485

12. Reddy SS, Shruthi K, Joy D, Reddy GB. 4-PBA prevents diabetic muscle atrophy in rats by modulating ER stress response and ubiquitin-proteasome system. *Chem Biol Interact*. 2019;306:70-77. doi:10.1016/j.cbi.2019.04.009

13. Shruthi K, Reddy SS, Reddy GB. Ubiquitin-proteasome system and ER stress in the retina of diabetic rats. *Arch Biochem Biophys*. 2017;627:10-20. doi:10.1016/j.abb.2017.06.006

14. Kang JQ, Shen W, Macdonald RL. Why does fever trigger febrile seizures? GABAA receptor gamma2 subunit mutations associated with idiopathic generalized epilepsies have temperature-dependent trafficking deficiencies. *J Neurosci Off J Soc Neurosci*. 2006;26(9):2590-2597. doi:10.1523/JNEUROSCI.4243-05.2006

15. Poliquin S, Kang JQ. Disruption of the Ubiquitin-Proteasome System and Elevated Endoplasmic Reticulum Stress in Epilepsy. *Biomedicines*. 2022;10(3):647. doi:10.3390/biomedicines10030647

16. Bowman AB, Yoo SY, Dantuma NP, Zoghbi HY. Neuronal dysfunction in a polyglutamine disease model occurs in the absence of ubiquitin-proteasome system impairment and inversely correlates with the degree of nuclear inclusion formation. *Hum Mol Genet*. 2005;14(5):679-691. doi:10.1093/hmg/ddi064

17. Hernández F, Díaz-Hernández M, Avila J, Lucas JJ. Testing the ubiquitin-proteasome hypothesis of neurodegeneration in vivo. *Trends Neurosci*. 2004;27(2):66-69. doi:10.1016/j.tins.2003.12.002

18. Bett JS, Goellner GM, Woodman B, Pratt G, Rechsteiner M, Bates GP. Proteasome impairment does not contribute to pathogenesis in R6/2 Huntington's disease mice: exclusion of proteasome activator REGgamma as a therapeutic target. *Hum Mol Genet*. 2006;15(1):33-44. doi:10.1093/hmg/ddi423

19. Díaz-Hernández M, Hernández F, Martín-Aparicio E, et al. Neuronal induction of the immunoproteasome in Huntington's disease. *J Neurosci Off J Soc Neurosci*. 2003;23(37):11653-11661.

20. Kang JQ, Shen W, Macdonald RL. Trafficking-deficient mutant GABRG2 subunit amount may modify epilepsy phenotype. *Ann Neurol*. 2013;74(4):547-559. doi:10.1002/ana.23947

21. Ding Q, Lewis JJ, Strum KM, et al. Polyglutamine expansion, protein aggregation, proteasome activity, and neural survival. *J Biol Chem*. 2002;277(16):13935-13942. doi:10.1074/jbc.M107706200

22. Seo H, Sonntag KC, Isacson O. Generalized brain and skin proteasome inhibition in Huntington's disease. *Ann Neurol*. 2004;56(3):319-328. doi:10.1002/ana.20207

23. Ge P, Ji X, Ding Y, et al. Celastrol causes apoptosis and cell cycle arrest in rat glioma cells. *Neurol Res*. 2010;32(1):94-100. doi:10.1179/016164109X12518779082273

24. Zhong YL, Xu GJ, Huang S, et al. Celastrol induce apoptosis of human multiple myeloma cells involving inhibition of proteasome activity. *Eur J Pharmacol*. 2019;853:184-192. doi:10.1016/j.ejphar.2019.03.036

25. Wang WB, Feng LX, Yue QX, et al. Paraptosis accompanied by autophagy and apoptosis was induced by celastrol, a natural compound with influence on proteasome, ER stress and Hsp90. *J Cell Physiol*. 2012;227(5):2196-2206. doi:10.1002/jcp.22956

26. Boridy S, Le PU, Petrecca K, Maysinger D. Celastrol targets proteostasis and acts synergistically with a heat-shock protein 90 inhibitor to kill human glioblastoma cells. *Cell Death Dis*. 2014;5:e1216. doi:10.1038/cddis.2014.182

27. Mu TW, Ong DST, Wang YJ, et al. Chemical and biological approaches synergize to ameliorate protein-folding diseases. *Cell*. 2008;134(5):769-781. doi:10.1016/j.cell.2008.06.037

28. Chow AM, Brown IR. Induction of heat shock proteins in differentiated human and rodent neurons by celastrol. *Cell Stress Chaperones*. 2007;12(3):237-244. doi:10.1379/csc-269.1

29. Sun H, Xu L, Yu P, Jiang J, Zhang G, Wang Y. Synthesis and preliminary evaluation of neuroprotection of celastrol analogues in PC12 cells. *Bioorg Med Chem Lett*. 2010;20(13):3844-3847. doi:10.1016/j.bmcl.2010.05.066

30. Petrović A, Kaur J, Tomljanović I, Nistri A, Mladinic M. Pharmacological induction of Heat Shock Protein 70 by celastrol protects motoneurons from excitotoxicity in rat spinal cord in vitro. *Eur J Neurosci*. 2019;49(2):215-231. doi:10.1111/ejn.14218

31. Konieczny J, Jantas D, Lenda T, et al. Lack of neuroprotective effect of celastrol under conditions of proteasome inhibition by lactacystin in in vitro and in vivo studies: implications for Parkinson's disease. *Neurotox Res*. 2014;26(3):255-273. doi:10.1007/s12640-014-9477-9

32. Chow AM, Tang DWF, Hanif A, Brown IR. Localization of heat shock proteins in cerebral cortical cultures following induction by celastrol. *Cell Stress Chaperones*. 2014;19(6):845-851. doi:10.1007/s12192-014-0508-5

33. Jantas D, Roman A, Kuśmierczyk J, et al. The extent of neurodegeneration and neuroprotection in two chemical in vitro models related to Parkinson's disease is critically dependent on cell culture conditions. *Neurotox Res*. 2013;24(1):41-54. doi:10.1007/s12640-012-9374-z

34. Kalmar B, Greensmith L. Activation of the heat shock response in a primary cellular model of motoneuron neurodegeneration-evidence for neuroprotective and neurotoxic effects. *Cell Mol Biol Lett*. 2009;14(2):319-335. doi:10.2478/s11658-009-0002-8

35. Gentil BJ, Mushynski WE, Durham HD. Heterogeneity in the properties of NEFL mutants causing Charcot-Marie-Tooth disease results in differential effects on neurofilament assembly and susceptibility to intervention by the chaperone-inducer, celastrol. *Int J Biochem Cell Biol*. 2013;45(7):1499-1508. doi:10.1016/j.biocel.2013.04.009

36. Bentea E, Van Liefferinge J, Verbruggen L, et al. Zonisamide attenuates lactacystin-induced parkinsonism in mice without affecting system xc<sup/>. *Exp Neurol*. 2017;290:15-28. doi:10.1016/j.expneurol.2016.12.009

37. Lottes EN, Cox DN. Homeostatic Roles of the Proteostasis Network in Dendrites. *Front Cell Neurosci*. 2020;14:264. doi:10.3389/fncel.2020.00264

38. Birdsall V, Waites CL. Autophagy at the synapse. *Neurosci Lett*. 2019;697:24-28. doi:10.1016/j.neulet.2018.05.033

39. Kabashi E, Agar JN, Taylor DM, Minotti S, Durham HD. Focal dysfunction of the proteasome: a pathogenic factor in a mouse model of amyotrophic lateral sclerosis. *J Neurochem*. 2004;89(6):1325-1335. doi:10.1111/j.1471-4159.2004.02453.x

40. Wang J, Wang CE, Orr A, Tydlacka S, Li SH, Li XJ. Impaired ubiquitin–proteasome system activity in the synapses of Huntington's disease mice. *J Cell Biol*. 2008;180(6):1177-1189. doi:10.1083/jcb.200709080

41. Tseng BP, Green KN, Chan JL, Blurton-Jones M, LaFerla FM. Abeta inhibits the proteasome and enhances amyloid and tau accumulation. *Neurobiol Aging*. 2008;29(11):1607-1618. doi:10.1016/j.neurobiolaging.2007.04.014

42. Chen L, Thiruchelvam MJ, Madura K, Richfield EK. Proteasome dysfunction in aged human α-synuclein transgenic mice. *Neurobiol Dis*. 2006;23(1):120-126. doi:10.1016/j.nbd.2006.02.004

43. Oh S, Hong HS, Hwang E, et al. Amyloid peptide attenuates the proteasome activity in neuronal cells. *Mech Ageing Dev*. 2005;126(12):1292-1299. doi:10.1016/j.mad.2005.07.006

44. Garret P, Ebstein F, Delplancq G, et al. Report of the first patient with a homozygous OTUD7A variant responsible for epileptic encephalopathy and related proteasome dysfunction. *Clin Genet*. 2020;97(4):567-575. doi:10.1111/cge.13709

45. Santiago-Sim T, Burrage LC, Ebstein F, et al. Biallelic Variants in OTUD6B Cause an Intellectual Disability Syndrome Associated with Seizures and Dysmorphic Features. *Am J Hum Genet*. 2017;100(4):676-688. doi:10.1016/j.ajhg.2017.03.001

46. Correa-Vela M, Lupo V, Montpeyó M, et al. Impaired proteasome activity and neurodegeneration with brain iron accumulation in FBXO7 defect. *Ann Clin Transl Neurol*. 2020;7(8):1436-1442. doi:10.1002/acn3.51095

47. Cheroni C, Marino M, Tortarolo M, et al. Functional alterations of the ubiquitin-proteasome system in motor neurons of a mouse model of familial amyotrophic lateral sclerosis†. *Hum Mol Genet*. 2009;18(1):82-96. doi:10.1093/hmg/ddn319

48. Engel T, Martinez-Villarreal J, Henke C, et al. Spatiotemporal progression of ubiquitin-proteasome system inhibition after status epilepticus suggests protective adaptation against hippocampal injury. *Mol Neurodegener*. 2017;12(1):21. doi:10.1186/s13024-017-0163-2

49. Ehlers MD. Activity level controls postsynaptic composition and signaling via the ubiquitin-proteasome system. *Nat Neurosci*. 2003;6(3):231-242. doi:10.1038/nn1013

50. Djakovic SN, Schwarz LA, Barylko B, DeMartino GN, Patrick GN. Regulation of the proteasome by neuronal activity and calcium/calmodulin-dependent protein kinase II. *J Biol Chem*. 2009;284(39):26655-26665. doi:10.1074/jbc.M109.021956

51. Bingol B, Schuman EM. Activity-dependent dynamics and sequestration of proteasomes in dendritic spines. *Nature*. 2006;441(7097):1144-1148. doi:10.1038/nature04769

# 3 Characterization of Autophagy in *GABRG2(Q390X)* Models

## 3.1 Introduction

Dravet syndrome is a severe developmental and epileptic encephalopathy (DEE) with diverse genetic causes. The most common causative gene, representing approximately 80% of cases, is *SCN1A*, which encodes $Na_V1.1$, the alpha subunit of the voltage-gated sodium channel.[1] These mutations are often nonsense mutations and result in no protein product.[1] However, a mutation in the γ2 subunit of the $GABA_A$ receptor, *GABRG2(Q390X)*, is also associated with Dravet syndrome.[2] This mutation results in a truncated protein that is severely misfolded and highly stable.[3] The γ2(Q390X) protein readily forms dimers and larger oligomers, including intracellular protein aggregates.[3,4] This is in stark contrast to the *SCN1A* mutations, and thus presents a very different molecular pathology, with implications for patient-specific selection of current therapeutics and for the development of additional therapeutics. Therefore, I have studied how the γ2(Q390X) mutant protein affects cellular proteostasis.

### 3.1.1 Autophagy and its role in healthy neurons

Cells have two primary pathways for disposing of misfolded proteins and other cellular waste, such as damaged organelles. One is the ubiquitin-proteasome system (UPS), by which individual proteins are fed into the proteasome and cleaved into small polypeptides. These polypeptides are recycled as amino acids for new proteins.[5] The

other pathway is autophagy, which can be further divided into microautophagy, chaperone mediated autophagy, and macroautophagy. This chapter focuses on macroautophagy, which will be henceforth referred to simply as “autophagy.” Autophagy uses a lipid bilayer to engulf cargo in a vesicle called the autophagosome, which then fuses with the lysosome to form an autolysosome.[6,7] The cargo is then broken down by the plethora of degradative enzymes contained within the lysosome.[7] Autophagy thus is more suited to larger complexes such as protein aggregates than is the UPS.[6] Because γ2(Q390X) forms aggregates, we asked if the continuous presence of misfolded, aggregated protein was taxing the autophagy system.

There are several key proteins involved in autophagy that will be explored in this chapter. The initiation of autophagosome formation is regulated by beclin-1; beclin-1 deficits therefore are associated with fewer autophagosomes.[8] Microtubule-associated proteins 1A/1B light chain 3B (LC3B) is involved in the expansion of the nascent autophagosome. LC3B is cleaved to produce LC3B-I, which is then conjugated with phosphatidylethanolamine to produce LC3B-II.[9] It is this conjugated form that is found in the autophagosomal membrane and is thus degraded in the final stages of autophagy.[10,11] An increase in LC3B-II consequently signifies an increase in the number of autophagosomes, which may be due to decreased degradation, or to induction of autophagy.[10] Therefore, investigating the ratio between the conjugated and unconjugated forms is an essential marker of autophagic flux.[9] LC3B – as well as related proteins like LC3A – directly interacts with another important autophagy protein, p62, also called sequestosome 1 (SQSTM1).[6] Like LC3B-II, p62 is also degraded in the final stages of autophagy, and thus inhibition of autophagy results in elevated p62.[6,12]

Finally the endoplasmic reticulum (ER) chaperone GRP78/BiP, which primarily assists folding of nascent proteins and regulates the unfolded protein response, also plays a crucial role in initiating autophagy.[13]

Neurons are highly sensitive to disruptions of autophagy, due to their post-mitotic state that prevents dispersal of protein aggregates and damaged organelles via mitosis, as well as due to their unique cytoarchitecture with far-reaching branches.[14,15] Autophagy is thus critical to neuronal survival.[16,17] Furthermore, properly balanced autophagy is necessary for neurodevelopment, and autophagy also plays a complex role in regulating synaptic proteins.[14,15] Unsurprisingly, then, healthy neurons have a high rate of autophagic flux, both rapidly inducing the formation of new autophagosomes when necessary and quickly degrading the contents.[18,19] The relationship between autophagy and neuronal health is complex, as autophagy impairments can lead to the accumulation of neurotoxic protein aggregates, and conversely the chronic presence of misfolded proteins can cause alterations in autophagy. Additionally, impaired autophagy can be both a cause and a result of seizure activity, which will be discussed in more detail below.

### 3.1.2 Autophagy in neurodegenerative diseases

The study of protein folding diseases, including neurodegenerative disorders, has been useful for developing understanding of the role of autophagy in neuronal health, as these diseases are generally associated with disruptions of autophagy. In the case of Huntington's disease (HD), autophagy is necessary to degrade mutant huntingtin (mHtt), as mHtt aggregates colocalize with p62 and LC3, and knockdown of p62 results

in increased apoptosis in cells transfected with GFP-HttQ68.[12] Similarly, beclin-1 knockdown results in formation of oligomers and aggregates of expanded polyQ Htt, by reducing the autophagic degradation of the mutant protein.[8] The functional deficit of beclin-1 is neurotoxic, as *Becn1*$^{+/-}$ mice have fewer autophagosomes and fewer synapses.[20] Conversely, expanded polyQ Htt interferes with the normal degradation of protein by beclin-1, by recruiting beclin-1 away from the trans-Golgi network to cytoplasmic aggregates.[8] Thus, there is a cycle whereby mutant protein oligomers sequester beclin-1, which impairs autophagy, which results in further accumulation of mutant protein.

Parkinson's disease (PD), too, is associated with changes in autophagy. P62 colocalizes with the Lewy bodies characteristic of PD.[6] Neurons overexpressing α-synuclein have reduced ability to upregulate autophagy in response to nutrient starvation.[21] However, these deficits can be overcome by overexpression of beclin-1, which reduces α-synuclein and prevents loss of synapses, by enhancing autophagy.[21]

Lafora disease is an excellent example of the crucial role autophagy plays in neuronal diseases. This genetic neurodegenerative and epileptic disease, characterized by intracellular inclusions of glycogen and protein dubbed Lafora bodies, is associated with impaired initiation of autophagy.[22–24] Lafora bodies colocalize with ubiquitin, BiP, and p62, which may sequester p62, hampering fulfillment of its normal roles.[23,24] Mutations in one of two proteins, laforin (*EPM2A*) and malin (*EPM2B*), account for the majority of Lafora disease cases.[24] Both proteins are directly involved in autophagy, ubiquitinating beclin-1 – and other components of the PI3KC3 complex that initiates autophagy – to stabilize it with K63-linked polyubiquitin chains.[22] Additionally, both

laforin and malin deficits are associated with lower LC3-II and poor initiation of autophagosome formation.[23,24] Furthermore, even under autophagy-inducing conditions, LC3-II remains low and fibroblasts demonstrate a diminished ability to upregulate autophagy.[23,24] Intriguingly, some of this pathology is seen well before the formation of Lafora bodies and the development of epilepsy, suggesting that impaired autophagy contributes to epilepsy, rather than being simply a consequence of seizures.[23]

### 3.1.3 Autophagy in epilepsy

Autophagy plays a complex role in genetic and acquired epilepsies. As mentioned above, deficits in autophagy can result in epilepsy, yet inversely, seizures can alter autophagic flux. Moreover, autophagy can play a neuroprotective role, preventing the neuronal death that follows seizures, or it can contribute to that death.

Epilepsy is common in congenital disorders of autophagy, and many genes have been implicated. The tuberous sclerosis genes *TSC1* and *TSC2* are perhaps some of the most well-understood, but many less prevalent mutations have been discovered in other components of the autophagy pathway, in patients with neurodevelopmental disorders and epilepsy.[14] Tuberous sclerosis results from mutations of the mTOR complex, which has a multitude of functions beyond regulation of autophagy; thus, it is possible the seizures that occur in tuberous sclerosis are not due to impaired autophagy but rather to deficits in other functions of mTOR.[14] To address this question, a conditional transgenic mouse, in which *Atg7* is knocked out in neurons that express CaMKIIα, was generated. ATG7 acts downstream of mTOR and is an E1-like ligase involved in the lipidation of LC3-I to form LC3-II and thus plays an important role in the

formation of autophagosomes.[25] In this Atg7$^{flox/flox}$; CaMKIIα-Cre model, almost no LC3-II was detected, as expected, while p62 was elevated.[25] Interestingly, approximately 75% of these *Atg7* KO mice developed spontaneous seizures, typically around postnatal week 8-10, confirming that disruption of autophagy is epileptogenic.[25] Further support for the epileptogenic nature of impaired autophagy comes from WDR45, a gene involved in the formation of autophagosomes.[26] Mutations in this gene are found in patients with beta-propeller protein-associated neurodegeneration (BPAN) and DEEs.[26]

Although the mechanisms by which autophagy deficits cause seizures are likely multifold, GABAergic signaling may be involved. The level of GABA itself may be altered, as the metabolic changes due to compromised autophagy may direct GABA into GABA shunt Krebs cycle for energy, thereby decreasing GABA.[27] GABA receptors are also affected by deficits in autophagy: in conditional *Atg7* KO mice, the ATG8-like proteins GABARAP, GABARAPL1, and GABARAPL2 are sequestered away in p62-positive aggregates.[28] These proteins are involved in the trafficking of GABR to the cell surface, so this sequestration results in less efficient trafficking of GABR and decreased GABR surface expression.[28] Similar effects on GABR expression were seen in a *Tsc2* knockdown.[28] Interestingly, the elevation of p62 caused by knockdown of Ulk2, a serine/threonine-protein kinase involved in activating autophagy, in *Ulk2*$^{+/-}$ mice resulted in decreased surface GABR, leading to imbalanced excitation and inhibition.[29] A similar connection between p62 and GABR surface expression is seen in a mouse model of depression, confirming that autophagic dysregulation of p62 governs GABR trafficking.[30]

In acquired epilepsies, perturbations of autophagy are also observed. After induction of status epilepticus (SE) in rats, autophagy is upregulated within hours and remains elevated for several days.[31–33] Apoptotic cell death occurred within 48 hr of SE, suggesting that this elevation of autophagy may be harmful.[33] Similar changes to LC3-II/LC3-I ratio, beclin-1, and p62, as well as widespread apoptosis, were seen at 4 weeks in an SE mouse model.[34] Additionally, this study found that HMGB1, an inducer of autophagy, was upregulated after SE.[34] They therefore treated mice with either an antibody for HMGB1 or the autophagy inhibitor 3-methyladenine (3-MA), and found that both treatments attenuated the changes in autophagy-related proteins and reduced the amount of apoptosis that occurred after SE.[34] Astrocytes, too, die after SE and have increased autophagy, further supporting the hypothesis that excess autophagy after seizures is detrimental.[35]

However, upregulation of autophagy has also been suggested to be protective. After inducing SE in mice, inspection of the hippocampus revealed upregulated autophagy and lysosomal activity in specific populations of neurons, while the apoptosis marker cleaved caspase-3 was only found in different cells.[36] Hence, the upregulated autophagy in hippocampal neurons may be protective.[36] Additionally, upregulating autophagy prior to SE induction via activation of the cannabinoid receptor type 2 (CB2R) mitigated neuronal loss.[37] Interestingly, autophagy was also upregulated to a lesser extent in untreated animals, compared to control mice that did not have seizures evoked, leading the authors to conclude that autophagy is protective and apoptosis occurs only after autophagy has failed to maintain neuronal health after SE.[37] Of note, however, is a study that found only transient changes in the LC3-II/LC3-I ratio,

indicating that SE results in temporary impairment of lysosomal degradation rather than upregulation of autophagy.[38] Thus, while it is clear that autophagy and seizures are linked, the exact nature of the association is not yet fully understood.

In non-neuronal cells, the interplay between autophagy and cell health is also complex. Suppression of autophagy can lead to ER stress, more polyubiquitinated proteins, and apoptosis.[11] Relatedly, in the presence of misfolded proteins – like the mutant α1-antitrypsin Z protein and polyglutamine expansion proteins – that induce ER stress and autophagy, the inhibition of autophagy increases cytotoxicity.[11,39] Yet, genetically or pharmacologically autophagy-deficient cells have *less* apoptosis after treatment with various ER stress inducers, compared to control cells.[11] The authors suggest that, in cells with a large capacity for protein degradation, induction of autophagy may excessively remove "bystander" proteins, with negative consequences for cell viability.[11]

It is clear, however, that the GABRG2(Q390X) mutation almost certainly results in dysregulated autophagy, between the impact of chronic epilepsy on autophagy and the presence of misfolded protein aggregates. It is important to disentangle the contributions of these two factors, as dysregulated autophagy due to seizures can likely be at least partially attenuated by AEDs, while the misfolded proteins more resembles a neurodegenerative disorder. Autophagy impairment due to misfolded proteins would be a fairly novel mechanism in an epilepsy and opens the door to new classes of treatments. In order to tease apart the mechanism, we utilized two model systems. One

model is transfected HEK293T cells. These non-excitable cells do not have seizure activity, and thus are a model only of proteostasis impairments.

Our second set of experiments involved two different mouse lines: *Scn1a*$^{+/-}$ and *Gabrg2*$^{+/Q390X}$. Both mouse lines are models of Dravet syndrome and have very similar phenotypes. For instance, the onset of spontaneous seizures is in the end of the third postnatal week for both lines: P19 for *Gabrg2*$^{+/Q390X}$ and P21 for *Scn1a*$^{+/-}$ mice.[4,40] Because of the recurrent seizures, both lines are both expected to have dysregulated autophagy. However, the disease-causing mutation in *Gabrg2*$^{+/Q390X}$ results in misfolded protein while *Scn1a*$^{+/-}$ has a null allele. Therefore, any differences in proteostasis between these two mice is likely due to the mutation-specific effect of chronic presence of misfolded protein.

## 3.2 Methods

### 3.2.1 Cell culture and polyethyleneimine transfection

Human embryonic kidney 293 T (HEK293T) cells were grown in Dulbecco's Modified Eagle's Medium (DMEM) supplemented with 10% FBS and 1% penicillin/streptomycin. 24 hours after plating the cells, they were transfected with cDNA for wildtype rat GABR γ2S or γ2S(Q390X) subunits (referred to hereafter simply as γ2 or γ2(Q390X) subunits, respectfully), human GABR α1 subunit, human GABR β2 subunit, and/or empty vector pcDNA. cDNA was combined with polyethyleneimine (PEI) at a ratio of 2.5 µL PEI per 1 µg cDNA. Brefeldin-A (BFA) (Sigma-Aldrich B6542) was dissolved in dimethyl sulfoxide (DMSO) and used at a concentration of 5 µg/mL.

### 3.2.2 Immunoblot

Cells were harvested 48 hr after transfection. Cells were washed with cold phosphate buffered saline (PBS) and lysed with RIPA-PI solution containing 20 mM Tris, 20 mM EGTA, 1 mM DTT, 1 mM benzamidine, 0.01 mM PMSF, 0.005 µg/mL leupeptin, and 0.005 µg/mL pepstatin. Protein concentration was measured and samples were subjected to standard SDS polyacrylamide gel electrophoresis (SDS-PAGE) procedures and immunoblotted. Primary antibodies used were anti-α1 1:500 (Millipore Sigma MABN489), anti-γ2 1:1,000 (Synaptic Systems 224003), anti-beclin-1 1:1,500 (Novus Biologicals NBP1-00088), anti-BiP 1:300 (BD Biosciences 610979), anti-LC3 1:1,000 (Novus Biologicals NB100-2220), anti-p62 1:300 (Abnova H00008878-M01), anti-β-actin 1:6,000 (ABclonal AC006), and anti-ATPase 1:1,000 (Developmental Studies Hybridoma Bank a6F). Secondary antibodies were LI-COR IRDye 680LT Goat anti-Mouse IgG Secondary Antibody (926-68020) and IRDye 800CW Goat anti-Rabbit IgG Secondary Antibody (926-32211), both 1:10,000.

Blots were imaged with an Odyssey DLx digital fluorescence scanner and LI-COR Image Studio Lite 5.2 software. Protein bands were quantified by circumscribing the band of interest and correcting for background signal. Integrated density values (IDVs) for the protein of interest were normalized to the IDV for the loading control, ATPase. The values were then normalized to loading controls and then the normalized IDV of the control lane (generally, wildtype or untreated), which was arbitrarily taken as equal to 1.

### 3.2.3 Mice

The generation of the *Gabrg2*$^{+/Q390X}$ mouse is described previously[4] and the line was maintained in C57BL/6J (Jackson Labs stock #000664). *Scn1a*$^{+/-}$ mice (Jackson Laboratory #024761) were generously provided by Dr. Jennifer Kearney at Vanderbilt University and maintained on a C57BL/6J × 129S6/SvEvTac background.[41] Animals were housed in standard facilities with ad libitum food and water access.

### 3.2.4 Immunohistochemistry

At postnatal day 21 (P21), mice were anesthetized with isoflurane and sacrificed via decapitation. Brains were harvested, fixed in 4% paraformaldehyde for 30 minutes, and stored in 30% sucrose at 4°C overnight. Both paraformaldehyde and sucrose solutions were in 0.1 M phosphate buffer (0.1 M $NaH_2PO_4$ + 0.1 M $Na_2HPO_4$) pH 7.4. Next, the brains were frozen in Tissue-Tek OCT Compound (#4583) on dry ice before being coronally sectioned on a cryostat to create slices 30 µM thick. Primary antibodies were anti-parvalbumin 1:300 – 1:100 (GenScript A01439) and anti-p62 1:200 – 1:100 (Abnova H00008878-M01). Secondary antibodies were Alexa Fluor 488 donkey anti-mouse (Invitrogen A21202) and Alexa Fluor 555 goat anti-rabbit (Invitrogen A21429), both 1:400. TO-PRO-3 1:500 (Invitrogen T3605) was used as a nuclear marker.

### 3.2.5 Data analysis

Data were analyzed using GraphPad Prism 9.4 and is reported as mean ± standard error of the mean (SEM). For the cell culture experiments, two-way analysis of variance (ANOVA) tests were performed and post-hoc analyses were performed as reported in the text, corrected for multiple comparisons. For the mouse immunohistochemistry

experiments, one-way ANOVAs and Šídák's multiple comparisons post-hoc analysis were performed. Statistical significance was taken as $p < 0.05$ throughout.

## 3.3 Results

### 3.3.1 Dose-dependent effects on LC3 from γ2 but not γ2(Q390X)

To investigate the effects of γ2(Q390X) on autophagy, HEK293T cells were transfected with increasing amounts of cDNA for wildtype γ2 or mutant γ2(Q390X) (total cDNA was normalized to 4 μg with empty vector pcDNA). Beclin-1, BiP, LC3, and p62 were examined. For beclin-1, no differences were seen across genotype or cDNA dose. P62 and BiP likewise had no difference. For LC3, we examined the ratio between LC3B-II and LC3B-I, as it gives a better view of autophagic flux. The ratio LC3B-II/LC3B-I was elevated for the 4 μg dose of γ2, compared to the 0.5 μg dose. Conversely, for γ2(Q390X), all conditions were equal to the low dose of γ2. The change in ratio was driven by a large increase in LC3B-II, while LC3B-I remained stable.

***Table 3.1. p values of the effects of increasing amounts of cDNA, genotype of γ2, and the interaction of these factors on various autophagy factors.***

| | µg cDNA | Genotype | Interaction |
|---|---|---|---|
| Beclin-1 | 0.2840 | 0.8439 | 0.8340 |
| BiP | 0.2972 | 0.5288 | 0.5732 |
| LC3B-II/LC3B-I | 0.0650 | **0.0199** | 0.0564 |
| LC3B-I | 0.6794 | 0.8685 | 0.4721 |
| LC3B-II | 0.1755 | **0.0201** | 0.0803 |
| p62 | 0.5913 | 0.1215 | 0.9413 |
| γ2 | **0.0006** | **<0.0001** | 0.5455 |

Expression of LC3B-II differs in the presence of mutant γ2(Q390X) protein compared to wildtype γ2 protein. Significant values ($p < 0.05$) are bolded. Two-way ANOVA, $n$ = 5-6.

***Table 3.2. Post-hoc analysis of LC3.***

| | 0.5 | 1 | 2 | 4 |
|---|---|---|---|---|
| LC3B-II/LC3B-I | | | | |
| WT | | 1.346 ± 0.221; 0.2217 | 1.354 ± 0.138; 0.2066 | **1.798 ± 0.090; 0.0011** |
| Q390X | 1.156 ± 0.076 | 1.050 ± 0.235; 0.9129 | 1.168 ± 0.094; 0.9999 | 1.140 ± 0.125; 0.9999 |
| | | | | |
| LC3B-I | | | | |
| WT | | 1.432 ± 0.568; 0.9446 | 1.354 ± 0.332; 0.9680 | 2.094 ± 0.851; 0.5437 |
| Q390X | 1.272 ± 0.267 | 2.325 ± 1.542; 0.5533 | 1.036 ± 0.353; 0.9899 | 0.896 ± 0.193; 0.9622 |
| | | | | |
| LC3B-II | | | | |
| WT | | 1.590 ± 0.519; 0.7048 | 1.824 ± 0.536; 0.4688 | **3.250 ± 0.998; 0.0052** |
| Q390X | 1.296 ± 0.194 | 1.072 ± 0.227; 0.9742 | 1.004 ± 0.202; 0.9462 | 1.046 ± 0.280; 0.9649 |
| | | | | |
| γ2 | | | | |
| WT | | 2.957 ± 1.027; 0.9824 | 7.105 ± 4.535; 0.6822 | 14.882 ± 5.825; 0.1065 |
| Q390X | 10.542 ± 2.519 | 15.493 ± 3.535; 0.8089 | 23.722 ± 4.004; 0.1541 | **37.632 ± 9.095; 0.0010** |

The genotype difference in LC3B-II/LC3B-I is due to an increase in LC3B-II in cells expressing high amounts of γ2 protein. Values are expressed as mean ± SEM and the *p* value of the comparison to the 0.5 μg cDNA condition for that respective genotype. Significant values ($p < 0.05$) are bolded. Dunnett's multiple comparisons test, $n = 5$-6.

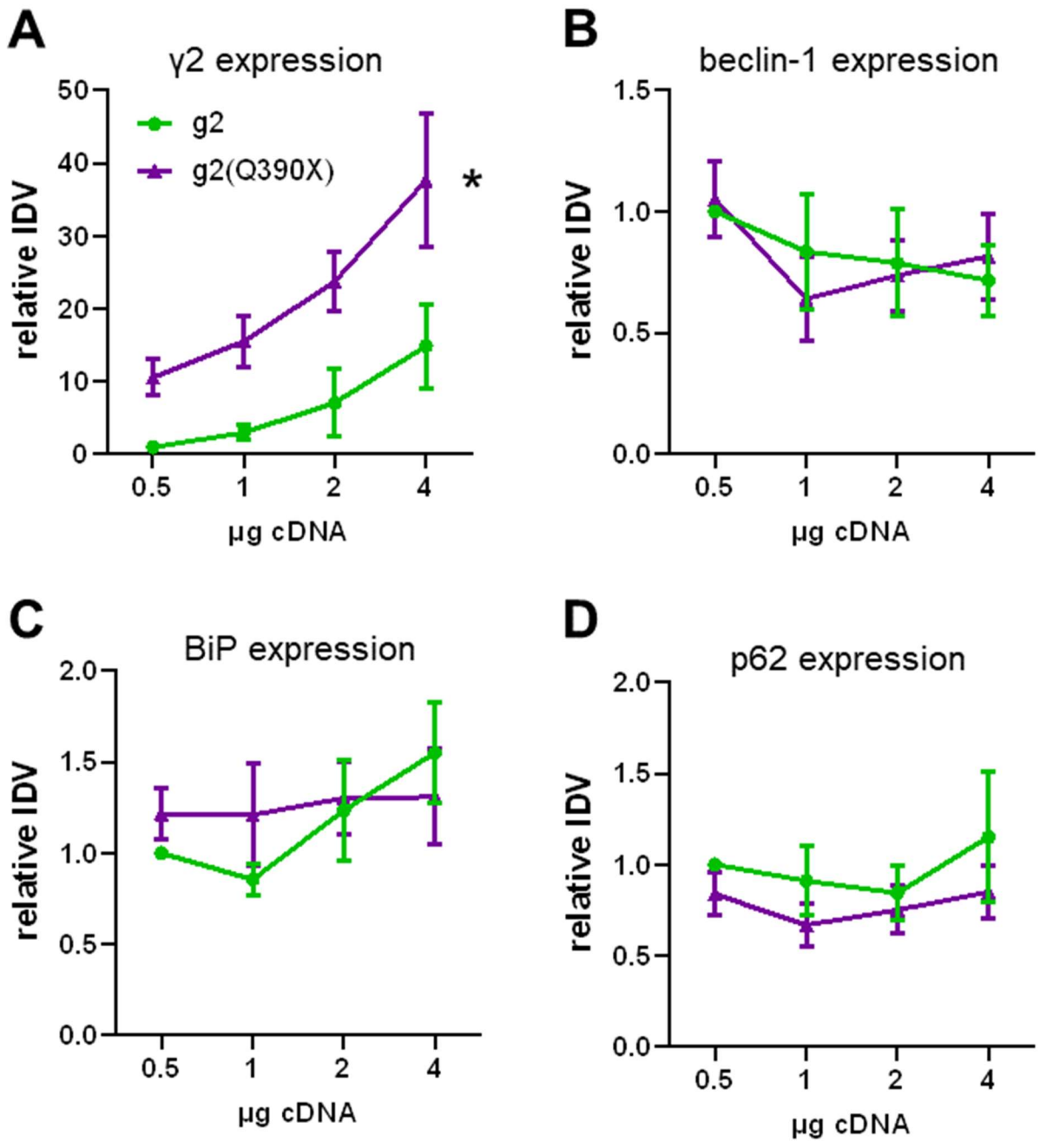


***Figure 3.1. Increased expression of neither γ2 nor γ2(Q390X) had any effect on beclin-1, BiP, or p62 expression.***
The expression of γ2, however, does increase with the transfection of more cDNA. Values are normalized to normalized to 0.5 µg γ2 cDNA. * represents significant genotype differences. *n* = 5-6.

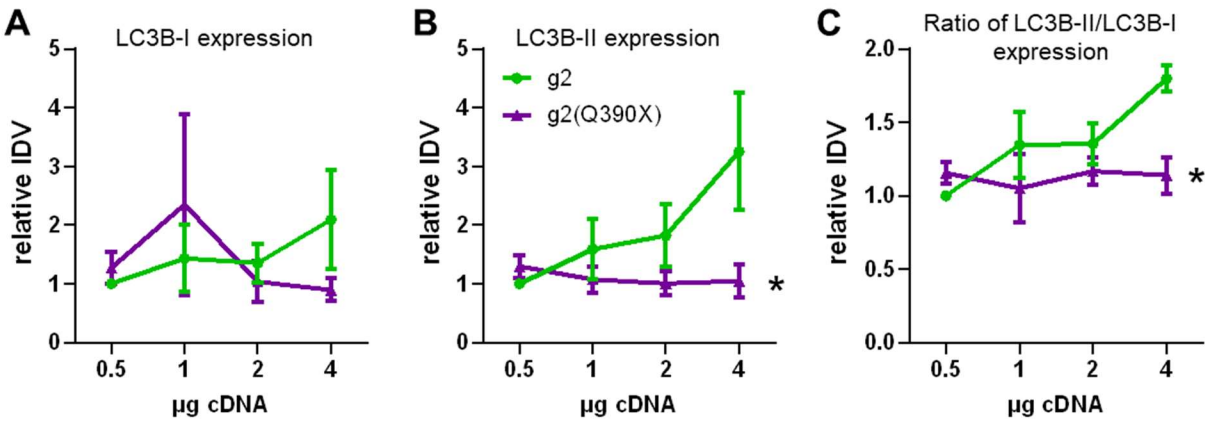


***Figure 3.2. The LC3B-II/LC3B-I ratio is elevated in response to increasing amounts of wildtype γ2 cDNA, but not to increasing amounts of mutant γ2(Q390X).***
This is due to the increase in LC3B-II, as LC3B-I is unchanged across all conditions. Values are normalized to normalized to 0.5 µg γ2 cDNA. * represents significant genotype differences. *n* = 5-6.

### 3.3.2 Effect of ER stress inducer Brefeldin-A is not different between α1β2γ2 and α1β2γ2(Q390X)

We next induced cellular stress with Brefeldin-A (BFA) (5 µg/mL, 1 hr), a compound that blocks transport from the ER to the Golgi.[10] This accumulation of proteins in the ER causes ER stress, as measured by CHOP expression, and increased autophagy, as measured by LC3-II expression, in a time and dose dependent manner.[10]

Even under this ER-stress-inducing condition, there were no changes in autophagy as measured by total expression of BiP or p62, or by the ratio between LC3B-II and LC3B-I. This may be due to the treatment schedule – 5 µg/mL is a high dose but 1 hr may have been too short.[10] Beclin-1 did reveal a significant source of variation from drug treatment ($p$ = 0.0488) but post hoc Sidak's multiple comparisons test did not find any one condition to be different from vehicle-treated wildtype. Because there was no effect from genotype or from the interaction of drug treatment and genotype, this

indicates that the mutant γ2(Q390X) protein had, in this model, no effect on beclin-1. In accordance with our previous studies, α1 and γ2 had genotype effects ($p$ = 0.0007 and 0.0026, respectively), but interestingly only α1 had drug variation ($p$ = 0.0219) while γ2 did not ($p$ = 0.1926).

***Table 3.3. p values of the effects of BFA treatment, the genotype of the GABR expressed, and the interaction of these factors on various autophagy factors.***

| | BFA | Genotype | Interaction |
|---|---|---|---|
| α1 | **0.0219** | **0.0007** | 0.9287 |
| γ2 | 0.1926 | **0.0026** | 0.8955 |
| Beclin-1 | **0.0488** | 0.6181 | 0.8158 |
| BiP | 0.1058 | 0.4525 | 0.8544 |
| LC3B-II/LC3B-I | 0.1595 | 0.9356 | 0.1309 |
| LC3B-I | 0.2013 | 0.7669 | 0.1982 |
| LC3B-II | 0.1115 | 0.7124 | 0.7542 |
| p62 | 0.1471 | 0.3481 | 0.8485 |

The ER stress inducer BFA alters the expression of beclin-1, but not other proteins associated with autophagy. Significant values ($p < 0.05$) are bolded. Two-way ANOVA, $n$ = 3-5.

***Table 3.4. The ER stress inducer BFA alters the expression of beclin-1, but post-hoc analysis shows no individual differences.***

| Beclin-1 | Vehicle | BFA |
|---|---|---|
| Wt | | 1.152 ± 0.116; 0.7920 |
| Het | 1.100 ± 0.175 | 1.288 ± 0.098; 0.6678 |
| Hom | 0.942 ± 0.126 | 1.250 ± 0.167; 0.2721 |

Values are expressed as mean ± SEM and the $p$ value of the comparison to the vehicle-treated control for the respective genotype. Sidak's multiple comparisons test, $n$ = 5.

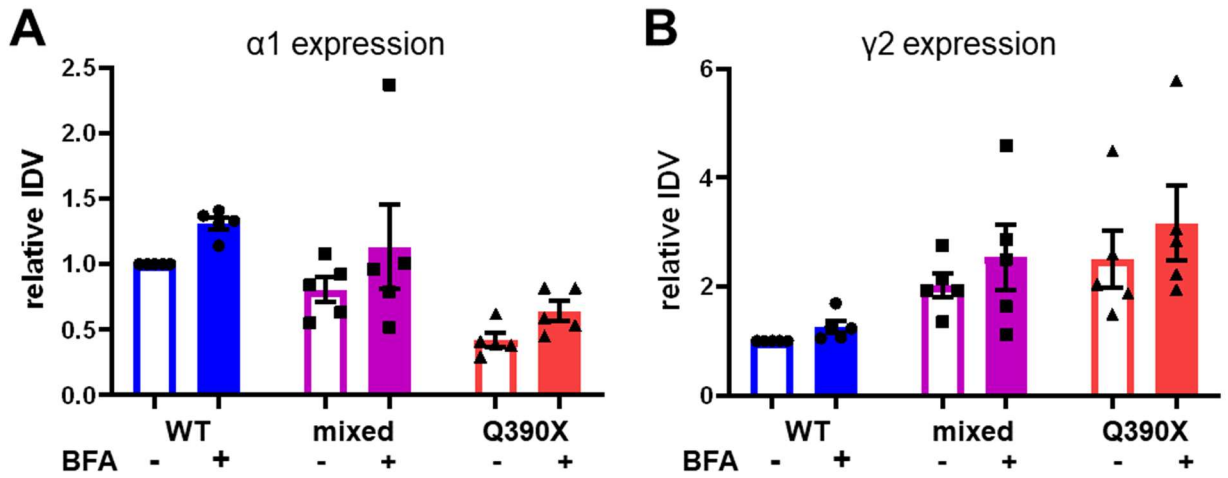


***Figure 3.3. 2(Q390X) alters expression of the GABR subunits α1 and γ2.***
BFA increases the expression of α1. Values are normalized to vehicle-treated WT α1β2γ2. *n* = 5.

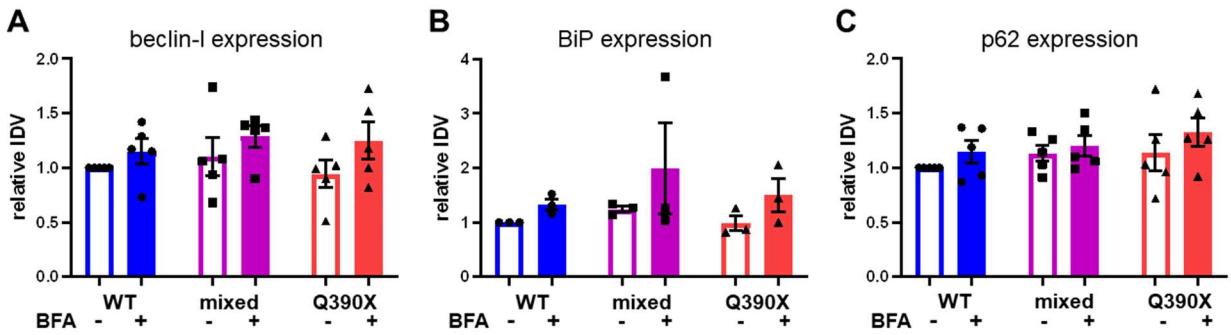


***Figure 3.4. BFA increases beclin-1 expression, regardless of the composition of the expressed GABR.***
Values are normalized to vehicle-treated WT α1β2γ2. *n* = 3-5.

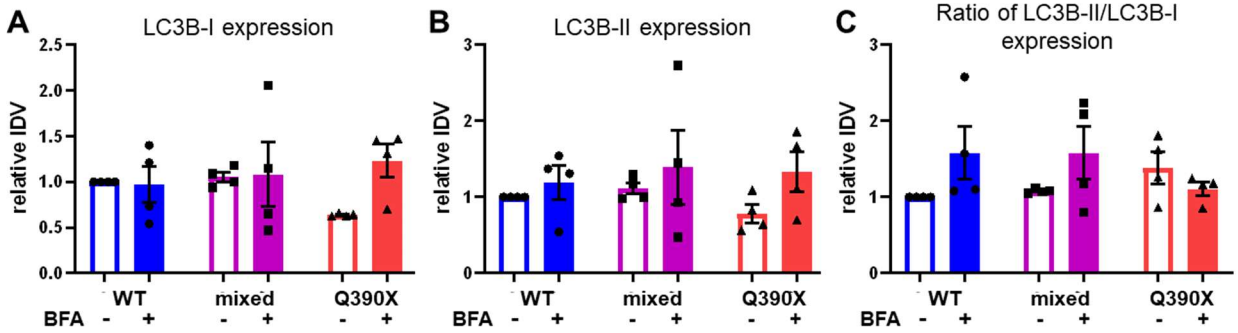


***Figure 3.5. BFA may have genotype-dependent effects on LC3B.***
Values are normalized to vehicle-treated WT α1β2γ2. *n* = 4.

### 3.3.3 Investigating parvalbumin-positive interneuron selective vulnerability

Loss of GABAergic neurons occurs in older *Gabrg2*$^{+/Q390X}$ mice.[4] We suspected that this neuronal death may be in part due to deficits in autophagy, as apoptosis eventually results from autophagy failure.[11,37] Additionally, we hypothesized that there may be specific types of neurons especially vulnerable to death resulting from altered autophagy.[36] Parvalbumin interneurons (PVIN) were a likely target for two reasons: These neurons are known to generally have high vulnerability, and PVIN dysfunction is central to the pathology of *SCN1A*-associated Dravet syndrome. The vulnerability of PVIN is due to their fast-spiking nature – PVIN have a high demand for energy, in order to maintain their spike rate, and thus disruptions to homeostasis can easily impact these neurons.[42] PVIN are known to be damaged after seizures,[43,44] and loss of PVIN is associated with epileptogenesis, preceding spontaneous seizures.[45,46]

Furthermore, PVIN have impaired excitability in *Scn1a* haploinsufficiency models. While the *GABRG2(Q390X)* mutation is associated with Dravet syndrome, the majority (~80%) of DS patients have mutations in *SCN1A*.[47] Given the clinical similarities of the two groups, it would not be surprising to find that *Gabrg2*$^{+/Q390X}$ mice also have decreased PVIN activity. Typically, these mutations result in loss-of-function of the encoded voltage-gated sodium channel, $Na_V1.1$, although gain-of-function mutations may also be possible.[47] $Na_V1.1$ is preferentially located to PVIN, as most hippocampal and cortical $Na_V1.1$ cells co-stain for PV, and a majority of PV positive cells co-staining for $Na_V1.1$.[48,49] Supporting the critical involvement of PVIN in *SCN1A*-mutation Dravet syndrome, conditional heterozygous knockout of *Scn1a* in PV cells results in

spontaneous seizures and increased susceptibility to induced seizures, and neither phenotype was seen in the model of pyramidal cell specific knockout.[49]

Haploinsufficiency of $Na_V1.1$ alters activity of PVIN, as PVIN from *Scn1a*$^{+/-}$ and *Scn1a*$^{+/R1407X}$ have a decreased ability to sustain fast spiking, a phenotype not seen in pyramidal cells.[48,50] These neurons also have decreased excitability, although this may, however, be transient, as one study found that PVIN activity normalized by P35.[51] But, despite the normal activity at later ages, these neurons were not entirely identical to wildtype, as the spike initiation zone remained more distal than in wildtype mice.[51] It is important to note, however, that some studies have failed to find impairments of interneurons and some have even found evidence of intrinsic hyperexcitability of excitatory neurons, suggesting that PVIN alterations alone are not responsible for the phenotype of Dravet syndrome.[52]

PVIN are important in other forms of epilepsy beyond Dravet syndrome, as is the perineuronal net (PNN), an extracellular structure surrounding neurons that determines excitability of PVIN and aid in fast-spiking behavior.[53] In a mouse model of malformation of cortical development (MCD) utilizing a dorsal progenitor cell specific KO of *Depdc5* in the cortex, the PNN began degrading and PVIN began dying before the onset of seizures at P15.[46] In a model of acquired epilepsy, too, PVIN were decreased as soon as 24 hr post SE, preceding the development of spontaneous seizures around day 15.[45] Furthermore, the number of PVIN negatively correlated with number of spontaneous seizures after SE.[45] Breakdown of the PNN can occur after SE as well, and enzymatic degradation of PNN resulted in more seizures in PTZ-treated mice, although seizure

onset was delayed.[54] Additionally, in an electrical stimulation model of epilepsy, the rats that developed spontaneous seizures after the induced SE had a mild decrease in the number of PVIN, while rats that did not develop seizures had no change.[43] Moreover, this post-SE loss of PVIN can progress with time.[44]

It is worth noting that reductions in PVIN are not the sole driver of epileptogenesis, as multiple studies have found that the loss of PVIN did not always correlate with seizure severity, [43,55] or that the loss of additional types of cells – such as somatostatin or calretinin interneurons – also plays a role.[43,45] However, even when multiple cell types are lost, PVIN are likely still very important: In sea lions with TLE, granule cells were also decreased in addition to PVIN, but not to the same extent, resulting in a greater ratio of granule cells to PVIN.[56]

As a whole, given the susceptibility of PVIN to cellular stress, the importance of PVIN to epilepsy, and the phenotypical similarities to models with known deficits in PVIN signaling, we hypothesized that PVIN in *Gabrg2*$^{+/Q390X}$ mice degenerate due to altered autophagy. Because seizure activity itself is detrimental to PVIN, a suitable control is necessary. In contrast to truncated γ2 proteins, neither truncated nor missense mutant $Na_V1.1$ protein forms intracellular aggregates.[1] The *Scn1a*$^{+/-}$ mouse models the haploinsufficiency of *SCN1A*-mutation Dravet syndrome via a heterozygous knockout, so there will be no misfolded mutant protein. Consequently, comparison of these two models provides an opportunity to determine which neuronal changes may be due to seizures, and what is due to underlying alterations to proteostasis caused by the γ2(Q390X) protein.

I planned to investigate brains from *Gabrg2*$^{+/Q390X}$ and *Scn1a*$^{+/-}$ mice – and wildtype littermates – at P21, which is shortly after seizure onset; at 6 months, which when neuronal death is first detected in *Gabrg2*$^{+/Q390X}$ mice; and at 12 months.[4] I chose to focus on somatosensory cortex because of the role of the thalamocortical circuit in seizures,[4] and on the dentate gyrus, because damage to hippocampal PVIN is associated with development of epilepsy.[43–45,56]

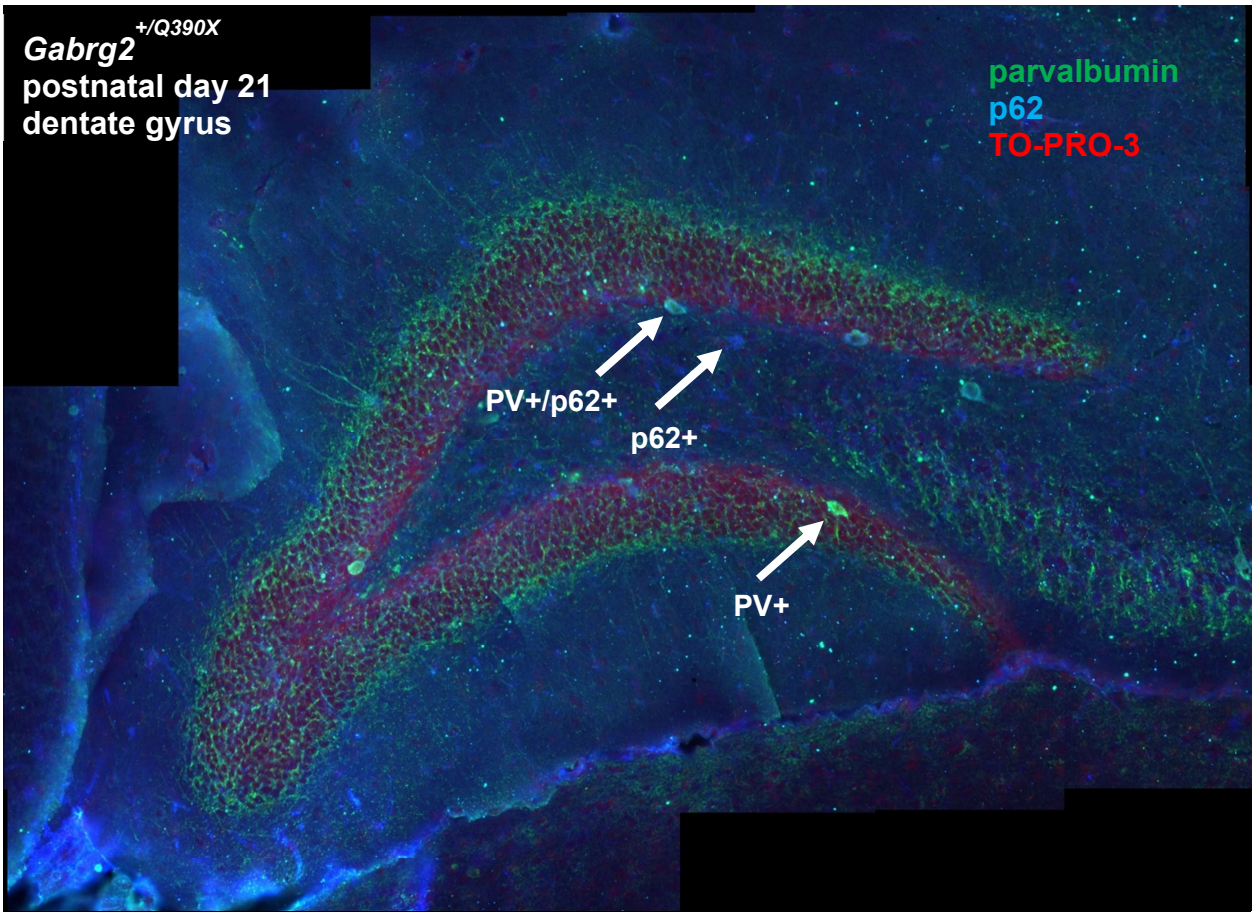


***Figure 3.6. Coronal section of the dentate gyrus of a P21* Gabrg2$^{+/Q390X}$ *mouse.*** Green is parvalbumin, blue is p62, and red is nuclear marker TO-PRO-3.

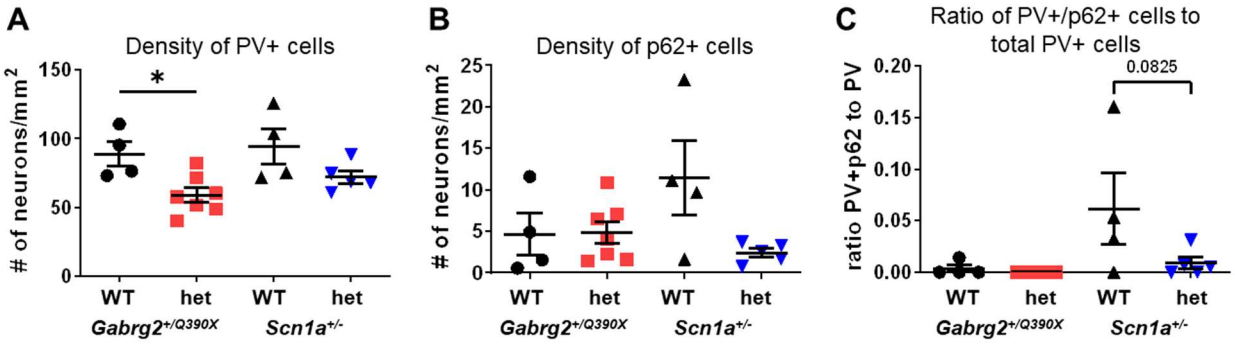


***Figure 3.7. In the somatosensory cortex, Gabrg2$^{+/Q390X}$ mice have fewer PV+ neurons than wildtype littermates.***
Neurons positive for p62 are unchanged. One-way ANOVA, Sidak's multiple comparisons test, $n$ = 4-7 slices total from 1-2 mice per genotype. * denotes $p < 0.05$.

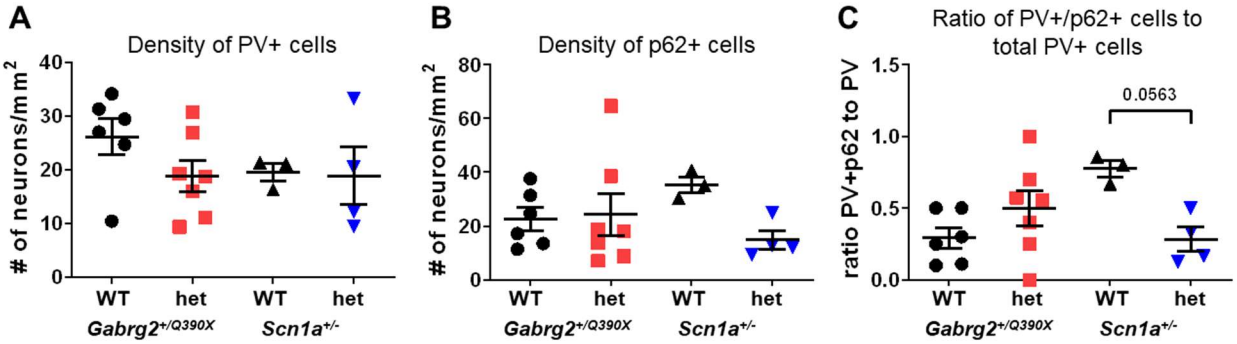


***Figure 3.8. In the dentate gyrus, there is no change in the number of PV+ or p62+ neurons for either Gabrg2$^{+/Q390X}$ or Scn1a$^{+/-}$ mice.***
One-way ANOVA, Sidak's multiple comparisons test, $n$ = 3-7 slices total from 1-2 mice per genotype.

This preliminary data suggests some possible changes to PVIN density at P21. In the somatosensory cortex, *Gabrg2$^{+/Q390X}$* mice had fewer PV+ neurons than their wildtype littermates (58.94 ± 5.38 vs 88.85 ± 8.75, $p = 0.0456$), but *Scn1a$^{+/-}$* mice had no change compared to their wildtype littermates (72.15 ± 4.63 vs 94.11 ± 12.69, $p = 0.2463$). In the dentate gyrus, there were no differences between any genotype. For p62, neither brain region shows any change, for either Dravet syndrome model. The ratio between PV/p62 double positive cells and total PV+ cells is likewise not changed,

although a very strong trend is seen for *Scn1a*$^{+/-}$ mice (somatosensory cortex: WT 0.06165 ± 0.03473, het 0.00871 ± 0.00581, $p$ = 0.0825; dentate gyrus: WT 0.7746 ± 0.0564, het 0.2813 ± 0.0857, $p$ = 0.0563).

## 3.4 Conclusions

### 3.4.1 Differential response of autophagy proteins to γ2 and γ2(Q390X) subunits

The γ2(Q390X) subunit results in some changes to autophagy proteins, compared to the response to the wildtype γ2 subunit. For γ2(Q390X), expression of all autophagy proteins measured (beclin-1, BiP, LC3B-I and LC3B-II, and p62) is constant for all amounts of γ2(Q390X) cDNA tested. However, increasing γ2 protein causes LC3B-II expression – and thus the LC3B-II/LC3B-I ratio – to rise, although, curiously, beclin-1 and p62 are unchanged. Because p62 and LC3B-II are both degraded during the final steps of autophagy, after fusion with the lysosome, failure of this step generally results in a correlation between the expression of these two proteins. Alternatively, elevated LC3B-II due to induction of autophagy is associated with increased beclin-1. So, it is unexpected that no other proteins investigated were differentially regulated.

However, LC3 is also involved in cellular functions unrelated to autophagy, which could explain the lack of concomitant increase in p62 or beclin-1. Non-autophagy roles such as bacteria phagocytosis and cytokine secretion[57,58] are unlikely to be involved in these experiments. Functions such as the formation of endosomes,[59,60] the fusion of lysosomes with the cell membrane,[61] and loading of extracellular vesicles[62] also do not seem particularly relevant. More promising is the fine-tuning of ERAD via the formation

of EDEMosomes, but only LC3-I – and not LC3-II – is reported in this process.[63,64] Additionally, LC3 can be sequestered by protein aggregates independent of autophagy, although this process is dependent on p62;[65,66] therefore, an increase in LC3B-II levels due to association with aggregates should also be accompanied by an increase in p62. Because wildtype γ2 is only moderately disposed towards aggregation, and p62 levels were unchanged, it is unlikely that the increase in LC3B-II is due to non-autophagic involvement with protein aggregates.

Due to the lack of change in beclin-1, BiP, and p62, it seems that transfected HEK293T cells do not upregulate autophagy in response to large amounts of exogenous protein, nor is the autophagic capacity noticeably overwhelmed. However, both LC3 and p62 can be transcriptionally regulated, obfuscating changes to protein synthesis and turnover.[9] As such, the correlation between LC3B-II and p62 is not always as expected, even under confirmed conditions of autophagy induction. While the cause of the change to specifically LC3B-II is not clear, it is noteworthy that cells expressing γ2(Q390X) did not have the same increase. This suggests that this likely autophagy-independent function of LC3 is differentially regulated by the presence of the γ2(Q390X) subunit.

Interestingly, the data from GABR-transfected cells treated with the ER stress inducer BFA did not show changes in either form of LC3. However, beclin-1 was affected by BFA, as each transfection condition shows an upward trend with drug treatment. The lack of significant changes in other proteins may be due to the experiment being slightly underpowered (n = 3-5), as p62 displays a trend similar to beclin-1.

### 3.4.2 Decreased parvalbumin staining in *Gabrg2*$^{+/Q390X}$

I detected a decrease in the number of PV+ neurons in the somatosensory cortex of P21 *Gabrg2*$^{+/Q390X}$ mice, and there is a trend towards a decreased proportion of PV+ neurons co-staining for p62 in *Scn1a*$^{+/-}$ mice. While preliminary, this data does suggest that interesting differences may already be present at this young age, although more study is required. This is of particular interest because young neurons are far more adaptable than older neurons. Indeed, while increased somatic γ2 expression is noted even at P0 in *Gabrg2*$^{+/Q390X}$ mice, aggregates of γ2 are not detectable until 5-6 months and do not become prominent until 12 months.[4] Cleaved caspase-3, likewise, is first detected at 5-6 months and becomes more prevalent with age.[4] Given those prior findings and the lack of obvious trend in the number of p62+ cells at P21, it thus is plausible that any changes in PVIN count at P21 are not likely due to apoptosis resulting from altered autophagy. Because it takes several months for the misfolded protein present in *Gabrg2*$^{+/Q390X}$ – and absent from *Scn1a*$^{+/-}$ – to accumulate, any potential differences between *Gabrg2*$^{+/Q390X}$ and *Scn1a*$^{+/-}$ mice may not emerge until at least 6 months of age.

While disturbances to protein quality control, as revealed by the ER stress marker CHOP/GADD153, has been shown *in vitro*, we have not yet shown this *in vivo*.[4,67] But, because ~6 months is when proteostasis begins to become seriously impaired – based on the presence of intracellular protein aggregates – changes in ER stress and autophagy are likely present around at this time as well.

Similar to what was discussed in the chapter on the UPS, multiple ages of mice should be examined, especially old mice 12+ months of age. It is difficult to predict exactly when changes in autophagy markers will become evident, as this varies across disease models. The intersection between genetic epilepsy and autophagy has not yet been studied much, beyond epilepsies caused by congenital disruptions of the autophagy pathway itself. This category primarily includes the tuberous sclerosis genes *TSC1* and *TSC2*, but also includes genes less commonly mutated in epilepsy, such as the endosome and lysosome membrane protein V-ATPase[68] and WIPI4, a protein involved in biogenesis of autophagosomes.[69] However, one study examined autophagy in a *Kcnma1* knockout model of epileptic encephalopathy caused by mutations in the potassium channel KCNMA1, which is not directly involved in the autophagic process. This epileptic mouse has impaired fusion of autophagosomes and lysosomes at 10-12 weeks old,[70] so if the progression of this disease is similar to Dravet syndrome, perhaps at that age is when clear deficits will be detected.

Much more study has been directed to autophagy in genetic models of neurodegenerative diseases. Impaired autophagy is detected at 2.7 months for the aggressive 5xFAD model of AD, while the same defects are seen at 20 months in the late-onset model APP51.[7] For transgenic mouse models of Parkinson's disease, aberrant autophagy is observed at 9 months in mice overexpressing the A53T α-synuclein mutant[71] and 18 months in a LRRK2(R1441G) knockin mouse.[72] The accelerated HD mouse model HdhQ200 has increased LC3 and p62 as early as 9 weeks, as well as mHtt protein aggregates,[73] while autophagy was only investigated at 15 months in a zQ175 mouse.[74] Note, though, that the presence of protein aggregates

is not a guarantee for observable alterations in autophagy: In the HD model R6/2, autophagy is not altered at 4, 8, or 12 weeks, although aggregates are present.[75] Conversely, in the Tg2576 AD model, autophagy deficits occur by 5 months of age although amyloid plaques are not present until 10-12 months.[7]

The degree to which autophagy is impaired may vary over time, as the lysosome deficits seen at 5 months in the Tg2576 AD mouse are more severe at 12 months.[7] Alternatively, the nature of the changes to autophagy may shift with disease progression, as early-stage AD APPswe/PS1dE9 mice (6 months old) have increased beclin-1 and LC3B-II:I ratio, while the inverse is true at 12 months, representing the late stage of the disease.[76]

Additionally, it is important to investigate multiple brain regions, as region-specific pathology is possible. Study of the BACHD mouse revealed no changes in protein expression of autophagy markers at any in the hypothalamus or striatum, while in the cortex there was a decrease in LC3B-II/LC3B-I ratio at 12 months.[77]

In regard to neuronal death, this will likely require study of old *Gabrg2*$^{+/Q390X}$ mice. Neurodegeneration, as measured by a decrease in NeuN staining, is observed in *Gabrg2*$^{+/Q390X}$ mice 14-18 months old, in the somatosensory cortex and thalamus.[4] However, total neuronal counts in the dentate gyrus, CA1, and CA3 regions of the hippocampus are unchanged in 14-18 month old animals.[4] Nevertheless, this does not preclude the possibility of cell-type specific vulnerability in this region, if that cell population is rare. Interneurons as a whole constitute 10-15% of the neurons in the hippocampus,[78] and PV+ interneurons will be only a subset of that group, so even a total loss of PV+ interneurons would result in only a small change to NeuN staining.

Losses that are quantitatively minor, however, can have important pathological effects, such as altering the ratio of excitatory and inhibitory neurons.[56]

An important caveat to note is, the *Gabrg2*$^{+/Q390X}$ mice are in the C57BL/6J genetic background, and this mouse strain is known to be less prone to neuronal death after induced seizures.[79,80] While the mechanism(s) of protection are not yet known, one study hypothesizes that enhanced autophagy may be protective.[36] Conversely, the *Scn1a*$^{+/-}$ animals used for these experiments were an F1 hybrid of C57BL/6J and 129S6/SvEvTac, with the latter being a strain more susceptible to neuronal death after seizures. However, the C57BL/6 line confers some protection when hybridized with FVB/N, another vulnerable strain.[80] Thus, the *Scn1a*$^{+/-}$ F1 hybrids may also have some of the protection as the C57BL/6J *Gabrg2*$^{+/Q390X}$ mice, making direct comparisons more appropriate. But, the traits of these strains should be kept in mind, as these mice may have some protection against proteostatic impairments, and thus cell death may be more severe in other mouse strains and in human patients with Dravet syndrome.

This data on P21 mice serves as a valuable starting point for a longitudinal study on proteostasis and neuronal health in *Gabrg2*$^{+/Q390X}$ Dravet syndrome mice. Although the most prominent changes are likely in old mice (12 months), this data on young mice will allow a timeline of the development of these changes. It is not surprising that moderate differences in PVIN number are seen so early: Epilepsy-causing *SCN1A* and *GABRG2* mutations are generally germline mutations, and thus the mutation is present from conception onwards. Neurons therefore are suffering ramifications of the mutation once

that particular gene becomes expressed (in humans, γ2 expression is found throughout multiple brain regions by 29-31 GW[81] and $Na_V1.1$ becomes detectable at 19-22 GW[82]) and cellular changes may have preceded the first seizure. Indeed, a recent proteomic study of the hippocampus of *Scn1a*$^{+/A1783V}$ Dravet syndrome mice found that over two hundred proteins differed in expression levels compared to wildtype controls, at just two weeks old.[83]

### 3.4.3 Future directions

It would be valuable to repeat the *in vitro* experiments in different cell types, as cell types vary in their autophagic and proteasomal capacities, suggesting variable responses to the presence of mutant proteins.[19,84] One such cell line may be L929. Transfection is not nearly as efficient in this cell type but may be better at showing alterations to ER stress and autophagy. The lack of prominent disruptions to autophagy seen in these experiments may be to an exceptional resilience of the proteostasis network in HEK cells. More clinically-relevant findings will come from investigating autophagy in neurons cultured from *Gabrg2*$^{+/Q390X}$ mice.

In addition to the use of BFA, which induces ER stress by blocking the transport of proteins from the ER and provides insight to the resilience of the unfolded protein response, an autophagy inhibitor such as 3-MA would also be useful. This would allow study of the effect of the γ2(Q390X) subunit on the reserve capacity of the autophagy pathway. Given that HEK293T cells expressing γ2(Q390X) protein do not adapt to large amounts of protein by increasing LC3B-II as cells expressing γ2 do, they may be closer to failure of autophagy, and thus the resulting apoptosis.

The only marker of autophagy examined so far in mice was p62. Because increased p62 can imply upregulation of autophagy or a failing of the final stages (e.g., lysosomal degradation), it will be important to investigate other components of the autophagy/lysosome system, such as beclin-1 and LAMP-1/LAMP-2. Furthermore, p62, like LC3, is recruited in an autophagy-independent manner to protein aggregates.[65] Thus, examining multiple components of the autophagy/lysosome pathway will present a clearer picture of the potential changes to autophagy in the parvalbumin interneurons of *Gabrg2*$^{+/Q390X}$ and *Scn1a*$^{+/-}$ mice.

Because some of these experiments were preliminary, and thus likely somewhat underpowered, it would be worthwhile to replicate the experiments, to build a more robust understanding. For the immunohistochemistry experiments quantifying PV and p62, only 1 or 2 mice were available at the time. Clearly, several more animals should be studied before strong conclusions can be made. Additionally, it is of great importance to continue the experiment across multiple ages, as planned. This will allow us to track the time course of any progressive neurodegeneration.

## 3.5 References


1. Marini C, Scheffer IE, Nabbout R, et al. The genetics of Dravet syndrome. *Epilepsia*. 2011;52 Suppl 2:24-29. doi:10.1111/j.1528-1167.2011.02997.x

2. Harkin LA, Bowser DN, Dibbens LM, et al. Truncation of the GABAA-receptor gamma2 subunit in a family with generalized epilepsy with febrile seizures plus. *Am J Hum Genet*. 2002;70(2):530-536. doi:10.1086/338710

3. Wang J, Shen D, Xia G, et al. Differential protein structural disturbances and suppression of assembly partners produced by nonsense GABRG2 epilepsy mutations: implications for disease phenotypic heterogeneity. *Scientific Reports*. 2016;6:srep35294. doi:10.1038/srep35294

4. Kang JQ, Shen W, Zhou C, Xu D, Macdonald RL. The human epilepsy mutation GABRG2(Q390X) causes chronic subunit accumulation and neurodegeneration. *Nat Neurosci*. 2015;18(7):988-996. doi:10.1038/nn.4024

5. Guerriero CJ, Brodsky JL. The delicate balance between secreted protein folding and endoplasmic reticulum-associated degradation in human physiology. *Physiol Rev*. 2012;92(2):537-576. doi:10.1152/physrev.00027.2011

6. Pankiv S, Clausen TH, Lamark T, et al. p62/SQSTM1 binds directly to Atg8/LC3 to facilitate degradation of ubiquitinated protein aggregates by autophagy. *J Biol Chem*. 2007;282(33):24131-24145. doi:10.1074/jbc.M702824200

7. Lee JH, Yang DS, Goulbourne CN, et al. Faulty autolysosome acidification in Alzheimer's disease mouse models induces autophagic build-up of Aβ in neurons, yielding senile plaques. *Nat Neurosci*. 2022;25(6):688-701. doi:10.1038/s41593-022-01084-8

8. Shibata M, Lu T, Furuya T, et al. Regulation of intracellular accumulation of mutant Huntingtin by Beclin 1. *J Biol Chem*. 2006;281(20):14474-14485. doi:10.1074/jbc.M600364200

9. Klionsky DJ, Abdel-Aziz AK, Abdelfatah S, et al. Guidelines for the use and interpretation of assays for monitoring autophagy (4th edition)1. *Autophagy*. 2021;17(1):1-382. doi:10.1080/15548627.2020.1797280

10. Kawakami T, Inagi R, Takano H, et al. Endoplasmic reticulum stress induces autophagy in renal proximal tubular cells. *Nephrol Dial Transplant*. 2009;24(9):2665-2672. doi:10.1093/ndt/gfp215

11. Ding WX, Ni HM, Gao W, et al. Differential effects of endoplasmic reticulum stress-induced autophagy on cell survival. *J Biol Chem*. 2007;282(7):4702-4710. doi:10.1074/jbc.M609267200

12. Bjørkøy G, Lamark T, Brech A, et al. p62/SQSTM1 forms protein aggregates degraded by autophagy and has a protective effect on huntingtin-induced cell death. *Journal of Cell Biology*. 2005;171(4):603-614. doi:10.1083/jcb.200507002

13. Li J, Ni M, Lee B, Barron E, Hinton DR, Lee AS. The unfolded protein response regulator GRP78/BiP is required for endoplasmic reticulum integrity and stress-induced autophagy in mammalian cells. *Cell Death Differ*. 2008;15(9):1460-1471. doi:10.1038/cdd.2008.81

14. Fassio A, Falace A, Esposito A, Aprile D, Guerrini R, Benfenati F. Emerging Role of the Autophagy/Lysosomal Degradative Pathway in Neurodevelopmental Disorders With Epilepsy. *Front Cell Neurosci*. 2020;14:39. doi:10.3389/fncel.2020.00039

15. Hoffmann S, Orlando M, Andrzejak E, et al. Light-Activated ROS Production Induces Synaptic Autophagy. *J Neurosci*. 2019;39(12):2163-2183. doi:10.1523/JNEUROSCI.1317-18.2019

16. Komatsu M, Waguri S, Chiba T, et al. Loss of autophagy in the central nervous system causes neurodegeneration in mice. *Nature*. 2006;441(7095):880-884. doi:10.1038/nature04723

17. Hara T, Nakamura K, Matsui M, et al. Suppression of basal autophagy in neural cells causes neurodegenerative disease in mice. *Nature*. 2006;441(7095):885-889. doi:10.1038/nature04724

18. Castillo K, Valenzuela V, Matus S, et al. Measurement of autophagy flux in the nervous system in vivo. *Cell Death Dis*. 2013;4:e917. doi:10.1038/cddis.2013.421

19. Boland B, Kumar A, Lee S, et al. Autophagy induction and autophagosome clearance in neurons: relationship to autophagic pathology in Alzheimer's disease. *J Neurosci*. 2008;28(27):6926-6937. doi:10.1523/JNEUROSCI.0800-08.2008

20. Pickford F, Masliah E, Britschgi M, et al. The autophagy-related protein beclin 1 shows reduced expression in early Alzheimer disease and regulates amyloid beta accumulation in mice. *J Clin Invest*. 2008;118(6):2190-2199. doi:10.1172/JCI33585

21. Spencer B, Potkar R, Trejo M, et al. Beclin 1 gene transfer activates autophagy and ameliorates the neurodegenerative pathology in alpha-synuclein models of Parkinson's and Lewy body diseases. *J Neurosci*. 2009;29(43):13578-13588. doi:10.1523/JNEUROSCI.4390-09.2009

22. Sanchez-Martin P, Lahuerta M, Viana R, Knecht E, Sanz P. Regulation of the autophagic PI3KC3 complex by laforin/malin E3-ubiquitin ligase, two proteins involved in Lafora disease. *Biochim Biophys Acta Mol Cell Res*. 2020;1867(2):118613. doi:10.1016/j.bbamcr.2019.118613

23. Criado O, Aguado C, Gayarre J, et al. Lafora bodies and neurological defects in malin-deficient mice correlate with impaired autophagy. *Human Molecular Genetics*. 2012;21(7):1521-1533. doi:10.1093/hmg/ddr590

24. Lahuerta M, Aguado C, Sánchez-Martín P, Sanz P, Knecht E. Degradation of altered mitochondria by autophagy is impaired in Lafora disease. *The FEBS Journal*. 2018;285(11):2071-2090. doi:10.1111/febs.14468

25. McMahon J, Huang X, Yang J, et al. Impaired autophagy in neurons after disinhibition of mammalian target of rapamycin and its contribution to epileptogenesis. *J Neurosci*. 2012;32(45):15704-15714. doi:10.1523/JNEUROSCI.2392-12.2012

26. Carvill GL, Liu A, Mandelstam S, et al. Severe infantile onset developmental and epileptic encephalopathy caused by mutations in autophagy gene WDR45. *Epilepsia*. 2018;59(1):e5-e13. doi:10.1111/epi.13957

27. Bejarano E, Rodríguez-Navarro JA. Autophagy and amino acid metabolism in the brain: implications for epilepsy. *Amino Acids*. 2015;47(10):2113-2126. doi:10.1007/s00726-014-1822-z

28. Hui KK, Takashima N, Watanabe A, et al. GABARAPs dysfunction by autophagy deficiency in adolescent brain impairs GABAA receptor trafficking and social behavior. *Sci Adv*. 2019;5(4):eaau8237. doi:10.1126/sciadv.aau8237

29. Sumitomo A, Yukitake H, Hirai K, et al. Ulk2 controls cortical excitatory–inhibitory balance via autophagic regulation of p62 and GABAA receptor trafficking in pyramidal neurons. *Human Molecular Genetics*. 2018;27(18):3165-3176. doi:10.1093/hmg/ddy219

30. Tomoda T, Sumitomo A, Shukla R, et al. BDNF controls GABAAR trafficking and related cognitive processes via autophagic regulation of p62. *Neuropsychopharmacology*. 2022;47(2):553-563. doi:10.1038/s41386-021-01116-0

31. Ni H, Gong Y, Yan JZ, Zhang LL. Autophagy inhibitor 3-methyladenine regulates the expression of LC3, Beclin-1 and ZnTs in rat cerebral cortex following recurrent neonatal seizures. *World J Emerg Med*. 2010;1(3):216-223.

32. Sun J, Gao X, Meng D, et al. Antagomirs Targeting MiroRNA-134 Attenuates Epilepsy in Rats through Regulation of Oxidative Stress, Mitochondrial Functions and Autophagy. *Front Pharmacol*. 2017;8:524. doi:10.3389/fphar.2017.00524

33. Li Q, Han Y, Du J, et al. Alterations of apoptosis and autophagy in developing brain of rats with epilepsy: Changes in LC3, P62, Beclin-1 and Bcl-2 levels. *Neurosci Res*. 2018;130:47-55. doi:10.1016/j.neures.2017.08.004

34. Ying C, Ying L, Yanxia L, Le W, Lili C. High mobility group box 1 antibody represses autophagy and alleviates hippocampus damage in pilocarpine-induced mouse epilepsy model. *Acta Histochem*. 2020;122(2):151485. doi:10.1016/j.acthis.2019.151485

35. Ryu HJ, Kim JE, Yeo SI, Kang TC. p65/RelA-Ser529 NF-κB subunit phosphorylation induces autophagic astroglial death (Clasmatodendrosis) following status epilepticus. *Cell Mol Neurobiol*. 2011;31(7):1071-1078. doi:10.1007/s10571-011-9706-1

36. Rami A, Benz A. Exclusive Activation of Caspase-3 in Mossy Fibers and Altered Dynamics of Autophagy Markers in the Mice Hippocampus upon Status Epilepticus Induced by Kainic Acid. *Mol Neurobiol*. 2018;55(5):4492-4503. doi:10.1007/s12035-017-0665-5

37. Wu Q, Zhang M, Liu X, Zhang J, Wang H. CB2R orchestrates neuronal autophagy through regulation of the mTOR signaling pathway in the hippocampus of developing rats with status epilepticus. *Int J Mol Med*. 2020;45(2):475-484. doi:10.3892/ijmm.2019.4439

38. Shacka JJ, Lu J, Xie ZL, Uchiyama Y, Roth KA, Zhang J. Kainic acid induces early and transient autophagic stress in mouse hippocampus. *Neurosci Lett*. 2007;414(1):57-60. doi:10.1016/j.neulet.2006.12.025

39. Teckman JH, Perlmutter DH. Retention of mutant α1-antitrypsin Z in endoplasmic reticulum is associated with an autophagic response. *American Journal of Physiology-Gastrointestinal and Liver Physiology*. 2000;279(5):G961-G974. doi:10.1152/ajpgi.2000.279.5.G961

40. Yu FH, Mantegazza M, Westenbroek RE, et al. Reduced sodium current in GABAergic interneurons in a mouse model of severe myoclonic epilepsy in infancy. *Nat Neurosci*. 2006;9(9):1142-1149. doi:10.1038/nn1754

41. Miller AR, Hawkins NA, McCollom CE, Kearney JA. Mapping genetic modifiers of survival in a mouse model of Dravet syndrome. *Genes Brain Behav*. 2014;13(2):163-172. doi:10.1111/gbb.12099

42. Cabungcal JH, Steullet P, Morishita H, et al. Perineuronal nets protect fast-spiking interneurons against oxidative stress. *Proc Natl Acad Sci U S A*. 2013;110(22):9130-9135. doi:10.1073/pnas.1300454110

43. Huusko N, Römer C, Ndode-Ekane XE, Lukasiuk K, Pitkänen A. Loss of hippocampal interneurons and epileptogenesis: a comparison of two animal models of acquired epilepsy. *Brain Struct Funct*. 2015;220(1):153-191. doi:10.1007/s00429-013-0644-1

44. Pavlov I, Huusko N, Drexel M, et al. Progressive loss of phasic, but not tonic, GABAA receptor-mediated inhibition in dentate granule cells in a model of post-traumatic epilepsy in rats. *Neuroscience*. 2011;194:208-219. doi:10.1016/j.neuroscience.2011.07.074

45. Drexel M, Preidt AP, Kirchmair E, Sperk G. Parvalbumin interneurons and calretinin fibers arising from the thalamic nucleus reuniens degenerate in the subiculum after kainic acid-induced seizures. *Neuroscience*. 2011;189:316-329. doi:10.1016/j.neuroscience.2011.05.021

46. Yang T, Hu S, Chang WC, Kao HY, Wang Y. Perineuronal Nets Degradation and Parvalbumin Interneuron loss in a Mouse Model of DEPDC5-related Epilepsy. *Dev Neurosci*. Published online May 17, 2022. doi:10.1159/000525039

47. Angus M, Peters CH, Poburko D, Brimble E, Spelbrink EM, Ruben PC. Case studies in neuroscience: a novel amino acid duplication in the NH2-terminus of the brain sodium channel NaV1.1 underlying Dravet syndrome. *J Neurophysiol*. 2019;122(5):1975-1980. doi:10.1152/jn.00491.2019

48. Ogiwara I, Miyamoto H, Morita N, et al. Nav1.1 localizes to axons of parvalbumin-positive inhibitory interneurons: a circuit basis for epileptic seizures in mice carrying an Scn1a gene mutation. *J Neurosci*. 2007;27(22):5903-5914. doi:10.1523/JNEUROSCI.5270-06.2007

49. Dutton SB, Makinson CD, Papale LA, et al. Preferential inactivation of Scn1a in parvalbumin interneurons increases seizure susceptibility. *Neurobiology of Disease*. 2013;49:211-220. doi:10.1016/j.nbd.2012.08.012

50. Tai C, Abe Y, Westenbroek RE, Scheuer T, Catterall WA. Impaired excitability of somatostatin- and parvalbumin-expressing cortical interneurons in a mouse model of Dravet syndrome. *Proc Natl Acad Sci USA*. 2014;111(30):E3139-3148. doi:10.1073/pnas.1411131111

51. Favero M, Sotuyo NP, Lopez E, Kearney JA, Goldberg EM. A Transient Developmental Window of Fast-Spiking Interneuron Dysfunction in a Mouse Model of Dravet Syndrome. *J Neurosci*. 2018;38(36):7912-7927. doi:10.1523/JNEUROSCI.0193-18.2018

52. Mattis J, Somarowthu A, Goff KM, et al. Corticohippocampal circuit dysfunction in a mouse model of Dravet syndrome. *Elife*. 2022;11:e69293. doi:10.7554/eLife.69293

53. Chaunsali L, Tewari BP, Sontheimer H. Perineuronal Net Dynamics in the Pathophysiology of Epilepsy. *Epilepsy Curr*. 2021;21(4):273-281. doi:10.1177/15357597211018688

54. Rankin-Gee EK, McRae PA, Baranov E, Rogers S, Wandrey L, Porter BE. Perineuronal net degradation in epilepsy. *Epilepsia*. 2015;56(7):1124-1133. doi:10.1111/epi.13026

55. Buckmaster PS, Abrams E, Wen X. Seizure frequency correlates with loss of dentate gyrus GABAergic neurons in a mouse model of temporal lobe epilepsy. *J Comp Neurol*. 2017;525(11):2592-2610. doi:10.1002/cne.24226

56. Cameron S, Lopez A, Glabman R, et al. Proportional loss of parvalbumin-immunoreactive synaptic boutons and granule cells from the hippocampus of sea lions with temporal lobe epilepsy. *J Comp Neurol*. 2019;527(14):2341-2355. doi:10.1002/cne.24680

57. Galluzzi L, Green DR. Autophagy-Independent Functions of the Autophagy Machinery. *Cell*. 2019;177(7):1682-1699. doi:10.1016/j.cell.2019.05.026

58. Schaaf MBE, Keulers TG, Vooijs MA, Rouschop KMA. LC3/GABARAP family proteins: autophagy-(un)related functions. *FASEB J*. 2016;30(12):3961-3978. doi:10.1096/fj.201600698R

59. Patel KK, Miyoshi H, Beatty WL, et al. Autophagy proteins control goblet cell function by potentiating reactive oxygen species production. *The EMBO Journal*. 2013;32(24):3130-3144. doi:10.1038/emboj.2013.233

60. Heckmann BL, Teubner BJW, Tummers B, et al. LC3-Associated Endocytosis Facilitates β-Amyloid Clearance and Mitigates Neurodegeneration in Murine Alzheimer's Disease. *Cell*. 2019;178(3):536-551.e14. doi:10.1016/j.cell.2019.05.056

61. DeSelm CJ, Miller BC, Zou W, et al. Autophagy proteins regulate the secretory component of osteoclastic bone resorption. *Dev Cell*. 2011;21(5):966-974. doi:10.1016/j.devcel.2011.08.016

62. Leidal AM, Debnath J. LC3-dependent extracellular vesicle loading and secretion (LDELS). *Autophagy*. 2020;16(6):1162-1163. doi:10.1080/15548627.2020.1756557

63. Calì T, Galli C, Olivari S, Molinari M. Segregation and rapid turnover of EDEM1 by an autophagy-like mechanism modulates standard ERAD and folding activities. *Biochem Biophys Res Commun*. 2008;371(3):405-410. doi:10.1016/j.bbrc.2008.04.098

64. Bernasconi R, Noack J, Molinari M. Unconventional roles of nonlipidated LC3 in ERAD tuning and coronavirus infection. *Autophagy*. 2012;8(10):1534-1536. doi:10.4161/auto.21229

65. Shvets E, Elazar Z. Autophagy-independent incorporation of GFP-LC3 into protein aggregates is dependent on its interaction with p62/SQSTM1. *Autophagy*. 2008;4(8):1054-1056. doi:10.4161/auto.6823

66. Kuma A, Matsui M, Mizushima N. LC3, an autophagosome marker, can be incorporated into protein aggregates independent of autophagy: caution in the interpretation of LC3 localization. *Autophagy*. 2007;3(4):323-328. doi:10.4161/auto.4012

67. Kang JQ, Shen W, Macdonald RL. Trafficking-deficient mutant GABRG2 subunit amount may modify epilepsy phenotype. *Ann Neurol*. 2013;74(4):547-559. doi:10.1002/ana.23947

68. Bott LC, Forouhan M, Lieto M, et al. Variants in ATP6V0A1 cause progressive myoclonus epilepsy and developmental and epileptic encephalopathy. *Brain Commun*. 2021;3(4):fcab245. doi:10.1093/braincomms/fcab245

69. Hor CHH, Tang BL. Beta-propeller protein-associated neurodegeneration (BPAN) as a genetically simple model of multifaceted neuropathology resulting from defects in autophagy. *Rev Neurosci*. 2019;30(3):261-277. doi:10.1515/revneuro-2018-0045

70. Yao Y, Qu D, Jing X, et al. Molecular Mechanisms of Epileptic Encephalopathy Caused by KCNMA1 Loss-of-Function Mutations. *Front Pharmacol*. 2021;12:775328. doi:10.3389/fphar.2021.775328

71. Zhang Y, Wu Q, Zhang L, et al. Caffeic acid reduces A53T α-synuclein by activating JNK/Bcl-2-mediated autophagy in vitro and improves behaviour and protects dopaminergic neurons in a mouse model of Parkinson's disease. *Pharmacol Res*. 2019;150:104538. doi:10.1016/j.phrs.2019.104538

72. Ho PWL, Leung CT, Liu H, et al. Age-dependent accumulation of oligomeric SNCA/α-synuclein from impaired degradation in mutant LRRK2 knockin mouse model of Parkinson disease: role for therapeutic activation of chaperone-mediated autophagy (CMA). *Autophagy*. 2020;16(2):347-370. doi:10.1080/15548627.2019.1603545

73. Heng MY, Duong DK, Albin RL, et al. Early autophagic response in a novel knock-in model of Huntington disease. *Hum Mol Genet*. 2010;19(19):3702-3720. doi:10.1093/hmg/ddq285

74. Abd-Elrahman KS, Hamilton A, Hutchinson SR, Liu F, Russell RC, Ferguson SSG. mGluR5 antagonism increases autophagy and prevents disease progression in the zQ175 mouse model of Huntington's disease. *Sci Signal*. 2017;10(510):eaan6387. doi:10.1126/scisignal.aan6387

75. Kumar MJV, Shah D, Giridharan M, Yadav N, Manjithaya R, Clement JP. Spatiotemporal analysis of soluble aggregates and autophagy markers in the R6/2 mouse model. *Sci Rep*. 2021;11(1):96. doi:10.1038/s41598-020-78850-w

76. Chen ML, Hong CG, Yue T, et al. Inhibition of miR-331-3p and miR-9-5p ameliorates Alzheimer's disease by enhancing autophagy. *Theranostics*. 2021;11(5):2395-2409. doi:10.7150/thno.47408

77. Baldo B, Soylu R, Petersén A. Maintenance of basal levels of autophagy in Huntington's disease mouse models displaying metabolic dysfunction. *PLoS One*. 2013;8(12):e83050. doi:10.1371/journal.pone.0083050

78. Pelkey KA, Chittajallu R, Craig MT, Tricoire L, Wester JC, McBain CJ. Hippocampal GABAergic Inhibitory Interneurons. *Physiological Reviews*. 2017;97(4):1619-1747. doi:10.1152/physrev.00007.2017

79. Schauwecker PE, Steward O. Genetic determinants of susceptibility to excitotoxic cell death: implications for gene targeting approaches. *Proc Natl Acad Sci U S A*. 1997;94(8):4103-4108. doi:10.1073/pnas.94.8.4103

80. Liu L, Hamre KM, Goldowitz D. Kainic acid-induced neuronal degeneration in hippocampal pyramidal neurons is driven by both intrinsic and extrinsic factors: analysis of FVB/N↔C57BL/6 chimeras. *J Neurosci*. 2012;32(35):12093-12101. doi:10.1523/JNEUROSCI.6478-11.2012

81. Kanaumi T, Takashima S, Iwasaki H, Mitsudome A, Hirose S. Developmental changes in the expression of GABAA receptor alpha 1 and gamma 2 subunits in human temporal lobe, hippocampus and basal ganglia: An implication for consideration on age-related epilepsy. *Epilepsy Research*. 2006;71(1):47-53. doi:10.1016/j.eplepsyres.2006.05.019

82. Wang W, Takashima S, Segawa Y, et al. The developmental changes of Na(v)1.1 and Na(v)1.2 expression in the human hippocampus and temporal lobe. *Brain Res*. 2011;1389:61-70. doi:10.1016/j.brainres.2011.02.083

83. Miljanovic N, Hauck SM, van Dijk RM, Di Liberto V, Rezaei A, Potschka H. Proteomic signature of the Dravet syndrome in the genetic Scn1a-A1783V mouse model. *Neurobiol Dis*. 2021;157:105423. doi:10.1016/j.nbd.2021.105423

84. Milan E, Perini T, Resnati M, et al. A plastic SQSTM1/p62-dependent autophagic reserve maintains proteostasis and determines proteasome inhibitor susceptibility in multiple myeloma cells. *Autophagy*. 2015;11(7):1161-1178. doi:10.1080/15548627.2015.1052928

# 4 Investigation of the Use of Chemical Chaperones to Rescue *GABRG2(Q390X)* Pathology

## 4.1 Introduction

In the previous chapters, I have presented some evidence that the *GABRG2(Q390X)* mutation results in potentially deleterious disruptions to cellular protein quality control mechanisms of autophagy and the ubiquitin-proteasome system. This builds on the prior findings of the lab that show that this mutation is dominant-negative in regards to $GABA_A$ receptor (GABR) function and neuronal health. Therefore, elimination of the mutant protein is a clearly apparent goal for therapeutic opportunities.

One prospective way to facilitate degradation of γ2(Q390X) is to stabilize the monomers and prevent the formation of multimers and aggregates. This could potentially be accomplished with chemical or pharmacological chaperones. Chemical chaperones provide a more favorable environment for protein folding, by altering the chemical environment of the ER, thereby stabilizing folded states and/or reducing aggregation tendencies.[1,2] Pharmacological chaperones, meanwhile, directly interact with the misfolding-prone protein, instead of altering the general folding environment.[1–4] Alternatively, proteostasis regulators that modulate endogenous molecular chaperones, such as BiP/GRP78 and heat shock proteins (HSPs), may also be therapeutic.

Chaperones have the potential to address the dominant-negative phenotype of *GABRG2(Q390X)* from another angle as well. Membrane proteins, such as the GABR subunits, are not folded and trafficked efficiently, and thus approximately only 20-30% of

newly synthesized protein is reaches the cell surface.[5] By retaining partnering subunits in the ER, the γ2(Q390X) subunit exacerbates this excessive degradation, reducing both total and surface expression of non-mutated partnering subunits. Stabilizing the wildtype subunits with chaperones may promote proper trafficking, by attenuating overactive degradation and providing more opportunities for assembly into full receptors.

### 4.1.1 PBA

Two chaperones were chosen: 4-phenyl butyric acid (PBA) and celastrol. PBA (brand name Buphenyl) is a chemical chaperone that is FDA-approved for urea cycle disorders, and it has shown promise in severe genetic neurological disorders, including *SLC6A1* associated disorders, STXBP1 encephalopathy, and Lafora disease. PBA has several mechanisms of action. It is a hydrophobic pharmacological chaperone, preventing aggregation of misfolded proteins, by interacting with exposed hydrophobic regions.[2] PBA is also an inhibitor of histone deacetylases (HDAC), and perhaps via this effect, PBA upregulates the molecular chaperones BiP, HSP70, and HSP90.[1,6]

*SLC6A1* neurodevelopmental disorder is caused by loss-of-function mutations in the protein encoded by *SLC6A1*, GABA transporter 1 (GAT1).[7,8] Many of the mutant GAT1 proteins are retained within the ER and consequently have reduced surface expression.[8–12] Application of PBA *in vitro* to cells expressing wildtype GAT1 increases GABA uptake activity in a time- and dose-dependent manner.[13] Additionally, two separate studies of GAT1 mutants with diverse types and locations of mutations (missense and truncations, C terminus and N terminus, etc), associated with a variety of neurological clinical phenotypes, found that PBA partially rescued the loss of GABA

uptake function of all mutants tested.[13,14] A similar rescue occurred in cultured neurons and astrocytes from *Slc6a1*$^{+/A288V}$ and *Slc6a1*$^{+/S295L}$ knockin mice, and reduced GAT1 expression was partially rescued in brain lysates.[13] Furthermore, PBA treatment decreased seizures in these epileptic mice, demonstrating that chemical chaperones are a viable therapy for genetic epilepsy.[13]

For disease-causing, aggregation-prone STXBP1 mutants, PBA not only increased the total levels of STXBP1 – including wildtype – but it also decreased the fraction of detergent-insoluble protein, indicating that less STXBP1 protein was in aggregates and thus even more was functional.[2] Importantly, no negative effect was observed from overexpression of wildtype STXBP1, indicating that concerns from boosting the mutant protein, in non-aggregated forms, should be minimal.[2] Aggregates were also decreased in *Caenorhabditis elegans* expressing the various mutants, and localization of the protein within the ventral nerve cord was restored.[2] Furthermore, PBA rescued locomotion deficits in mutant *C. elegans*.[2]

PBA improved motor and neurobehavioral phenotypes in the Lafora disease model *Epm2b*$^{-/-}$ mice.[6] This was due to a reduction of polyglucosan inclusions and polyubiquitinated protein aggregates in the brain, which prevented neuronal loss and dampened reactive gliosis.[6] For ATP1A3 mutants associated with a range of neurological impairments from hypotonia to severe infantile epilepsy, PBA promoted expression of the mutant protein in vitro by stabilizing them and promoting proper trafficking through the Golgi apparatus.[15] PBA also ameliorated trafficking defects for an ER-retained LGI1 mutant associated with autosomal dominant lateral temporal lobe epilepsy, LGI1(E383A).[16] When the protein was able to be secreted, it was able to

correctly bind to its receptor, and thus PBA ameliorated the epilepsy phenotype in mouse models.[16] Creatine transporter deficiency syndrome has several neurological symptoms including epilepsy and developmental delay, and is caused by mutations in the creatine transporter 1 (hCRT-1).[17] These mutations result in a misfolded protein that is retained in the ER, and PBA treatment restored trafficking to the plasma membrane and creatine uptake functionality of several mutants.[17]

In a non-epileptic neurological disorder, PBA also decreases ER stress resulting from dominant-negative mutations of Wolfram syndrome-causing WSF1.[18] Additionally, PBA improves behavioral phenotypes in Parkinson's disease and Alzheimer's disease mouse models, and aids folding of the protein Pael-R implicated in autosomal recessive juvenile parkinsonism.[19,20] In combination with taurursodiol, PBA slowed the progression of ALS in a recent clinical trial.[21] Another non-epileptic neurological disorder potentially aided by PBA is dystonia: PBA treatment alleviated ER stress in cells expressing mutant torsinA.[22] Multiple membrane proteins with neurological functions, such as the serotonin transporter (SERT)[23] and monocarboxylate transporter 8 (MCT8),[24] are also chaperoned by PBA. PBA is thus a very promising compound, reducing ER stress and facilitating proper folding and trafficking of many proteins connected to a wide spectrum of neurological disorders.

### 4.1.2 Celastrol

Celastrol is a naturally occurring compound in several plants, including *Tripterygium wilfordii*, which is commonly called the "thunder god vine" and is a component of traditional Chinese medicine. Celastrol has many reported mechanisms of action, including activation of heat shock factor 1 (HSF1).[25,26] HSF1 is a transcription factor that

regulates transcription of heat shock response genes, so celastrol treatment results in global upregulation of molecular chaperones.[3,25]

Amongst the upregulated chaperones is HSP70.[26–29] By upregulating HSP70 in cultured motor neurons, celastrol stabilized the Charcot-Marie-Tooth disease mutant NEFL(Q333P).[28] Similarly, mutations in glucocerebrosidase, associated with Gaucher disease, had increased binding with HSP70 after celastrol treatment, and consequently had increased glucocerebroside hydrolysis function.[27]

Celastrol also protects against polyglutamine toxicity by reducing aggregation of the polyglutamine protein, via HSF1 activation and the resulting upregulation of HSP70.[30] Similarly, celastrol reduces aggregation and expression of mutant PKCγ associated with spinocerebellar ataxia type 14.[31] Upregulation of HSP70 is believed to be the mechanism by which celastrol prevents neuronal death via excitotoxicity after spinal cord injury.[29] However, in contrast to another upregulator of HSP70, arimoclomol, celastrol could not protect cultured motoneurons from $H_2O_2$ or staurosporin induced death, and was in fact itself toxic, inducing caspase-3 activation.[32]

Another mechanism of celastrol is prevention of oxidative stress. Rotenone, a potent inducer of oxidative stress, results in cytotoxicity to neuroblastoma SH-SY5Y cells, but pretreatment with nanomolar concentrations of celastrol reduced the oxidative stress and consequent cell death.[33] Larger doses of celastrol (0.1-5 uM), however, have been shown to be toxic to SH-SY5Y cells.[34] Additionally, celastrol inhibits nicotinamide adenine dinucleotide phosphate (NADPH) oxidase (NOX), preventing the formation of radical oxygen species.[35]

Celastrol has also been shown to increase autophagosome formation in SH-SY5Y cells, as determined from an elevated LC3-II/LC3-I ratio and decreased p62.[36] This upregulation of autophagy provided protection against the cytotoxicity of MPP+, preventing motor deficits and dopaminergic death in MPTP treated mice.[36]

Additional studies have found that celastrol can rescue ER stress, including reducing BiP.[37] Celastrol also upregulates HSP90, which stabilizes phosphomannomutase 2 (PMM2) mutants associated with PMM2 deficiency congenital disorder of glycosylation and increases enzymatic activity.[3] Celastrol is also widely reported as a proteasome inhibitor, although this has primarily been studied in the context of cancer and tumor cells.

However, it is the chemical chaperone effect that interests us most, and is likely the mechanism behind promising preliminary data. In HEK239T cells transfected with wildtype a1b2g2 or mutant a1b2g2(Q390X) GABR, celastrol increased both total and surface expression of α1 across a range of concentrations (0.125-4 μM).[38] While HSP70 expression was increased in the mutant condition, it was unchanged in the wildtype condition, indicating that HSP70 upregulation is not the sole mechanism behind the increase in α1.[38] In *Gabrg2*$^{+/Q390X}$ mice, celastrol (0.3 mg/kg/day for 14 days) increased surface expression of α1 and γ2, which increased frequency and amplitude of mIPSCs. Unsurprisingly, then, celastrol reduced seizures in 2 month old *Gabrg2*$^{+/Q390X}$ mice, and early intervention beginning at P7 completely abolished mortality in two separate models of Dravet syndrome: *Gabrg2*$^{+/Q390X}$ and *Scn1a*$^{+/-}$ mice.[38] In addition to improving the seizure phenotype, celastrol also improved performance on the Barnes maze for

*Gabrg2*$^{+/Q390X}$ mice, as well as *Gabrb3*$^{+/-}$ mice, which model Angelman syndrome with severe seizures.[38,39]

## 4.2 Methods

### 4.2.1 Cell culture and polyethyleneimine transfection

Human embryonic kidney 293 T (HEK293T) cells were grown in Dulbecco's Modified Eagle's Medium (DMEM) supplemented with 10% FBS and 1% penicillin/streptomycin. 24 hours after plating the cells, they were transfected with cDNA for wildtype rat GABR γ2S, γ2S(Q390X), γ2S(W461X) subunits (referred to hereafter simply as γ2, γ2(Q390X), and γ2(W461X) subunits, respectfully), human GABR α1 subunit, human GABR β2 subunit, and/or empty vector pcDNA. cDNA was combined with polyethyleneimine (PEI) at a ratio of 2.5 µL PEI per 1 µg cDNA. Celastrol (Sigma-Aldrich C0869) and 4-phenylbutyric acid (PBA) (Sigma-Aldrich P21005) were dissolved in dimethyl sulfoxide (DMSO).

### 4.2.2 Immunoblot

Cells were harvested 48 hr after transfection. Cells were washed with cold phosphate buffered saline (PBS) and lysed with RIPA-PI solution containing 20 mM Tris, 20 mM EGTA, 1 mM DTT, 1 mM benzamidine, 0.01 mM PMSF, 0.005 µg/mL leupeptin, and 0.005 µg/mL pepstatin. Protein concentration was measured and samples were subjected to standard SDS polyacrylamide gel electrophoresis (SDS-PAGE) procedures and immunoblotted. Primary antibodies used were anti-α1 1:500 (Millipore Sigma MABN489), anti-γ2 1:1,000 (Synaptic Systems 224003), and anti-ATPase 1:1,000 (Developmental Studies Hybridoma Bank a6F). Secondary antibodies were LI-COR

IRDye 680LT Goat anti-Mouse IgG Secondary Antibody (926-68020) and IRDye 800CW Goat anti-Rabbit IgG Secondary Antibody (926-32211), both 1:10,000.

Blots were imaged with an Odyssey DLx digital fluorescence scanner and LI-COR Image Studio Lite 5.2 software. Protein bands were quantified by circumscribing the band of interest and correcting for background signal. Integrated density values (IDVs) for the protein of interest were normalized to the IDV for the loading control, ATPase. The values were then normalized to loading controls and then the normalized IDV of the control lane (generally, wildtype or untreated), which was arbitrarily taken as equal to 1.

### 4.2.3 Mice

The generation of the *Gabrg2*$^{+/Q390X}$ mouse is described previously[40] and the line was maintained in C57BL/6J (Jackson Labs stock #000664). Animals were housed in standard facilities with ad libitum food and water access.

### 4.2.4 Drug administration and brain tissue preparation in *Gabrg2*$^{+/Q390X}$ mice

Beginning at 1-1.5 months of age, heterozygous *Gabrg2*$^{+/Q390X}$ animals and wildtype littermates, both male and female, were treated daily with vehicle or 100 mg/kg PBA injected intraperitoneally for 7 days. PBA (Sigma-Aldrich P21005) was dissolved in 10% dimethyl sulfoxide (DMSO) and 90% 0.9% saline, for a final concentration of 20 mg/mL. After 7 days of treatment, the mice were anesthetized with isoflurane and decapitated. The brain was removed, and the somatosensory cortex, cerebellum, thalamus, and hippocampus were dissected.

### 4.2.5 EEG acquisition and scoring

Around 2-3 months of age, male and female *Gabrg2*$^{+/Q390X}$ mice were surgically implanted with head mounts from Pinnacle Technology that have two bipolar electroencephalogram (EEG) channels and one subcutaneous nuchal electromyogram (EMG) channel (Pinnacle 8201: 2 EEG/1 EMG Mouse Headmount). After recovering from head mount surgery for 7 days, a 24 hr baseline recording was acquired, with EEG and EMG channels and simultaneous video. Mice were then treated daily with 100 mg/kg PBA injected intraperitoneally for 7 days and on the 8$^{th}$ day a 24 hr EEG recording was again acquired. EEGs were acquired with Sirenia Acquisition, with the sampling rate set at 400 Hz with a pre-amplifier gain of 100 Hz. EEG and EMG channels have a filter set at 25 Hz.

EEGs are scored by a blinded skilled scorer with Sirenia Seizure Pro software. A power analysis of the theta frequency band of 5-7 Hz is used to identify seizures, as 5-7 Hz spike-and-wave discharges (SWDs) are the mouse correlate of human 2-4 Hz SWDs. Suspected seizure events were confirmed with the video recording.

### 4.2.6 Data analysis

Data were analyzed using GraphPad Prism 9.4 and is reported as mean ± standard error of the mean (SEM). For the cell culture experiments, two-way analysis of variance (ANOVA) tests were performed and post-hoc analyses were performed as reported in the text, corrected for multiple comparisons. For the mouse immunohistochemistry experiments, one-way ANOVAs and Šídák's multiple comparisons post-hoc analysis were performed. Statistical significance was taken as $p < 0.05$ throughout.

## 4.3 Results

### 4.3.1 PBA reduces seizures in *Gabrg2*$^{+/Q390X}$ mice

Because PBA works extremely well to reduce seizures in mice with GAT1 mutations by modulating protein expression,[13] I tested the efficacy in *Gabrg2*$^{+/Q390X}$ mice. Compared with baseline, mice treated with 100 mg/kg PBA for 7 days had dramatically fewer seizures, as defined by 5-7 Hz spike-and-wave discharges (SWDs). Seizures were entirely eliminated in one mouse, while the other had only one 5-7 Hz SWD event during the 24 hr recording (baseline 29.0 ± 4.0, PBA 0.5 ± 0.5, $p = 0.0097$). The one seizure that did occur was much shorter than the average seizure duration at baseline (1.339 s vs 3.369 ± 0.065 s, $p = 0.0284$). Thus, the average total time spent seizing was radically reduced from 97.96 ± 15.36 s to 0.6695 ± 0.6695 s ($p = 0.0120$).

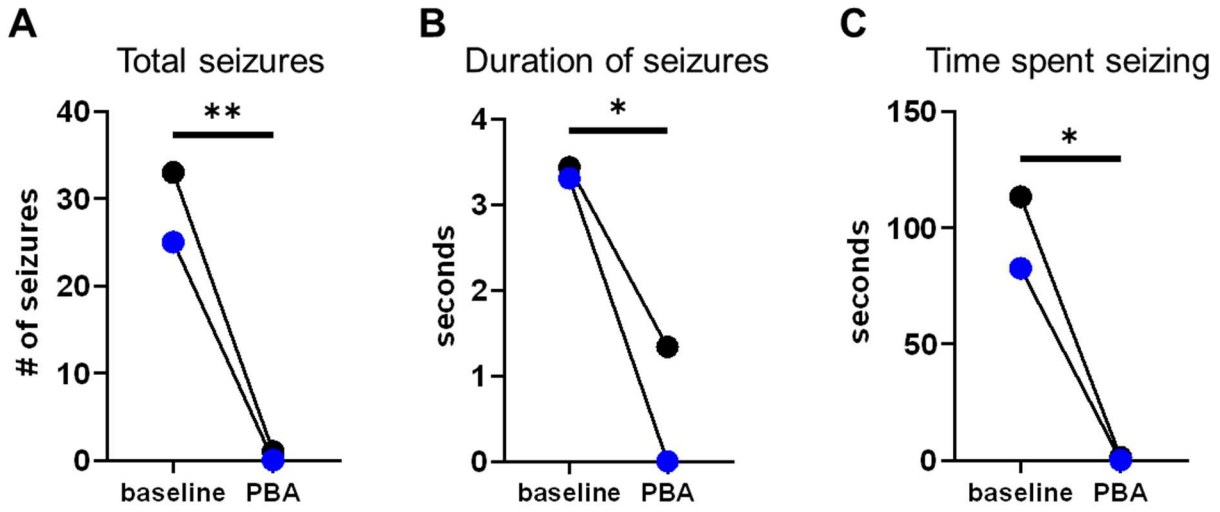


***Figure 4.1. PBA reduced 5-7 Hz SWDs in* Gabrg2$^{+/Q390X}$ *mice.***

### 4.3.2 PBA and celastrol fail to alter total protein expression of $GABA_A$ receptor subunits *in vitro*

To confirm if the anti-seizure effect of PBA was due to changes in protein expression, HEK293T cells were transfected with a full GABR in wildtype (α1β2γ2) or heterozygous mutant conditions (α1β2γ2/γ2(Q390X) and α1β2γ2/γ2(W461X)) and treated with 2 mM PBA for 24 hours or 1 μM celastrol for 6 hours. γ2(W461X) is an epilepsy-associated truncation mutation like γ2(Q390X) but it is less stable than wildtype γ2 and does not form protein aggregates or exert a dominant-negative effect on wildtype GABR subunits, although it does cause mild ER stress.[41] This mutation thus serves to provide further insight into any mutation-specific effects of the proteostasis regulators on expression of GABR subunits.

Interestingly, only α1 expression was affected by treatment with the drugs ($p$ = 0.0168). β2 and γ2 had strong genotype effects ($p < 0.0001$ for both β2 and γ2), in accordance with previous data, but there was no significant effect from drug treatment ($p$ = 0.0810 and 0.4214, respectively). Post-hoc analysis revealed that no single condition was significantly altered, although celastrol showed a very strong trend towards a reduction of α1 in the α1β2γ2/γ2(W461X) condition (untreated 1.157 ± 0.120; PBA 1.017 ± 0.215, $p$ = 0.6815 versus untreated; celastrol 0.731 ± 0.057, $p$ = 0.0561 versus untreated). And, there was no interaction between drug treatment and GABR condition, for any subunit, meaning that there were no mutation-specific drug effects.

For the α1β2γ2/γ2(Q390X) condition, I hypothesized that the drugs may affect wildtype and mutant γ2 differently, and thus in addition to quantifying total γ2 signal of all forms, I also examined γ2 and γ2(Q390X) monomers specifically. Wildtype γ2 and

mutant γ2(Q390X) were both unchanged by either drug (γ2: untreated 1 ± 0; PBA 1.108 ± 0.142, $p$ = 0.6771; celastrol0.819 ± 0.151, $p$ = 0.3611. γ2(Q390X): untreated 1 ± 0, PBA 1.073 ± 0.087, $p$ = 0.8428; celastrol 0.946 ± 0.160, $p$ = 0.9088).

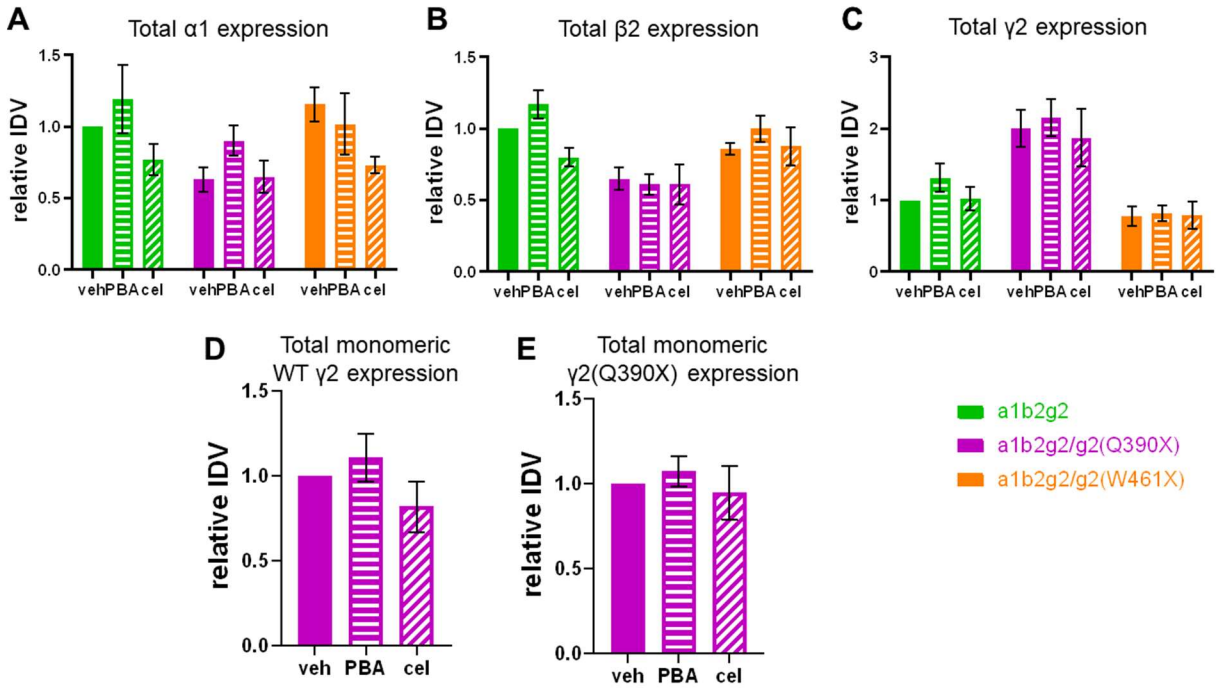


***Figure 4.2. Neither PBA nor celastrol affects total expression of GABR subunits in vitro.***

***Table 4.1. p values of analysis of total GABR subunit expression in cells expressing different GABRs and treated with PBA or celastrol.***

| | Drug | Genotype | Interaction |
|---|---|---|---|
| α1 | **0.0168** | **0.0459** | 0.4626 |
| β2 | 0.0810 | **<0.0001** | 0.2554 |
| γ2 | 0.4214 | **<0.0001** | 0.9378 |

Significant values ($p$ < 0.05) are bolded. 2-way ANOVA, n = 4-7.

***Table 4.2. Analysis of total GABR subunit expression in cells expressing different GABRs and treated with PBA or celastrol.***

| | vehicle | PBA | celastrol |
|---|---|---|---|
| **α1** | | | |
| α1β2γ2 | 1 ± 0 | 1.190 ± 0.238; 0.4810 | 0.770 ± 0.110; 0.3225 |
| α1β2γ2/γ2(Q390X) | 0.633 ± 0.085 | 0.903 ± 0.103; 0.3067 | 0.650 ± 0.113; 0.9946 |
| α1β2γ2/γ2(W461X) | 1.157 ± 0.120 | 1.017 ± 0.215; 0.6815 | *0.731 ± 0.057; 0.0561* |
| | | | |
| **β2** | | | |
| α1β2γ2 | 1 ± 0 | 1.171 ± 0.099; 0.2551 | 0.798 ± 0.065; 0.1610 |
| α1β2γ2/γ2(Q390X) | 0.649 ± 0.079 | 0.611 ± 0.071; 0.9380 | 0.611 ± 0.141; 0.9371 |
| α1β2γ2/γ2(W461X) | 0.859 ± 0.038 | 1.001 ± 0.092; 0.4379 | 0.877 ± 0.132; 0.9852 |
| | | | |
| **γ2** | | | |
| α1β2γ2 | 1 ± 0 | 1.316 ± 0.191; 0.3970 | 1.025 ± 0.161; 0.9938 |
| α1β2γ2/γ2(Q390X) | 1.999 ± 0.258 | 2.155 ± 0.255; 0.8145 | 1.870 ± 0.404; 0.8785 |
| α1β2γ2/γ2(W461X) | 0.778 ± 0.133 | 0.819 ± 0.107; 0.9849 | 0.788 ± 0.188; 0.9990 |
| | | | |
| **γ2, WT monomer** | | | |
| α1β2γ2/γ2(Q390X) | 1 ± 0 | 1.108 ± 0.142; 0.6771 | 0.819 ± 0.151; 0.3611 |
| | | | |
| **γ2, QX monomer** | | | |
| α1β2γ2/γ2(Q390X) | 1 ± 0 | 1.073 ± 0.087; 0.8428 | 0.946 ± 0.160; 0.9088 |

Values are expressed relative to the IDV of vehicle-treated α1β2γ2, which was taken as 1. Values presented are mean ± SEM and *p* value, compared to vehicle treated controls. Significant values ($p < 0.05$) are bolded. 2-way ANOVA, Dunnett's multiple comparisons test; n = 4-7. For γ2 monomers, 1-way ANOVA, Dunnett's multiple comparisons test; n = 6-7.

### 4.3.3 Celastrol, but not PBA, altered surface expression of γ2 protein

Despite the minimal change in total protein expression, it is possible that the proteostasis regulators did stabilize the degradation-prone proteins and increased functional levels, without a change in total protein expression. So, wildtype α1β2γ2 or mutant α1β2γ2/γ2(Q390X) GABR were expressed in HEK293T cells and surface expression of the GABR subunits was measured.

As expected, the genotype had very strong effects on surface expression of all three subunits. Additionally, drug treatment did influence α1 and β2 surface expression, although post-hoc analysis showed no individual condition was significantly altered compared to the respective untreated condition. A closer look at γ2 did, however, yield interesting findings. In these experimental conditions, dimers of γ2 are detected on the membrane, but functional receptors contain only a single γ2, with two α1 and 2 β2 subunits. Therefore, I quantified the total amount of γ2 signal detected, and separately quantified the single band representing the monomeric wildtype γ2 subunit. While the total amount of γ2 of all forms expressed at the surface was not changed by either drug, celastrol did influence monomeric wildtype γ2. In the wildtype GABR condition, celastrol treatment reduced monomeric γ2 surface expression (untreated 1 ± 0; celastrol 0.705 ± 0.071; $p = 0.0421$), but there was no effect for the mutant α1β2γ2/γ2(Q390X) GABR (untreated 1 ± 0; celastrol 0.287 ± 0.051; $p = 0.9536$). PBA had no effect.

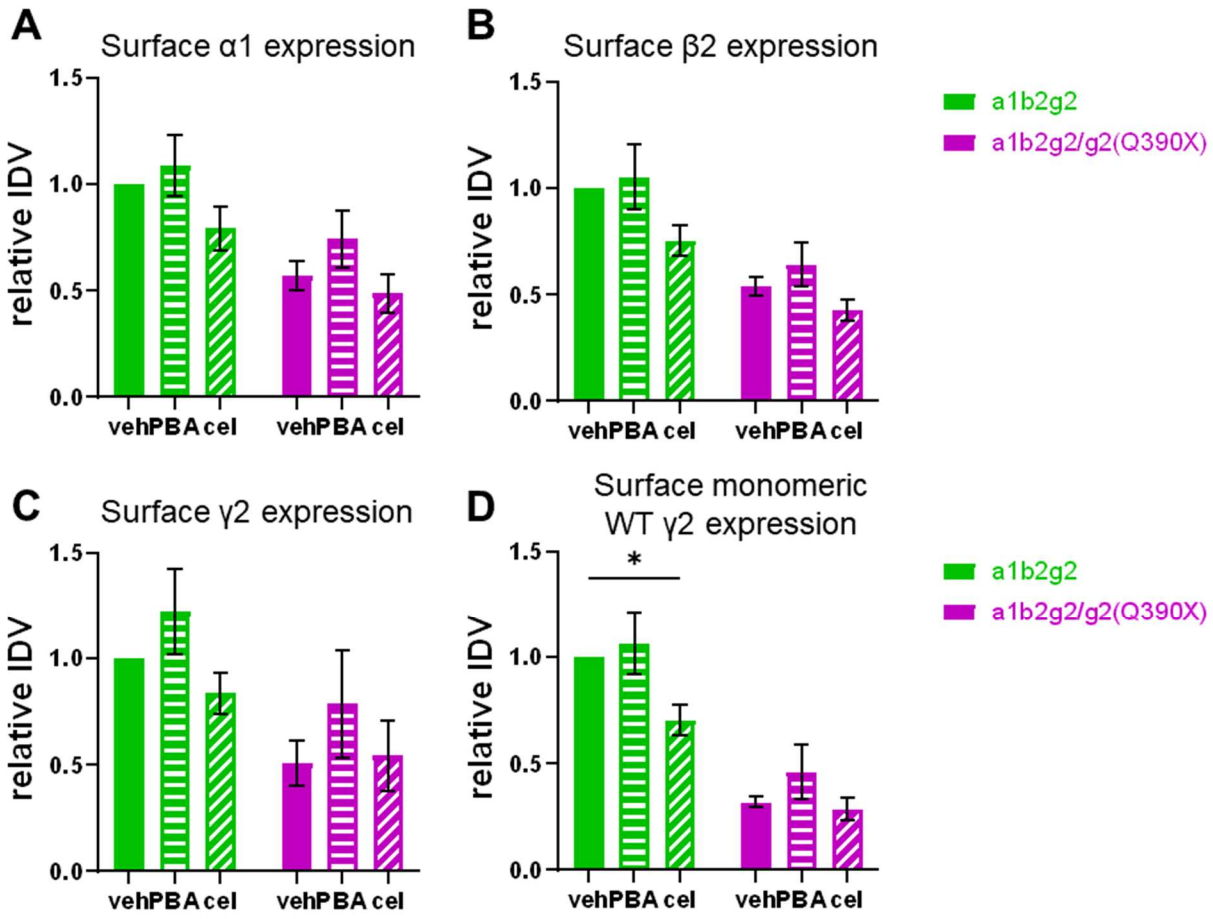


***Figure 4.3. Celastrol, but not PBA, reduced surface expression of γ2.***
Surface expression of α1 and β2 subunits was unaffected by either drug.

***Table 4.3. p values of analysis of surface GABR subunit expression in cells expressing different GABRs and treated with PBA or celastrol.***

| | Drug | Genotype | Interaction |
|---|---|---|---|
| α1 | **0.0373** | **0.0002** | 0.8273 |
| β2 | **0.0161** | **<0.0001** | 0.7289 |
| γ2 | 0.1306 | **0.0036** | 0.8161 |
| γ2, WT monomer | **0.0152** | **<0.0001** | 0.3133 |

Significant values ($p < 0.05$) are bolded. 2-way ANOVA, n = 6-7.

***Table 4.4. Analysis of surface GABR subunit expression in cells expressing different GABRs and treated with PBA or celastrol.***

| | vehicle | PBA | celastrol |
|---|---|---|---|
| **α1** | | | |
| α1β2γ2 | 1 ± 0 | 1.088 ± 0.142; 0.7698 | 0.792 ± 0.105; 0.2692 |
| α1β2γ2/γ2(Q390X) | 0.571 ± 0.068 | 0.743 ± 0.134; 0.3933 | 0.486 ± 0.092; 0.7817 |
| | | | |
| **β2** | | | |
| α1β2γ2 | 1 ± 0 | 1.054 ± 0.155; 0.8658 | 0.754 ± 0.071; 0.0907 |
| α1β2γ2/γ2(Q390X) | 0.540 ± 0.042 | 0.642 ± 0.103; 0.6125 | 0.429 ± 0.048; 0.5602 |
| | | | |
| γ2 | | | |
| α1β2γ2 | 1 ± 0 | 1.222 ± 0.204; 0.5222 | 0.836 ± 0.097; 0.6920 |
| α1β2γ2/γ2(Q390X) | 0.507 ± 0.106 | 0.785 ± 0.252; 0.3733 | 0.542 ± 0.168; 0.9832 |
| | | | |
| γ2, WT monomer | | | |
| α1β2γ2 | 1 ± 0 | 1.066 ± 0.147; 0.8148 | **0.705 ± 0.071; 0.0421** |
| α1β2γ2/γ2(Q390X) | 0.319 ± 0.025 | 0.460 ± 0.128; 0.4254 | 0.287 ± 0.051; 0.9536 |

Values are expressed relative to the IDV of vehicle-treated α1β2γ2, which was taken as 1. Values presented are mean ± SEM and *p* value, compared to vehicle treated controls. Significant values ($p < 0.05$) are bolded. 2-way ANOVA, Dunnett's multiple comparisons test; n = 6-7.

### 4.3.4 PBA did not alter total protein expression in *Gabrg2*$^{+/Q390X}$ mice

Mice 1-1.5 months of age were treated with PBA (100 mg/kg/day for 7 days). I examined α1, β2, γ2, and the ER chaperones BiP and calnexin. I also examined GAT1 to be able to draw comparisons to our GAT1 mouse models, as we have already shown that PBA increases GAT1 expression in these animals. Additionally, I measured Hrd1 and Sel1L, to provide possible insight on the mechanism of the hypothesized changes

to the GABR subunits, as well as allowing comparisons to zonisamide treatment (see Chapter 5).

Consistent with the *in vitro* data from transfected HEK293T cells, PBA treatment did not alter α1, β2, or γ2 total expression in any brain region, although GABR subunit expression did vary based on genotype, as expected. In contrast to work from our lab on PBA in *Slc6a1*$^{+/A288V}$ and *Slc6a1*$^{+/S295L}$ mice, in which an increase in GAT1 was seen in the cortex, hippocampus, and thalamus of 2-month-old mice,[13] there was no change in GAT1 for the PBA-treated *Gabrg2*$^{+/Q390X}$ mice or wildtype littermates.

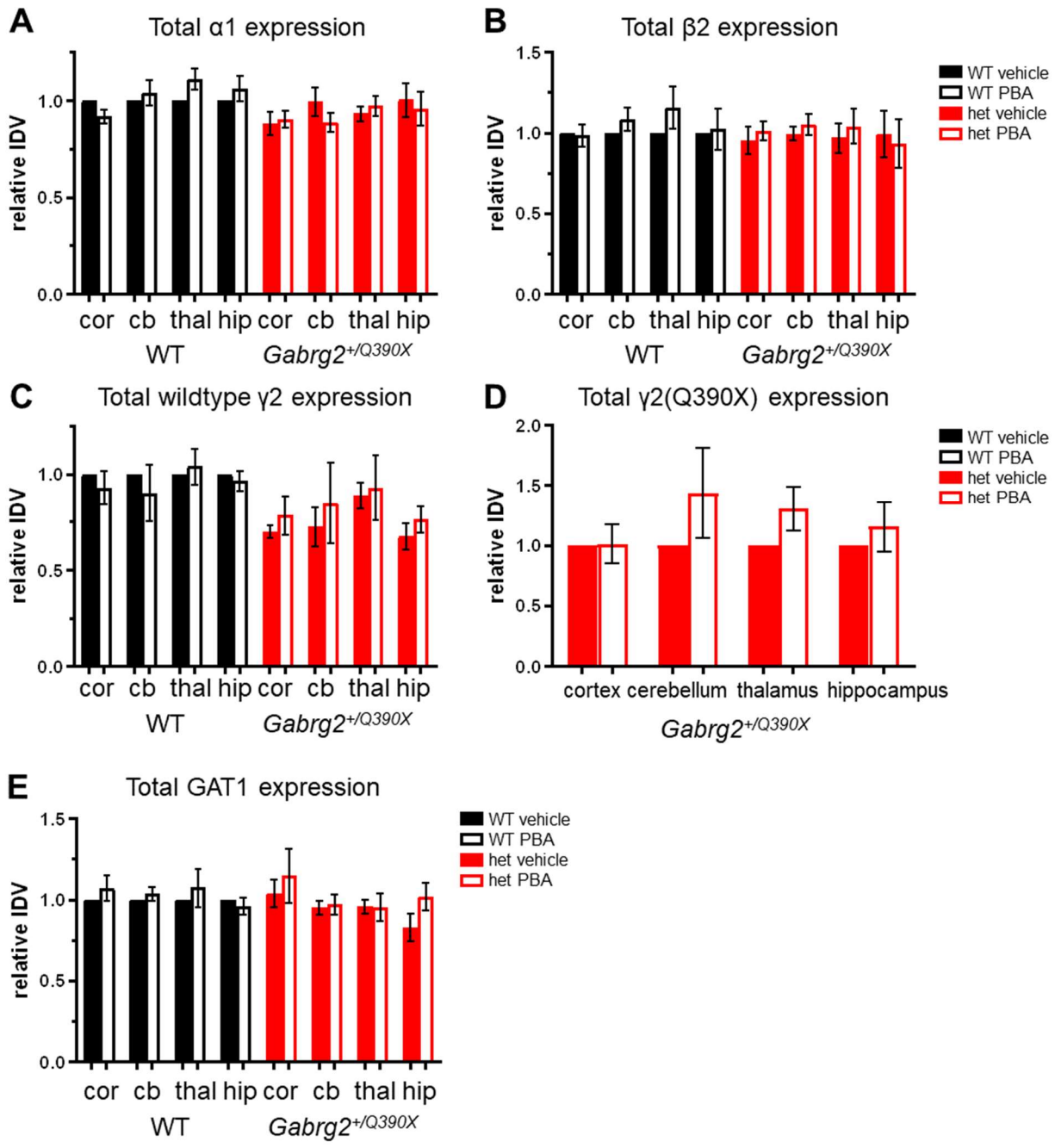


***Figure 4.4. PBA did not alter total expression of GABR subunits or GAT1 in* Gabrg2$^{+/Q390X}$ *mice.***

Interesting differences were found for the proteostasis elements. Calnexin expression was affected by PBA treatment and by mouse genotype in the cortex, although there was no interaction between these two factors. Post-hoc analysis, however, suggests upregulation in the mutant animals is driving the difference, while calnexin expression in the wildtype animals is unchanged (WT: 1 ± 0 untreated vs 1.083 ± 0.056 PBA, $p = 0.5260$; het: 1.065 ± 0.046 untreated vs 1.260 ± 0.090 PBA, $p = 0.0567$). In the cerebellum, a strong trend ($p = 0.0544$) was detected for drug effects.

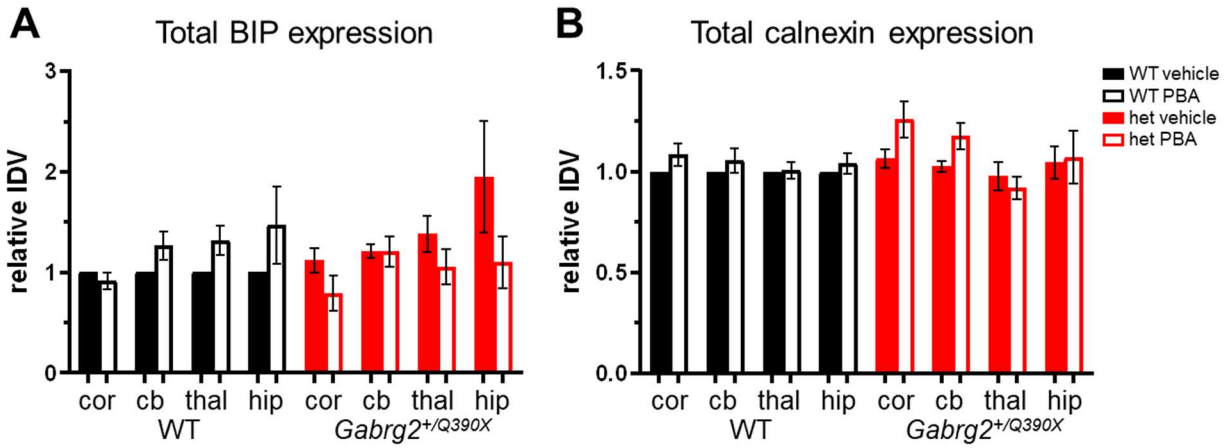


***Figure 4.5. PBA did not alter total expression of ER chaperones in* Gabrg2$^{+/Q390X}$ *mice.***

PBA also affected Sel1L expression in the cortex and cerebellum. As with calnexin, the mutant mice show the most change (cortex: WT: 1 ± 0 untreated vs 1.029 ± 0.112 PBA, $p = 0.9791$; het: 0.897 ± 0.099 untreated vs 1.353 ± 0.170 PBA, $p = 0.0218$). In

the thalamus and hippocampus, however, there was no difference in calnexin or Sel1L. BiP and Hrd1 were not influenced by PBA or genotype.

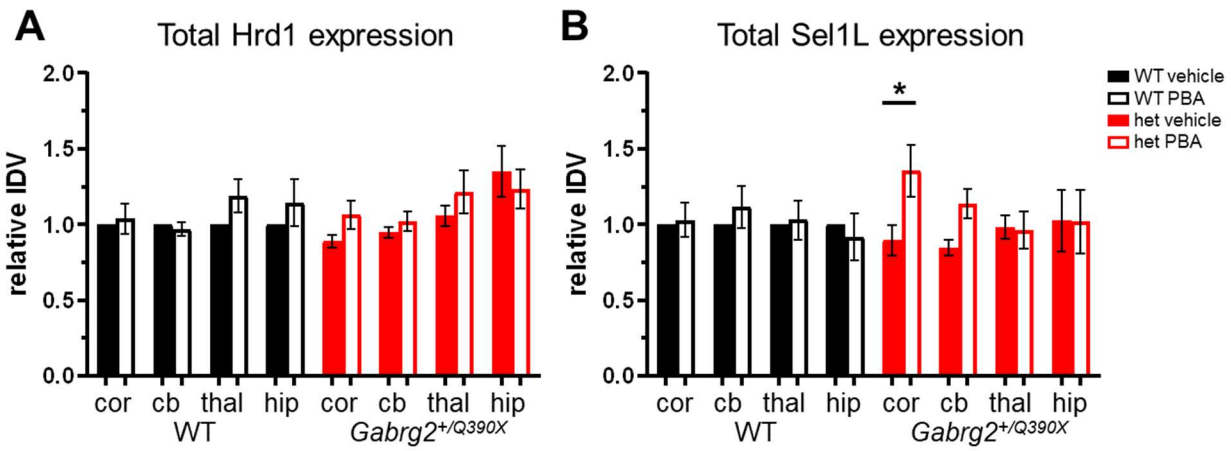


***Figure 4.6. PBA upregulated Sel1L but not Hrd1 in* Gabrg2$^{+/Q390X}$ *mice.***

***Table 4.5. p values of analysis of total protein expression in wildtype and* Gabrg2$^{+/Q390X}$ *mice treated with PBA.***

| Protein of interest, brain region | **PBA** | **Genotype** | **Interaction** |
|---|---|---|---|
| **Calnexin** | | | |
| Cortex | **0.0252** | **0.0491** | 0.3425 |
| Cerebellum | *0.0544* | 0.1521 | 0.3603 |
| Thalamus | 0.6028 | 0.2764 | 0.4989 |
| Hippocampus | 0.6760 | 0.6388 | 0.9302 |
| | | | |
| **Sel1L** | | | |
| Cortex | **0.0445** | 0.3426 | 0.0739 |
| Cerebellum | **0.0428** | 0.4911 | 0.3606 |
| Thalamus | 0.9578 | 0.6762 | 0.8084 |
| Hippocampus | 0.7939 | 0.7115 | 0.8218 |

Significant values ($p < 0.05$) are bolded. 2-way ANOVA, Sidak's multiple comparisons test; n = 6-7.

***Table 4.6. Analysis of total protein expression in wildtype and* Gabrg2$^{+/Q390X}$ *mice treated with PBA.***

| Protein of interest, brain region | **Wildtype, vehicle** | **Wildtype, PBA** | ***p*, vs vehicle** | **Heterozygous, vehicle** | **Heterozygous, PBA** | ***p*, vs vehicle** |
|---|---|---|---|---|---|---|
| **α1** | | | | | | |
| Cortex | 1 ± 0 | 0.920 ± 0.035 | 0.3142 | 0.881 ± 0.060 | 0.904 ± 0.044 | 0.9049 |
| Cerebellum | 1 ± 0 | 1.040 ± 0.066 | 0.8556 | 0.994 ± 0.076 | 0.888 ± 0.050 | 0.3808 |
| Thalamus | 1 ± 0 | 1.113 ± 0.054 | 0.1439 | 0.933 ± 0.039 | 0.974 ± 0.052 | 0.7698 |
| Hippocampus | 1 ± 0 | 1.061 ± 0.066 | 0.7829 | 1.005 ± 0.087 | 0.960 ± 0.086 | 0.8844 |
| | | | | | | |
| **β2** | | | | | | |
| Cortex | 1 ± 0 | 0.986 ± 0.069 | 0.9854 | 0.956 ± 0.086 | 1.014 ± 0.061 | 0.7864 |
| Cerebellum | 1 ± 0 | 1.087 ± 0.073 | 0.4756 | 0.994 ± 0.044 | 1.052 ± 0.066 | 0.7349 |
| Thalamus | 1 ± 0 | 1.157 ± 0.132 | 0.4757 | 0.969 ± 0.092 | 1.041 ± 0.108 | 0.8638 |
| Hippocampus | 1 ± 0 | 1.022 ± 0.128 | 0.9897 | 0.992 ± 0.144 | 0.936 ± 0.151 | 0.9408 |
| | | | | | | |
| **γ2, WT** | | | | | | |
| Cortex | 1 ± 0 | 0.929 ± 0.089 | 0.7354 | 0.699 ± 0.032 | 0.786 ± 0.103 | 0.6557 |
| Cerebellum | 1 ± 0 | 0.903 ± 0.147 | 0.8577 | 0.725 ± 0.102 | 0.849 ± 0.211 | 0.7929 |
| Thalamus | 1 ± 0 | 1.041 ± 0.092 | 0.9493 | 0.890 ± 0.068 | 0.929 ± 0.171 | 0.9573 |
| Hippocampus | 1 ± 0 | 0.966 ± 0.053 | 0.8826 | 0.675 ± 0.068 | 0.765 ± 0.068 | 0.4651 |
| | | | | | | |
| **γ2, QX** | | | | | | |
| Cortex | | | | 1 ± 0 | 1.015 ± 0.159 | 0.9267 |
| Cerebellum | | | | 1 ± 0 | 1.439 ± 0.373 | 0.2665 |
| Thalamus | | | | 1 ± 0 | 1.309 ± 0.186 | 0.1276 |
| Hippocampus | | | | 1 ± 0 | 1.157 ± 0.205 | 0.4728 |
| | | | | | | |
| **GAT1** | | | | | | |
| Cortex | 1 ± 0 | 1.071 ± 0.077 | 0.8547 | 1.03 ±9 0.088 | 1.150 ± 0.167 | 0.7015 |
| Cerebellum | 1 ± 0 | 1.035 ± 0.043 | 0.8074 | 0.952 ± 0.042 | 0.971 ± 0.061 | 0.9416 |
| Thalamus | 1 ± 0 | 1.075 ± 0.119 | 0.7635 | 0.957 ± 0.041 | 0.955 ± 0.084 | 0.9997 |

| | | | | | | |
|---|---|---|---|---|---|---|
| Hippocampus | 1 ± 0 | 0.959 ± 0.053 | 0.8803 | 0.830 ± 0.084 | 1.018 ± 0.085 | 0.1100 |
| | | | | | | |
| **BiP** | | | | | | |
| Cortex | 1 ± 0 | 0.915 ± 0.083 | 0.8361 | 1.120 ± 0.120 | 0.791 ± 0.178 | 0.1100 |
| Cerebellum | 1 ± 0 | 1.263 ± 0.141 | 0.2030 | 1.213 ± 0.072 | 1.207 ± 0.149 | 0.9993 |
| Thalamus | 1 ± 0 | 1.316 ± 0.146 | 0.2474 | 1.383 ± 0.179 | 1.056 ± 0.173 | 0.2502 |
| Hippocampus | 1 ± 0 | 1.470 ± 0.387 | 0.5969 | 1.947 ± 0.554 | 1.098 ± 0.256 | 0.2288 |
| | | | | | | |
| **Calnexin** | | | | | | |
| Cortex | 1 ± 0 | 1.083 ± 0.056 | 0.5260 | *1.065 ± 0.046* | *1.260 ± 0.090* | *0.0567* |
| Cerebellum | 1 ± 0 | 1.055 ± 0.062 | 0.6817 | 1.027 ± 0.027 | 1.175 ± 0.067 | 0.1004 |
| Thalamus | 1 ± 0 | 1.008 ± 0.041 | 0.9918 | 0.979 ± 0.071 | 0.919 ± 0.057 | 0.6493 |
| Hippocampus | 1 ± 0 | 1.040 ± 0.050 | 0.9191 | 1.044 ± 0.079 | 1.070 ± 0.130 | 0.9670 |
| | | | | | | |
| **Hrd1** | | | | | | |
| Cortex | 1 ± 0 | 1.039 ± 0.100 | 0.9195 | 0.891 ± 0.042 | 1.065 ± 0.095 | 0.2384 |
| Cerebellum | 1 ± 0 | 0.970 ± 0.046 | 0.8817 | 0.950 ± 0.034 | 1.021 ± 0.067 | 0.5271 |
| Thalamus | 1 ± 0 | 1.190 ± 0.107 | 0.3106 | 1.056 ± 0.068 | 1.216 ± 0.140 | 0.4556 |
| Hippocampus | 1 ± 0 | 1.145 ± 0.155 | 0.6943 | 1.349 ± 0.167 | 1.236 ± 0.132 | 0.8093 |
| | | | | | | |
| **Sel1L** | | | | | | |
| Cortex | 1 ± 0 | 1.029 ± 0.112 | 0.9791 | **0.897 ± 0.099** | **1.353 ± 0.170** | **0.0218** |
| Cerebellum | 1 ± 0 | 1.115 ± 0.137 | 0.6264 | 0.846 ± 0.052 | 1.137 ± 0.097 | 0.0855 |
| Thalamus | 1 ± 0 | 1.030 ± 0.130 | 0.9716 | 0.982 ± 0.080 | 0.962 ± 0.122 | 0.9890 |
| Hippocampus | 1 ± 0 | 0.919 ± 0.152 | 0.9250 | 1.024 ± 0.204 | 1.018 ± 0.212 | 0.9996 |

Values are expressed relative to the IDV of vehicle-treated wildtype mice, which was taken as 1. Values presented are mean ± SEM and *p* value, compared to vehicle-treated controls of the same genotype. Significant values ($p < 0.05$) are bolded. Values approaching significance are italicized. 2-way ANOVA, Sidak's multiple comparisons test; n = 6-7. For γ2(Q390X), t-test; n = 4-7.

## 4.4 Discussion and future directions

PBA unequivocally reduced the total number of 5-7 SWD seizure events and the total amount of time spent seizing, in *Gabrg2*$^{+/Q390X}$ mice. However, the mechanism by which PBA reduces seizures in this Dravet syndrome model merits further investigation. Unlike models of *SLC6A1* mutations, in which PBA upregulates GAT1 total and surface expression and increases GABA uptake activity, PBA does not seem to alter total GABR subunit expression *in vivo* or *in vitro*.

Surprisingly, PBA does affect total expression of the ER chaperone calnexin and the ERAD component Sel1L, in a brain region specific manner. In the somatosensory cortex and cerebellum of *Gabrg2*$^{+/Q390X}$ mice, calnexin and Sel1L are either clearly upregulated or show a strong trend towards upregulation. Wildtype littermates, however, are not as affected. This indicates that the seizure control may be due to reductions in ER stress. Although *in vitro* data did not show an effect of PBA (only celastrol) on surface expression, the combination of seizure reduction and increased ER chaperone expression suggests that surface trafficking of functional GABR subunits may be facilitated *in vivo* by PBA. Brain slice electrophysiology will be vital in investigating this possibility.

PBA is well established as an ER stress reducer, and in a model of hyperoxaluria, PBA treatment alleviates elevated calnexin and BiP.[42] However, a study in chondrocytes found that PBA did not rescue expression of molecular chaperones like calnexin, although PBA did normalize ER stress markers.[43] The precise effects of PBA on components of protein quality control, therefore, may depend on cell type and the specific disease.

It is interesting that Hrd1 was not also upregulated, in correlation with the changes in Sel1L. Reducing Sel1L results in a marked decrease of Hrd1 protein expression[44,45] and increased Sel1L is associated with upregulation of Hrd1.[46]

Celastrol decreased surface expression of monomeric γ2 in HEK293T cells transfected with wildtype α1β2γ2 GABR, which suggests the number of functional receptors in the cell membrane is likely decreased. The trend in α1 and β2 towards lower surface expression supports this. Because there was no change in total protein expression, this indicates that celastrol is altering maturation and trafficking of the subunits, although glycan digestion with glycosidases Endoglycosidase H and PNGase F would provide more evidence. Microscopy to visualize subcellular locations of the GABR subunits could also be helpful.

The reduction in cell surface expression of the wildtype γ2 subunit in transfected HEK293T cells was unexpected. Celastrol upregulates many heat shock response components, including HSP70, via activation of HSF1.[25,26] Upregulation of molecular chaperones such as HSP70 was predicted to stabilize the GABR subunits and result in increased surface expression. However, the effect on HSP70 is cell type specific: In cultured cerebral cortex, celastrol administration only influenced HSP70 in cortical neurons, and not glial cells.[47] And, in cultured dorsal root ganglion, celastrol upregulated Hsp70 in motor neurons but not in sensory neurons.[28] Interestingly, celastrol had the opposite effect on HSPB1/HSP27, which was upregulated in sensory neurons and not in motor neurons, possibly because HSP27 is not normally expressed in motor neurons.[28] So, in the HEK293T cells used in my experiments, celastrol may have not

upregulated the expected molecular chaperones, and indeed prior lab data had suggested that HSP70 was not upregulated in cells expressing wildtype GABR.[38] The interaction between HSPs, celastrol, and GABR subunits merits further investigation.

Additionally, in contrast to the γ2 surface expression reduction in HEK293T cells transfected with wildtype GABR caused by celastrol treatment, in cells expressing mutant α1β2γ2/γ2(Q390X) GABR there was no difference in any subunit, compared to vehicle-treated controls. Mutation-specific effects of celastrol have been reported, such as for mutations in neurofilament light chain (NEFL) that result in for Charco-Marie-Tooth disease. Neurofilament assembly of NEFL(Q333P) was rescued – but only in motor neurons, not sensory neurons – while NEFL(P8R) assembly was not rescued.[28] Despite the persistence of cytoskeletal abnormalities, toxicity of NEFL was mitigated by celastrol, but only in sensory neurons.[28] The efficacy of HSP70 and other HSPs to promote degradation of mutant γ2(Q390X) protein, stabilize wildtype GABR subunits, and/or facilitate surface trafficking of wildtype subunits should be investigated, perhaps through gene overexpression *in vitro*.

The suitability of celastrol for treatment of epilepsy is not certain. In the amygdala kindling model of epilepsy, mice treated with celastrol (1 mg/kg) actually had a reduced seizure threshold after kindling, although the threshold for initial seizures was unchanged.[25] Additionally, these mice had more activated microglia than vehicle-treated control animals, while celastrol-treated HSP70 knockout mice did not, indicating a deleterious inflammatory response mediated by HSP70.[25]

Taken together, the data in this chapter suggest that proteostasis regulators like pharmacological chaperones and molecular chaperone upregulators can be used to modulate surface expression of GABR subunits. This thus opens up an entire class of drugs as potential ASDs.

## 4.5 References


1. Guerriero CJ, Brodsky JL. The delicate balance between secreted protein folding and endoplasmic reticulum-associated degradation in human physiology. *Physiol Rev*. 2012;92(2):537-576. doi:10.1152/physrev.00027.2011

2. Guiberson NGL, Pineda A, Abramov D, et al. Mechanism-based rescue of Munc18-1 dysfunction in varied encephalopathies by chemical chaperones. *Nat Commun*. 2018;9(1):3986. doi:10.1038/s41467-018-06507-4

3. Vilas A, Yuste-Checa P, Gallego D, et al. Proteostasis regulators as potential rescuers of PMM2 activity. *Biochim Biophys Acta Mol Basis Dis*. 2020;1866(7):165777. doi:10.1016/j.bbadis.2020.165777

4. Ciana G, Dardis A, Pavan E, et al. In vitro and in vivo effects of Ambroxol chaperone therapy in two Italian patients affected by neuronopathic Gaucher disease and epilepsy. *Mol Genet Metab Rep*. 2020;25:100678. doi:10.1016/j.ymgmr.2020.100678

5. Di XJ, Wang YJ, Han DY, et al. Grp94 Protein Delivers γ-Aminobutyric Acid Type A (GABAA) Receptors to Hrd1 Protein-mediated Endoplasmic Reticulum-associated Degradation. *J Biol Chem*. 2016;291(18):9526-9539. doi:10.1074/jbc.M115.705004

6. Berthier A, Payá M, García-Cabrero AM, et al. Pharmacological Interventions to Ameliorate Neuropathological Symptoms in a Mouse Model of Lafora Disease. *Mol Neurobiol*. 2016;53(2):1296-1309. doi:10.1007/s12035-015-9091-8

7. Mattison KA, Butler KM, Inglis GAS, et al. SLC6A1 variants identified in epilepsy patients reduce γ-aminobutyric acid transport. *Epilepsia*. 2018;59(9):e135-e141. doi:10.1111/epi.14531

8. Mermer F, Poliquin S, Rigsby K, et al. Common molecular mechanisms of SLC6A1 variant-mediated neurodevelopmental disorders in astrocytes and neurons. *Brain*. 2021;144(8):2499-2512. doi:10.1093/brain/awab207

9. Mermer F, Poliquin S, Zhou S, et al. Astrocytic GABA transporter 1 deficit in novel SLC6A1 variants mediated epilepsy: Connected from protein destabilization to seizures in mice and humans. *Neurobiol Dis*. 2022;172:105810. doi:10.1016/j.nbd.2022.105810

10. Poliquin S, Hughes I, Shen W, et al. Genetic mosaicism, intrafamilial phenotypic heterogeneity, and molecular defects of a novel missense SLC6A1 mutation associated with epilepsy and ADHD. *Exp Neurol*. 2021;342:113723. doi:10.1016/j.expneurol.2021.113723

11. Wang J, Poliquin S, Mermer F, et al. Endoplasmic reticulum retention and degradation of a mutation in SLC6A1 associated with epilepsy and autism. *Mol Brain*. 2020;13(1):76. doi:10.1186/s13041-020-00612-6

12. Cai K, Wang J, Eissman J, et al. A missense mutation in SLC6A1 associated with Lennox-Gastaut syndrome impairs GABA transporter 1 protein trafficking and function. *Exp Neurol*. 2019;320:112973. doi:10.1016/j.expneurol.2019.112973

13. Nwosu G, Mermer F, Flamm C, et al. 4-Phenylbutyrate restored γ-aminobutyric acid uptake and reduced seizures in SLC6A1 patient variant-bearing cell and mouse models. *Brain Commun*. 2022;4(3):fcac144. doi:10.1093/braincomms/fcac144

14. Piniella D, Canseco A, Vidal S, et al. Experimental and Bioinformatic Insights into the Effects of Epileptogenic Variants on the Function and Trafficking of the GABA Transporter GAT-1. *Int J Mol Sci*. 2023;24(2):955. doi:10.3390/ijms24020955

15. Arystarkhova E, Ozelius LJ, Brashear A, Sweadner KJ. Misfolding, altered membrane distributions, and the unfolded protein response contribute to pathogenicity differences in Na,K-ATPase ATP1A3 mutations. *J Biol Chem*. 2021;296:100019. doi:10.1074/jbc.RA120.015271

16. Yokoi N, Fukata Y, Kase D, et al. Chemical corrector treatment ameliorates increased seizure susceptibility in a mouse model of familial epilepsy. *Nat Med*. 2015;21(1):19-26. doi:10.1038/nm.3759

17. El-Kasaby A, Kasture A, Koban F, et al. Rescue by 4-phenylbutyrate of several misfolded creatine transporter-1 variants linked to the creatine transporter deficiency syndrome. *Neuropharmacology*. 2019;161:107572. doi:10.1016/j.neuropharm.2019.03.015

18. Batjargal K, Tajima T, Jimbo EF, Yamagata T. Effect of 4-phenylbutyrate and valproate on dominant mutations of WFS1 gene in Wolfram syndrome. *J Endocrinol Invest*. 2020;43(9):1317-1325. doi:10.1007/s40618-020-01228-2

19. Omura T, Kaneko M, Okuma Y, Matsubara K, Nomura Y. Endoplasmic reticulum stress and Parkinson's disease: the role of HRD1 in averting apoptosis in neurodegenerative disease. *Oxid Med Cell Longev*. 2013;2013:239854. doi:10.1155/2013/239854

20. Kolb PS, Ayaub EA, Zhou W, Yum V, Dickhout JG, Ask K. The therapeutic effects of 4-phenylbutyric acid in maintaining proteostasis. *Int J Biochem Cell Biol*. 2015;61:45-52. doi:10.1016/j.biocel.2015.01.015

21. Paganoni S, Macklin EA, Hendrix S, et al. Trial of Sodium Phenylbutyrate–Taurursodiol for Amyotrophic Lateral Sclerosis. *N Engl J Med*. 2020;383(10):919-930. doi:10.1056/NEJMoa1916945

22. Cho JA, Zhang X, Miller GM, Lencer WI, Nery FC. 4-Phenylbutyrate Attenuates the ER Stress Response and Cyclic AMP Accumulation in DYT1 Dystonia Cell Models. *PLOS ONE*. 2014;9(11):e110086. doi:10.1371/journal.pone.0110086

23. Fujiwara M, Yamamoto H, Miyagi T, et al. Effects of the chemical chaperone 4-phenylbutylate on the function of the serotonin transporter (SERT) expressed in COS-7 cells. *J Pharmacol Sci*. 2013;122(2):71-83. doi:10.1254/jphs.12194fp

24. Braun D, Schweizer U. The Protein Translocation Defect of MCT8L291R Is Rescued by Sodium Phenylbutyrate. *Eur Thyroid J*. 2020;9(5):269-280. doi:10.1159/000507439

25. von Rüden EL, Wolf F, Gualtieri F, et al. Genetic and Pharmacological Targeting of Heat Shock Protein 70 in the Mouse Amygdala-Kindling Model. *ACS Chem Neurosci*. 2019;10(3):1434-1444. doi:10.1021/acschemneuro.8b00475

26. Walcott SE, Heikkila JJ. Celastrol can inhibit proteasome activity and upregulate the expression of heat shock protein genes, hsp30 and hsp70, in Xenopus laevis A6 cells. *Comp Biochem Physiol A Mol Integr Physiol*. 2010;156(2):285-293. doi:10.1016/j.cbpa.2010.02.015

27. Yang C, Swallows CL, Zhang C, et al. Celastrol increases glucocerebrosidase activity in Gaucher disease by modulating molecular chaperones. *Proc Natl Acad Sci U S A*. 2014;111(1):249-254. doi:10.1073/pnas.1321341111

28. Gentil BJ, Mushynski WE, Durham HD. Heterogeneity in the properties of NEFL mutants causing Charcot-Marie-Tooth disease results in differential effects on neurofilament assembly and susceptibility to intervention by the chaperone-inducer, celastrol. *Int J Biochem Cell Biol*. 2013;45(7):1499-1508. doi:10.1016/j.biocel.2013.04.009

29. Petrović A, Kaur J, Tomljanović I, Nistri A, Mladinic M. Pharmacological induction of Heat Shock Protein 70 by celastrol protects motoneurons from excitotoxicity in rat spinal cord in vitro. *Eur J Neurosci*. 2019;49(2):215-231. doi:10.1111/ejn.14218

30. Zhang YQ, Sarge KD. Celastrol inhibits polyglutamine aggregation and toxicity though induction of the heat shock response. *J Mol Med (Berl)*. 2007;85(12):1421-1428. doi:10.1007/s00109-007-0251-9

31. Nakazono A, Adachi N, Takahashi H, et al. Pharmacological induction of heat shock proteins ameliorates toxicity of mutant PKCγ in spinocerebellar ataxia type 14. *J Biol Chem*. 2018;293(38):14758-14774. doi:10.1074/jbc.RA118.002913

32. Kalmar B, Greensmith L. Activation of the heat shock response in a primary cellular model of motoneuron neurodegeneration-evidence for neuroprotective and neurotoxic effects. *Cell Mol Biol Lett*. 2009;14(2):319-335. doi:10.2478/s11658-009-0002-8

33. Choi BS, Kim H, Lee HJ, et al. Celastrol from “Thunder God Vine” protects SH-SY5Y cells through the preservation of mitochondrial function and inhibition of p38 MAPK in a rotenone model of Parkinson’s disease. *Neurochem Res*. 2014;39(1):84-96. doi:10.1007/s11064-013-1193-y

34. Jantas D, Roman A, Kuśmierczyk J, et al. The extent of neurodegeneration and neuroprotection in two chemical in vitro models related to Parkinson’s disease is critically dependent on cell culture conditions. *Neurotox Res*. 2013;24(1):41-54. doi:10.1007/s12640-012-9374-z

35. Malkov A, Ivanov AI, Latyshkova A, Bregestovski P, Zilberter M, Zilberter Y. Activation of nicotinamide adenine dinucleotide phosphate oxidase is the primary trigger of epileptic seizures in rodent models. *Ann Neurol*. 2019;85(6):907-920. doi:10.1002/ana.25474

36. Lin MW, Lin CC, Chen YH, Yang HB, Hung SY. Celastrol Inhibits Dopaminergic Neuronal Death of Parkinson’s Disease through Activating Mitophagy. *Antioxidants (Basel)*. 2019;9(1):E37. doi:10.3390/antiox9010037

37. Luo D, Fan N, Zhang X, et al. Covalent inhibition of endoplasmic reticulum chaperone GRP78 disconnects the transduction of ER stress signals to inflammation and lipid accumulation in diet-induced obese mice. *Elife*. 2022;11:e72182. doi:10.7554/eLife.72182

38. Kang JQ. Treatment Methods Using Celastrol. Published online February 8, 2018. Accessed August 1, 2022. https://patentscope.wipo.int/search/en/detail.jsf?docId=WO2018026810&_cid=P21-L6B2LC-41571-1

39. DeLorey TM, Handforth A, Anagnostaras SG, et al. Mice Lacking the β3 Subunit of the GABAA Receptor Have the Epilepsy Phenotype and Many of the Behavioral Characteristics of Angelman Syndrome. *J Neurosci*. 1998;18(20):8505-8514. doi:10.1523/JNEUROSCI.18-20-08505.1998

40. Kang JQ, Shen W, Zhou C, Xu D, Macdonald RL. The human epilepsy mutation GABRG2(Q390X) causes chronic subunit accumulation and neurodegeneration. *Nat Neurosci*. 2015;18(7):988-996. doi:10.1038/nn.4024

41. Kang JQ, Shen W, Macdonald RL. Trafficking-deficient mutant GABRG2 subunit amount may modify epilepsy phenotype. *Ann Neurol*. 2013;74(4):547-559. doi:10.1002/ana.23947

42. Bhardwaj R, Bhardwaj A, Dhawan DK, Tandon C, Kaur T. 4-PBA rescues hyperoxaluria induced nephrolithiasis by modulating urinary glycoproteins: Cross talk between endoplasmic reticulum, calcium homeostasis and mitochondria. *Life Sci*. 2022;305:120786. doi:10.1016/j.lfs.2022.120786

43. Tan L, Register TC, Yammani RR. Age-Related Decline in Expression of Molecular Chaperones Induces Endoplasmic Reticulum Stress and Chondrocyte Apoptosis in Articular Cartilage. *Aging Dis*. 2020;11(5):1091-1102. doi:10.14336/AD.2019.1130

44. Sun S, Shi G, Han X, et al. Sel1L is indispensable for mammalian endoplasmic reticulum-associated degradation, endoplasmic reticulum homeostasis, and survival. *Proc Natl Acad Sci U S A*. 2014;111(5):E582-591. doi:10.1073/pnas.1318114111

45. Omura T, Matsuda H, Nomura L, et al. Ubiquitin ligase HMG-CoA reductase degradation 1 (HRD1) prevents cell death in a cellular model of Parkinson's disease. *Biochem Biophys Res Commun*. 2018;506(3):516-521. doi:10.1016/j.bbrc.2018.10.094

46. Omura T, Asari M, Yamamoto J, et al. HRD1 levels increased by zonisamide prevented cell death and caspase-3 activation caused by endoplasmic reticulum stress in SH-SY5Y cells. *J Mol Neurosci*. 2012;46(3):527-535. doi:10.1007/s12031-011-9638-8

47. Chow AM, Tang DWF, Hanif A, Brown IR. Localization of heat shock proteins in cerebral cortical cultures following induction by celastrol. *Cell Stress Chaperones*. 2014;19(6):845-851. doi:10.1007/s12192-014-0508-5

# 5 Pharmacological facilitation of $GABA_A$ receptor subunit trafficking *in vitro* and seizure reduction in genetic epilepsy mouse *Gabrg2*$^{+/Q390X}$

Manuscript in revision at *Journal of Biological Chemistry*. Reprinted with permission from all co-authors.

Sarah Poliquin,[1, 2] Gerald Nwosu,[2, 3, 4] Karishma Randhave,[4] Wangzhen Shen,[4] Carson Flamm,[4] Jing-Qiong Kang[4, 5, 6]

[1]Neuroscience Graduate Program, Vanderbilt University, Nashville, TN 37232, USA; [2]Vanderbilt Brain Institute, Vanderbilt University, Nashville, TN 37232, USA; [3]Department of Neuroscience and Pharmacology, Meharry Medical College, Nashville, TN 37208, USA; [4]Department of Neurology, Vanderbilt University Medical Center, 465 21st Ave South, Nashville, TN 37232, USA; [5]Department of Pharmacology, Vanderbilt University, Nashville, TN 37232, USA; [6]Vanderbilt Kennedy Center of Human Development, Vanderbilt Brain Institute, Vanderbilt University, Nashville, TN 37232, USA.

## 5.1 Abstract

A significant number of patients with genetic epilepsy do not obtain seizure freedom, despite developments of new antiseizure drugs, suggesting a need for novel therapeutic approaches. Many genetic epilepsies are associated with misfolded mutant proteins, including *GABRG2(Q390X)*-associated Dravet syndrome, which we have previously shown to result in intracellular accumulation of mutant $GABA_A$ receptor γ2(Q390X) subunit protein. Thus, a potentially promising therapeutic approach is modulation of proteostasis, such as increasing endoplasmic reticulum (ER) associated degradation (ERAD). To that end, we have here identified an ERAD-associated E3 ubiquitin ligase, HRD1, as a modulator of wildtype and mutant γ2 subunit expression. By overexpressing HRD1 *in vitro*, we reduced the total expression of γ2 and γ2(Q390X).

Additionally, we show that zonisamide (ZNS) – an antiseizure drug reported to upregulate HRD1 – reduces seizures in the *Gabrg2*$^{+/Q390X}$ mouse model of Dravet syndrome. We propose that a possible mechanism for this effect is a partial rescue of surface trafficking of $GABA_A$ receptors, which are otherwise sequestered in the ER due to the dominant-negative effect of the γ2(Q390X) subunit. Furthermore, this partial rescue was not due to changes in ER chaperones BiP and calnexin, as total expression of these chaperones was unchanged in γ2(Q390X) models. Our results here suggest that leveraging the endogenous ERAD pathway may present a potential method to degrade neurotoxic mutant proteins like the γ2(Q390X) subunit. We also demonstrate a pharmacological means of regulating proteostasis, as ZNS alters protein trafficking, providing further support for the use of proteostasis regulators for the treatment of genetic epilepsies.

## 5.2 Keywords

epilepsy; GABA receptor; endoplasmic-reticulum-associated protein degradation (ERAD); E3 ubiquitin ligase; proteostasis; intracellular trafficking; Dravet syndrome

## 5.3 Highlights

- The E3 ubiquitin ligase HRD1 can facilitate degradation of both wildtype and mutant γ2 subunits, despite the altered conformation of the mutant γ2(Q390X) subunit
- The antiseizure drug zonisamide, primarily used for partial seizures in adults, reduced seizures in the Dravet syndrome model *Gabrg2*$^{+/Q390X}$

- Zonisamide partially rescued trafficking of $GABA_AR$ subunits, which is suppressed by the γ2(Q390X) subunit

## 5.4 Introduction

Genetic epilepsies are associated with mutations in a variety of proteins, and these mutations can impact protein folding, trafficking, and stability. Many of these epilepsy-associated mutations affect the main inhibitory pathway in the central nervous system, which utilizes γ-aminobutyric acid (GABA) and GABA receptors. The GABA type A receptor ($GABA_AR$) is the primary receptor mediating GABAergic signaling. Thus, many studies have focused on mutations in several subunits of the heteropentameric $GABA_AR$, which is typically composed of two α, two β, and 1 γ subunit. A number of mutations have been identified in the γ2 subunit, and these mutations are associated with a range of neurological phenotypes, from anxiety and childhood absence epilepsy on one end to Dravet syndrome on the other end.[1-10] Truncation mutations of the γ2 subunit not only lead to loss of functionality of the shortened γ2 protein, they can also alter the trafficking and degradation of the partnering α and β subunits that together comprise the whole $GABA_AR$.[11-15] This effect on proteostasis is especially pronounced in the dominant-negative phenotype caused by the γ2(Q390X) subunit, a mutation associated with Dravet syndrome, a severe developmental and epileptic encephalopathy (DEE).[16,17]

The γ2(Q390X) subunit is markedly misfolded, as the truncation deletes the 78 amino acids constituting the a majority of the intracellular loop and all of the 4$^{th}$ transmembrane domain, dramatically altering the conformation of the remaining

polypeptide.[11,16,17] However, the γ2(Q390X) subunit is still capable of interacting with the α1 and β2 subunits, as well as the wildtype γ2 subunit.[11,13] Due to the inability to assume the proper conformation, the γ2(Q390X) subunit is largely retained by the protein quality control mechanisms of the endoplasmic reticulum (ER), and is thereby prevented from traveling through the secretory pathway to the plasma membrane.[11] Because the γ2(Q390X) subunit is still capable of assembling with partnering subunits, the retention of the γ2(Q390X) subunit in the ER also results in the trapping of these wildtype subunits.[11,13] This results in a dominant-negative effect on $GABA_AR$ trafficking, with fewer receptors at the cell surface than in wildtype conditions or even compared to simple haploinsufficiency conditions in heterozygous knockout *Gabrg2*$^{+/-}$ mice.[17]

In addition to these $GABA_AR$ trafficking deficits, the retention of the γ2(Q390X) subunit in the ER can cause other difficulties. A chronic presence of misfolded proteins in the ER can cause ER stress, and in turn, prolonged ER stress can result in apoptosis.[18] Neuronal death is indeed seen in *Gabrg2*$^{+/Q390X}$.[17] Therefore, we have investigated a potential method of promoting degradation, utilizing the endogenous ER-associated degradation (ERAD) system.

Membrane proteins, such as the $GABA_AR$ subunits, are folded in the ER before passing through the rest of the secretory pathway.[19] Protein quality control mechanisms target terminally-misfolded proteins for degradation.[20] A key step in this process is the ubiquitination of the misfolded protein by an E3 ubiquitin ligase.[20-22] E3 ligases are known to be involved in many diverse neurological disorders, including Parkinson's disease, Alzheimer's disease, Angelman syndrome, Fragile X syndrome, and genetic epilepsies.[21-24] In this paper, we probed the ability of several E3 ligases to alter

expression of the γ2(Q390X) mutant subunit, and chose HRD1 for further study. We present evidence that a drug previously reported to upregulate HRD1 reduces seizures in *Gabrg2*$^{+/Q390X}$ mice and facilitates surface trafficking of $GABA_AR$ subunits *in vitro*.

## 5.5 Experimental procedures

### 5.5.1 Cell culture and polyethyleneimine transfection

Human embryonic kidney 293 T (HEK293T) cells were grown in Dulbecco's Modified Eagle's Medium (DMEM) supplemented with 10% FBS and 1% penicillin/streptomycin. 24 hours after plating the cells, they were transfected with cDNA for wildtype rat γ2S or γ2S(Q390X) subunits (referred to hereafter simply as γ2 or γ2(Q390X) subunits, respectfully), human α1 subunit, and/or human β2 subunit. cDNA was combined with polyethyleneimine (PEI) at a ratio of 2.5 µL PEI per 1 µg cDNA. Additional cDNA included myc-tagged HRD1 and HA-tagged SEL1L, kindly shared by Dr. Nobuko Hosokawa at the Institute for Frontier Life and Medical Sciences, Kyoto University. Zonisamide (ZNS) (Tocris 2625) dissolved in dimethyl sulfoxide (DMSO) was used in varying concentrations specified in text.

### 5.5.2 Immunoblot

Cells were harvested 48 h after transfection. Cells were washed with cold phosphate buffered saline (PBS) and lysed with RIPA-PI solution containing 20 mM Tris, 20 mM EGTA, 1 mM DTT, 1 mM benzamidine, 0.01 mM PMSF, 0.005 µg/mL leupeptin, and 0.005 µg/mL pepstatin. Protein concentration was measured, and samples were subjected to standard SDS polyacrylamide gel electrophoresis (SDS-PAGE) procedures and immunoblotted. Primary antibodies used were anti-α1 1:500 (Millipore Sigma

MABN489), anti-β2 1:1,000 (Millipore Sigma AB5561), anti-γ2 1:1,000 (Synaptic Systems 224003), anti-BiP 1:500 (BD Biosciences 610979), anti-calnexin 1:1,000 (Enzo Life Sciences ADI-SPA-860-F), anti-RNF34 *pending* (Novus Biologicals NBP2-56413) (RNF34 antibody was on backorder at the time of this thesis submission but will arrive shortly after and will be included in the revised manuscript submitted to *JBC*), anti-NEDD4L 1:1,000 (Cell Signaling Technology 4013), anti-UBE3A 1:1,000 (Atlas Antibodies HPA039410), anti-HRD1 1:1,000 (Novus Biologicals NB100-2526), anti-SEL1L 1:1,000 (Novus Biologicals NBP2-93746), anti-HA 1:300 (Cell Signaling Technology 3724S), anti-myc (Millipore Sigma 05-724), and anti-ATPase 1:1,000 (Developmental Studies Hybridoma Bank a6F). Secondary antibodies were LI-COR IRDye 680LT Goat anti-Mouse IgG Secondary Antibody (926-68020) and IRDye 800CW Goat anti-Rabbit IgG Secondary Antibody (926-32211), both 1:10,000.

Blots were imaged with an Odyssey DLx digital fluorescence scanner and LI-COR Image Studio Lite 5.2 software. Protein bands were quantified by circumscribing the band of interest and correcting for background signal. Integrated density values (IDVs) for the protein of interest were normalized to the IDV for the loading control, ATPase. The values were then normalized to loading controls and then the normalized IDV of the control lane (generally, wildtype or untreated), which was arbitrarily taken as equal to 1.

### 5.5.3 Biotinylation

Transfected HEK293T cells were gently washed with room-temperature PBS-Ca-Mg (PBS with 0.1 mM $CaCl_2$ and 1 mM $MgCl_2$) and then incubated with EZ-Link Sulfo-NHS-SS-biotin (Thermo Scientific 21331) in PBS-Ca-Mg. The biotinylation reaction was

then quenched with 0.1 M glycine in PBS-Ca-Mg. Cells were then collected and lysed in standard RIPA-PI buffer. Biotinylated proteins were purified by incubating the cell lysates overnight with high capacity Neutravidin agarose resin beads (Thermo Scientific 29202). After incubation, the beads were washed with RIPA-PI to remove non-biotinylated protein and biotinylated protein was next eluted from the beads with Laemmli sample buffer containing β-mercaptoethanol. Samples were then subjected to standard immunoblot procedures.

### 5.5.4 *Gabrg2*$^{+/Q390X}$ mouse model of Dravet syndrome

The generation of the *Gabrg2*$^{+/Q390X}$ mouse is described previously.[17]

### 5.5.5 Drug administration and brain tissue preparation in *Gabrg2*$^{+/Q390X}$ mice

*Gabrg2*$^{+/Q390X}$ mice in the C57BL/6J (Jackson Labs stock 000664) background were bred with wildtype C57BL/6J mice. Animals were housed in standard facilities with ad libitum food and water access. Beginning at 1-1.5 months of age, heterozygous animals and wildtype littermates, both male and female, were treated daily with vehicle or 20 mg/kg ZNS injected intraperitoneally for 7 days. ZNS (Tocris 2625) was dissolved in 10% DMSO and 90% 0.9% saline, for a final concentration of 5 mg/mL. After 7 days of treatment, the mice were anesthetized with isoflurane and decapitated. The brain was removed, and the somatosensory cortex, cerebellum, thalamus, and hippocampus were dissected.

### 5.5.6 EEG acquisition and scoring

Around 2-3 months of age, male and female *Gabrg2*$^{+/Q390X}$ mice were surgically implanted with head mounts from Pinnacle Technology that have two bipolar

electroencephalogram (EEG) channels and one subcutaneous nuchal electromyogram (EMG) channel (Pinnacle 8201: 2 EEG/1 EMG Mouse Headmount). After recovering from head mount surgery for 7 days, a 24 h baseline recording was acquired, with EEG and EMG channels and simultaneous video. Mice were then treated daily with 20 mg/kg ZNS injected intraperitoneally for 7 days and on the 8$^{th}$ day a 24 h EEG recording was again acquired. EEGs were acquired with Sirenia Acquisition, with the sampling rate set at 400 Hz with a pre-amplifier gain of 100 Hz. EEG and EMG channels have a filter set at 25 Hz.

EEGs are scored by a blinded skilled scorer with Sirenia Seizure Pro software. A power analysis of the theta frequency band of 5-7 Hz was used to identify seizures, as 5-7 Hz spike-and-wave discharges (SWDs) are the mouse correlate of human 2-4 Hz SWDs. Suspected seizure events were confirmed with the video recording.

### 5.5.7 Data analysis

Data were analyzed using GraphPad Prism 9.4 and is reported as mean ± standard error of the mean (SEM). For cell culture experiments overexpressing HRD1 and SEL1L, one-way analysis of variance (ANOVA) tests were performed. Each condition was compared to all other conditions using Tukey's test for post-hoc analysis, corrected for multiple comparisons. For EEG data, paired t-tests were used. Simple linear regression was used to evaluate the dose-response effect of ZNS on HRD1 expression. For other cell culture and mouse experiments utilizing ZNS, two-way ANOVAs were performed, fitting a full interaction model. Post-hoc analysis was done with Šídák's multiple comparisons, examining simple effects within drug treatments. Statistical significance was taken as $p < 0.05$ throughout.

## 5.6 Results

### 5.6.1 The *GABRG2(Q390X)* mutation results in γ2 dimers and reduces expression of α1 and β2 subunits

As we have shown before, the mutant γ2(Q390X) subunit is prone to self-dimerization, resulting in dimers and larger oligomers (Figure 1A).[17,25] Because this protein cannot fold properly, it is retained in the ER, which also results in the ER retention of partnering α1 and β2 subunits.[11,13] Due to the trafficking impediment, the α1 and β2 subunits are subjected to increased degradation, lowering the total protein expression of these subunits.[11,26] In line with these previous findings, HEK293T cells expressing α1β2γ2(Q390X) $GABA_AR$ had a 34.5 ± 8.1% reduction in the expression of the α1 subunit ($p$ = 0.0017) and a 36.9 ± 11.6% reduction in β2 subunit expression ($p$ = 0.0128), compared to cells expressing α1β2γ2 $GABA_AR$ (Fig 1B, 1C).

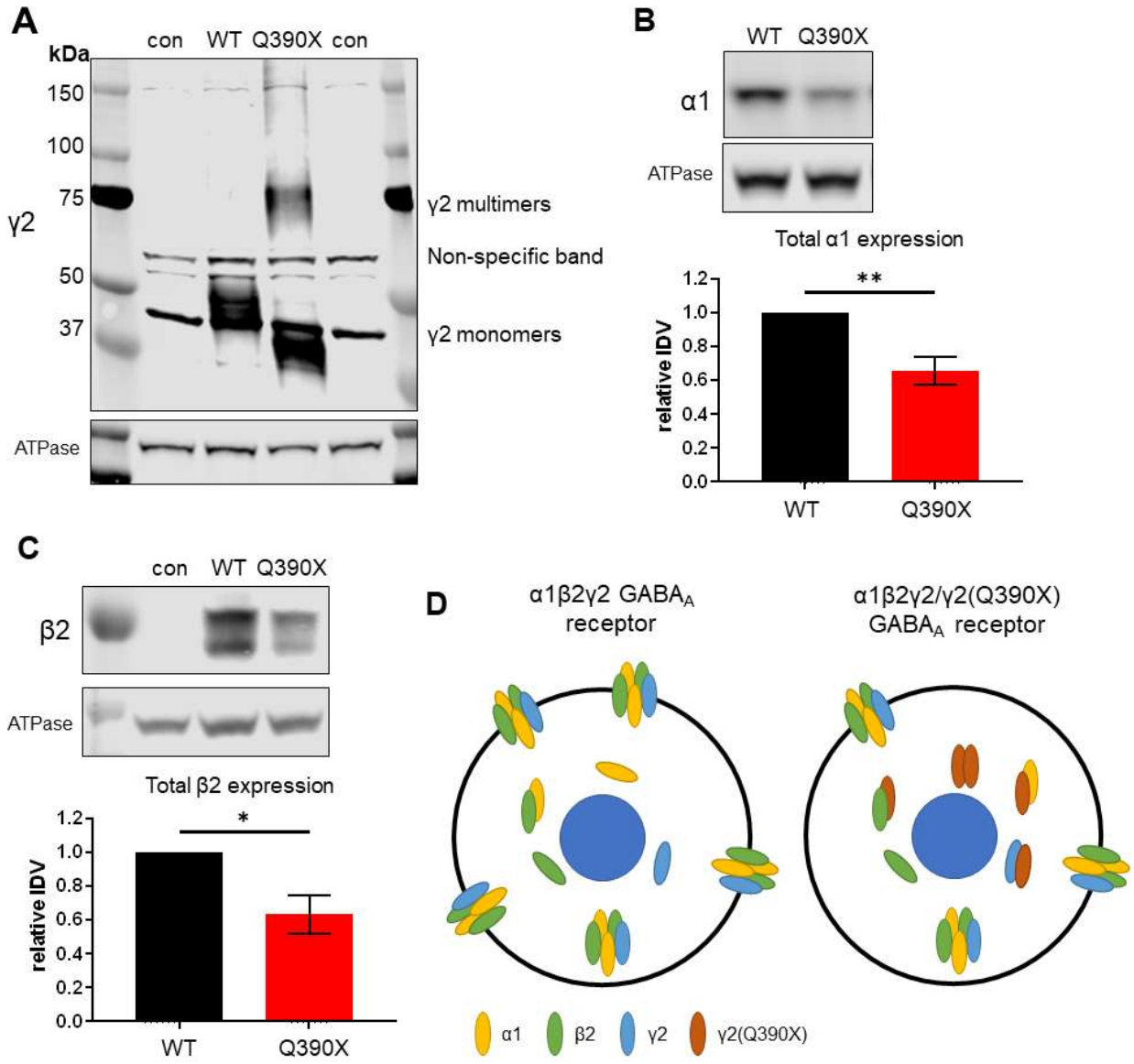


***Figure 5.1. The GABRG2(Q390X) mutation resulted in γ2 dimers and reduced expression of α1 and β2 subunits.***

A-C. HEK293T cells were transfected with wildtype γ2 or γ2 truncation mutations, and wildtype α1 and β2 (total cDNA: 3 μg per 60 mm dish). Con is untransfected control. 48 hr after transfection, cells were harvest and lysed. Lysates were subjected to SDS-PAGE. A. Immunoblot for γ2 (1:1,000). Monomers of γ2 can be seen on the bottom half of the membrane, and dimers and larger multimers can be seen on the top half. γ2 runs slightly below the predicted size of 55 kDa, consistently running at ~45 kDa. The band near 60 kDa is non-specific. B. Immunoblot for α1 (1:500) and graph showing integrated density values (IDVs) normalized to the loading control and then to the wildtype α1β2γ2 condition. C. Immunoblot for β2 (1:1,000) and graph of normalized IDVs. D. Cartoon demonstrating that the γ2(Q390X) mutant subunit forms oligomers and retains partnering wildtype α1, β2, and γ2 subunits intracellularly, hampering proper trafficking

of $GABA_ARs$ to the cell surface. N = 5-6 separate transfections. Unpaired t-tests were used to evaluate statistical significance. * $p < 0.05$, ** $p < 0.01$. Values are expressed as mean ± S.E.M.

### 5.6.2 Overexpression of an E3 ubiquitin ligase increased γ2(Q390X) subunit degradation

We sought to facilitate the degradation of mutant γ2(Q390X) protein, with the goal of alleviating the negative effects of the mutant protein. Misfolded proteins are tagged for degradation by the addition of ubiquitin proteins, which are added by substrate-specific E3 ubiquitin ligases.[20] Although hundreds of E3 ligases have been identified, their substrates are not always known. Therefore, we tested several E3 ligases that are known or suspected to ubiquitinate proteins related to the γ2 subunit: HMG-CoA reductase degradation protein 1 (HRD1), ubiquitin-protein ligase E3A (UBE3A), neural precursor cell expressed developmentally down-regulated gene 4-like (NEDD4L, also called NEDD4-2), and ring finger protein 34 (RNF34).

HRD1, also called synoviolin 1 (SVN1), is an ERAD-associated E3 ubiquitin ligase known to ubiquitinate the α1 subunit, which has high similarity to the γ2 subunit.[19,27] UBE3A, also known as E6AP ubiquitin-protein ligase (E6AP), is postulated to influence *GABRB3* expression via repressor element 1 (RE1)-silencing transcription factor (REST).[28] Additionally, UBE3A interacts with plic-1, which is known to stabilize the β3 subunit.[29,30] Indeed, unpublished data from our previous study of the *Ube3a*$^{-/-}$ mouse[31] suggested that Ube3a regulates expression of the β3 subunit in mice. NEDD4L, meanwhile, is an epilepsy-associated protein that regulates expression of the α-amino-3-hydroxy-5-methyl-4-isoxazolepropionic acid (AMPA) receptor subunit

GluA1.[32-34] GluA1, also referred to as GluR-1, has 20% sequence identity to the γ2 $GABA_AR$ subunit and several similar domains. Additionally, NEDD4L regulates neuron excitability independently of AMPA receptors, which opens the possibility of other neurotransmitter receptors such as $GABA_AR$ also interacting with NEDD4L.[35] Thus, we chose to investigate whether HRD1, NEDD4L, or UBE3A overexpression affects the expression of the γ2(Q390X) mutant subunit. Finally, RNF34 has been shown to ubiquitinate the γ2 subunit for degradation, but RNF34 specifically interacts with a portion of the C-terminal region that is missing in the γ2(Q390X) subunit (amino acids 362-404).[36] We thus included RNF34 to confirm that it is not capable of decreasing the expression of the γ2(Q390X) subunit.

Each of these E3 ligases was co-transfected with γ2 or γ2(Q390X) subunits, and the expression of γ2 protein was assessed by Western blot. For the wildtype γ2 subunit, only HRD1 overexpression decreased the amount of γ2 protein, although the NEDD4L condition did near significance (compared to pcDNA control 1 ± 0: RNF34 0.935 ± 0.0336, $p = 0.764$; HRD1 0.559 ± 0.0433, $p < 0.0001$; NEDD4L 0.839 ± 0.0385, $p = 0.058$; UBE3A 0.888 ± 0.0725, $p = 0.294$) (Fig 2A, 2B). Likewise, only HRD1 overexpression altered expression of the γ2(Q390X) subunit. Because the γ2(Q390X) subunit is often detected as dimers, we quantified monomers, dimes, and the total amount of γ2(Q390X) protein. For γ2(Q390X) monomers, compared to pcDNA control 1 ± 0: RNF34 0.9849 ± 0.0751, $p > 0.999$; HRD1 0.681 ± 0.0644, $p = 0.0074$; NEDD4L 1.060 ± 0.0656, $p = 0.948$; UBE3A 0.966 ± 0.0876, $p = 0.994$ (Fig 2C). Similarly, for γ2(Q390X) dimers, compared to pcDNA control 1 ± 0: RNF34 1.041 ± 0.0685, $p = 0.983$; HRD1 0.606 ± 0.0302, $p = 0.0004$; NEDD4L 0.921 ± 0.0807, $p = 0.846$; UBE3A

0.835 ± 0.0829, $p = 0.246$ (Fig 2D). And, for total γ2(Q390X) expression, compared to pcDNA control 1 ± 0: RNF34 0.989 ± 0.0762, $p > 0.999$; HRD1 0.656 ± 0.0575, $p = 0.0027$; NEDD4L 1.037 ± 0.0643, $p = 0.990$; UBE3A 0.947 ± 0.0859, $p = 0.963$ (Fig 2E). Expression of the E3 ligases is shown in Supplementary Figure 1.

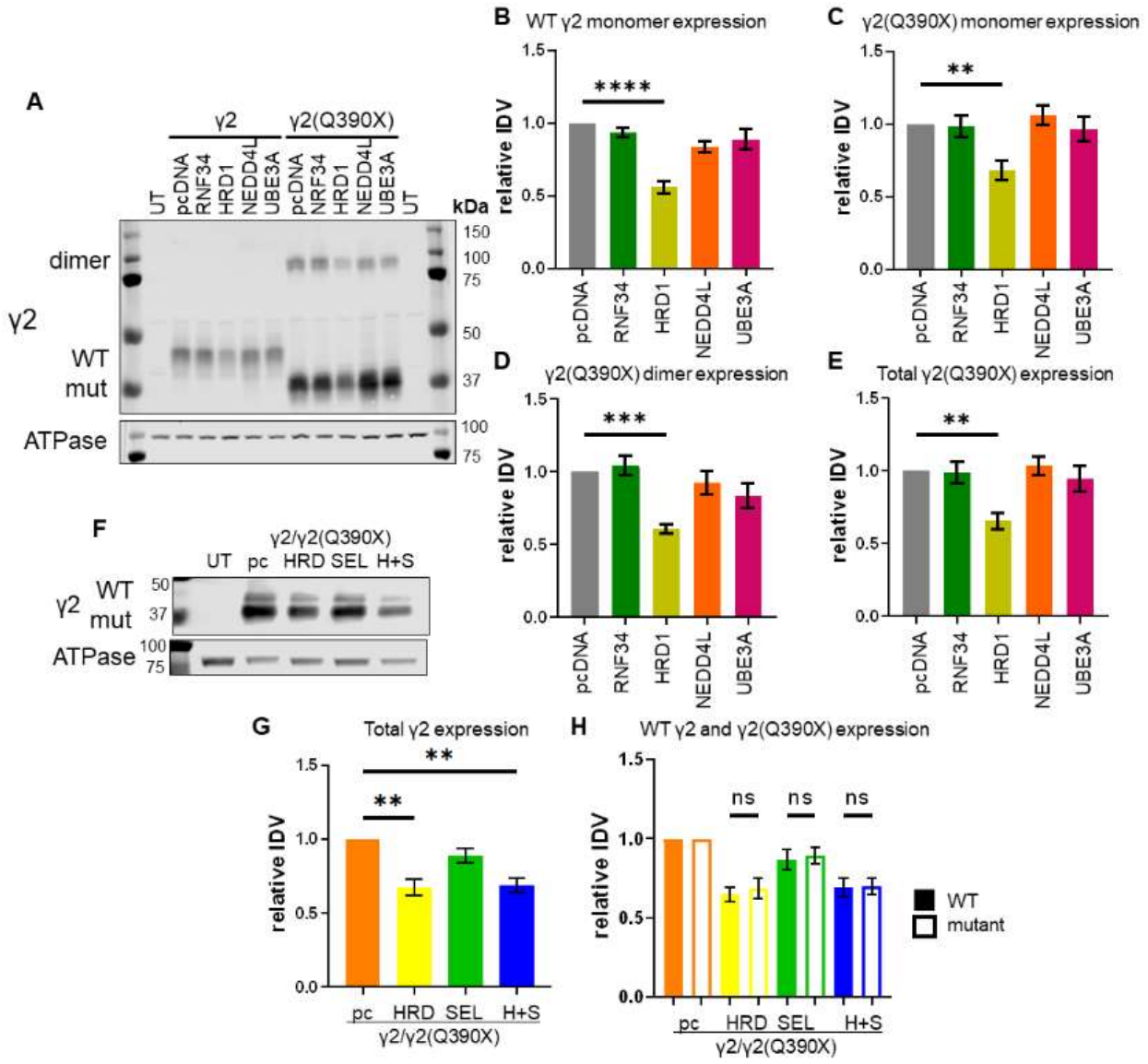


***Figure 5.2. Overexpression of the E3 ubiquitin ligase HRD1 increased γ2(Q390X) degradation.***

A-E. HEK293T cells were transfected with γ2 or γ2(Q390X) (3 μg) and pcDNA, HA-RNF34, HRD1-myc, HA-NEDD4L, or UBE3A-HA (0.5 μg). A. 48 h post transfection, cells were collected, lysed, and subjected to SDS-PAGE. The membrane was immunoblotted with an anti-γ2 antibody (1:1,000). B. A graph of the IDVs of the wildtype γ2 band ~45 kDa, normalized first to the loading control ATPase (1:1,000) and then to the γ2 + pcDNA condition. C. A graph of the IDVs of the γ2(Q390X) monomers (lower band, 39 kDa). D. A graph of the IDVs of the γ2(Q390X) dimers (upper band, ~80 kDa). E. A graph of the total γ2(Q390X) signal, the sum of the upper and lower bands. C-E. IDVs were normalized to ATPase (1:1,000) and then to the γ2(Q390X) + pcDNA control condition. F-H. HEK293T cells were transfected with γ2 and γ2(Q390X) (1.5 μg each). They were cotransfected with HRD1-myc (labeled HRD) or HA-SEL1L (labeled SEL) or both HRD1-myc and HA-SEL1L (labeled H+S), using 0.5 μg of these plasmids. Total

cDNA was normalized to 4 μg with empty vector pcDNA. pc is γ2 and γ2(Q390X) + pcDNA. UT is untransfected controls. F. An SDS-PAGE membrane was immunoblotted with γ2 (1:1,000). Wildtype γ2 runs at ~45 kDa and γ2(Q390X) runs at ~39 kDa and can thus be seen separately. G. Graph showing γ2 IDVs normalized first to the loading control, ATPase (1:1,000) and then to the control condition, γ2 + γ2(Q390X) + pcDNA. The sum of both wildtype γ2 and mutant γ2(Q390X) is presented here. H. Normalized IDVs of the wildtype γ2 and mutant γ2(Q390X) bands in (F) are shown individually, with wildtype as the solid bars and mutant as the outlined bars. N = 7 separate transfections. One-way ANOVA and Tukey's test for post-hoc analysis, corrected for multiple comparisons, were used to evaluate statistical significance. * $p < 0.05$, ** $p < 0.01$, *** $p < 0.001$, **** $p < 0.0001$. Values are expressed as mean ± S.E.M.

Intrigued by the success of HRD1, we were curious about another protein that acts as an adaptor and stabilizer for HRD1, suppressor of lin-12-like protein 1 (SEL1L). Thus, we asked if overexpression of both HRD1 and SEL1L together may further aid degradation of the γ2(Q390X) subunit. Because patients with epilepsy-associated *GABRG2* mutations are heterozygous for their mutation, we mimicked this heterozygosity by transfecting HEK293T cells with equal amounts of wildtype and mutant γ2 subunit cDNA (1.5 μg each). Cells were cotransfected with 0.5 μg of HRD1-myc, HA-SEL1L, or both HRD1-myc and HA-SEL1L, and empty vector pcDNA was used to normalize the transfection to 4 μg for all conditions. Expression of total γ2 protein – wildtype and mutant combined – was found to be decreased in cells transfected with HRD1-myc (0.675 ± 0.055, $p = 0.0001$) or HRD1-myc + HA-SEL1L (0.690 ± 0.048, $p = 0.0002$), but not HA-SEL1L alone (0.889 ± 0.046, $p = 0.284$) (Fig 2F, 2G).

Because the mutant γ2(Q390X) subunit is toxic to cells while the wildtype γ2 subunit is functional, the optimal therapeutic outcome would be targeted degradation of primarily the mutant form of the γ2 subunit. Therefore, we then quantified separately the

wildtype and mutant γ2 subunits to determine if the mutant γ2(Q390X) subunit was decreased more than the functional wildtype γ2 subunit. The expression of each subunit was normalized to the pcDNA control condition for that subunit, and then we compared the relative reduction between the two subunits for each transfection condition. Interestingly, wildtype γ2 and γ2(Q390X) subunits were affected identically for all conditions: HRD1-myc (0.646 ± 0.046 WT vs 0.688 ± 0.065 Q390X, $p = 0.906$) and HRD1-myc + HA-SEL1L (0.692 ± 0.059 WT vs 0.698 ± 0.050 Q390X, $p = 0.999$) reduced the levels of wildtype and mutant protein equally, and transfection with HA-SEL1L had no effect on either form of γ2 subunit (0.865 ± 0.065 WT vs 0.893 ± 0.050 Q390X, $p = 0.971$) (Fig 2H).

Transfection of HEK293T cells with HRD1-myc cDNA resulted in overexpression, approximately tripling HRD1 expression compared to endogenous levels (Supplementary Fig 2A). However, transfection with HA-SEL1L did not alter SEL1L expression compared to endogenous levels, although immunoblotting for the HA tag does show a band at the expected molecular weight, indicating a successful transfection (Supplementary Fig 2B).

### 5.6.3 A suggested HRD1 upregulator, ZNS, increased surface expression of $GABA_AR$ subunits *in vitro*

We then sought to upregulate HRD1 via pharmacological methods. ZNS is an antiseizure drug generally used to treat partial seizures in adults. However, it is also used in low doses as an add-on therapy for Parkinson's disease. Evidence suggests that the usefulness for Parkinson's disease comes from the ability of ZNS to elevate HRD1 levels.[37-40] Therefore, we predicted that ZNS-induced upregulation of HRD1 would have similar effects on $GABA_AR$ subunits as HRD1 overexpression. Based on

effective doses used in other, independent studies, a dose of 3 μM was chosen for these experiments.[38,40,41] Additionally, our preliminary data suggested no difference between 3 and 30 μM ZNS.

Because the γ2(Q390X) subunit has a dominant-negative effect on $GABA_AR$ subunit trafficking, we hypothesized that decreased expression of the γ2(Q390X) subunit would relieve the other subunits from the ER retention and allow normal surface trafficking. Therefore, surface protein expression was investigated in HEK293T cells transfected with α1β2γ2/γ2(Q390X), and treated with ZNS (3 μM, 24 hr) or cotransfected with HRD1-myc, HA-SEL1L, or both HRD1-myc and HA-SEL1L. These conditions were compared to wildtype α1β2γ2. As before, empty vector pcDNA was used to normalize total cDNA mass.

ZNS treatment partially rescued $GABA_AR$ trafficking to the cell surface in cells expressing α1β2γ2/γ2(Q390X), while HRD1-myc overexpression further reduced surface expression (Fig 3). Investigating the monomeric wildtype γ2 isoform – the component of functional $GABA_ARs$ – we found that, as expected, surface expression of the γ2 subunit was lower in the α1β2γ2/γ2(Q390X) + pcDNA (henceforth Q390X) condition than the α1β2γ2 + pcDNA (henceforth WT) condition (0.474 ± 0.027, $p < 0.0001$). The ZNS-treated α1β2γ2/γ2(Q390X) + pcDNA condition showed a trend towards an increase (0.572 ± 0.017) but this was not statistically different from Q390X ($p = 0.106$) and was still lower than WT ($p < 0.0001$) (Fig 3A). However, for the α1 subunit, ZNS treatment rescued the reduction seen in the Q390X condition (Q390X 0.747 ± 0.057, compared to WT 1 ± 0, $p = 0.032$; compared to ZNS 0.998 ± 0.074, $p = 0.033$), such that the ZNS-treated α1β2γ2/γ2(Q390X) + pcDNA condition was

indistinguishable from WT (1 ± 0 WT vs 0.998 ± 0.074 ZNS, $p > 0.999$) (Fig 3B). For the β2 subunit, the Q390X condition showed lower expression than WT (0.671 ± 0.068, $p = 0.019$), and the ZNS-treated α1β2γ2/γ2(Q390X) + pcDNA condition rescued the β2 subunit expression (0.934 ± 0.117) to be not different from WT ($p = 0.978$) but this increase failed to reach statistical significance compared to the untreated Q390X condition ($p = 0.088$) (Fig 3C). ZNS therefore partially rescued the deleterious effect of the γ2(Q390X) subunit on the surface trafficking of $GABA_AR$ subunits.

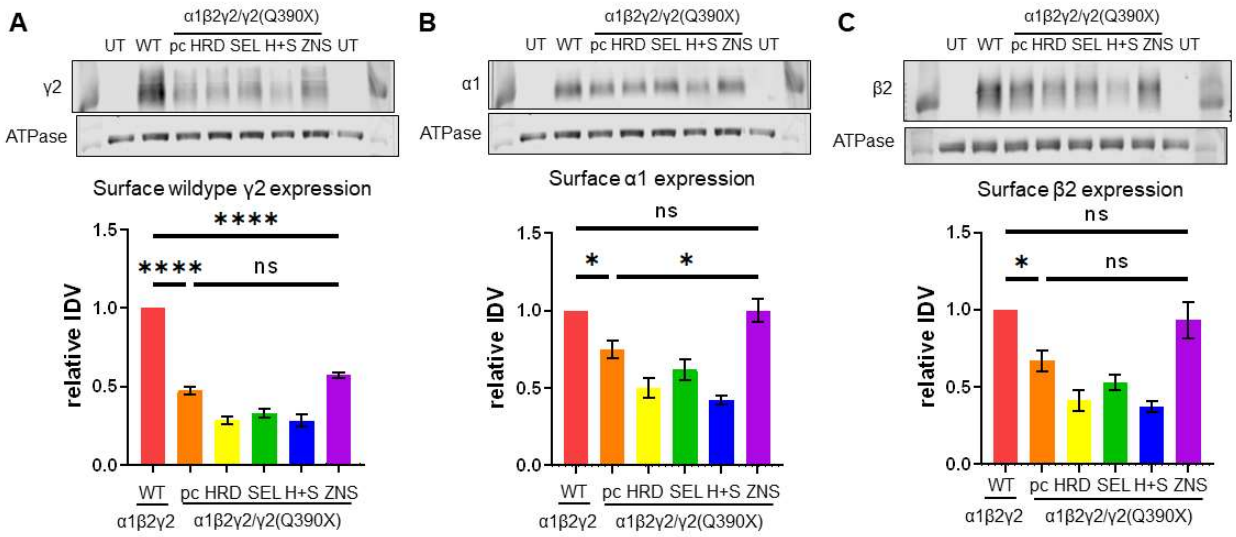


***Figure 5.3. ZNS facilitated trafficking of GABA$_A$R subunits.***
A-C. HEK293T cells in 100 mm dishes were transfected with α1, β2, γ2, and empty vector pcDNA (3 μg each) (labeled as WT). UT is untransfected controls. For all other conditions, the cells were transfected with α1, β2, γ2, and γ2(Q390X) (3:3:1.5:1.5 μg). They were cotransfected with HRD1-myc (labeled HRD) or HA-SEL1L (labeled SEL) or both HRD1-myc and HA-SEL1L (labeled H+S), using 1.5 μg of these plasmids. Total cDNA was normalized to 12 μg with empty vector pcDNA. pc is α1, β2, γ2, γ2(Q390X), and pcDNA (3:3:1.5:1.5 μg). ZNS is α1, β2, γ2, γ2(Q390X), and pcDNA (3:3:1.5:1.5 μg), treated with 3 μM ZNS, 24 h before harvesting. Living cells were treated with EZ-Link Sulfo-NHS-SS-biotin to biotinylate surface proteins, which were then purified and run on polyacrylamide gels. A. A membrane was immunoblotted for γ2 (1:1,000) and graph of IDVs. IDVs were normalized first to the loading control, ATPase (1:1,000), and then to the WT condition. Normalized IDVs are for monomeric wildtype γ2. B. Membrane and graph of normalized IDVs for α1 (1:500). C. Membrane immunoblotted for β2 (1:1,000) and graph of normalized IDVs. N = 5-6 separate transfections. One-way ANOVA and Tukey's test for post-hoc analysis, corrected for multiple comparisons, were used to evaluate statistical significance. * $p < 0.05$, **** $p < 0.0001$. Values are expressed as mean ± S.E.M.

### 5.6.4 ZNS had no effect on total expression of α1 or β2 subunits *in vitro*

Intrigued by the disparity between the effects of HRD1 overexpression and treatment with ZNS (3 μM, 24 hr) on GABA$_A$R subunit surface expression, we investigated total expression of α1, β2, and γ2 proteins after ZNS treatment. HEK293T

cells were transfected with the wildtype (α1β2γ2 1:1:1), mixed (α1β2γ2/γ2(Q390X) 1:1:0.5:0.5), or mutant (α1β2γ2(Q390X) 1:1:1) condition.

For the α1 and β2 subunits, ZNS (3 μM, 24 hr) had no effect in any transfection condition. Total protein expression of the α1 subunit was unchanged in all conditions (WT: 1 ± 0 vehicle vs 0.946 ± 0.023 ZNS, $p = 0.875$; mixed: 0.639 ± 0.060 vehicle vs 0.661 ± 0.073 ZNS, $p = 0.990$; mutant: 0.371 ± 0.066 vehicle vs 0.437 ± 0.072 ZNS, $p = 0.793$) (Fig 4A). The β2 subunit also had no differences (WT: 1 0 vehicle vs 0.966 ± 0.034 ZNS, $p = 0.907$; mixed: 0.705 ± 0.036 vehicle vs 0.715 ± 0.046 ZNS, $p = 0.997$; mutant: 0.461 ± 0.054 vehicle vs 0.539 ± 0.044 ZNS, $p = 0.433$) (Fig 4B).

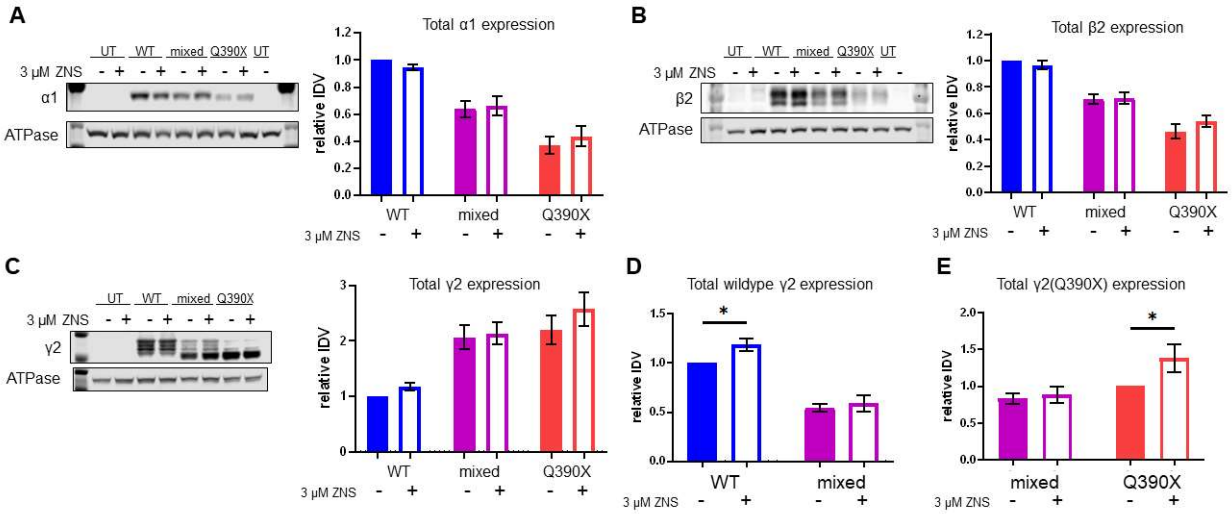


***Figure 5.4. In vitro, ZNS altered γ2 expression in a mutation-dependent manner, but not α1 or β2.***

A-E. HEK293T cells were transfected with α1, β2, and γ2 (1 μg each per 60 mm dish) (WT); α1, β2, and mixed γ2 and γ2(Q390X) (1:1:0.5:0.5); or α1, β2, and γ2(Q390X) (1:1:1) (mutant). Untransfected cells were used as controls (con). 24 h before harvesting, 3 μM ZNS or vehicle was applied. For A-D, IDVs were normalized to ATPase (1:1,000) and then to vehicle-treated WT. A. Immunoblot for α1 (1:500) and graph of normalized IDVs. B. Immunoblot for β2 (1:1,000) and graph of normalized IDVs. C. Immunoblot for γ2 (1:1,000) and graph of normalized IDVs. Quantification is for all γ2 signal: wildtype γ2 at 45 kDa, mutant γ2 at 39 kDa, and dimers between 80-100 kDa. D. Graph of normalized IDVs of only monomeric wildtype γ2 at 45 kDa. E. Graph of normalized IDVs of only monomeric γ2(Q390X) at 39 kDa. IDVs were normalized first to ATPase (1:1,000) and then to vehicle-treated mutant, which was taken as 1. A-E, N = 7-8 separate transfections. Two-way ANOVA and Šídák's multiple comparisons, examining simple effects within drug treatments, were used to evaluate statistical significance. * $p < 0.05$. Values are expressed as mean ± S.E.M.

### 5.6.5 ZNS had genotype-dependent effects on γ2 and γ2(Q390X) subunits *in vitro*

Next, expression of the γ2 subunit after ZNS (3 μM, 24 hr) treatment was evaluated. Data were analyzed for wildtype γ2 monomers alone, γ2(Q390X) monomers alone, and for total γ2 subunits, which refers to the sum of wildtype and mutant monomers and γ2 dimers. For total γ2 subunits, no differences were seen after ZNS

treatment (WT: 1 ± 0 vehicle vs 1.177 ± 0.067 ZNS, $p$ = 0.907; mixed: 2.064 ± 0.216 vehicle vs 2.136 ± 0.206 ZNS, $p$ = 0.993; mutant: 2.203 ± 0.258 vehicle vs 2.575 ± 0.308 ZNS, $p$ = 0.505) (Fig 4C). Interestingly, in the HEK293T cells transfected with the wildtype $GABA_AR$ condition, a slight increase in the wildtype γ2 subunit was observed with ZNS treatment, in contrast to the effects of HRD1 overexpression (WT: 1 ± 0 vehicle vs 1.190 ± 0.065 ZNS, $p$ = 0.045; mixed: 0.544 ± 0.041 vehicle vs 0.591 ± 0.081 ZNS, $p$ = 0.807) (Fig 4D). Similarly, ZNS treatment increased γ2(Q390X) subunit expression in the mutant condition (mixed: 0.834 ± 0.069 vehicle vs 0.886 ± 0.107 ZNS, $p$ = 0.937; mutant: 1 ± 0 vehicle vs 1.383 ± 0.192 ZNS, $p$ = 0.0496) (Fig 4E).

However, in the mixed condition – analogous to heterozygous patients – neither wildtype γ2 nor γ2(Q390X) subunit expression was altered with ZNS (3 μM, 24 hr) treatment *in vitro*. Because protein aggregates of γ2(Q390X) subunits are cytotoxic, and likely more difficult to degrade compared to monomers, we also investigated the relative amount of γ2 dimers, but saw no difference (mixed: 1 ± 0 vehicle vs 1.110 ± 0.175 ZNS, $p$ = 0.909; mutant: 1.683 ± 0.290 vehicle vs 1.428 ± 0.205 ZNS, $p$ = 0.607) (Supplementary Figure 3).

### 5.6.6 ZNS did not increase the expression of HRD1 *in vitro*

Given the opposing effects of HRD1 overexpression and ZNS treatment on both surface and total expression of $GABA_AR$ subunits, we sought to confirm that ZNS upregulates HRD1 in HEK293T cells. However, when we exposed HEK293T cells to varying doses of ZNS (0.3-30 μM) for 24 h, no effect on HRD1 was observed, compared to vehicle-treated cells ($p$ = 0.3451) (Fig 5A, 5B). SEL1L expression was likewise unaffected (data not shown).

Cells overexpressing exogenous protein via transfection, however, have altered proteostasis compared to untransfected cells, so ZNS was next tested in transfected cells expressing $GABA_ARs$. As before, HEK293T cells were transfected with the wildtype (α1β2γ2 1:1:1), mixed (α1β2γ2/γ2(Q390X) 1:1:0.5:0.5), or mutant (α1β2γ2(Q390X) 1:1:1) condition. Each condition then was treated with ZNS (3 μM, 24 hr) or vehicle, and expression of HRD1 and SEL1L was examined.

Similar to untransfected cells, HEK293T cells expressing WT, mixed, or mutant α1β2γ2 $GABA_ARs$ had no changes to HRD1 expression after ZNS (3 μM, 24 hr) exposure (WT: 1 ± 0 vehicle vs 1.062 ± 0.041 ZNS, $p = 0.742$; mixed: 1.031 ± 0.037 vehicle vs 1.161 ± 0.077 ZNS, $p = 0.168$; mutant: 1.083 ± 0.037 vehicle vs 1.178 ± 0.057 ZNS, $p = 0.418$) (Fig 5C). Likewise, no difference was seen for SEL1L (WT: 1 ± 0 vehicle vs 1.003 ± 0.028 ZNS, $p > 0.999$; mixed: 0.982 ± 0.039 vehicle vs 0.980 ± 0.068 ZNS, $p > 0.999$; mutant: 0.971 ± 0.051 vehicle vs 1.040 ± 0.097 ZNS, $p = 0.778$) (Fig 5D). Note, however, that for HRD1 expression, a very subtle but consistent trend towards an increase is observed with ZNS treatment for all conditions.

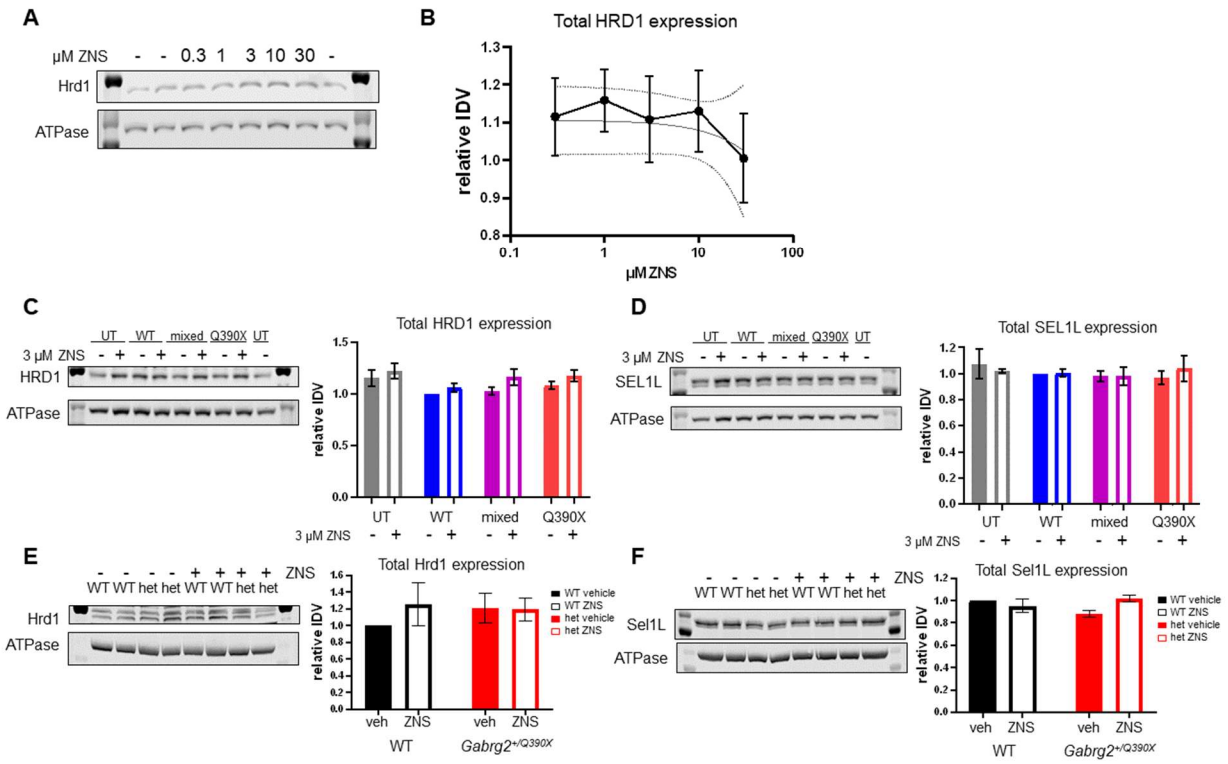


***Figure 5.5. ZNS did not upregulate HRD1.***
A-B. Untransfected HEK293T cells were treated with 0.3, 1, 3, 10, or 30 μM ZNS or vehicle, 48 h after passaging and 24 h before harvesting. A. The SDS-PAGE membrane was immunoblotted for HRD1 (1:1,000). B. HRD1 IDVs were normalized to the average of all vehicle-treated dishes. This average was taken as 1. A simple linear regression was performed, and the line of best fit (Y = -0.002712*X + 1.106) is shown in gray, with a 95% confidence interval as the dotted lines. C-D. HEK293T cells were transfected with α1, β2, and γ2 (1 μg each per 60 mm dish) (WT); α1, β2, and mixed γ2 and γ2(Q390X) (1:1:0.5:0.5); or α1, β2, and γ2(Q390X) (1:1:1) (mutant). Untransfected cells were used as controls (con). 24 h before harvesting, 3 μM ZNS or vehicle was applied. D. Immunoblot for HRD1 (1:1,1000) and graph of normalized IDVs. For C-D, IDVs were normalized to ATPase (1:1,000) and then to vehicle-treated WT. D. Immunoblot for SEL1L (1:1,000) and graph of normalized IDVs. E-F. Beginning at P30-45, *Gabrg2*$^{+/Q390X}$ mice and wildtype littermates were treated with 20 mg/kg ZNS or DMSO/saline vehicle for 7 days. Lysates of somatosensory cortex (cor), cerebellum (cb), thalamus (thal), and hippocampus (hip) were used for SDS-PAGE. Representative images from thalamus are shown. E. Membrane immunoblotted for Hrd1 (1:1,000) and graph of normalized IDVs. In E-F, IDVs were normalized to the loading control, ATPase (1:1,000), and then to a paired vehicle-treated wildtype animal. F. Immunoblot for Sel1L (1:1,000) and graph of normalized IDVs. For A-B, N = 9. For E, N = 8 separate transfections, and for F, N = 5 separate transfections. For E-F, N = 6-8 animals. Two-way ANOVA and Šídák's multiple comparisons, examining simple effects within drug treatments, were used to evaluate statistical significance. * $p < 0.05$. Values are expressed as mean ± S.E.M.

### 5.6.7 ZNS reduced seizures in *Gabrg2*$^{+/Q390X}$ mice

Although we found that ZNS does not upregulate HRD1 in HEK293T cells, we had nevertheless found a unique, potentially therapeutic effect of ZNS. The rescue of α1 and β2 subunit surface trafficking could help to normalize the decreased GABAergic signaling seen in *Gabrg2*$^{+/Q390X}$ mice.[17] Furthermore, because ZNS had been found to upregulate Hrd1 in rodents,[37-39] we remained hopeful that ZNS would increase Hrd1 expression in *Gabrg2*$^{+/Q390X}$ mice despite the lack of effect on HRD1 in HEK293T cells. Thus, we were curious whether ZNS could be beneficial for Dravet syndrome caused by the *GABRG2(Q390X)* mutation, by decreasing levels of the γ2(Q390X) subunit via Hrd1 modulation and/or facilitation of surface trafficking of α1 and β2 subunits via an Hrd1-independent mechanism. *Gabrg2*$^{+/Q390X}$ mice have spontaneous seizures beginning around P19, including absence seizures and generalized tonic-clonic seizures.[17] Compared to baseline recordings, mice 3 months of age that were treated with ZNS (20 mg/kg/day for 7 days) had fewer 5-7 Hz spike-and-wave discharges (SWDs) during a 24 h period (15.58 ± 4.987 baseline vs 3.667 ± 2.028 ZNS, $p = 0.0358$) and the total time spent seizing was reduced (90.04 ± 37.34 seconds baseline vs 28.10 ± 19.19 ZNS, $p = 0.0176$) (Fig 6). At this dose of ZNS, the duration of SWD events that did occur was not altered (5.106 ± 1.700 seconds baseline vs 4.050 ± 2.260 ZNS, $p = 0.2584$) (Fig 6D).

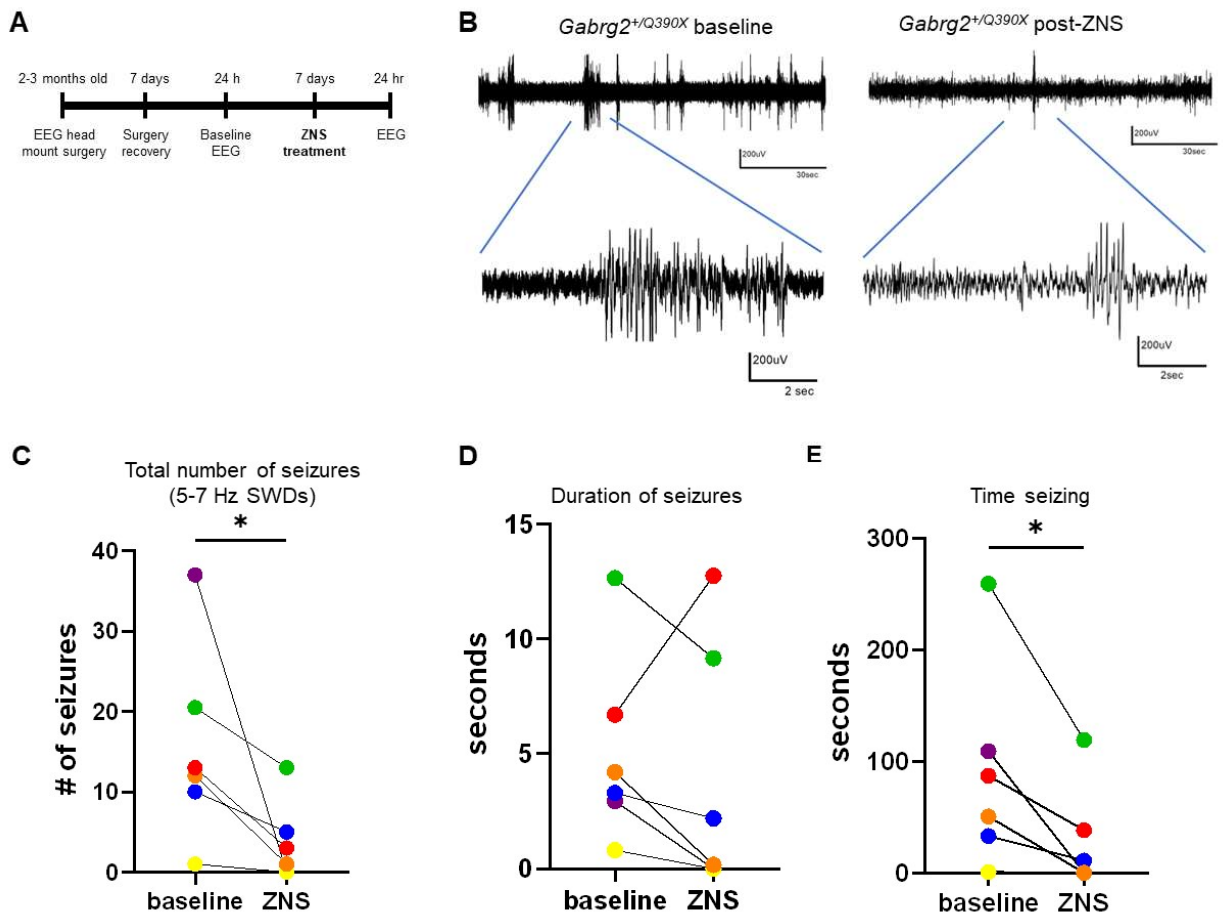


***Figure 5.6. ZNS reduced seizures in* Gabrg2$^{+/Q390X}$ *mice.***
A. Schematic showing EEG schedule. B. Representative traces from a *Gabrg2*$^{+/Q390X}$ mouse experiencing a 5-7 Hz spike-and-wave discharge (SWD) at baseline and after 7 days of ZNS treatment (20 mg/kg/day, administered intraperitoneally). A 60 second trace is zoomed in on a 10 second window. C. Total number of 5-7 Hz SWDs in 24 h, during baseline and after ZNS treatment. D. Average duration of 5-7 SWD events, during baseline and after ZNS treatment. E. Total time spent seizing in 5-7 Hz SWDs in 24 h, during baseline and after ZNS treatment. N = 3 female heterozygous *Gabrg2*$^{+/Q390X}$ mice. One-tailed paired t-tests were used to determine significance. * $p < 0.05$.

### 5.6.8 ZNS had differential effects on γ2 and γ2(Q390X) subunits in mice

We next investigated if the reduction of seizures in *Gabrg2*$^{+/Q390X}$ mice by ZNS treatment was due rescue of the expression of $GABA_AR$ subunits. Shortly after seizure onset (1-1.5 months of age), *Gabrg2*$^{+/Q390X}$ mice and wildtype littermates were treated with ZNS (20 mg/kg/day for 7 days). Following treatment, brain lysates were analyzed for total expression of α1, β2, and γ2 subunits. Multiple brain regions were examined: the somatosensory cortex and thalamus were chosen for their role in seizures via the thalamocortical circuit, and the cerebellum and hippocampus were chosen to enable comparisons to our prior work.[17,42]

Interestingly, the ZNS treatment affected γ2 subunit expression in both wildtype and heterozygous animals, but in opposite directions. In wildtype animals, γ2 subunit expression decreased by 22% in thalamus but was unchanged in other regions **(cortex:** 1 ± 0 vehicle vs 1.033 ± 0.076 ZNS, $p = 0.934$; **cerebellum:** 1 ± 0 vehicle vs 0.924 ± 0.084 ZNS, $p = 0.698$; **thalamus:** 1 ± 0 vehicle vs 0.784 ± 0.042 ZNS, $p = 0.004$; **hippocampus:** 1 ± 0 vehicle vs 0.871 ± 0.037 ZNS, $p = 0.146$) (Fig 7A, Supplementary Fig 4A). But in heterozygous mice, the wildtype form of the γ2 subunit exhibited 41% increased expression in the hippocampus compared to vehicle-treated mice, while other regions were unaffected (**cortex:** 0.786 ± 0.068 vehicle vs 0.841 ± 0.086 ZNS, $p = 0.831$; **cerebellum:** 0.739 ± 0.070 vehicle vs 0.912 ± 0.069 ZNS, $p = 0.176$; **thalamus:** 0.685 ± 0.039 vehicle vs 0.784 ± 0.057 ZNS, $p = 0.244$; **hippocampus:** 0.536 ± 0.026 vehicle vs 0.757 ± 0.073 ZNS, $p = 0.008$) (Fig 7A, Supplementary Fig 4A).

Curiously, in ZNS-treated *Gabrg2*$^{+/Q390X}$ mice, the mutant γ2(Q390X) subunit also demonstrated an increase in one of the four brain regions: 31% in the cerebellum (**cortex:** 1 ± 0 vehicle vs 1.452 ± 0.302 ZNS, $p = 0.315$; **cerebellum:** 1 ± 0 vehicle vs

1.314 ± 0.072 ZNs, $p = 0.0003$; **thalamus:** 1 ± 0 vehicle vs 1.262 ± 0.078 ZNS, $p = 0.097$; **hippocampus:** 1 ± 0 vehicle vs 1.285 ± 0.160 ZNS, $p = 0.301$) (Fig 7B, Supplementary Fig 4B).

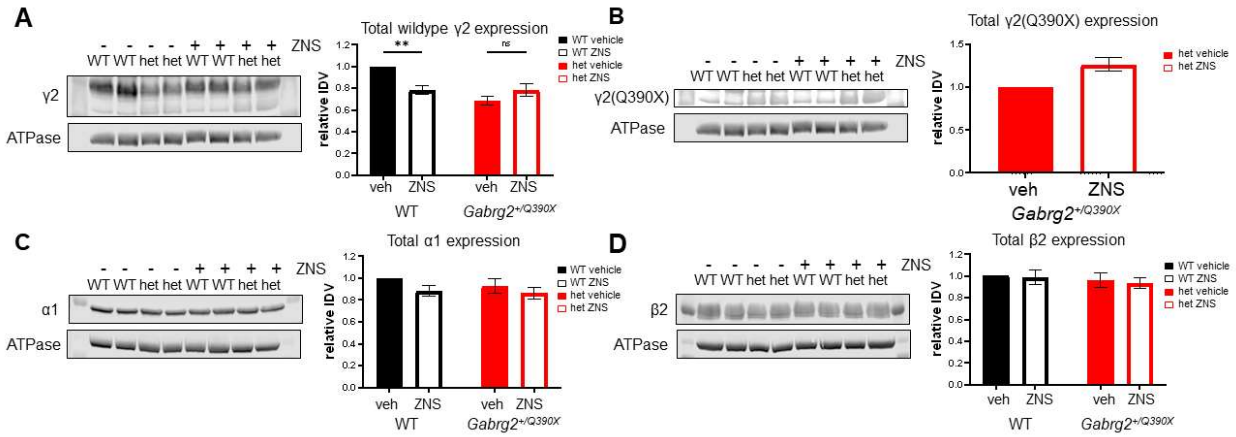


***Figure 5.7. ZNS altered γ2 expression in* Gabrg2$^{+/Q390X}$ *but not α1 or β2.***
A-D. Beginning at P30-45, *Gabrg2*$^{+/Q390X}$ mice and wildtype littermates were treated with 20 mg/kg ZNS or equal volume DMSO/saline vehicle, with daily intraperitoneal injections for 7 days. Brains were dissected and lysates of somatosensory cortex (cor), cerebellum (cb), thalamus (thal), and hippocampus (hip) were used for SDS-PAGE. Representative images from thalamus are shown. A. Immunoblot for γ2 (1:1,000) and graph of normalized IDVs. Wildtype γ2 can be seen at ~50 kDa and γ2(Q390X) is visible below. n A, B-C, IDVs were normalized to the loading control, ATPase (1:1,000), and then to a paired vehicle-treated wildtype animal. B. The membrane from (A) is presented with digitally manipulated contrast and brightness to better visualize the γ2(Q390X) band. This manipulation was performed after quantification and had no effect on measured IDVs. The graph is of IDVs normalized to ATPase (1:1,000) and then to paired vehicle-treated heterozygous *Gabrg2*$^{+/Q390X}$ animals. C. Immunoblot for α1 (1:500) and graph of normalized IDVs. D. Immunoblot of thalamus lysates probed for β2 (1:1,000) and graph of normalized IDVs. N = 6-8 animals. Two-way ANOVA and Šídák's multiple comparisons, examining simple effects within drug treatments, were used to evaluate statistical significance. ** $p < 0.01$, *** $p < 0.001$. Values are expressed as mean ± S.E.M.

### 5.6.9 ZNS had no effect on total expression of α1 or β2 subunits in mice

In contrast to the γ2 subunits, the partnering subunits were unchanged by ZNS treatment for either genotype (*Gabrg2*$^{+/Q390X}$ or wildtype littermates). For the α1 subunit, ZNS treatment resulted in no change in any brain region (**cortex:** WT: 1 ± 0 vehicle vs 0.944 ± 0.057 ZNS, $p = 0.761$; het: 0.931 ± 0.029 vehicle vs 0.956 ± 0.081 ZNS, $p = 0.944$; **cerebellum:** WT: 1 ± 0 vehicle vs 1.085 ± 0.085 ZNS, $p = 0.526$; het: 0.992 ±

0.056 vehicle vs 1.138 ± 0.063 ZNS, $p$ = 0.168; **thalamus:** WT: 1 ± 0 vehicle vs 0.883 ± 0.051 ZNS, $p$ = 0.227; het: 0.930 ± 0.065 vehicle vs 0.863 ± 0.055 ZNS, $p$ = 0.603; **hippocampus:** WT: 1 ± 0 vehicle vs 0.966 ± 0.047 ZNS, $p$ = 0.876; het: 0.866 ± 0.041 vehicle vs 0.942 ± 0.070 ZNS, $p$ = 0.702) (Fig 7C, Supplementary Fig 4C). Similarly, the β2 subunit was universally unchanged (**cortex:** WT: 1 ± 0 vehicle vs 1.102 ± 0.108 ZNS, $p$ = 0.621; het: 0.983 ± 0.082 vehicle vs 1.015 ± 0.065 ZNS, $p$ = 0.954; **cerebellum:** WT: 1 ± 0 vehicle vs 1.173 ± 0.111 ZNS, $p$ = 0.553; het: 1.072 ± 0.109 vehicle vs 1.383 ± 0.160 ZNS, $p$ = 0.164; **thalamus:** WT: 1 ± 0 vehicle vs 0.988 ± 0.069 ZNS, $p$ = 0.986; het: 0.960 ± 0.069 vehicle vs 0.937 ± 0.047 ZNS, $p$ = 0.951; **hippocampus:** WT: 1 ± 0 vehicle vs 1.211 ± 0.186 ZNS, $p$ = 0.404; het: 0.944 ± 0.111 vehicle vs 1.086 ± 0.037 ZNS, $p$ = 0.835) (Fig 7D, Supplementary Fig 4D).

### 5.6.10 ZNS had no effect on Hrd1 expression in mouse brain

Because ZNS treatment in mice had effects on γ2 subunit expression not consistent with the results of *in vitro* HRD1 overexpression, we sought to replicate studies that showed elevation of Hrd1 in rodents treated with ZNS.[37-39] Utilizing the same samples – *Gabrg2*$^{+/Q390X}$ mice and wildtype littermates 1-1.5 months of age, treated with ZNS (20 mg/kg/day) for 7 days – expression of Hrd1 and Sel1L was then examined.

Contrary to our initial hypothesis, Hrd1 was not upregulated in wildtype or heterozygous mouse brains after ZNS treatment **(cortex:** WT: 1 ± 0 vehicle vs 1.167 ± 0.158 ZNS, $p$ = 0.705; het: 1.026 ± 0.196 vehicle vs 0.888 ± 0.161 ZNS, $p$ = 0.786; **cerebellum:** WT: 1 ± 0 vehicle vs 1.064 ± 0.139 ZNS, $p$ = 0.947; het: 1.054 ± 0.181 vehicle vs 1.362 ± 0.182 ZNS, $p$ = 0.311; **thalamus:** WT: 1 ± 0 vehicle vs 1.254 ± 0.257

ZNS, $p$ = 0.569; het: 1.205 ± 0.177 vehicle vs 1.195 ± 0.136 ZNS, $p$ = 0.999; **hippocampus:** WT: 1 ± 0 vehicle vs 0.995 ± 0.074 ZNS, $p$ = 0.999; het: 0.972 ± 0.057 vehicle vs 1.111 ± 0.134 ZNS, $p$ = 0.510) (Fig 5E, Supplementary Fig 5A). Sel1L was also unaffected (**cortex:** WT: 1 ± 0 vehicle vs 1.091 ± 0.156 ZNS, $p$ = 0.928; het: 1.020 ± 0.192 vehicle vs 1.088 ± 0.238 ZNS, $p$ = 0.959; **cerebellum:** WT: 1 ± 0 vehicle vs 0.883 ± 0.087 ZNS, $p$ = 0.826; het: 0.906 ± 0.102 vehicle vs 1.217 ± 0.228 ZNS, $p$ = 0.283; **thalamus:** WT: 1 ± 0 vehicle vs 0.953 ± 0.058 ZNS, $p$ = 0.663; het: 0.880 ± 0.032 vehicle vs 1.017 ± 0.032 ZNS, $p$ = 0.053; **hippocampus:** WT: 1 ± 0 vehicle vs 0.923 ± 0.138 ZNS, $p$ = 0.865; het: 1.090 ± 0.157 vehicle vs 0.939 ± 0.066 ZNS, $p$ = 0.572) (Fig 5F, Supplementary Fig 5B).

### 5.6.11 Neither HRD1 overexpression nor ZNS treatment altered expression of BiP or calnexin *in vitro*

Our results so far show that ZNS facilitated surface trafficking of $GABA_AR$ subunits for HEK293T cells expressing α1β2γ2/γ2(Q390X) subunits, but ZNS had no effect on total protein expression in this mixed $GABA_AR$ condition. This is in contrast to the clear reduction in γ2 protein expression in HRD1-overexpressing conditions. Additionally, ZNS does not upregulate HRD1 or SEL1L in HEK293T cells or in young mice. We therefore investigated alternative mechanisms of action for ZNS. Because ZNS promoted surface trafficking of $GABA_AR$ subunits without altering the total expression of these proteins, we thus hypothesized that ZNS may be altering the secretory pathway, as it is through this pathway that membrane proteins like $GABA_AR$ subunits are trafficked to reach the cell surface. We have previously reported that the γ2(Q390X) subunit causes ER stress,[13,17] and there are reports of ZNS preventing ER

stress.[38-41] Therefore, we investigated the ER-localized molecular chaperones BiP/GRP78 and calnexin, which have been shown to interact with $GABA_AR$ subunits.[19,27]

However, in untransfected HEK293T cells or cells transfected with wildtype, mixed, or mutant $GABA_AR$, we found no difference in BiP expression after ZNS treatment (3 μM, 24 hr) (untransfected: 0.587 ± 0.101 vehicle vs 0.709 ± 0.086 ZNS, $p$ = 0.763; WT: 1 ± 0 vehicle vs 1.022 ± 0.052 ZNS, $p$ = 0.999; mixed: 1.225 ± 0.111 vehicle vs 1.097 ± 0.069 ZNS, $p$ = 0.725; mutant: 1.066 ± 0.097 vehicle vs 1.004 ± 0.089 ZNS, $p$ = 0.973) (Fig 8A). Likewise, calnexin displayed no changes post-treatment (untransfected: 0.921 ± 0.053 vehicle vs 0.854 ± 0.042 ZNS, $p$ = 0.828; WT: 1 ± 0 vehicle vs 1.073 ± 0.041 ZNS, $p$ = 0.778; mixed: 1.205 ± 0.056 vehicle vs 1.111 ± 0.041 ZNS, $p$ = 0.579; mutant: 1.099 ± 0.042 vehicle vs 1.140 ± 0.088 ZNS, $p$ = 0.966) (Fig 8B).

BiP and calnexin expression were also examined in HEK293T cells transfected with wildtype and mutant γ2 subunits, and pcDNA, HRD1-myc, HA-SEL1L, or both HRD1-myc and HA-SEL1L (same conditions as Figure 2). No differences were seen between any conditions (data not shown).

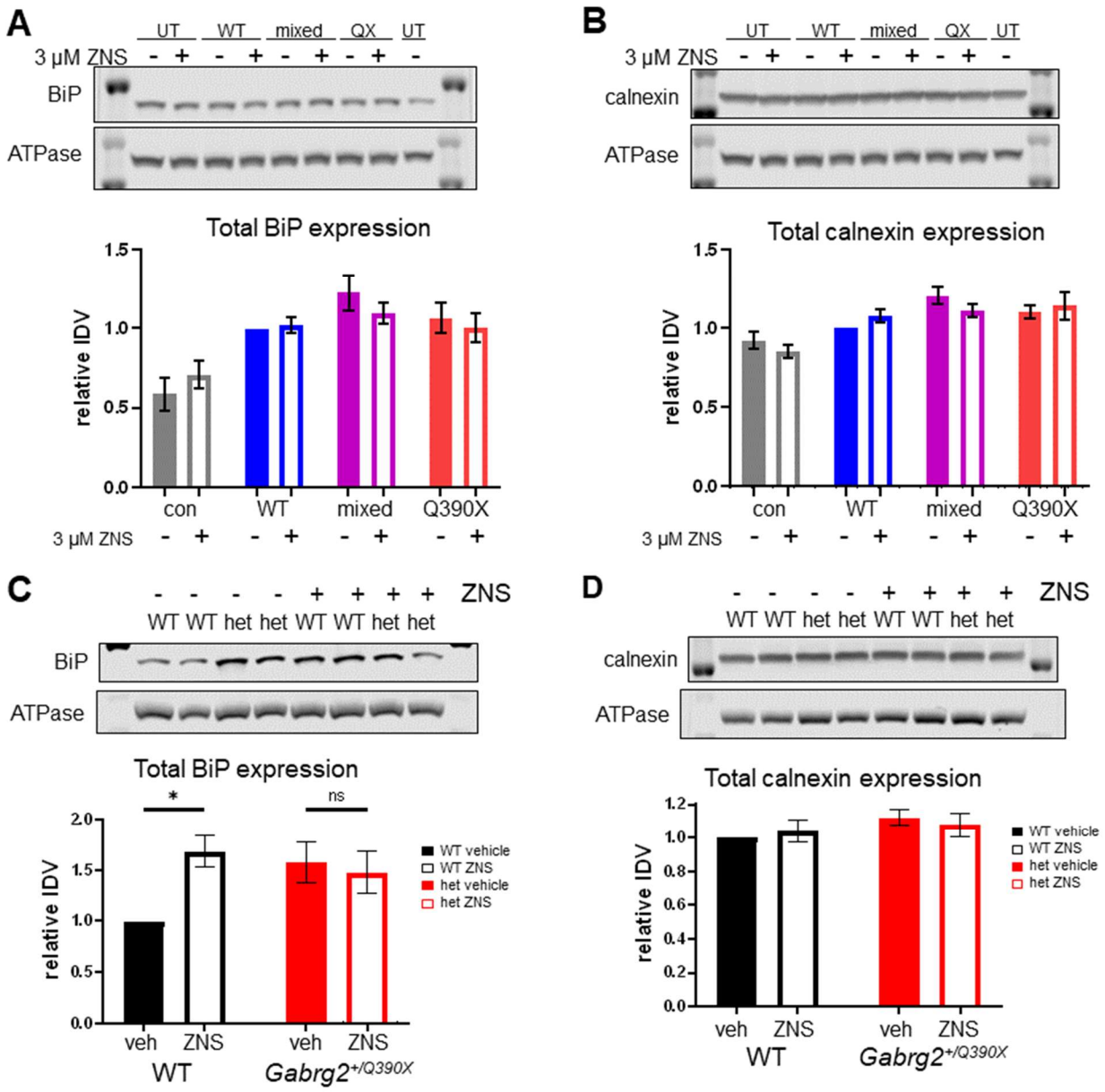


***Figure 5.8. ZNS did not normalize ER stress associated with γ2(Q390X).***
A-B. HEK293T cells were transfected with α1, β2, and γ2 (1 μg each per 60 mm dish) (WT); α1, β2, and mixed γ2 and γ2(Q390X) (1:1:0.5:0.5); or α1, β2, and γ2(Q390X) (1:1:1) (mutant). Untransfected cells were used as controls (con). 24 h before harvesting, 3 μM ZNS or vehicle was applied. IDVs were normalized to ATPase (1:1,000) and then to vehicle-treated WT. A. Membrane immunoblotted for BiP/GRP78 (1:500) and graph of normalized IDVs. B. Immunoblot for calnexin (1:1,000) and graph of normalized IDVs. C-D. Beginning at P30-45, *Gabrg2*$^{+/Q390X}$ mice and wildtype littermates were treated with 20 mg/kg ZNS or equal volume DMSO/saline vehicle, with daily intraperitoneal injections for 7 days. Brains were dissected and lysates of somatosensory cortex (cor), cerebellum (cb), thalamus (thal), and hippocampus (hip) were used for SDS-PAGE. Representative images from thalamus are shown. C.

Immunoblot for BiP (1:500) and graph of normalized IDVs. D. Immunoblot for calnexin (1:1,000) and graph of normalized IDVs. A-B, N = 7-8 separate transfections. C-D, N = 6-8 animals. Two-way ANOVA and Šídák's multiple comparisons, examining simple effects within drug treatments, were used to evaluate statistical significance. * $p < 0.05$. Values are expressed as mean ± S.E.M.

### 5.6.12 ZNS upregulated BiP in wildtype mice, but not in *Gabrg2*$^{+/Q390X}$

In addition to transfected HEK293T cells, we also interrogated the effect of ZNS on ER chaperones in mice. Curiously, mice did display changes in BiP expression after ZNS treatment (20 mg/kg/day for 7 days) – but only the wildtype littermates (Fig 8C, Supplementary Fig 7A). BiP was highly upregulated in WT animals post-ZNS in two of the four brain regions investigated: cerebellum (WT: 1 ± 0 vehicle vs 1.352 ± 0.059 ZNS, $p = 0.023$; het: 1.282 ± 0.128 vehicle vs 1.272 ± 0.111 ZNS, $p = 0.997$) and thalamus (WT: 1 ± 0 vehicle vs 1.680 ± 0.155 ZNS, $p = 0.023$; het: 1.575 ± 0.202 vehicle vs 1.480 ± 0.211 ZNS, $p = 0.914$). Hippocampus showed a strong trend that failed to reach statistical significance (WT: 1 ± 0 vehicle vs 1.495 ± 0.200 ZNS, $p = 0.064$; het: 1.605 ± 0.123 vehicle vs 1.291 ± 0.148 ZNS, $p = 0.300$). Only in the cortex was there no difference for either genotype (WT: 1 ± 0 vehicle vs 1.389 ± 0.114 ZNS, $p = 0.149$; het: 1.496 ± 0.219 vehicle vs 1.285 ± 0.163 ZNS, $p = 0.546$). Post-hoc unpaired t-tests of vehicle-treated mice revealed that BiP is upregulated in *Gabrg2*$^{+/Q390X}$ mice compared to wildtype littermates in cortex, thalamus, and hippocampus, and the difference in cerebellum closely approaches significance (**cortex:** WT 1 ± 0 vs het 1.496 ± 0.219, $p = 0.0470$; **cerebellum:** WT 1 ± 0 vs het 1.282 ± 0.128, $p = 0.0522$; **thalamus:** WT 1 ± 0 vs het 1.575 ± 0.202, $p = 0.0172$; **hippocampus:** WT 1 ± 0 vs het 1.605 ± 0.123, $p = 0.0006$) (Supplementary Figure 6).

Calnexin, however, was not altered in any brain region examined for either genotype (**cortex:** WT: 1 ± 0 vehicle vs 1.258 ± 0.131 ZNS, $p = 0.376$; het: 1.279 ± 0.299 vehicle vs 1.158 ± 0.117 ZNS, $p = 0.799$; **cerebellum:** WT: 1 ± 0 vehicle vs 0.983 ± 0.048 ZNS, $p = 0.937$; het: 1.037 ± 0.026 vehicle vs 0.991 ± 0.038 ZNS, $p = 0.630$; **thalamus:** WT: 1 ± 0 vehicle vs 1.040 ± 0.065 ZNS, $p = 0.866$; het: 1.123 ± 0.046 vehicle vs 1.078 ± 0.070 ZNS, $p = 0.838$; **hippocampus:** WT: 1 ± 0 vehicle vs 0.917 ± 0.055 ZNS, $p = 0.569$; het: 0.971 ± 0.051 vehicle vs 0.805 ± 0.080 ZNS, $p = 0.122$) (Fig 8D, Supplementary Fig 7B).

## 5.7 Discussion

### 5.7.1 An epilepsy-associated truncation mutation in the γ2 subunit impairs $GABA_AR$ expression

We have recapitulated here that the γ2(Q390X) mutant protein, associated with the severe DEE Dravet syndrome, reduces the total expression of the partnering $GABA_AR$ subunits α1 and β2. This reduction is accompanied by a decrease in $GABA_AR$ surface expression, which results in diminished amplitude of miniature inhibitory postsynaptic currents (mIPSCs) and of GABA-evoked currents.[11,13,17] Because impaired GABAergic signaling is known to be an important contributor to epilepsy, this suggests that the ER retention of α1 and β2 subunits by γ2(Q390X) is responsible for the seizure pathology.[17]

### 5.7.2 The E3 ligase HRD1 facilitates degradation of the mutant γ2(Q390X) subunit

Our previous studies have demonstrated that epilepsy-associated mutant $GABA_AR$ subunits are degraded in part through ERAD.[43,44] The ERAD component

HRD1, an E3 ubiquitin ligase, has been shown to ubiquitinate the α1 subunit, thereby marking the α1 subunit for degradation via the ubiquitin-proteasome system.[19,27] As the α1 and γ2 subunits share 44% sequence identity, it was probable that HRD1 may also be capable of targeting the γ2 subunit. Indeed, pharmacological inhibition of HRD1 not only slowed the degradation of an α1 mutant subunit that is normally rapidly degraded, it also elevated expression of two epilepsy-associated missense γ2 subunit mutations.[27] Here we provide further evidence that HRD1 is involved in the degradation of the γ2 subunit. Importantly, HRD1 can modulate the expression of both the wildtype γ2 subunit and the severely misfolded mutant γ2(Q390X) subunit.

E3 ligases are substrate-specific, and although ~600 E3 ligases have been discovered, their substrates remain largely unidentified. However, E3 ligases are commonly linked with neurological phenotypes, including Angelman syndrome, tuberous sclerosis complex, autism spectrum disorder, and many genetic epilepsies.[21,22,45] In fact, one review found that 83 distinct E3 ligases were associated with a wide range of neurological diseases, comprising 70 diseases in total.[22] Therefore, to identify E3 ligases with the γ2 subunit as a substrate, we tested two E3 ligases associated with epilepsy: NEDD4L and UBE3A. However, neither robustly influenced expression of the γ2 or γ2(Q390X) subunit. Another E3 ligase, ring finger protein 34 (RNF34), had also been reported to ubiquitinate the γ2 subunit for degradation, but RNF34 specifically interacts with a portion of the C-terminal region that is missing in the γ2(Q390X) subunit (amino acids 362-404).[36] It was therefore suspected that RNF34 would decrease expression of the wildtype γ2 subunit and not the γ2(Q390X) subunit. However, RNF34 failed to modulate expression of either the γ2 or γ2(Q390X) subunit.

As the authors of that initial study had also used HEK293 cells and rat cDNA for the short isoform of γ2, known as γ2S, the reason for this discrepancy is not immediately clear.

Unexpectedly, cotransfection with HA-SEL1L had no effect on γ2 or γ2(Q390X) subunit expression, and this may be related to the fact that the HA-SEL1L transfection failed to increase SEL1L expression. Because the HA tag robustly appears on immunoblots, it is unlikely that the transfection itself was unsuccessful. Instead, it may be that expression of Sel1L in HEK293T cells is tightly regulated, such that endogenous expression is reduced in response to exogenous plasmids.[46]

Although HRD1 decreased the expression of the functional wildtype γ2 subunit as well as the mutant γ2(Q390X) subunit, leveraging HRD1 may still be useful. The *GABRG2(Q390X)* mutation is dominant-negative. Neurons from *Gabrg2*$^{+/Q390X}$ mice have decreased miniature inhibitory postsynaptic current amplitude and frequency, compared to *Gabrg2*$^{+/-}$ mice, due to ER retention and subsequent increased degradation and impaired surface trafficking of other $GABA_AR$ subunits.[17] This indicates that the presence of the mutant subunit is more deleterious than simple heterozygous lack of wildtype γ2. Therefore, decreasing the expression of γ2(Q390X) via HRD1-related mechanisms may reduce ER retention of wildtype γ2, allowing for more efficient trafficking of $GABA_ARs$ to the cell surface. Although increased HRD1 activity may reduce the total amount of wildtype γ2 further, the increase in surface trafficking of functional receptors by removing γ2(Q390X) may offset the decrease of total γ2. Some deficit of γ2 is permissible to neurons: *Gabrg2*$^{+/-}$ mice have a much milder phenotype than *Gabrg2*$^{+Q390X-}$ mice, and indeed in some genetic backgrounds these heterozygous

knockout mice have no seizures at all.[17,47] While our *in vitro* experiments did not show rescued γ2 surface trafficking with HRD1 overexpression, *in vivo* results may differ and this should be explored.

Additionally, we only investigated one dose of HRD1-myc cDNA. It is possible that lower doses may preferentially target the misfolded mutant γ2(Q390X) protein. Furthermore, chemical chaperones that stabilize wildtype proteins – such as 4-phenylbutyrate , a compound we have recently reported restoring GABA transporter 1 function[42] – may help preserve properly-folded wildtype γ2 subunits from HRD1-mediated degradation, further enabling selective degradation of primarily the mutant γ2(Q390X) subunit.

### 5.7.3 ZNS partially ameliorated the suppression of the γ2(Q390X) subunit on surface trafficking of $GABA_AR$ subunits

ZNS is approved by the United States Food and Drug Administration (FDA) for use in adults with partial-onset seizures, but is sometimes used for pediatric Dravet syndrome patients, in combination with other therapies. The antiseizure mechanism of ZNS is complex,[48,49] but our work here suggests that increased surface expression of $GABA_ARs$ may be another component. The γ2(Q390X) subunit has a dominant-negative effect on $GABA_AR$ surface expression, as the mutant protein retains wildtype α1 and β2 subunits in the ER. We found that ZNS fully rescued the surface trafficking of α1 and β2 subunits. The γ2 subunit was not significantly rescued, so it is probable that the primary makeup of the added surface receptors is α1β2 receptors. Although α1β2 receptors are generally rare, this possibility should still be explored. Electrophysiology experiments will be helpful to determine if the number of α1β2γ2 receptors is also increased.

This increase in $GABA_AR$ subunit trafficking is especially noteworthy for clinical applications, because epilepsy patients often build tolerance to antiseizure drugs. In the case of benzodiazepines, drug tolerance is hypothesized to be due – at least in part – to changes in receptor localization. More specifically, in response to chronic exposure to benzodiazepines, $GABA_ARs$ become internalized and the proportion of $GABA_ARs$ at the cell surface decreases.[50,51] It would quite insightful to investigate the possibility of zonisamide ameliorating the $GABA_AR$ internalization that occurs in response to long-term use of benzodiazepines.

### 5.7.4 ZNS had mixed effects on γ2 and γ2(Q390X) subunit expression

While ZNS had no effect on total expression of α1 or β2 subunits in mouse brains or HEK293T cells, for any genotype, some interesting findings on γ2 subunits were obtained, suggesting differential changes in different brain regions and between different genotypes upon ZNS treatment. ZNS treatment resulted in an increase in the wildtype γ2 subunit expression in the hippocampus of *Gabrg2*$^{+/Q390X}$ mice, as well as an increase in the mutant γ2(Q390X) subunit in the cerebellum of the same mice. Conversely, in wildtype littermates, the γ2 subunit was actually lower in the thalamus of ZNS-treated animals compared to vehicle-treated controls. It is curious that mutant protein increased in *Gabrg2*$^{+/Q390X}$ mice but ZNS still decreased seizures so effectively. This is likely due to the brain regions affected: γ2(Q390X) was only elevated in the cerebellum, which is not involved in absence seizures.

In contrast to the decreased γ2 expression in wildtype mouse brain lysates, in HEK293T cells expressing wildtype $GABA_ARs$, there was a 19% increase in γ2 subunit expression after exposure to ZNS. Somewhat similar to the elevated γ2(Q390X)

expression seen in *Gabrg2*$^{+/Q390X}$ mice treated with ZNS, the mutant condition in HEK293T cells also had an increase in the expression of the γ2(Q390X) subunit. However, this mutant condition (α1β2γ2(Q390X)) is the equivalent of a homozygous animal, and heterozygous animals are analogous to the mixed $GABA_AR$ condition in HEK293T cells. In the mixed condition, no differences are seen.

The discrepancies between *in vivo* and *in vitro* data may be due to the different amounts of $GABA_AR$ protein: the transfected HEK293T cells overexpress these proteins. Alternatively, proteostasis mechanisms in neurons may be different from those in HEK293T cells. Finally, the concentration of ZNS likely differs between the two experimental setups. A study utilizing 19.1 mg/kg ZNS in mice found that the concentration in the brain was 2.95 ± 0.27 μg/mL, or 13.9 μM, 30 min after a single injection.[48] This is several-fold higher than the concentration applied to HEK293T cells, but the mice used for biochemistry experiments were sacrificed approximately 24 h after the last injection, and brain and serum concentrations are drastically decreased by 6 h post injection.[52] Thus, the concentration of ZNS in the brains of mice was likely much lower than 13.9 μM at the time of collection. The precise concentration at the time of collection and the average concentration during the week of treatment, however, are unknown.

### 5.7.5 ZNS did not increase HRD1 expression in mice or HEK293T cells

We chose to investigate ZNS because it has been reported to upregulate HRD1, by transcriptional upregulation of the adaptor protein SEL1L. However, we failed to find any effect of ZNS (20 mg/kg/day for 7 days) on Hrd1 or Sel1L in brain lysates from juvenile *Gabrg2*$^{+/Q390X}$ mice or wildtype littermates. HEK293T cells also revealed no

significant in HRD1 expression after 24 h of 0.3-30 μM ZNS. However, a very modest yet consistent upward trend is present. It is possible that, for these models, a different dose or treatment schedule is needed to detect robust changes to HRD1. Additionally, it is possible that the statistically insignificant increase of approximately 10% may be biologically relevant.

### 5.7.6 ZNS reduces seizures in the *Gabrg2*$^{+/Q390X}$ model of Dravet syndrome

Despite the failure to support the initial hypothesis that ZNS upregulates Hrd1, here we show that ZNS, at the dose of 20 mg/kg/day, was effective in reducing the number of spontaneous 5-7 Hz SWD seizures in 3-month-old *Gabrg2*$^{+/Q390X}$ mice. The average duration of a single seizure event was not reduced, although most mice showed a downward trend. Nevertheless, the total time spent seizing was 69% lower than baseline. Thus, ZNS may be useful for *GABRG2(Q390X)*-associated Dravet syndrome. In addition to seizures, it will be interesting to evaluate other Dravet-associated phenotypes in ZNS-treated *Gabrg2*$^{+/Q390X}$ mice, such as anxiety, social abnormalities, and spatial memory.[17]

### 5.7.7 *Gabrg2*$^{+/Q390X}$ mice had a dampened response to the effect of ZNS on the expression of the ER chaperone BiP

Because ZNS does not alter HRD1 in our models, and had only inconsistent effects on γ2 subunit expression, we considered other explanations for the effect of ZNS on $GABA_AR$ subunit trafficking. Previous studies have suggested a protective role for ZNS against ER stress.[38-41] Relief of ER stress can aid in protein processing and forward trafficking, so we investigated if expression of two components of ER stress – BiP and calnexin – were affected by ZNS treatment.

In HEK293T cells, ZNS did not change total expression of either BiP or calnexin, regardless of what $GABA_AR$ configuration the cells were transfected with. There are many proteins involved in the ER stress and unfolded protein response pathways, such as ATF6, PERK, IRE1α, and CHOP, so these additional factors should be investigated to obtain a more comprehensive understanding of the interaction between ZNS, $GABA_AR$ subunits, and protein processing.

In the brains of young mice, a different response occurred. Like in HEK293T cells, calnexin was not affected. However, BiP was strongly upregulated by ZNS, but, interestingly, only in the wildtype animals. This disparity suggests that the ER stress pathway is altered in *Gabrg2*$^{+/Q390X}$ mice, as they did not respond in this manner to ZNS. Indeed, BiP expression is approximately 50% higher in *Gabrg2*$^{+/Q390X}$ mice compared to littermates, in all four brain regions examined. This is in line with our prior *in vitro* findings that the γ2(Q390X) protein is associated with increased expression of the ER-stress-induced pro-apoptotic factor GADD153/CHOP.[13,17] The elevated expression of BiP at baseline and lack of response to ZNS raises the possibility of a ceiling effect, wherein the molecular chaperones in the ER of neurons of *Gabrg2*$^{+/Q390X}$ mice are operating at full capacity. The γ2(Q390X) subunit may deplete the reserve capacity of protein folding pathways, such that these cells are perhaps not capable of promoting further protein quality control measures. More research is necessary to fully characterize the effects of the γ2(Q390X) subunit mutation on ER stress and proteostasis.

### 5.7.8 Conclusion

ERAD is known to be altered in some genetic diseases with epilepsy, including familial encephalopathy with neuroserpin inclusion bodies (FENIB)[53] and RNF13-associated infantile neurodegeneration.[54] Additionally, many other genetic epilepsies are associated with misfolded and/or mistrafficked proteins, such as those caused by mutations in *SLC6A1*,[55,56] *STXBP1*,[57,58] and *KCNQ2*.[59] Together, this points towards a possible avenue of treatment: modulation of proteostasis. In this paper, we identified a component of ERAD, an endogenous protein quality control pathway, that can decrease expression of the neurotoxic γ2(Q390X) subunit. This component – the E3 ubiquitin ligase HRD1 – is a druggable target. Dinoprost (DNP) and dihydroergocristine (DHEC) inhibit HRD1, allowing mutant $GABA_AR$ subunits that are subject to overactive degradation to instead insert into receptors with partial functionality.[27] In contrast to those mutations that have partial function and are degraded too rapidly, the γ2(Q390X) subunit is nonfunctional and forms intracellular aggregates.[17] We therefore attempted to increase γ2(Q390X) degradation by upregulating HRD1 via ZNS. While our work does not support the prior reports that ZNS can upregulate HRD1, we did still find promising effects of ZNS on γ2 subunits and $GABA_ARs$. Further investigation is necessary to elucidate how ZNS modulates $GABA_AR$ subunits. This topic is of great interest, as recently there has been an increase in the study of protein folding, trafficking, and quality control in the context of epilepsy. Our findings on ZNS suggest that this potential proteostasis regulator may be applicable to a range of disorders.

## 5.8 Supplementary Figures

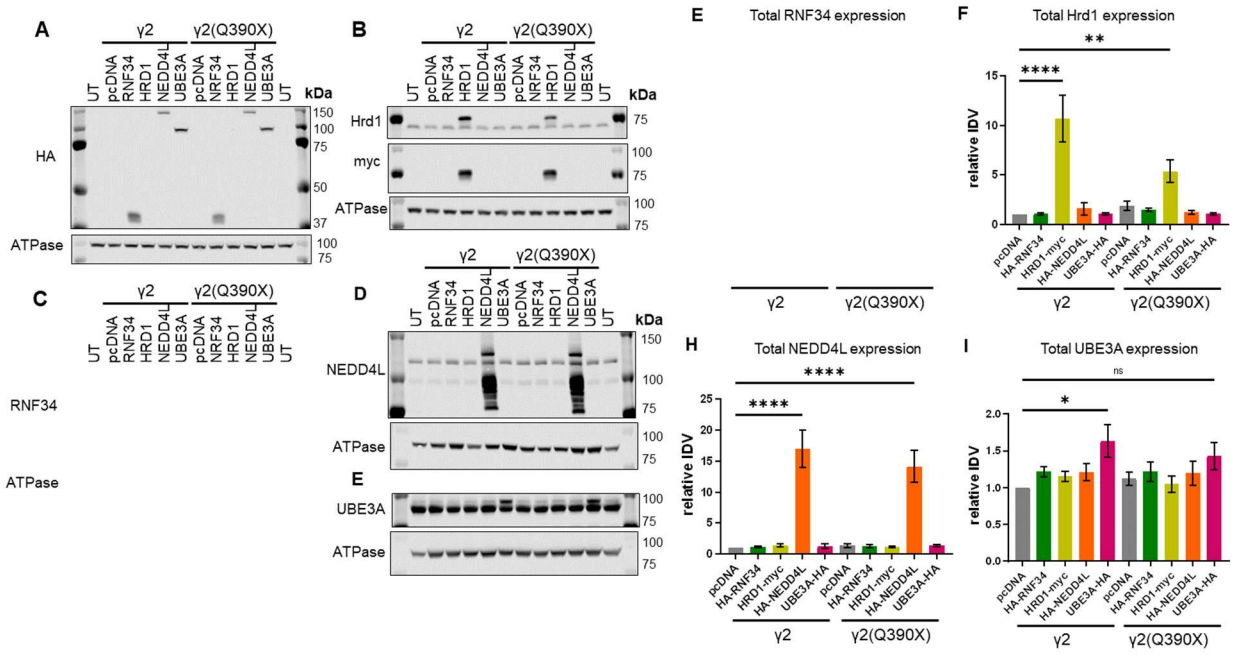


***Figure 5.9. Supplementary Figure 1: E3 ubiquitin ligases were overexpressed with γ2 or γ2(Q390X) subunits.***
HEK293T cells were transfected with γ2 or γ2(Q390X) (3 µg) and pcDNA, HA-RNF34, HRD1-myc, HA-NEDD4L, or UBE3A-HA (0.5 µg). 48 h post transfection, cells were collected, lysed, and subjected to SDS-PAGE. A. The membrane was immunoblotted with an anti-HA antibody (1:300). B. A membrane immunoblotted for HRD1 (1:1,000) and myc (1:500). C. Immunoblot for RNF34 (1: *pending* ). D. Immunoblot for NEDD4L (1:1,000). E. Immunoblot for UBE3A (1:1,000). F-I. Graphs of the IDVs, normalized first to the loading control ATPase (1:1,000) and then to the γ2 + pcDNA condition. One-way ANOVA and Tukey's test for post-hoc analysis, corrected for multiple comparisons, were used to evaluate statistical significance. * $p < 0.05$, ** $p < 0.01$, *** $p < 0.001$, **** $p < 0.0001$. Values are expressed as mean ± S.E.M. *RNF34 antibody on backorder; data to be completed after submission of this dissertation.*

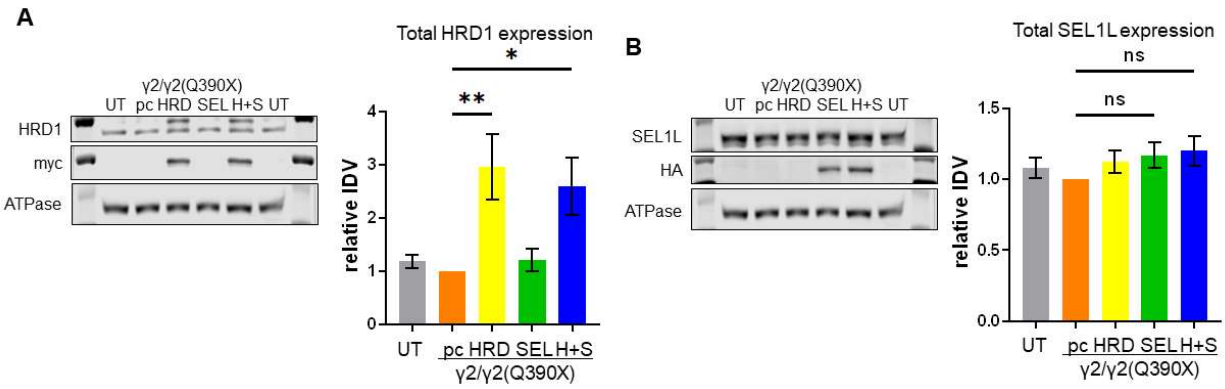


***Figure 5.10. Supplementary Figure 2: ERAD components were overexpressed with γ2 and γ2(Q390X) subunits.***

HEK293T cells were transfected with γ2 and γ2(Q390X) (1.5 µg each). They were cotransfected with HRD1-myc (labeled HRD) or HA-SEL1L (labeled SEL) or both HRD1-myc and HA-SEL1L (labeled H+S), using 0.5 µg of these plasmids. Total cDNA was normalized to 4 µg with empty vector pcDNA. pc is γ2 and γ2(Q390X) + pcDNA. UT is untransfected controls. A. Immunoblot for HRD1 (1:1,000) and myc (1:500) and graph of normalized HRD1 IDVs. Although the myc tag is only 10 amino acids (1.2 kDa), it appears to result in the heterologous HRD1-myc protein having a noticeable upward shift compared to the endogenous HRD1. Quantification is for the area encompassing both bands. For A-B, UT was graphed as the average of the normalized IDVs of each UT lane. B. Immunoblot for SEL1L (1:1,000) and HA (1:300) and graph of normalized SEL1L IDVs. N = 7 separate transfections. One-way ANOVA and Tukey's test for post-hoc analysis, corrected for multiple comparisons, were used to evaluate statistical significance. * $p < 0.05$, ** $p < 0.01$. Values are expressed as mean ± S.E.M.

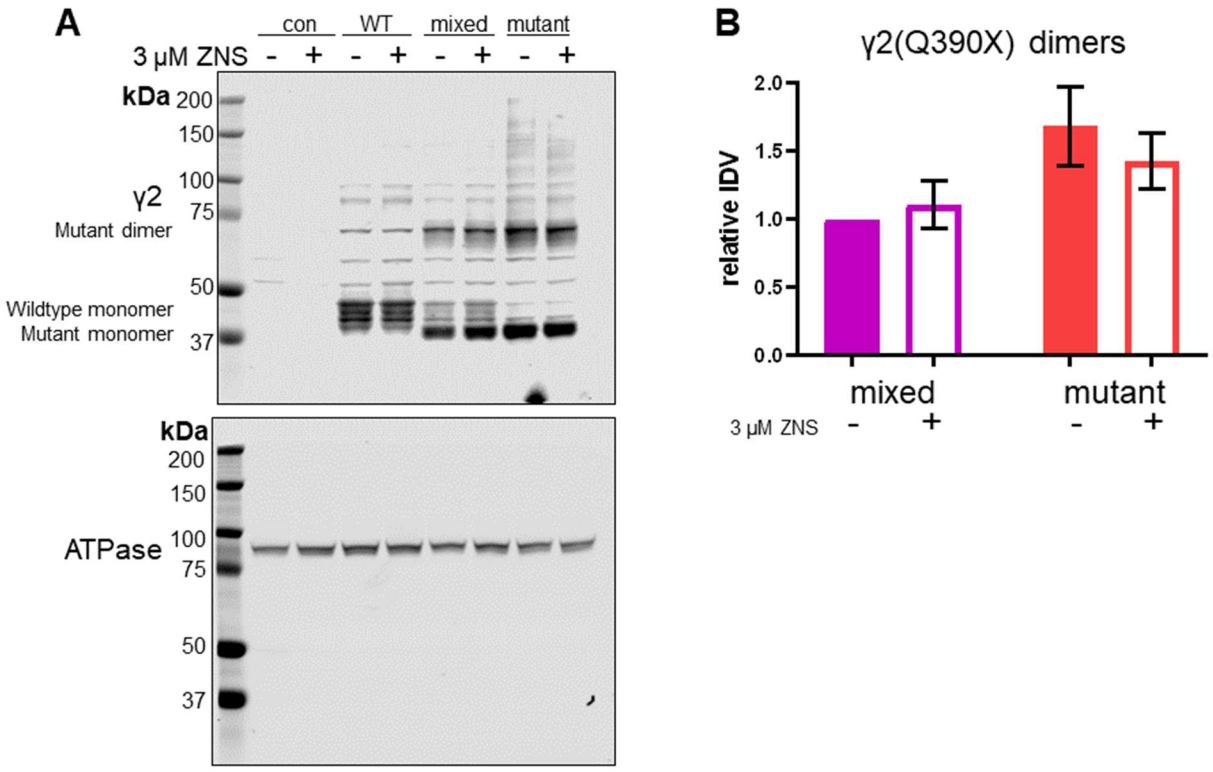


***Figure 5.11. Supplementary Figure 3: ZNS did not affect oligomerization of the γ2(Q390X) subunit.***

HEK293T cells were transfected with α1, β2, and γ2 (1 μg each per 60 mm dish) (WT); α1, β2, and mixed γ2 and γ2(Q390X) (1:1:0.5:0.5); or α1, β2, and γ2(Q390X) (1:1:1) (mutant). Untransfected cells were used as controls (con). 24 h before harvesting, 3 μM ZNS or vehicle was applied. Lysates were subjected to SDS-PAGE and immunoblotted. A. Uncropped immunoblot for γ2 (1:1,000), showing monomers (39 and 45 kDa) and dimers (80-100 kDa). B. Graph of normalized IDVs. IDVs were normalized first to ATPase (1:1,000) and then to vehicle-treated mixed, which was taken as 1. A-E, N = 8 separate transfections. Two-way ANOVA and Šídák's multiple comparisons, examining simple effects within drug treatments, were used to evaluate statistical significance. Values are expressed as mean ± S.E.M.

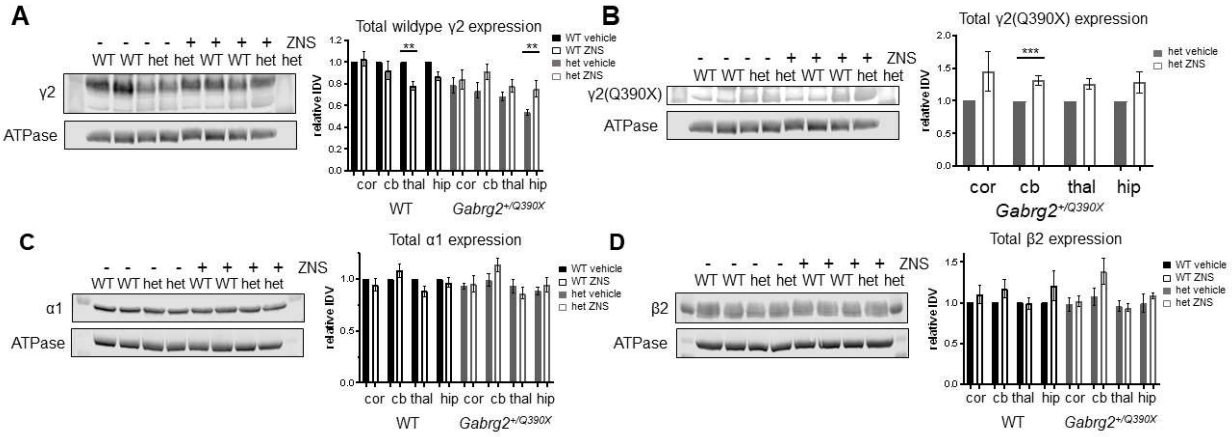


***Figure 5.12. Supplementary Figure 4: ZNS altered γ2 expression in* Gabrg2$^{+/Q390X}$ *but not α1 or β2.***

A-D. Beginning at P30-45, *Gabrg2*$^{+/Q390X}$ mice and wildtype littermates were treated with 20 mg/kg ZNS or equal volume DMSO/saline vehicle, with daily intraperitoneal injections for 7 days. Brains were dissected and lysates of somatosensory cortex (cor), cerebellum (cb), thalamus (thal), and hippocampus (hip) were used for SDS-PAGE. Representative images from thalamus are shown. A. Immunoblot for γ2 (1:1,000) and graph of normalized IDVs. Wildtype γ2 can be seen at ~50 kDa and γ2(Q390X) is visible below. In A, C-D, IDVs were normalized to the loading control, ATPase (1:1,000), and then to a paired vehicle-treated wildtype animal. B. The membrane from (A) is presented with digitally manipulated contrast and brightness to better visualize the γ2(Q390X) band. This manipulation was performed after quantification and had no effect on measured IDVs. The graph is of IDVs normalized to ATPase (1:1,000) and then to paired vehicle-treated heterozygous *Gabrg2*$^{+/Q390X}$ animals. C. Immunoblot for α1 (1:500) and graph of normalized IDVs. D. Immunoblot of thalamus lysates probed for β2 (1:1,000) and graph of normalized IDVs. C. N = 6-8 animals. Two-way ANOVA and Šídák's multiple comparisons, examining simple effects within drug treatments, were used to evaluate statistical significance. ** $p < 0.01$, *** $p < 0.001$. Values are expressed as mean ± S.E.M.

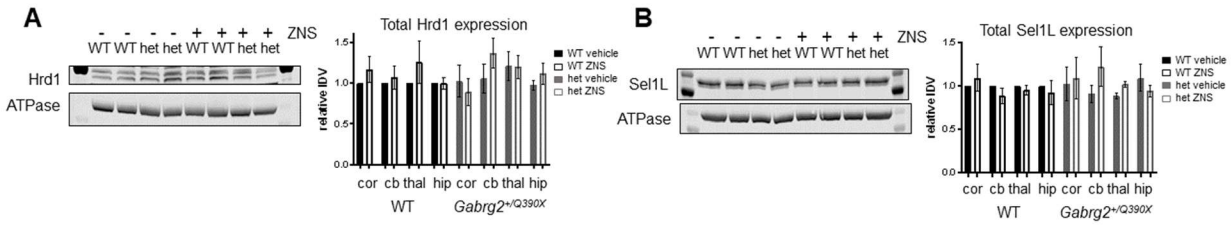


***Figure 5.13. Supplementary Figure 5: ZNS did not alter Hrd1 or Sel1L expression in* Gabrg2$^{+/Q390X}$.**

Beginning at P30-45, *Gabrg2*$^{+/Q390X}$ mice and wildtype littermates were treated with 20 mg/kg ZNS or equal volume DMSO/saline vehicle, with daily intraperitoneal injections for 7 days. Brains were dissected and lysates of somatosensory cortex (cor), cerebellum (cb), thalamus (thal), and hippocampus (hip) were used for SDS-PAGE. Representative images from thalamus are shown. A. Immunoblot for Hrd1 (1:1,000) and graph of normalized IDVs. In A-B, IDVs were normalized to the loading control, ATPase (1:1,000), and then to a paired vehicle-treated wildtype animal. B. Immunoblot of thalamus lysates probed for Sel1L (1:1,000) and graph of normalized IDVs.

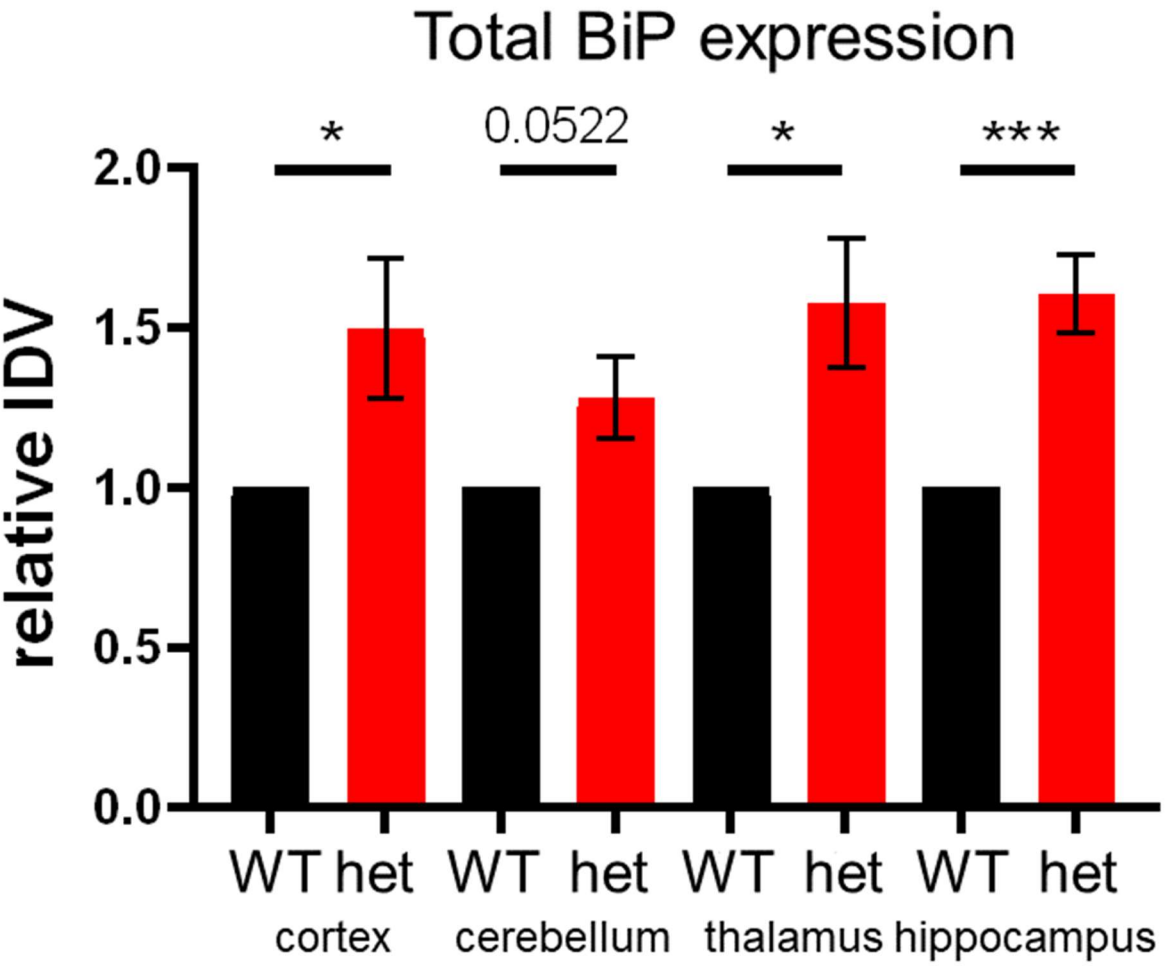


***Figure 5.14. Supplementary Figure 6: Elevated BiP in* Gabrg2$^{+/Q390X}$ *mice.***
Beginning at P30-45, *Gabrg2*$^{+/Q390X}$ mice and wildtype littermates were treated with 20 mg/kg ZNS or equal volume DMSO/saline vehicle, with daily intraperitoneal injections for 7 days. Brains were dissected and lysates of somatosensory cortex (cor), cerebellum (cb), thalamus (thal), and hippocampus (hip) were used for SDS-PAGE. Here, only the vehicle-treated animals are shown, to present baseline levels of BiP expression. Lysates were immunoblotted with BiP (1:500) and IDVs normalized to the loading control, ATPase (1:1,000), and then to a paired vehicle-treated wildtype littermate, are graphed. Unpaired t-tests were used to evaluate statistical significance. * $p < 0.05$, *** $p < 0.001$. Values are expressed as mean ± S.E.M.

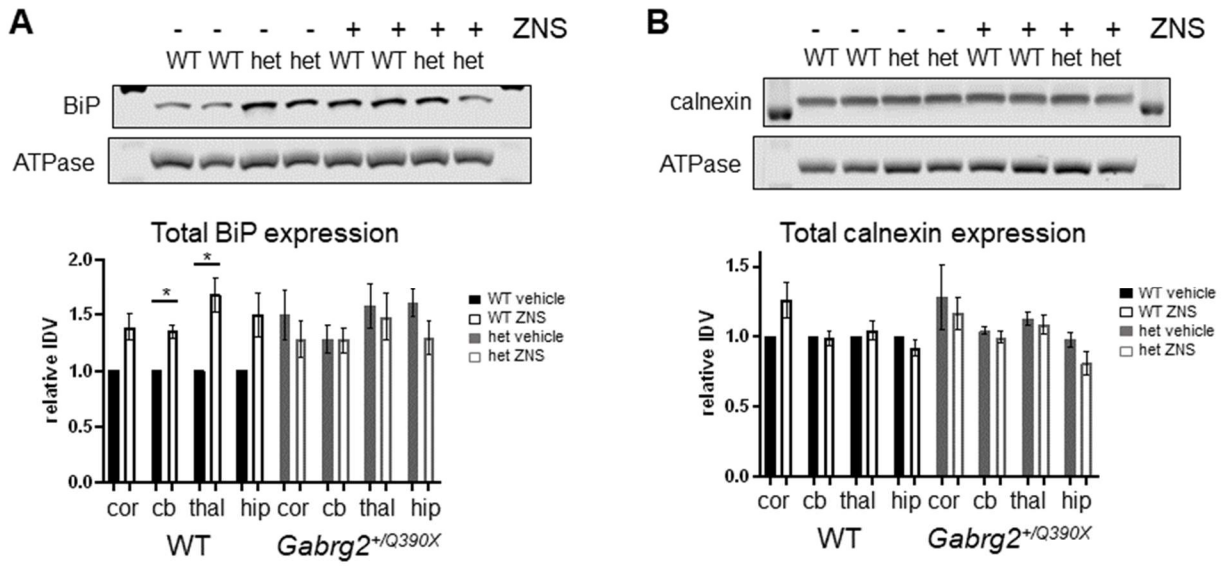


***Figure 5.15. Supplementary Figure 7: ZNS did not normalize ER stress associated with* Gabrg2$^{+/Q390X}$.**

Beginning at P30-45, *Gabrg2*$^{+/Q390X}$ mice and wildtype littermates were treated with 20 mg/kg ZNS or equal volume DMSO/saline vehicle, with daily intraperitoneal injections for 7 days. Brains were dissected and lysates of somatosensory cortex (cor), cerebellum (cb), thalamus (thal), and hippocampus (hip) were used for SDS-PAGE. Representative images from thalamus are shown. A. Immunoblot for BiP (1:500) and graph of normalized IDVs. In A-B, IDVs were normalized to the loading control, ATPase (1:1,000), and then to a paired vehicle-treated wildtype animal. B. Immunoblot of thalamus lysates probed for calnexin (1:1,000) and graph of normalized IDVs. * $p < 0.05$. Values are expressed as mean ± S.E.M.

## 5.9 Declarations

### 5.9.1 Data availability

The datasets used and/or analyzed during the current study are available from the corresponding author on reasonable request.

### 5.9.2 Supporting information

This article contains supporting information.


### 5.9.3 Funding

National Institute of Neurological Disease and Stroke (NINDS) R01 NS082635 and NS121718. The content is solely the responsibility of the authors and does not necessarily represent the official views of the National Institutes of Health.


### 5.9.4 Conflict of interest

The authors declare that they have no conflicts of interest with the contents of this article.

### 5.9.5 Author contributions

SP conceptualized the project, performed biochemistry experiments, and wrote the paper. GN performed EEG surgeries and acquired and analyzed EEG data. KR assisted with animal care. WS performed biochemistry experiments. CF analyzed EEG data. JQK conceptualized the project, edited the paper, and acquired funding. All authors read and approved the final manuscript.

## 5.10 References


1. Wallace RH, Marini C, Petrou S, Harkin LA, Bowser DN, Panchal RG, et al. Mutant GABA(A) receptor gamma2-subunit in childhood absence epilepsy and febrile seizures. Nat Genet. 2001 May;28(1):49–52.

2. Marini C, Harkin LA, Wallace RH, Mulley JC, Scheffer IE, Berkovic SF. Childhood absence epilepsy and febrile seizures: a family with a GABA(A) receptor mutation. Brain. 2003 Jan;126(Pt 1):230–40.

3. Audenaert D, Schwartz E, Claeys KG, Claes L, Deprez L, Suls A, et al. A novel GABRG2 mutation associated with febrile seizures. Neurology. 2006 Aug 22;67(4):687–90.

4. Shi X, Huang MC, Ishii A, Yoshida S, Okada M, Morita K, et al. Mutational analysis of GABRG2 in a Japanese cohort with childhood epilepsies. J Hum Genet. 2010 Jun;55(6):375–8.

5. Lachance-Touchette P, Brown P, Meloche C, Kinirons P, Lapointe L, Lacasse H, et al. Novel α1 and γ2 GABAA receptor subunit mutations in families with idiopathic generalized epilepsy. Eur J Neurosci. 2011 Jul;34(2):237–49.

6. Boillot M, Morin-Brureau M, Picard F, Weckhuysen S, Lambrecq V, Minetti C, et al. Novel GABRG2 mutations cause familial febrile seizures. Neurol Genet. 2015 Dec;1(4):e35.

7. Epi4K consortium, Epilepsy Phenome/Genome Project. Ultra-rare genetic variation in common epilepsies: a case-control sequencing study. Lancet Neurol. 2017 Feb;16(2):135–43.

8. Zou F, McWalter K, Schmidt L, Decker A, Picker JD, Lincoln S, et al. Expanding the phenotypic spectrum of GABRG2 variants: a recurrent GABRG2 missense variant associated with a severe phenotype. J Neurogenet. 2017;31(1–2):30–6.

9. Komulainen-Ebrahim J, Schreiber JM, Kangas SM, Pylkäs K, Suo-Palosaari M, Rahikkala E, et al. Novel variants and phenotypes widen the phenotypic spectrum of GABRG2-related disorders. Seizure. 2019 Jul;69:99–104.

10. Saleem T, Maqbool H, Sheikh N, Tayyeb A, Mukhtar M, Ashfaq A. GABRG2 C588T Polymorphism Is Associated with Idiopathic Generalized Epilepsy but Not with Antiepileptic Drug Resistance in Pakistani Cohort. Biomed Res Int. 2022;2022:3460792.

11. Kang JQ, Shen W, Macdonald RL. The GABRG2 mutation, Q351X, associated with generalized epilepsy with febrile seizures plus, has both loss of function and dominant-negative suppression. J Neurosci. 2009 Mar 4;29(9):2845–56.

12. Tian M, Macdonald RL. The Intronic GABRG2 Mutation, IVS6+2T→G, Associated with Childhood Absence Epilepsy Altered Subunit mRNA Intron Splicing, Activated Nonsense-Mediated Decay, and Produced a Stable Truncated γ2 Subunit. J Neurosci. 2012 Apr 25;32(17):5937–52.

13. Kang JQ, Shen W, Macdonald RL. Trafficking-deficient mutant GABRG2 subunit amount may modify epilepsy phenotype. Ann Neurol. 2013 Oct 1;74(4):547–59.

14. Johnston AJ, Kang JQ, Shen W, Pickrell WO, Cushion TD, Davies JS, et al. A Novel GABRG2 Mutation, p.R136*, in a family with GEFS+ and extended phenotypes. Neurobiol Dis. 2014 Apr;64:131–41.

15. Ishii A, Kanaumi T, Sohda M, Misumi Y, Zhang B, Kakinuma N, et al. Association of nonsense mutation in GABRG2 with abnormal trafficking of GABAA receptors in severe epilepsy. Epilepsy Res. 2014 Mar;108(3):420–32.

16. Harkin LA, Bowser DN, Dibbens LM, Singh R, Phillips F, Wallace RH, et al. Truncation of the GABAA-receptor gamma2 subunit in a family with generalized epilepsy with febrile seizures plus. Am J Hum Genet. 2002 Feb;70(2):530–6.

17. Kang JQ, Shen W, Zhou C, Xu D, Macdonald RL. The human epilepsy mutation GABRG2(Q390X) causes chronic subunit accumulation and neurodegeneration. Nat Neurosci. 2015 Jul;18(7):988–96.

18. Haynes CM, Titus EA, Cooper AA. Degradation of misfolded proteins prevents ER-derived oxidative stress and cell death. Mol Cell. 2004 Sep 10;15(5):767–76.

19. Di XJ, Wang YJ, Han DY, Fu YL, Duerfeldt AS, Blagg BSJ, et al. Grp94 Protein Delivers γ-Aminobutyric Acid Type A (GABAA) Receptors to Hrd1 Protein-mediated Endoplasmic Reticulum-associated Degradation. J Biol Chem. 2016 Apr 29;291(18):9526–39.

20. Pohl C, Dikic I. Cellular quality control by the ubiquitin-proteasome system and autophagy. [cited 2021 Oct 7]; Available from: https://www.science.org/doi/epdf/10.1126/science.aax3769

21. Zhu J, Tsai NP. Ubiquitination and E3 Ubiquitin Ligases in Rare Neurological Diseases with Comorbid Epilepsy. Neuroscience. 2020 Jan 21;428:90–9.

22. George AJ, Hoffiz YC, Charles AJ, Zhu Y, Mabb AM. A Comprehensive Atlas of E3 Ubiquitin Ligase Mutations in Neurological Disorders. Front Genet. 2018;9:29.

23. Potjewyd FM, Axtman AD. Exploration of Aberrant E3 Ligases Implicated in Alzheimer's Disease and Development of Chemical Tools to Modulate Their Function. Front Cell Neurosci. 2021;15:768655.

24. Lescouzères L, Bomont P. E3 Ubiquitin Ligases in Neurological Diseases: Focus on Gigaxonin and Autophagy. Front Physiol. 2020;11:1022.

25. Kang JQ, Shen W, Lee M, Gallagher MJ, Macdonald RL. Slow degradation and aggregation in vitro of mutant GABAA receptor gamma2(Q351X) subunits associated with epilepsy. J Neurosci. 2010 Oct 13;30(41):13895–905.

26. Warner TA, Shen W, Huang X, Liu Z, Macdonald RL, Kang JQ. Differential molecular and behavioural alterations in mouse models of GABRG2 haploinsufficiency versus dominant negative mutations associated with human epilepsy. Hum Mol Genet. 2016 Aug 1;25(15):3192–207.

27. Di XJ, Wang YJ, Cotter E, Wang M, Whittsette AL, Han DY, et al. Proteostasis Regulators Restore Function of Epilepsy-Associated GABAA Receptors. Cell Chem Biol. 2021 Jan 21;28(1):46-59.e7.

28. Tanaka M, DeLorey TM, Delgado-Escueta A, Olsen RW. GABRB3, Epilepsy, and Neurodevelopment. In: Noebels JL, Avoli M, Rogawski MA, Olsen RW, Delgado-Escueta AV, editors. Jasper's Basic Mechanisms of the Epilepsies [Internet]. 4th ed. Bethesda (MD): National Center for Biotechnology Information (US); 2012 [cited 2023 Mar 2]. Available from: http://www.ncbi.nlm.nih.gov/books/NBK98178/

29. Saliba RS, Pangalos M, Moss SJ. The ubiquitin-like protein Plic-1 enhances the membrane insertion of GABAA receptors by increasing their stability within the endoplasmic reticulum. J Biol Chem. 2008 Jul 4;283(27):18538–44.

30. Kleijnen MF, Shih AH, Zhou P, Kumar S, Soccio RE, Kedersha NL, et al. The hPLIC proteins may provide a link between the ubiquitination machinery and the proteasome. Mol Cell. 2000 Aug;6(2):409–19.

31. Delahanty RJ, Zhang Y, Bichell TJ, Shen W, Verdier K, Macdonald RL, et al. Beyond Epilepsy and Autism: Disruption of GABRB3 Causes Ocular Hypopigmentation. Cell Rep. 2016 Dec 20;17(12):3115–24.

32. Lee KY, Jewett KA, Chung HJ, Tsai NP. Loss of fragile X protein FMRP impairs homeostatic synaptic downscaling through tumor suppressor p53 and ubiquitin E3 ligase Nedd4-2. Hum Mol Genet. 2018 Aug 15;27(16):2805–16.

33. Zhu J, Lee KY, Jewett KA, Man HY, Chung HJ, Tsai NP. Epilepsy-associated gene Nedd4-2 mediates neuronal activity and seizure susceptibility through AMPA receptors. PLoS Genet. 2017 Feb;13(2):e1006634.

34. Jewett KA, Zhu J, Tsai NP. The tumor suppressor p53 guides GluA1 homeostasis through Nedd4-2 during chronic elevation of neuronal activity. J Neurochem. 2015 Oct;135(2):226–33.

35. Zhu J, Lee KY, Jong TT, Tsai NP. C2-lacking isoform of Nedd4-2 regulates excitatory synaptic strength through GluA1 ubiquitination-independent mechanisms. J Neurochem. 2019 Nov;151(3):289–300.

36. Jin H, Chiou TT, Serwanski DR, Miralles CP, Pinal N, De Blas AL. Ring finger protein 34 (RNF34) interacts with and promotes γ-aminobutyric acid type-A receptor degradation via ubiquitination of the γ2 subunit. J Biol Chem. 2014 Oct 17;289(42):29420–36.

37. Wu Q, Tian JH, He YX, Huang YY, Huang YQ, Zhang GP, et al. Zonisamide alleviates cardiac hypertrophy in rats by increasing Hrd1 expression and inhibiting endoplasmic reticulum stress. Acta Pharmacol Sin. 2021 Oct;42(10):1587–97.

38. Tian J hui, Wu Q, He Y xiang, Shen Q ying, Rekep M, Zhang G ping, et al. Zonisamide, an antiepileptic drug, alleviates diabetic cardiomyopathy by inhibiting endoplasmic reticulum stress. Acta Pharmacol Sin. 2021 Mar;42(3):393–403.

39. He YX, Shen QY, Tian JH, Wu Q, Xue Q, Zhang GP, et al. Zonisamide Ameliorates Cognitive Impairment by Inhibiting ER Stress in a Mouse Model of Type 2 Diabetes Mellitus. Front Aging Neurosci. 2020;12:192.

40. Omura T, Asari M, Yamamoto J, Kamiyama N, Oka K, Hoshina C, et al. HRD1 levels increased by zonisamide prevented cell death and caspase-3 activation caused by endoplasmic reticulum stress in SH-SY5Y cells. J Mol Neurosci. 2012 Mar;46(3):527–35.

41. Tsujii S, Ishisaka M, Shimazawa M, Hashizume T, Hara H. Zonisamide suppresses endoplasmic reticulum stress-induced neuronal cell damage in vitro and in vivo. Eur J Pharmacol. 2015 Jan 5;746:301–7.

42. Nwosu G, Mermer F, Flamm C, Poliquin S, Shen W, Rigsby K, et al. 4-Phenylbutyrate restored γ-aminobutyric acid uptake and reduced seizures in SLC6A1 patient variant-bearing cell and mouse models. Brain Commun. 2022;4(3):fcac144.

43. Gallagher MJ, Shen W, Song L, Macdonald RL. Endoplasmic reticulum retention and associated degradation of a GABAA receptor epilepsy mutation that inserts an aspartate in the M3 transmembrane segment of the alpha1 subunit. J Biol Chem. 2005 Nov 11;280(45):37995–8004.

44. Kang JQ, Shen W, Macdonald RL. Two molecular pathways (NMD and ERAD) contribute to a genetic epilepsy associated with the GABAA receptor GABRA1 PTC mutation, 975delC, S326fs328X. J Neurosci. 2009 Mar 4;29(9):2833–44.

45. Poliquin S, Kang JQ. Disruption of the Ubiquitin-Proteasome System and Elevated Endoplasmic Reticulum Stress in Epilepsy. Biomedicines. 2022 Mar;10(3):647.

46. Hattori T, Hanafusa K, Wada I, Hosokawa N. SEL1L degradation intermediates stimulate cytosolic aggregation of polyglutamine-expanded protein. The FEBS Journal. 2021;288(15):4637–54.

47. Crestani F, Lorez M, Baer K, Essrich C, Benke D, Laurent JP, et al. Decreased GABAA-receptor clustering results in enhanced anxiety and a bias for threat cues. Nat Neurosci. 1999 Sep;2(9):833–9.

48. Borowicz KK, Luszczki JJ, Sobieszek G, Ratnaraj N, Patsalos PN, Czuczwar SJ. Interactions between zonisamide and conventional antiepileptic drugs in the mouse maximal electroshock test model. Eur Neuropsychopharmacol. 2007 Mar;17(4):265–72.

49. Sonsalla PK, Wong LY, Winnik B, Buckley B. The antiepileptic drug zonisamide inhibits MAO-B and attenuates MPTP toxicity in mice: clinical relevance. Exp Neurol. 2010 Feb;221(2):329–34.

50. Ali NJ, Olsen RW. Chronic benzodiazepine treatment of cells expressing recombinant GABAA receptors uncouples allosteric binding: studies on possible mechanisms. Journal of Neurochemistry. 2001;79(5):1100–8.

51. Tehrani MH, Barnes EM. Sequestration of gamma-aminobutyric acidA receptors on clathrin-coated vesicles during chronic benzodiazepine administration in vivo. J Pharmacol Exp Ther. 1997 Oct;283(1):384–90.

52. Nagatomo I, Akasaki Y, Hashiguchi W, Tominaga M, Uchida M, Takigawa M. A solvent used for antiepileptic drugs increases serum and brain zonisamide concentrations in seizure-susceptible el mice. Epilepsy Behav. 2001 Aug;2(4):357–62.

53. Ying Z, Wang H, Fan H, Wang G. The endoplasmic reticulum (ER)-associated degradation system regulates aggregation and degradation of mutant neuroserpin. J Biol Chem. 2011 Jun 10;286(23):20835–44.

54. Edvardson S, Nicolae CM, Noh GJ, Burton JE, Punzi G, Shaag A, et al. Heterozygous RNF13 Gain-of-Function Variants Are Associated with Congenital Microcephaly, Epileptic Encephalopathy, Blindness, and Failure to Thrive. Am J Hum Genet. 2019 Jan 3;104(1):179–85.

55. Carvill GL, McMahon JM, Schneider A, Zemel M, Myers CT, Saykally J, et al. Mutations in the GABA Transporter SLC6A1 Cause Epilepsy with Myoclonic-Atonic Seizures. Am J Hum Genet. 2015 May 7;96(5):808–15.

56. Wang J, Poliquin S, Mermer F, Eissman J, Delpire E, Wang J, et al. Endoplasmic reticulum retention and degradation of a mutation in SLC6A1 associated with epilepsy and autism. Mol Brain. 2020 May 12;13(1):76.

57. Saitsu H, Kato M, Mizuguchi T, Hamada K, Osaka H, Tohyama J, et al. De novo mutations in the gene encoding STXBP1 (MUNC18-1) cause early infantile epileptic encephalopathy. Nat Genet. 2008 Jun;40(6):782–8.

58. Guiberson NGL, Pineda A, Abramov D, Kharel P, Carnazza KE, Wragg RT, et al. Mechanism-based rescue of Munc18-1 dysfunction in varied encephalopathies by chemical chaperones. Nat Commun. 2018 Sep 28;9(1):3986.

59. Kim EC, Zhang J, Pang W, Wang S, Lee KY, Cavaretta JP, et al. Reduced axonal surface expression and phosphoinositide sensitivity in Kv7 channels disrupts their function to inhibit neuronal excitability in Kcnq2 epileptic encephalopathy. Neurobiol Dis. 2018 Oct;118:76–93.

# 6 Conclusions and Future Directions

## 6.1 Conclusions

The data presented in these chapters suggests that proteostasis is impaired by the γ2(Q390X) protein, which is a radical departure from the traditional view of epilepsies as ion channel disorders. I observe deviations in autophagy proteins, molecular chaperones, and in ubiquitin-proteasome system function, compared to conditions using the wildtype γ2 protein. While the autophagy protein and ubiquitin-proteasome system (UPS) activity differences were discovered *in vitro*, the change to the expression pattern of the molecular chaperone BiP occurred in the brains of *Gabrg2*$^{+/Q390X}$ mice, suggesting real-world relevancy to the pathophysiology of epileptic encephalopathies such as Dravet syndrome.

Additionally, I began biochemical characterization of mutations in another protein associated with genetic epilepsy, the GABA transporter 1 (GAT1). Because GAT1 is expressed in astrocytes as well as neurons,[1] proteostatic impairments caused by genetic epilepsies may occur throughout multiple types of brain cells, rather than being limited to neurons.

This work contributes to the emerging field of studying the importance of proteostasis in genetic epilepsy. In addition to demonstrating aberrations of proteostasis resulting from the γ2(Q390X) protein, I also suggest a potential avenue for future therapeutics: I show that expression of the dominant-negative, aggregate-forming γ2(Q390X) protein can be decreased via modulation of the endogenous endoplasmic reticulum (ER) associated degradation (ERAD) system. This can perhaps be translated

to other genetic epilepsies with potentially harmful misfolded proteins, such as STXBP1 encephalopathy,[2] KCNQ2 encephalopathy,[3] and *SLC6A1* disorders.[4]

## 6.2 Future Directions

### 6.2.1 Autophagy and UPS over lifespan

As mentioned in Chapters 2 and 3, it will be important to characterize the protein degradation pathways in *Gabrg2*$^{+/Q390X}$ mice across their lifespan. This includes examining autophagic markers in brain slices from *Gabrg2*$^{+/Q390X}$ and *Scn1a*$^{+/-}$ mice, and how that may correlate with the number of parvalbumin-positive interneurons (PVIN). Additionally, UPS activity should be investigated at multiple timepoints. As discussed in Chapter 3, it is possible that the deficits may shift and evolve over the life of the animal, such that different abnormalities may be identified at different ages. Useful timepoints might include the neonatal period preceding seizure onset; P21, the approximate age of seizure onset; early adulthood before γ2(Q390X) protein noticeably accumulates; 6 months of age, when γ2(Q390X) aggregates become readily detectable; and 12 months of age, when neuronal loss has been detected.[5]

### 6.2.2 Firing properties of PV IN in *Gabrg2*$^{+/Q390X}$

Irrespective of what the previous experiment may find regarding the viability of PVIN, it will be useful to investigate the functionality of PVIN in *Gabrg2*$^{+/Q390X}$ mice. Surviving PVIN – whether that is a number comparable to wildtype mice or much lower – may have an impaired ability to fire action potential trains, similar to what is seen in *Scn1a* Dravet syndrome models.[6–8] Alternatively, hyperexcitability of PVIN is possible. Because PVIN express GABR, the dominant-negative effects of the γ2(Q390X) subunit

on GABR surface expression identified in other cell types presumably apply to these neurons as well. This would reduce the inhibition received and potentially result in hyperexcitability, which is not incompatible with the pathophysiology of epilepsy. Although decreased PVIN activity is associated with seizures, elevated PVIN firing can also contribute to seizures and epileptiform activity.[9–11]

### 6.2.3 Is seizure control sufficient to normalize proteostasis?

As has been discussed at length, particularly in Chapter 1, the relationship between genetic epilepsy and proteostasis is complex, due to dual influence of both mutated protein and epileptic activity on proteostasis networks. This raises the question of whether seizure suppression is sufficient to normalize autophagy and the UPS. While comparisons between the *Scn1a*$^{+/-}$ and *Gabrg2*$^{+/Q390X}$ models can provide some insight into the role of mutant protein, as the lack of mutant protein is the primary difference between these two mouse models of Dravet syndrome, the *Scn1a*$^{+/-}$ mouse it is still a different model, despite great phenotypic similarity. Thus, a diligent experiment would attempt to modulate the γ2(Q390X) protein or seizures within the same mouse line, *Gabrg2*$^{+/Q390X}$. Regulation of the γ2(Q390X) subunit can likely be achieved by chronic treatment with PBA. For comparison, it will be insightful to utilize an ASD that does not significantly alter expression of γ2(Q390X) protein or directly affect proteostasis, but does effectively control seizures. With these two treatments targeting separate aspects of pathophysiology, the effects on autophagy and the UPS in these chronically treated animals could be compared.

It may take extensive preliminary work, however, to identify a suitable ASD. For example, ZNS is not a good candidate because it does alter GABR proteostasis.

Carbamazepine is also not suited, as it has been shown to enhance both autophagy and proteasome activity.[12–14] Similarly, valproate has effects on ER stress that would confound this study.[15–17] Benzodiazepines are well-known for altering GABR trafficking and subunit composition.[18–20] GAT1 inhibitors like tiagabine, meanwhile, may result in GABR changes due to the chronically elevated extracellular GABA levels.[21,22] Finally, while the above-mentioned drugs have been tested in several models, only ZNS has been extensively characterized in γ2(Q390X) models. Thus, even ASDs that are not currently known to directly modify proteostasis or GABR expression may still have that effect in γ2(Q390X) models. Therefore, if multiple candidate compounds can be identified, it may be prudent to use more than one in this study, to ensure consistent effects and rule out unknown confounding variables.

### 6.2.4 Assess autophagic reserve capacity

Because the nonfunctional γ2(Q390X) protein is likely degraded at least in part through autophagy, and this protein is constitutively expressed, the autophagic pathway may be overtaxed. Thus, it would be worthwhile to investigate the autophagic reserve capacity. In other words, are cells expressing the γ2(Q390X) subunit still capable of upregulating autophagy in response to autophagy-inducing conditions? Rapamycin is an inhibitor of the mTOR pathway and a potent inducer of autophagy. Incubation of cells in low-nutrient medium is also a conventional method of upregulating autophagy. Cultured cells expressing γ2(Q390X) or γ2 subunits could be exposed to these conditions, and autophagic flux between the wildtype and mutant conditions could be compared.

Furthermore, the γ2(Q390X) protein may render cells more sensitive to deleterious effects from deficits in autophagy. For instance, cells may be more vulnerable to apoptosis when treated with an autophagy inhibitor such as 3-methyladenine (3-MA). A simple trypan blue cell counting assay could be utilized, or samples could be evaluated for markers of apoptosis such as cleaved caspase-3.

### 6.2.5 Rapamycin as a therapeutic compound

Depending on the results of the prior study, it might be worthwhile to explore the use of rapamycin in *Gabrg2*$^{+/Q390X}$ mice. Rapamycin is used clinically to treat multiple symptoms of tuberous sclerosis, including seizures, and rapamycin may also have antiepileptogenic properties for other epilepsies, although this has not yet been verified clinically.[23,24] In γ2(Q390X) models, autophagy upregulation via rapamycin treatment may reduce expression of γ2(Q390X) protein. This could have robust disease-modifying effects beyond seizure reduction, as the decreased load of protein aggregates may lessen the extent of neurodegeneration. Thus, in addition to our standard acquisition of EEG recordings to assess anti-seizure treatment efficacy, mice treated with rapamycin should be put through a battery of neurobehavioral tests to investigate the effects on cognition and social behaviors. Moreover, biochemical analysis of brain tissue should be conducted, especially on tissue from old mice, to evaluate whether rapamycin is neuroprotective in *Gabrg2*$^{+/Q390X}$ mice.

It is important to note, however, that standard ASDs may also have some benefits to cognition and neuronal health, because Dravet syndrome is a developmental and epileptic encephalopathy – the seizures contribute to developmental delay. By decreasing seizures, it would be expected to see an improvement in the course of the

encephalopathy. Thus, rapamycin treatment must be compared to another compound equally effective at reducing seizures, in order to rigorously elucidate the autophagy-specific effects of rapamycin.

### 6.2.6 Impact of γ2(Q390X) on molecular chaperones and the unfolded protein response

In addition to perturbations of autophagy and the UPS, the findings concerning the upregulation of BiP in wildtype animals after ZNS treatment – but not in *Gabrg2*$^{+/Q390X}$ animals – suggest a possibility that the γ2(Q390X) protein induces broad changes to the protein quality control networks. Calnexin was investigated and total expression was found to be unaltered in any condition; however, *in vitro* experiments had discovered a dramatic increase in the interaction between calnexin and the γ2(Q390X) subunit, compared to the γ2 subunit.[25] Total expression of other molecular chaperones, such as GRP94, calreticulin, and HSP70, should also be examined, as well as their interaction with the γ2(Q390X) subunit. The basal levels may differ between wildtype and *Gabrg2*$^{+/Q390X}$ mice, and/or the response to ZNS treatment may be disparate.

### 6.2.7 Synergism of proteostasis regulators

My work with PBA suggests a statistically insignificant trend towards increased surface expression of α1, β2, and wildtype γ2, in HEK293T cells transfected with α1β2γ2/γ2(Q390X). Meanwhile, ZNS robustly rescued surface expression of α1 and β2 – but not γ2. It would be fascinating if these two compounds could act synergistically, to increase the surface expression of full α1β2γ2 GABR. It is imperative to explore this possibility. Electrophysiological confirmation that upregulated surface expression does indeed correspond to functional receptors will of great use.

### 6.2.8 Selective targeting of γ2(Q390X)

Although the discovery that Hrd1 overexpression can decrease expression of the overly-stable γ2(Q390X) protein is groundbreaking, it is limited by the fact that expression of wildtype γ2 protein was reduced by the same magnitude. Thus, it will be useful to investigate other E3 ubiquitin ligases in the aims of achieving more selective degradation of the γ2(Q390X) subunit. An extensive literature review will be necessary, to guide the decisions of which E3 ligases will be studied. Databases such as UbiNet 2.0, which lists thousands of known E3 ligase-substrate interactions as well as substrate motifs targeted by various E3 ligases, will be helpful.[26] An alternative, and perhaps complementary, approach is selective inhibition of the degradation of wildtype GABR subunits, although this will not fully protect neurons from the dominant-negative effects of the γ2(Q390X) protein. A promising candidate for this approach is RNF34, which targets the γ2 subunit for degradation and requires lysine residues near the C-terminus that are deleted from the truncated γ2(Q390X) protein.[27] Additionally, if a selective E3 ligase can be identified – or engineered – then the interaction between the E3 ligase and the γ2(Q390X) subunit can be facilitated with a proteolysis targeting chimera (PROTAC).[28]

### 6.2.9 Relationship between HRD1, γ2(Q390X), and ZNS

I've shown that overexpression of HRD1 is associated with decreased total and surface expression of γ2 and γ2(Q390X) subunits. However, to more fully argue for causation, the effect of HRD1 knockdown or inhibition should be examined. If decreased HRD1 activity results in increased expression of γ2 and γ2(Q390X) subunits, this further validates that HRD1 is involved in the degradation of the γ2(Q390X) subunit.

Robust pharmacological reduction of HRD1 mRNA and protein levels can be obtained with DNP and DHEC.[29] Knockdown of HRD1 will serve another purpose: insight into the mechanism of ZNS. Although ZNS is reported to upregulate HRD1, I did not replicate those findings. However, if knockdown of HRD1 prevents the effects of ZNS on GABR subunit trafficking, that suggests that ZNS does indeed have an interaction with HRD1. It is possible that my methods were not sensitive enough to detect a small (but biologically relevant) change in HRD1 expression. Alternatively, ZNS may be acting on GABR subunits through HRD1, but in a manner that does not influence HRD1 expression levels. For example, ZNS may alter the affinity of HRD1 for a substrate, such that a change in HRD1 levels are not necessary to amplify HRD1-mediated degradation of that substrate.

### 6.2.10 Mechanism by which ZNS promotes GABR subunit trafficking

In Chapter 5, I showed that ZNS upregulated surface expression – but not total expression – of the α1 and β2 subunits, in HEK293T cells transfected with a1β2γ2/γ2(Q390X) GABR. However, I was not yet able to determine the mechanism by which ZNS promotes trafficking of GABR subunits. It would be insightful to examine how ZNS may be altering how the γ2(Q390X) subunit interacts with other proteins. For example, immunoprecipitation could be used to investigate if the increased surface trafficking of α1 and β2 subunits is due to interruption of the partnering of the wildtype subunits with the γ2(Q390X) protein, thereby mitigating ER retention of these subunits. Alternatively, the upregulated protein trafficking may be independent of the γ2(Q390X) subunit. Therefore, it would be of use to interrogate the effects of ZNS on wildtype α1β2γ2 GABRs. Possibilities that are not heavily genotype-dependent could include

altered expression of secretory pathway proteins. Furthermore, crucially, the increased surface expression of GABR subunits must be confirmed *in vivo*, through brain surface biotinylation, microscopy, and/or electrophysiology.

### 6.2.11 Impact of this study on other epilepsy-associated mutations and proteostasis

Finally, it has been my hope throughout all my studies that the findings on *GABRG2(Q390X)* may be translatable to other epilepsy-causing genetic mutations. In my introductory chapter, I mentioned aberrant proteostasis associated with several other genetic epilepsies, including excessive ERAD of α1(A322D)[30] and γ2(R177G) GABR subunits;[31] loss of function of E3 ubiquitin ligases like *UBE3A*[32,33] and of deubiquitinases such as *OTUD7A*;[34] and impaired UPS function in progressive myoclonus epilepsy type 1.[35] Additionally, intracellular protein aggregates are associated with many genetic epilepsies beyond *GABRG2(Q390X)*, including STXBP1 encephalopathy,[2] KCNQ2 encephalopathy,[3] and Lafora disease.[36,37]

A gene that would be especially interesting to investigate is *SLC6A1*, which encodes GAT1. Several mutations in this gene, although identified in patients with diverse phenotypes, have been shown to be partially retained with the ER.[38–41] Furthermore, evidence points towards ER retention of several more mutations so far less thoroughly characterized, as the mutant proteins have reduced surface expression compared to wildtype GAT1 while total protein expression is unchanged.[4] However, the consequences of ER retention have not yet been studied in these models. Additionally, it may be worthwhile to modulate ERAD, either upregulating components to decrease expression of deleterious mutant proteins – as I did with Hrd1 overexpression to reduce

γ2(Q390X) expression – or inhibiting elements to allow mutant proteins with partial function to more efficiently traffic to the cell surface.

The GAT1(S295L) mutation is of particular interest, as it is almost fully retained within the ER and has no GABA uptake function,[4] analogous to the prominent ER retention and accumulation of γ2(Q390X) protein and lack of GABR activity for receptors containing the γ2(Q390X) subunit. I briefly investigated the effect of GAT1(S295L) on the UPS and observed a trend towards decreased GFPu intensity compared to non-excitable cells transfected with wildtype GAT1. This preliminary work suggests that UPS activity is altered in a genetic epilepsy other than *GABRG2(Q390X)*-associated Dravet syndrome, as a direct consequence of the mutated protein. The Kang lab has recently acquired a mouse harboring this mutation, the *Slc6a1*$^{+/S295L}$ line, which will allow for valuable *in vivo* experimentation. Aspects of proteostasis such as ER stress, autophagy, and proteasome activity should be studied in this mouse and in other models of genetic epilepsies. Thus, this study will have a broad impact on understanding genetic epilepsies and treatment interventions.

## 6.3 References


1. Fattorini G, Melone M, Conti F. A Reappraisal of GAT-1 Localization in Neocortex. *Front Cell Neurosci*. 2020;14:9. doi:10.3389/fncel.2020.00009

2. Guiberson NGL, Pineda A, Abramov D, et al. Mechanism-based rescue of Munc18-1 dysfunction in varied encephalopathies by chemical chaperones. *Nat Commun*. 2018;9(1):3986. doi:10.1038/s41467-018-06507-4

3. Kim EC, Zhang J, Pang W, et al. Reduced axonal surface expression and phosphoinositide sensitivity in Kv7 channels disrupts their function to inhibit neuronal excitability in Kcnq2 epileptic encephalopathy. *Neurobiol Dis*. 2018;118:76-93. doi:10.1016/j.nbd.2018.07.004

4. Mermer F, Poliquin S, Rigsby K, et al. Common molecular mechanisms of SLC6A1 variant-mediated neurodevelopmental disorders in astrocytes and neurons. *Brain*. 2021;144(8):2499-2512. doi:10.1093/brain/awab207

5. Kang JQ, Shen W, Zhou C, Xu D, Macdonald RL. The human epilepsy mutation GABRG2(Q390X) causes chronic subunit accumulation and neurodegeneration. *Nat Neurosci*. 2015;18(7):988-996. doi:10.1038/nn.4024

6. Ogiwara I, Miyamoto H, Morita N, et al. Nav1.1 localizes to axons of parvalbumin-positive inhibitory interneurons: a circuit basis for epileptic seizures in mice carrying an Scn1a gene mutation. *J Neurosci*. 2007;27(22):5903-5914. doi:10.1523/JNEUROSCI.5270-06.2007

7. Tai C, Abe Y, Westenbroek RE, Scheuer T, Catterall WA. Impaired excitability of somatostatin- and parvalbumin-expressing cortical interneurons in a mouse model of Dravet syndrome. *Proc Natl Acad Sci USA*. 2014;111(30):E3139-3148. doi:10.1073/pnas.1411131111

8. Favero M, Sotuyo NP, Lopez E, Kearney JA, Goldberg EM. A Transient Developmental Window of Fast-Spiking Interneuron Dysfunction in a Mouse Model of Dravet Syndrome. *J Neurosci*. 2018;38(36):7912-7927. doi:10.1523/JNEUROSCI.0193-18.2018

9. Anstötz M, Fiske MP, Maccaferri G. Impaired KCC2 Function Triggers Interictal-Like Activity Driven by Parvalbumin-Expressing Interneurons in the Isolated Subiculum In Vitro. *Cereb Cortex*. 2021;31(10):4681-4698. doi:10.1093/cercor/bhab115

10. Ellender TJ, Raimondo JV, Irkle A, Lamsa KP, Akerman CJ. Excitatory effects of parvalbumin-expressing interneurons maintain hippocampal epileptiform activity via synchronous afterdischarges. *J Neurosci*. 2014;34(46):15208-15222. doi:10.1523/JNEUROSCI.1747-14.2014

11. Sessolo M, Marcon I, Bovetti S, et al. Parvalbumin-Positive Inhibitory Interneurons Oppose Propagation But Favor Generation of Focal Epileptiform Activity. *J Neurosci*. 2015;35(26):9544-9557. doi:10.1523/JNEUROSCI.5117-14.2015

12. Meng Q, Chen X, Sun L, Zhao C, Sui G, Cai L. Carbamazepine promotes Her-2 protein degradation in breast cancer cells by modulating HDAC6 activity and acetylation of Hsp90. *Mol Cell Biochem*. 2011;348(1-2):165-171. doi:10.1007/s11010-010-0651-y

13. Hidvegi T, Ewing M, Hale P, et al. An autophagy-enhancing drug promotes degradation of mutant alpha1-antitrypsin Z and reduces hepatic fibrosis. *Science*. 2010;329(5988):229-232. doi:10.1126/science.1190354

14. Sarkar S, Floto RA, Berger Z, et al. Lithium induces autophagy by inhibiting inositol monophosphatase. *J Cell Biol*. 2005;170(7):1101-1111. doi:10.1083/jcb.200504035

15. Batjargal K, Tajima T, Jimbo EF, Yamagata T. Effect of 4-phenylbutyrate and valproate on dominant mutations of WFS1 gene in Wolfram syndrome. *J Endocrinol Invest*. 2020;43(9):1317-1325. doi:10.1007/s40618-020-01228-2

16. Bown CD, Wang JF, Chen B, Young LT. Regulation of ER stress proteins by valproate: therapeutic implications. *Bipolar Disord*. 2002;4(2):145-151. doi:10.1034/j.1399-5618.2002.t01-1-40201.x

17. Fu J, Peng L, Wang W, et al. Sodium Valproate Reduces Neuronal Apoptosis in Acute Pentylenetetrzole-Induced Seizures via Inhibiting ER Stress. *Neurochem Res*. 2019;44(11):2517-2526. doi:10.1007/s11064-019-02870-w

18. Tehrani MH, Barnes EM. Sequestration of gamma-aminobutyric acidA receptors on clathrin-coated vesicles during chronic benzodiazepine administration in vivo. *J Pharmacol Exp Ther*. 1997;283(1):384-390.

19. Ali NJ, Olsen RW. Chronic benzodiazepine treatment of cells expressing recombinant GABAA receptors uncouples allosteric binding: studies on possible mechanisms. *Journal of Neurochemistry*. 2001;79(5):1100-1108. doi:10.1046/j.1471-4159.2001.00664.x

20. Foitzick MF, Medina NB, Iglesias García LC, Gravielle MC. Benzodiazepine exposure induces transcriptional down-regulation of GABAA receptor α1 subunit gene via L-type voltage-gated calcium channel activation in rat cerebrocortical neurons. *Neurosci Lett*. 2020;721:134801. doi:10.1016/j.neulet.2020.134801

21. Mhatre MC, Ticku MK. Chronic GABA treatment downregulates the GABAA receptor alpha 2 and alpha 3 subunit mRNAS as well as polypeptide expression in primary cultured cerebral cortical neurons. *Brain Res Mol Brain Res*. 1994;24(1-4):159-165. doi:10.1016/0169-328x(94)90128-7

22. Platt KP, Zwartjes RE, Bristow DR. The effect of GABA stimulation on GABAA receptor subunit protein and mRNA expression in rat cultured cerebellar granule cells. *Br J Pharmacol*. 1996;119(7):1393-1400. doi:10.1111/j.1476-5381.1996.tb16051.x

23. Klein P, Friedman A, Hameed MQ, et al. Repurposed molecules for antiepileptogenesis: Missing an opportunity to prevent epilepsy? *Epilepsia*. 2020;61(3):359-386. doi:10.1111/epi.16450

24. Canpolat M, Gumus H, Kumandas S, Coskun A, Per H. The use of rapamycin in patients with tuberous sclerosis complex: Long-term results. *Epilepsy Behav*. 2018;88:357-364. doi:10.1016/j.yebeh.2018.09.020

25. Shen W, Poliquin S, Macdonald RL, Dong M, Kang JQ. Endoplasmic reticulum stress increases inflammatory cytokines in an epilepsy mouse model Gabrg2+/Q390X knockin: A link

between genetic and acquired epilepsy? *Epilepsia*. 2020;61(10):2301-2312. doi:10.1111/epi.16670

26. Li Z, Chen S, Jhong JH, et al. UbiNet 2.0: a verified, classified, annotated and updated database of E3 ubiquitin ligase-substrate interactions. *Database (Oxford)*. 2021;2021:baab010. doi:10.1093/database/baab010

27. Jin H, Chiou TT, Serwanski DR, Miralles CP, Pinal N, De Blas AL. Ring finger protein 34 (RNF34) interacts with and promotes γ-aminobutyric acid type-A receptor degradation via ubiquitination of the γ2 subunit. *J Biol Chem*. 2014;289(42):29420-29436. doi:10.1074/jbc.M114.603068

28. Tomoshige S, Ishikawa M. PROTACs and Other Chemical Protein Degradation Technologies for the Treatment of Neurodegenerative Disorders. *Angew Chem Int Ed Engl*. 2021;60(7):3346-3354. doi:10.1002/anie.202004746

29. Di XJ, Wang YJ, Cotter E, et al. Proteostasis Regulators Restore Function of Epilepsy-Associated GABAA Receptors. *Cell Chem Biol*. 2021;28(1):46-59.e7. doi:10.1016/j.chembiol.2020.08.012

30. Di XJ, Wang YJ, Han DY, et al. Grp94 Protein Delivers γ-Aminobutyric Acid Type A (GABAA) Receptors to Hrd1 Protein-mediated Endoplasmic Reticulum-associated Degradation. *J Biol Chem*. 2016;291(18):9526-9539. doi:10.1074/jbc.M115.705004

31. Todd E, Gurba KN, Botzolakis EJ, Stanic AK, Macdonald RL. GABAA receptor biogenesis is impaired by the γ2 subunit febrile seizure-associated mutation, GABRG2(R177G). *Neurobiology of Disease*. 2014;69:215-224. doi:10.1016/j.nbd.2014.05.013

32. Zhu J, Tsai NP. Ubiquitination and E3 Ubiquitin Ligases in Rare Neurological Diseases with Comorbid Epilepsy. *Neuroscience*. 2020;428:90-99. doi:10.1016/j.neuroscience.2019.12.030

33. Lopez SJ, Segal DJ, LaSalle JM. UBE3A: An E3 Ubiquitin Ligase With Genome-Wide Impact in Neurodevelopmental Disease. *Front Mol Neurosci*. 2018;11:476. doi:10.3389/fnmol.2018.00476

34. Garret P, Ebstein F, Delplancq G, et al. Report of the first patient with a homozygous OTUD7A variant responsible for epileptic encephalopathy and related proteasome dysfunction. *Clin Genet*. 2020;97(4):567-575. doi:10.1111/cge.13709

35. Polajnar M, Zavašnik-Bergant T, Škerget K, et al. Human Stefin B Role in Cell's Response to Misfolded Proteins and Autophagy. *PLOS ONE*. 2014;9(7):e102500. doi:10.1371/journal.pone.0102500

36. Berthier A, Payá M, García-Cabrero AM, et al. Pharmacological Interventions to Ameliorate Neuropathological Symptoms in a Mouse Model of Lafora Disease. *Mol Neurobiol*. 2016;53(2):1296-1309. doi:10.1007/s12035-015-9091-8

37. Rao SNR, Maity R, Sharma J, et al. Sequestration of chaperones and proteasome into Lafora bodies and proteasomal dysfunction induced by Lafora disease-associated mutations of malin. *Hum Mol Genet*. 2010;19(23):4726-4734. doi:10.1093/hmg/ddq407

38. Cai K, Wang J, Eissman J, et al. A missense mutation in SLC6A1 associated with Lennox-Gastaut syndrome impairs GABA transporter 1 protein trafficking and function. *Exp Neurol*. 2019;320:112973. doi:10.1016/j.expneurol.2019.112973

39. Poliquin S, Hughes I, Shen W, et al. Genetic mosaicism, intrafamilial phenotypic heterogeneity, and molecular defects of a novel missense SLC6A1 mutation associated with epilepsy and ADHD. *Exp Neurol*. 2021;342:113723. doi:10.1016/j.expneurol.2021.113723

40. Wang J, Poliquin S, Mermer F, et al. Endoplasmic reticulum retention and degradation of a mutation in SLC6A1 associated with epilepsy and autism. *Mol Brain*. 2020;13(1):76. doi:10.1186/s13041-020-00612-6

41. Mermer F, Poliquin S, Zhou S, et al. Astrocytic GABA transporter 1 deficit in novel SLC6A1 variants mediated epilepsy: Connected from protein destabilization to seizures in mice and humans. *Neurobiol Dis*. 2022;172:105810. doi:10.1016/j.nbd.2022.105810